



Virginia Commonwealth University
VCU Scholars Compass

Theses and Dissertations

Graduate School

2015

Development of Irreversible Substrate Competitive Probes for PKA Activity

Robert A. Coover
Virginia Commonwealth University

Follow this and additional works at: <https://scholarscompass.vcu.edu/etd>

 Part of the [Medicinal Chemistry and Pharmaceutics Commons](#)

© The Author

Downloaded from

<https://scholarscompass.vcu.edu/etd/3907>

This Dissertation is brought to you for free and open access by the Graduate School at VCU Scholars Compass. It has been accepted for inclusion in Theses and Dissertations by an authorized administrator of VCU Scholars Compass. For more information, please contact libcompass@vcu.edu.

© Robert A. Coover 2015

All Rights Reserved

**DEVELOPMENT OF IRREVERSIBLE SUBSTRATE COMPETITIVE PROBES FOR
PKA ACTIVITY**

A dissertation submitted in partial fulfillment of the requirements for the degree of Doctor of
Philosophy at Virginia Commonwealth University.

by

Robert Anthony Coover

Bachelor of Science, University of North Carolina at Greensboro, May 2011

Director: Keith C. Ellis

Assistant Professor, Department of Medicinal Chemistry

Acknowledgement

I would like to send my humblest and most sincere thanks to so many people. I would like to thank my wife Candace for her constant love, patience, and strength. My family, for always reminding me what's most important. A special nod to those family who can't see this now, I miss you all.

I would like to thank my advisor and mentor Dr. Keith C. Ellis. You allowed me to be as passionate as I can be about this project and I believe it let me achieve so much. I have had the privilege of learning under your tutelage.

I would like to thank my committee members: Dr. Glen Kellogg, Dr. Martin Safo, Dr. Darrell Peterson, and Dr. Frank Gupton. Thank you all for the career and guidance support. Special thanks for your patience and time as I'm sure I can take a fair amount of both.

Thanks to my fellow lab mates, past and present, who keep spirits high and are a source of encouragement.

Finally, I would like to thank my support system of friends. The bonds that keep true friends around don't weather with time, they simply grow stronger.

Table of Contents

Acknowledgements	ii
List of Tables	v
List of Figures	vi
Abstract	x
List of Abbreviations	xii
Chapter:	
1. Introduction to Proteomic Strategies	
1.1. Proteomics.....	1
1.2. Chemical Proteomics	2
1.3. Irreversible Inhibitors of the Kinome	8
1.4. Activity-Based Protein Profiling	20
1.5. General Hypothesis	25
2. Background on the cAMP-Dependent Protein Kinase	
2.1. cAMP-dependent protein kinase (PKA)	26
2.2. Structure of PKA	27
2.3. Expression and Regulation of PKA	29
2.4. Healthy and Diseased PKA Activity.....	34
2.5 Current Methods to Detect PKA and PKA α activity	40

3. Development of ABPs for PKAC α	
3.1. Background on the Heat-Stable Protein Kinase Inhibitor (PKI)	46
3.2. PKI Selectivity.....	49
3.4. Single Amino Acid Analogues.....	55
3.5. Production and Evaluation of Longer Peptide-Based Probes.....	65
3.6. First Protein Production Experiments.....	76
3.7. Biological Characterization of 38 as a Probe for PKAC α	80
3.8. Preparation of Rh-PKI(14-22)Gly-CMK.....	87
3.9. Biological Characterization of 41 as a Probe for PKAC α	91
3.10. The Fluoromethyl Ketone Electrophile.....	106
3.11. Expression of Phosphorylated PKAC α	110
3.12. Biological Characterization of 48 as a Probe for PKAC α	117
3.13. Development of a Biotinylated Peptide-Based Probe.....	130
3.14. Results, Discussion, and Future Directions.	137
4. Experimentals	
4.1. ClustalX Sequence Alignment.....	139
4.2. General Chemical Methods.....	150
4.3. General Procedure for the Formation of Weinreb Amide Intermediates.....	151
4.4. General Procedure for the Grignard Reactions with Weinreb Amides.....	154
4.5. Synthesis of Remaining Single Amino Acid Analogues	158
4.6. Alternative Route to Chloromethyl Ketone	163
4.7. Diazomethane Route to Chloromethyl Ketone	165
4.8. Synthesis of Rhodamine Derivatives	168

4.9. General Protocol for Probe Assembly	170
4.10. Synthesis of Fluoromethyl Ketone.....	180
4.11. Synthesis of Remaining Peptide Probes	184
4.12. Biology Experiments	189
Literature Cited	207

List of Tables

	Page
Table 1: Representative selective electrophiles	5
Table 2: Examples of irreversible kinase inhibitors	10
Table 3: Selection of Known A-Kinase Anchoring Proteins (AKAPs).....	32
Table 4: Selected substrates of PKAC α	35
Table 5: Proteins whose expression is increased or decreased directly by PKA activity	36
Table 6: Fragments of PKI and the corresponding K_i values for PKAC α	47
Table 7: Structure-activity relationship analysis by amino acid substitution	48
Table 8: Sequence alignment of DFG---APE regions of PKA and PKG	49
Table 9: Representative PKI fragments and their corresponding affinity for PKG.....	50
Table 10: PKAC α IC ₅₀ s by Z'LYTE Assay.....	62
Table 11: Summary information of AKT1 and PKAC α inhibition	64
Table 12: Trypsin digest mass spec results.....	122
Table 13: Results of Bradford assay for MCF7 cell lysates	192
Table 14: Results of Bradford assay for MDA-MB-231 cell lysates.....	193
Table 15: Results of Bradford assay for bovine heart lysates.....	194
Table 16: Results of Bradford assay for mouse heart lysates	196

List of Figures

	Page
Figure 1: Major components of an activity-based probe (ABP).....	4
Figure 2: Activity-based probes linker and recognition scaffold containing.....	6
Figure 3: Representative fluorophores and a click handle.....	7
Figure 4: Representative affinity labels and click handle.....	8
Figure 5: Peptide-based inactivators of PKB by a Type IV binding mechanism.....	13
Figure 6: Small molecules use by Taylor et al to inactivate PKA at Cys199.....	14
Figure 7: First designed irreversible peptide-based inactivator of PKA.....	14
Figure 8: Inhibitors used by Shaltiel et al to characterize the active site of PKA.....	15
Figure 9: Peptide-based active site directed affinity labels for PKA by Kaiser et al.....	16
Figure 10: Peptide-based affinity labels for PKA, representatives from Lawrence et al.....	18
Figure 11: Mechanism-based quenched fluorescent probe of PKA.....	19
Figure 12: Adenine base and representative activity-based probes for the kinome.....	24
Figure 13: Major regions interacting with the active-site.....	29
Figure 14: PKI(14-24) 2-D representation of intermolecular interactions with PKAC α	31
Figure 15: Schematic representation of cAMP-dependent activation of PKA.....	34
Figure 16: PKA's role in heart contractility and energy consumption.....	38
Figure 17: Substrate-based probe of PKAC α catalytic activity.....	42
Figure 18: Active-site directed probe with electrophile directed towards Cys343.....	43

Figure 19: Sox residue used for selective detection of Mg ²⁺ binding	44
Figure 20: Distance analysis of relevant alpha carbons to the side chain of Cys199	52
Figure 21: View of critical amino acids in PKI for affinity for PKAC α	54
Figure 22: Close up on Ile22 and proximity to Cys199	56
Figure 23: Synthesis of Boc vinylketone amino acid derivatives	58
Figure 24: Synthesis of Poc vinylketone amino acid derivatives	59
Figure 25: Synthesis of various amino acid—electrophile derivatives	60
Figure 26: PKAC α inhibition graphs	62
Figure 27: AKT1 inhibition	64
Figure 28: Alternative route to glycine chloromethyl ketone	68
Figure 29: Diazomethane route to chloromethyl ketone formation	70
Figure 30: Synthesis of Rhodamine-NHS ester	71
Figure 31: Solid phase synthesis of the pentapeptide	73
Figure 32: Solid phase addition of rhodamine tag and soft cleavage	74
Figure 33: Coupling of the electrophile to 37 to generate 38	76
Figure 34: Coomassie stain of purified recombinant PKAC α	78
Figure 35: Evaluation of 35	79
Figure 36: Examination of Probe 38 with wt PKAC α	81
Figure 37: Examination of A= 38 , B = fluoresceine-maleimide, and C = 35	83
Figure 38: Iterative solid phase synthesis of 39	88
Figure 39: Mixed solid phase and solution phase chemical assembly of 41	90
Figure 40: Protein concentration detection analysis	92
Figure 41: Labeling analysis with wild-type and C199A PKAC α	94

Figure 42: Coomassie and fluorescence image overlap from Figure 42	95
Figure 43: Saturability of labeling	97
Figure 44: Examination of the effects of cysteine oxidation on labeling	99
Figure 45: Analysis of pH effects on labeling	101
Figure 46: Overlap of fluorescence and Coomassie gel images from Figure 46.....	102
Figure 47: PKAC α treated with PDK1 analysis with 41	104
Figure 48: Synthesis of fluoromethyl ketone	106
Figure 49: Production of peptide on resin.....	107
Figure 50: Assembly of Rh-PKI(14-22)-G-(FMK)	109
Figure 51: Examination of labeling on treated PKAC α	112
Figure 52: Agarose gel electrophoresis of PDK1 plasmid and pRSF duet.....	114
Figure 53: Examination of coexpressed PKAC α and PDK1 labeling with 48	116
Figure 54: Saturability of labeling of probe 48	118
Figure 55: Cysteine oxidation effect of labeling by Ellman's reagent	119
Figure 56: Selectivity labeling experiment with wild-type and mutant PKAC α	120
Figure 57: Labeling in the presence of ATP and MgCl ₂	121
Figure 58: Labeling in MCF7 cell lysates.....	123
Figure 59: Examination of MDA-MB-231 lysates with compound 48	125
Figure 60: Examination of bovine heart lysates with compound 48	126
Figure 61: Examination of mouse heart lysates with compound 48	127
Figure 62: Synthesis of Biotin-NHS	130
Figure 63: Synthesis of Biotin-PKI(14-22)-G-(FMK).....	131
Figure 64: Western blot of the pull-down sample with pThr197 antibody.....	132

Figure 65: Western blot of the pull-down sample with streptavidin-HRP	133
Figure 66: Coomassie stain of pull-down sample, major bands highlighted	133
Figure 67: Synthesis of Bioin-Aoc-PKI(14-22)-G-(FMK).....	135
Figure 68: Detection of recombinant PKAC α labeled with 51 and 54	136
Figure 69: Human kinome DFG-APE sequence alignment.....	139
Figure 70: Bradford assay graph for MCF7 lysates.....	192
Figure 71: Bradford assay graph for MDA-MB-231 cell lysates	193
Figure 72: Bradford assay graph for bovine heart lysates	194
Figure 73: Bradford assay graph for mouse heart lysates.....	196

Abstract

DEVELOPMENT OF IRREVERSIBLE SUBSTRATE COMPETITIVE PROBES FOR PKA ACTIVITY

By Robert A. Coover, Ph.D.

A dissertation submitted in partial fulfillment of the requirements for the degree of Doctor of Philosophy at Virginia Commonwealth University.

Virginia Commonwealth University, 2015.

Major Director: Keith C. Ellis Assistant Professor, Department of Medicinal Chemistry

The current environment for drug discovery and disease treatment relies heavily on genomic analysis, structural biology and chemical biology techniques. With the enormous advances in genomic analysis and structural biology, the use of and desire for targeted therapies has increased. However, as more genomic data for cancer disease state pathology becomes available we must ask increasingly difficult questions and even produce new technologies, such as activity-based probes, to answer these questions.

In particular, targeted kinase inhibitors for the treatment of cancer has become a mainstay for drug development for both industry and academia, but it is evident that the genomic data is not always indicative of protein expression. Additionally, protein expression alone does not completely characterize functional activity. Therefore, in order to more accurately validate drug

targets and predict drug efficacy, we must not only identify possible targets but also determine their activity *in vivo*.

The goal of this work was to develop a probe for Protein Kinase A that would act by alkylating a conserved cysteine in the substrate-binding pocket of the enzyme. We hypothesized that by targeting the substrate-binding pocket we could effectively utilize the natural substrate selectivity filters as well as take into account multiple endogenous regulatory mechanisms. We produced probes utilizing portions of the pseudosubstrate inhibitor PKI that demonstrate the ability to label the catalytic subunit of Protein Kinase A in an activity-dependent manner, thus making it an important first step in a new class of activity-based probes for the kinome.

List of Abbreviations

Å – angstrom	Fmoc – 9-Fluorenylmethoxycarbonyl
2-CTC – 2-chlorotrityl chloride resin	g – gram
ABP – activity-based probe	H ₂ – molecular hydrogen
ABPP – activity-based protein profiling	H ₂ O – water
Ac – acetyl	HCl – hydrochloric acid
ACN – Acetonitrile	HOBt – 1-hydroxybenzotriazole
ADP – adenosine diphosphate	IC ₅₀ – concentration of inhibitor required for
atm – atmospheres	50% inhibition
ATP – adenosine triphosphate	M – molarity
Bn – benzyl	L – liter
Boc – tert-butoxycarbonyl	NMM – 4-methylmorpholine
°C – degrees celcius	PKA – Protein Kinase A
cAMP – cyclic adenosine monophosphate	PKA α – the alpha subunit of PKA
DNA – deoxyribose nucleic acid	PKG – Protein Kinase G
DCM – dichloromethane	PyBOP – (benzotriazol-1-
DMF – dimethylformamide	oxy)tripyrrolidinophosphonium
DMSO – dimethyl sulfoxide	hexafluorophosphate
<i>E. coli</i> – Escherichia coli	SDS-Page – Sodium dodecyl sulfate
EDCI – 1-ethyl-3-(3-	polyacrylamide gel electrophoresis
dimethylaminopropyl)carbodiimide	THF - tetrahydrofuran
Et – ethyl	V - volts
EtOAc – ethyl acetate	

Chapter 1: Introduction

1.1: Proteomics

The sequencing of the human genome has yielded a complete image of the possible products of gene expression in the body.¹ As the technology has advanced, sequencing has been increasingly used to characterize disease states with fascinating results. However, the genomic data does not always directly correlate to the phenotype.^{2,3} Which is partly due to the genotype not always being indicative of the cellular environment, especially the post-translational modifications that may occur.² This is particularly true in human malignancies, where multiple genetics mutations may provide phenotypes with increased survival advantages that result from downstream effects.⁴

In general, the field of proteomics seeks to determine actual protein amounts and general characteristics of the phenotype.⁵ Proteomic data can be acquired in a multitude of ways, ranging from qualitative to quantitative analysis.^{6,7} Important tools and technologies available for proteomic analysis are continuously improved upon and invented. However, some mainstay technologies and techniques are: molecular probes, gel electrophoresis, chromatography, mass spectrometry, and immunochemistry. It is only through the appropriate execution of these experiments and expert interpretation that the data obtained gains significant value.

Proteomics has influenced oncology for many decades, with examples dating back to the early twentieth century where researchers analyzed blood plasma by gel electrophoresis to link increased protein expression with the cancer phenotype.⁸ Since early publication such as this, proteomics has been utilized in various ways to delineate the cancer disease state.^{8,9} While this information is very useful, it does not have the level of detail required to link protein activity with expression. This disconnect has provided a new frontier for characterizing phenotypic

function in diseased states thus expanding traditional proteomics to include a new area known as chemical proteomics.¹⁰

1.2: Chemical Proteomics

In the field of proteomics, the gap of data between protein levels and functions has formed a specialized application. That is, activity-based proteomics, or chemical proteomics. Activity-based proteomics utilizes small molecules, known as activity-based probes (ABPs), to selectively react with a residue only in the active form of an enzyme.¹¹⁻¹³ This selective reactivity enables tagging of enzymes exclusively in their active state for analysis. This direct measurement technique allows the quantification of aberrantly active enzymes and can help to identify novel drug targets, inhibitors, and relevant pathways. Clarifying the relationship of expression and activity is the major task of activity-based proteomics, the process of conducting such experiments with an ABP is known as activity-based protein profiling (ABPP).¹⁴⁻¹⁷

1.2.1: Activity-Based Probes

To conduct ABPP, an activity-based probe must be developed, and there are many criteria and factors to consider. Activity based probes (ABPs) must be covalent inhibitors and selective for the active form of the enzyme. For different classes of enzyme, there are different approaches to achieve this type of selectivity.¹⁸⁻²¹ Identifying a mechanism of action that will allow a probe to label in an activity-dependent manner is the first step. With some enzyme classes, this challenge is more obvious than with others. The cysteine proteases, for example, have a nucleophilic cysteine in the active-site that is critical for activity. This active site not only serves as an important location to target, but by its nature will yield an inhibitor that behaves in an activity dependent manner.²⁰ In general, kinases do not utilize a nucleophilic amino acid for phosphoryl transfer, this in turn provides a challenge for developing an activity-based probe. The

few examples of known ABPs in the kinome target a cysteine that is found in the ATP-binding pocket. While these cysteines do not directly participate in catalysis, their alkylation causes inhibition of the enzyme. It is also suggested that by binding in the nucleotide binding site they are acting in an activity-dependent manner. While this approach has proved valuable for developing ABPs and irreversible inhibitors for a number of kinases, the bulk of the kinome remains without such probes.¹⁷ This is in part due to the conservation of nucleotide binding pockets across not only the kinome but the entire proteome. Therefore, we set out to develop a new strategy to target kinases in an activity-dependent manner that does not rely on targeting the ATP-binding site (see Chapter 3).

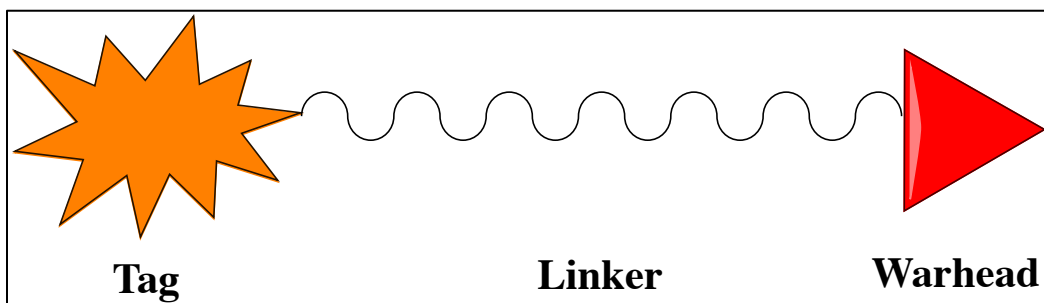
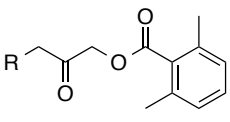
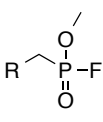
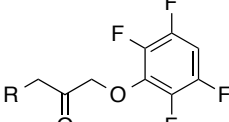
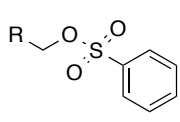
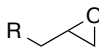
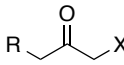
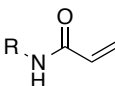
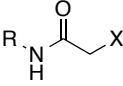
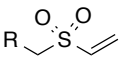
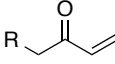
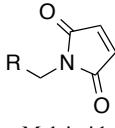
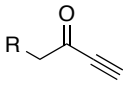


Figure 1: Major components of an activity-based probe (ABP).

ABPs consist of three major components (Figure 1). First, there is a reactive moiety (electrophile) i.e., warhead, for selective covalent modification of the desired residue. These electrophiles can range from moieties geared towards specific side chains containing nitrogen, sulfur, or oxygen to actual substrates that become covalently attached when the enzyme acts upon it (Table 1). Selection of the electrophile is an important decision when designing a probe. Some of the major considerations one should factor is whether their goal is to produce a family selective or a target selective probe. If the goal is to develop a family selective probe, the warhead is selected solely on selective reactivity. The acyloxymethylketone (AOMK) moiety is a

prime example of a reactive moiety being selected to produce a family selective ABP. It is a very selective electrophile, and inherently only weakly electrophilic. Only by placement in close proximity to the nucleophilic residue does the reaction occur (in biological systems). The halomethylketone moieties have seen widespread application, their reactivity can be attenuated significantly by the leaving group halogen. Iodomethyl ketone for example is not an ideal electrophile for developing a selective ABP because it is very reactive towards cysteine (and other nucleophilic residues). However, iodomethyl ketone has been appended onto a generic scaffold and used in conjunction with click chemistry to characterize the cysteinome. Similarly, the bromomethyl ketone is generally too reactive for the development of a selective ABP. The chloromethyl ketone can be utilized in a variety of different applications. For instance, chloromethyl ketones are a primary ingredient in protease inhibitor cocktails. In contrast to the iodo- bromo- and chloromethyl ketone is the fluoromethyl ketone which has a significantly reduced reactivity profile.

Table 1: Representative selective electrophiles

 <p>Acyloxymethylketone</p>	 <p>Fluorophosphonate</p>	 <p>Phenoxyethylketone</p>	 <p>Sulfonate-ester</p>
 <p>Epoxide</p>	 <p>Halomethylketone</p>	 <p>Acrylamide</p>	 <p>Chloro/Iodoacetamides</p>
 <p>Methylvinylsulfone</p>	 <p>Vinylketone</p>	 <p>Maleimide</p>	 <p>Propargyl Ketone</p>

Second, there must be a linker, or recognition sequence, to connect the warhead and tag. The difference between the two can be reduced to whether your probe is selective for a family of proteins or a single target. In general, a generic hydrocarbon linker is chosen when the purpose is to develop a family selective ABP (Figure 2, FP-biotin). With a linker the most important variables are length and desired physical properties (if required for solubility/cell permeability). The recognition sequence provides the greatest selectivity as it serves as the primary scaffold and can have the greatest variability and this is utilized when the desired outcome is a target selective ABP (Figure 2, fmk-pa).¹⁰ The scaffold can and should be optimized to have greater affinity and selectivity than a simple linker.²² Common examples of recognition sequences include small molecules, peptide substrate sequences (proteases), and adenosine triphosphate (ATP) analogues (kinases).

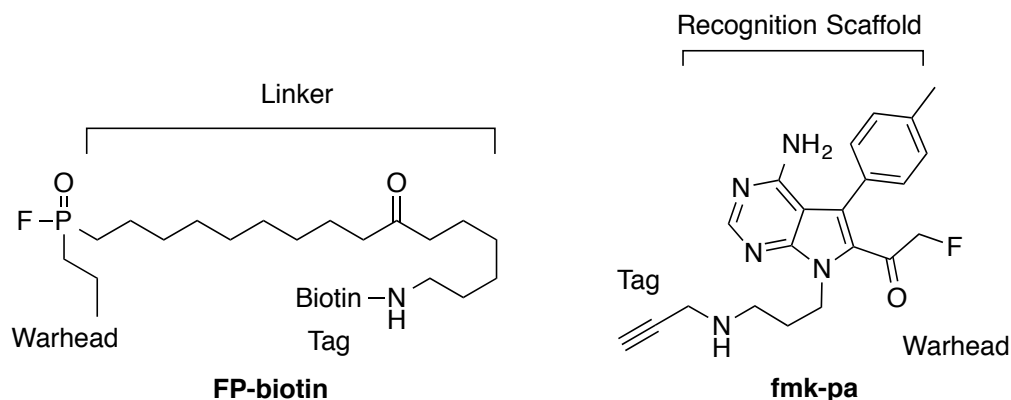


Figure 2: Activity-based probes with different linker styles, family and target selective.

The final requirement is a detectable tag for quantification. Selection of a tag is generally limited to fluorescent, affinity, and click based tags (Figure 3, 4). There are many fluorescent options available and are quite often dependent on the selected system. For example, when examining isolated proteins or lysates by gel electrophoresis, one does not need to consider cell permeability or background fluorescence. In such a case, generic rhodamine or rhodamine derivative is acceptable. However, if the probe is destined for use *in vivo*, a fluorophore such as BODIPY should be considered due to its physical properties allowing for cell permeability. Additional probes with varying absorption and emission properties are commercially available, allowing a researcher to select Stoke shift values, wavelengths, and quantum yields. Having appropriately tailored fluororophores is particularly important when FRET based applications are to be considered.

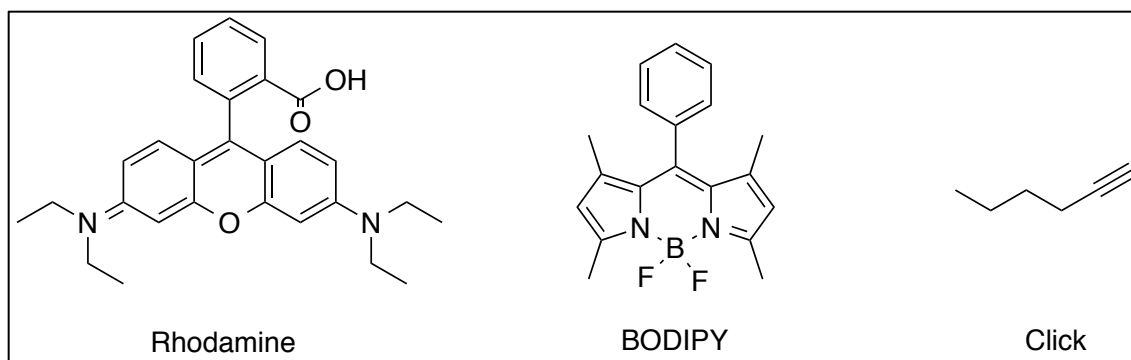


Figure 3. Representative fluorophores and a click handle.

Affinity tags can also vary greatly. Deciding on an affinity tag relies heavily on the application. For small molecule/probe development, biotin is the most commonly used affinity handle (Figure 4). This is due to its favorable size and known high affinity for streptavidin. Biotin is also easily appended onto a peptide or small molecule by simple chemical transformations and its solubility can be attenuated for different labeling applications. Other affinity tags may take the form as short peptides and quite often are used on the target itself and not the probe: histidine (His tag), Myc tag, human influenza hemagglutinin (HA tag), and etc. (see Figure 4). These may be appended by chemical or biological methods and offer high selectivity; however, size/steric bulk becomes an issue when attempting to use the peptide-based affinity tags.

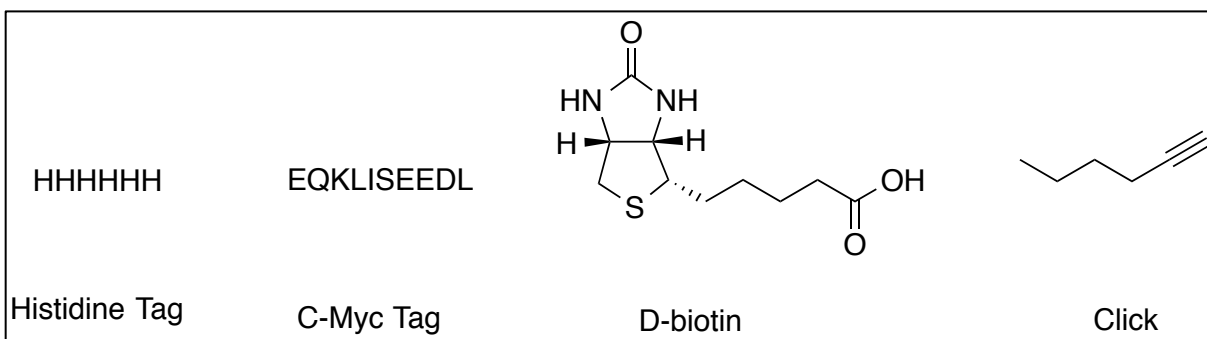


Figure 4: Representative affinity labels and click handle.

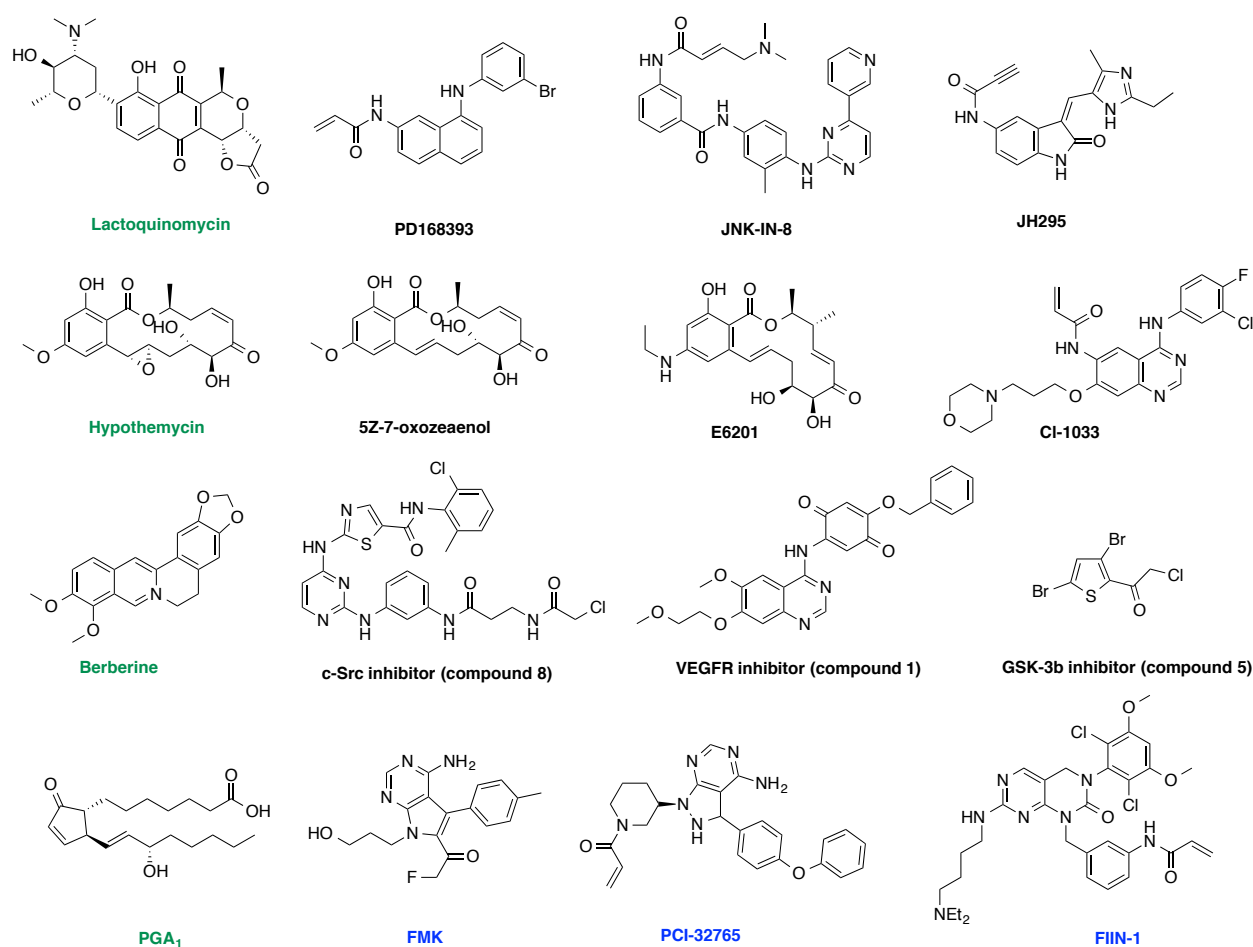
1.3: Irreversible Inhibitors of the Kinome

The beginnings of an activity-based probe lay within the development of irreversible inhibitors. The development of selective irreversible inhibitors is a critical first step in the production of an activity-based probe, because one of the requirements for ABPP is that the ABP be irreversible. The kinome is one of the most numerous and varied class of enzymes found in nature. Kinases catalyze the transfer of a phosphate group from a nucleotide to a substrate. This post-translational modification has significant effects on cell signaling, phenotype, and disease state. This central role to the basic foundations of life have caused many kinases to be the center of drug discovery efforts.¹⁷ The vast majority of kinase inhibitors are competitive inhibitors of the ATP-binding pocket, which is highly conserved.²³ Because of this conserved binding site and mechanism of action by the inhibitors, off-target activity is always a consideration. There is a concerted effort to develop selective inhibitors by capitalizing on different mechanisms of action for inhibition. Of particular interest is the focus on the irreversible targeting of cysteines in the kinome.

Targeting cysteines for the regulation of kinase activity has long been used, if not well understood. Numerous examples exist dating back long before their binding mechanisms were

fully developed. These range from allosteric to orthosteric cysteine alkylating compounds. The solution of many crystal structures has enabled a structure-based design push for selective kinase inhibitors. The interest in irreversible kinase inhibitors has increased, and the most prevalent approach in the literature utilizing a nucleophilic cysteine is a strategy that targets the ATP-binding site (Table 2). Through the use of multiple selectivity filters, residue binding interactions, gatekeeper interactions, and location of the target cysteines, a significant number of irreversible inhibitors for the kinome, many with clinical relevance, have been produced. Indeed, many screening platforms have been developed to determine off-target activity/selectivity for the kinome. However, the development of selective kinase inhibitors has only been completed for a small fraction of the kinome.

Table 2: Examples of irreversible kinase inhibitors (green are natural products, blue have been further developed into ABPs, and black are generic Type I irreversible inhibitors).



The prevailing strategy for the development of irreversible kinase inhibitors is producing a number of Type I inhibitors. Many reversible inhibitors that bind in the ATP-binding pocket with a known cysteine in close proximity have been altered with medicinal chemistry techniques to produce irreversible inhibitors. This successful approach has resulted in major efforts to develop new strategies for producing irreversible kinase inhibitors. The current set of cysteines being *actively* targeted reside in four distinct positions within the ATP-binding pocket: roof

region, DFG region, glycine-rich loop region, and the hinge binding region. Each of these regions has examples of being targeted by irreversible kinase inhibitors; however, some are more effective than others. This set of irreversible kinase inhibitors that bind exclusively to the ATP-binding pocket, and are competitive with ATP, are known as Type I binding inhibitors.

Diverse examples exist in the literature of type I cysteine modifying inhibitors of the kinome that target each of the four cysteines. Dual specificity mitogen-activated protein kinase 7 (MAP2K7) is involved in mitochondrial cell death and its inhibition has been of interest. The inhibitor 5Z-7-Oxozeaenol (5Z7O, Table 2) has been demonstrated to inhibit MAP2K7 in a Type I binding mechanism by crystallography and shown to alkylate Cys218, which is located at the outskirts of the hinge region.²⁴ It was also pointed out that there are 11 such similar cysteines in the kinome, i.e., this conserved cysteine is also targeted by EGFR, Nek2, KDR, IKKb, ITX, BMX, JMK1-3, and BTK inhibitors.²⁵ A cysteine located in the β -strand (DFG region) is targeted by the activity-based probe “FMK” for the kinase RSK.²⁶ Similar cysteines in the β -strand have been targeted effectively against TAK1, ERK2, GSK3b, and MEK1.²⁷⁻²⁹ Cysteines located in the glycine-rich loop region have been effectively targeted against FGFR1-4 and have been the subject of ABPP.^{30,31} A cysteine identified in the roof region has been targeted in Her2 and has shown increased efficacy over reversible inhibitors. This strategy has thus far proven effective at producing efficacious kinase inhibitors with the potential for turning into ABPs.¹⁷ However, selectivity does continue to be an issue that requires additional binding interactions to address.²⁵

Much effort has since been put forth to develop Type II inhibitors. Type II inhibitors also bind to the ATP-binding pocket and take advantage of the DFG-out configuration. It has been demonstrated that, by utilizing the additional binding interactions from the DFG-out

configuration as a selectivity filter, increased-kinome wide selectivity can be achieved.²⁸ This approach has also found applications in the production of irreversible kinase inhibitors, as Type II inhibitors have been altered with medicinal chemistry techniques to produce cysteine alkylating Type II inhibitors.²⁸ These representative examples have produced highly selective and efficacious inhibitors but their application to the kinome is limited and certainly would not be applicable as an ABP, as the DFG-out configuration is inactive. Targeting other cysteines outside of the ATP-binding pocket would provide a route to produce inhibitors with access to more kinases. Type III inhibitors (allosteric inhibitors) have had sporadic success as reversible inhibitors, and few examples (if any) exist that conclusively display irreversible inhibition that is also saturable.³²

Substrate competitive, or type IV binding, irreversible inhibitors are becoming more prominent, as it is suggested that the natural selectivity filters involved with the substrate-binding site will provide similarly increased selectivity in complex biological mixtures.³³ Many examples exist and a predominant case is with Protein Kinase B (PKB, or AKT). AKT has been the subject of numerous inhibition studies for various disease implications, most notably cancer. AKT1 has a number of solvent exposed cysteine residues that when alkylated modulate activity, most notably Cys310 in the substrate-binding site, specifically the activation loop (or T-loop). This particular cysteine has been demonstrated to be alkylated by peptidomimetic compounds (TPCK, Boc-Phe-VK), and natural products (lactoquinomycin, wortmanin, and berberine); upon alkylation, inhibition of catalytic activity is resultant.³⁴⁻³⁶

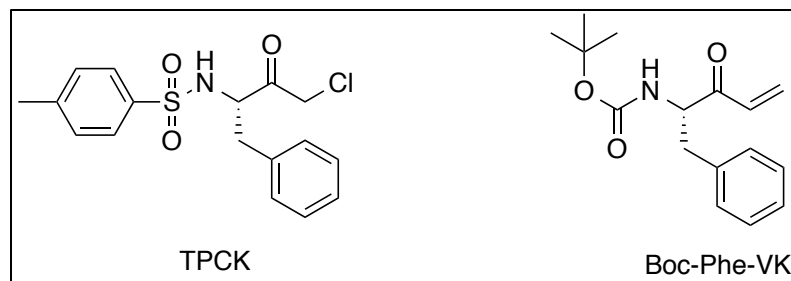


Figure 5: Peptide-based inactivators of PKB by a Type IV binding mechanism.

Protein Kinase A (PKA, or cAMP-dependent protein kinase) is the prototype kinase and has been the first in many regards for various studies and is the target of this thesis. The pathway to the development of an ABP goes through irreversible inhibitor design, and a thorough knowledge of the available data on irreversible inhibition of your target is required to avoid repetitious results therefore a brief overview of Type IV inhibitors of the prototype kinase is below.

Protein Kinase A (PKA) is the prototype kinase with two cysteine residues that have been thoroughly investigated throughout the years, and one in particular has been shown to modulate catalytic activity: Cys199.³⁷⁻⁴¹ Cys199 is located in the substrate-binding pocket, specifically the activation loop (T-loop) and alkylating or oxidizing this residue inhibits catalytic activity.^{42,43} Cys199 has been shown to be nucleophilic and react with a variety of different electrophiles and inhibitors. Taylor and colleagues demonstrated that oxidation at Cys199 by glutathione was an endogenous regulatory mechanism.³⁷ Additionally, in separate studies conducted by Taylor, Cys199 was alkylated by Michael acceptors, sulfhydryl moieties, and halomethyl ketones (Figure 6).⁴⁴⁻⁴⁶ More early (1982) work by Taylor and colleagues, produced a peptide based affinity probe that formed a disulfide bond with Cys199; this probe contained the sequence LRRACLG with the cysteine oxidized with Npys so that it will selectively oxidize Cys199 (Figure 7).⁴⁴

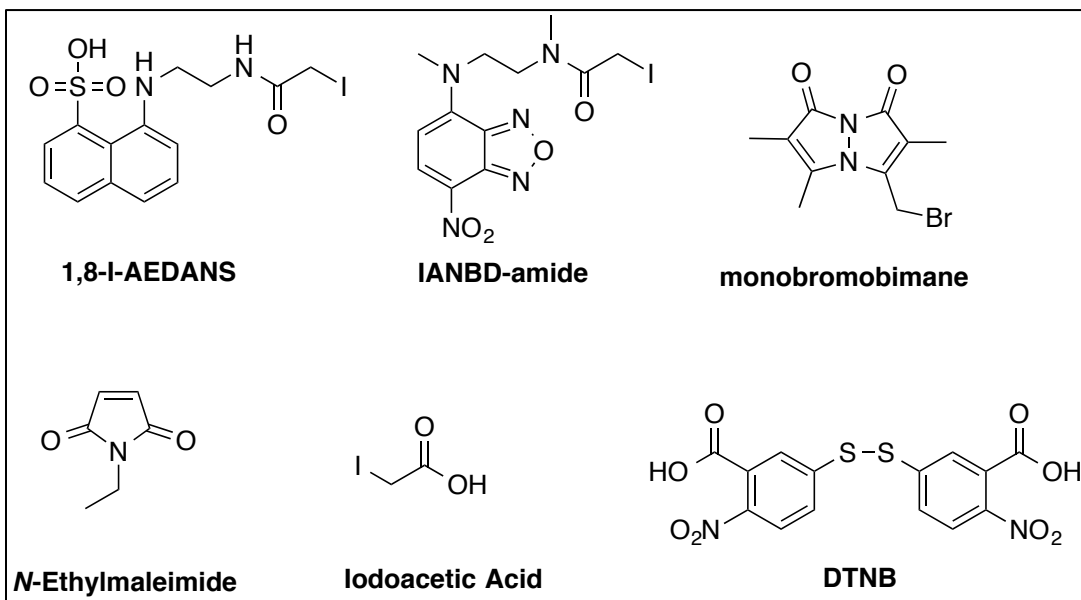


Figure 6: Small molecules used by Taylor et al to inactivate PKA at Cys199.

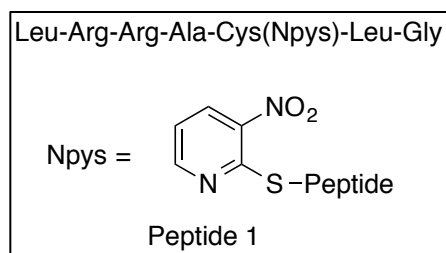


Figure 7: First designed irreversible peptide-based inactivator of PKA

A number of other groups have also taken advantage of the substrate-binding pocket and the nucleophilic cysteine located in the activation loop. Shaltiel and colleagues used a combination of known amino acid substrate sequences to hypothesize that: 1) both a basic and hydrophobic moiety, 2) or only the basic moiety were important recognition elements, and that by producing these one would develop an active site directed labeling compound.⁴⁷ They examined the inhibitory effects of *N*^α-tosyl-L-lysine chloromethyl ketone (TLCK) and *N*^α-tosyl-L-phenylalanine chloromethyl ketone (TPCK) to test this hypothesis (Figure 8). It was

determined that both labeled Cys199 and inactivated PKA α by this mechanism, and reagents such as chloroacetamide and chloroacetic acid did not. This was important early work in characterizing not only the promiscuity of previously thought to be selective trypsin and chymotrypsin inhibitors, but in mapping the active site of PKA. It is important to note however, that their labeling was greatly affected by their simulated biological conditions. Specifically, it was noted that when MgATP was added to their labeling conditions, inactivation of PKA α was prevented.⁴⁷ In another publication it was demonstrated that this could be an additional regulatory mechanism in which substrate specificity is altered by the immediate environment of the cell (a type of reversible spatial regulation). Finally, the reactivity of the sulfhydryl groups in response to these stimuli was determined, and it was indeed affected greatly.⁴⁸

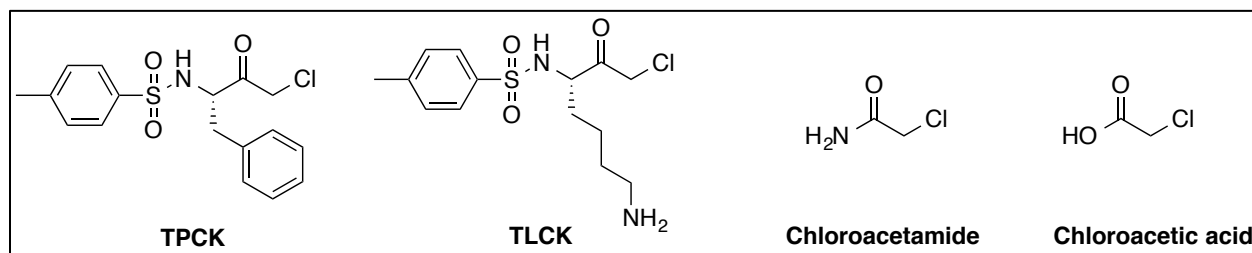


Figure 8: Inhibitors used by Shaltiel et al to characterize the active site of PKA.

E. T. Kaiser (1938-1988) also pioneered significant early work with PKA and produced multiple publications in the development of active site (Type IV) directed affinity labels for PKA α (Figure 9). Kaiser's work centered on peptide based affinity labels. He coauthored with Taylor the 1982 paper that detailed disulfide bond mechanism based peptide affinity labels.⁴⁴ They went on to further examine the substrate-binding pocket by synthesizing a number of subsequent peptide based affinity labels incorporating bromoacetamides and chloroacetamides in addition to the oxidized cysteine residues used to form the disulfide at Cys199. However, only

the bromoacetamides showed any labeling activity. Their radiolabeled probes and trypsin digestion experiments help form early models of the substrate-binding site (prior to crystal structure). They hypothesized that the conserved nature of this cysteine among known kinases (considerably fewer at the time), would provide a general strategy to develop affinity labels that work by a similar mechanism to determine active site sequences.⁴⁹ Kaiser and Miller also produced a peptide based photoaffinity label that produced similar results when used to discover the residues responsible for substrate recognition.⁵⁰ Further they characterized a small library of their peptide based covalent inactivators and known ones (the disulfide forming compounds explored previously, Figure 9). Their results were particularly noteworthy in light of what we now know in that, in addition to them further demonstrating the amino acids that play a role in substrate recognition, their probes were prevented from covalent labeling in the presence of physiologically relevant concentrations of MgATP.⁵¹

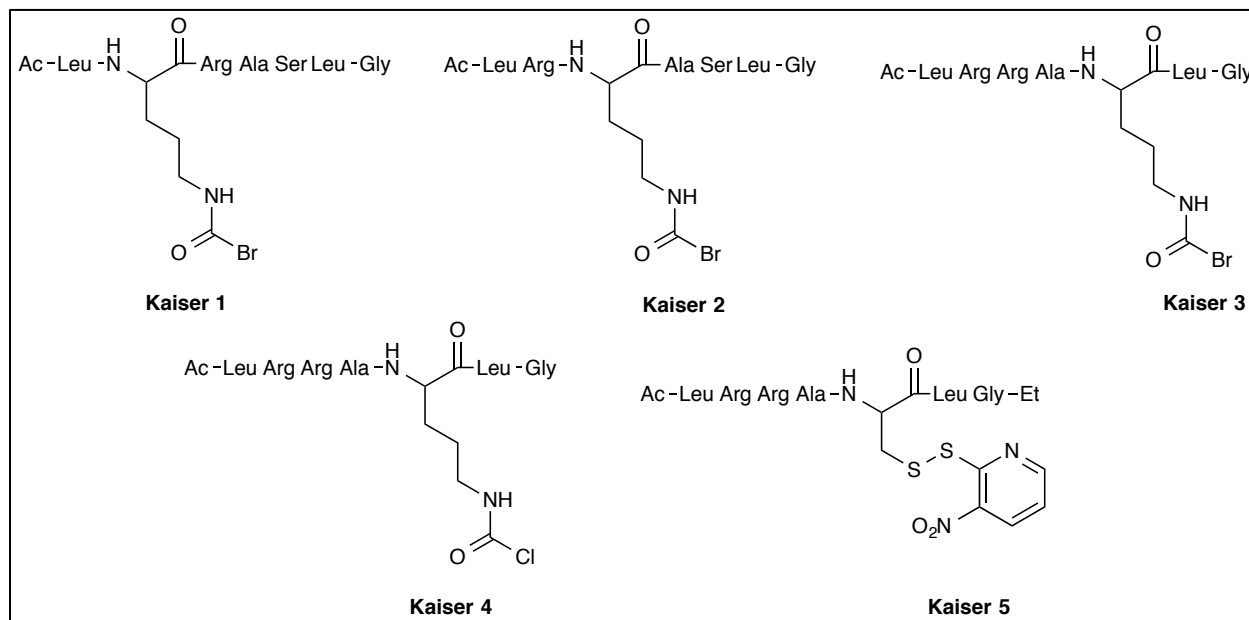


Figure 9: Peptide-based active site directed affinity labels for PKA by Kaiser et al.

Contemporary to the work of Kaiser et al., two other groups produced Type IV irreversible inhibitor studies. Glass and colleagues produced a photoaffinity labeling peptide based on the PKI(6-22) scaffold and show that it does label the catalytic subunit of PKA. They cite “soon to be published” work in complex biological mixtures, but that work was never published.⁵² A group at Louisiana State University published a study detailing the fluorescent affinity labeling of the catalytic subunit with a small molecule. They propose a novel mechanism of action in that their small molecule reacts with two residues, lysine-72 and cysteine-199, by forming an isoindole derivative with PKA α .⁵³ However, in a simultaneous publication they note the similar mechanism and inhibitory activity against Protein Kinase G (cGMP-dependent protein kinase, or PKG).⁵⁴

Lawrence and colleagues attempted similar affinity labels with the aid of the now available kinase crystal structures, and the ability to express recombinant PKA α (previous groups had been using purchased or isolated mammalian proteins from various mammalian sources). They essentially demonstrated the structure-based design principle of our approach by synthesizing multiple affinity probes and performing substrate analysis. Early work was focused on appending an oxidized cysteine at the C-terminal end of a peptide inhibitor to selectively oxidize Cys199 (Figure 10). These peptides were effective at inhibiting PKA α by reacting specifically with Cys199. Interestingly, ATP blocked labeling of their peptide probes as well, lending support to the hypothesis that there is a conformational change of the cysteine in the presence of a nucleotide.⁵⁵ They state that they were continuing structure-activity relationship studies on these series of peptides but nothing has been published with them since (although a different strategy was used in 2011 and is discussed in chapter 2). They do note, however, that in addition to labeling Cys199 they also labeled a similar cysteine in Protein Kinase G, PKG.⁵⁶

Selectivity between the two similar kinases was not achieved at first but they were able to tune for PKG over PKA in a later paper.^{55,57} However, they moved into methods to detect PKA activity while not inhibiting and will be discussed in chapter 2, methods to detect PKA activity.

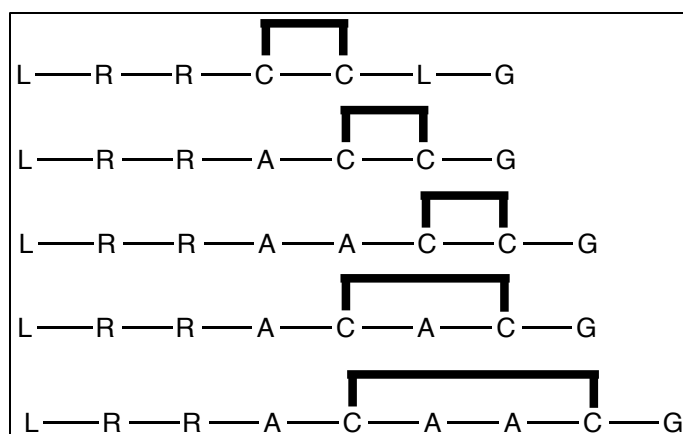


Figure 10: Peptide-based affinity labels for PKA, representative peptides from Lawrence et al.

A contemporary example of peptide-based affinity labels that target the Cys199 of PKA α in the activation loop comes from Tung et al. They utilize a mechanism-based inactivation method that effectively is silent until it labels the free catalytic subunit of PKA (Figure 11).⁵⁸ This example is particularly interesting in that the probe was designed to remain quenched until reacting with PKA α , effectively only reporting the amount of catalytic subunit not bound to regulatory subunits or inhibited by any other substrate competitive mechanism. Tung et al examine their probe in various conditions to display selectivity in biological mixtures and quantitate levels of the protein in various ways with the hypothesis that this could be used to

detect PKA levels in cancer patients. The mechanism and lead compound are shown below in Figure 11. The researchers did not however publish data concerning the protective effects of ATP (or lack thereof) against their probe.⁵⁸

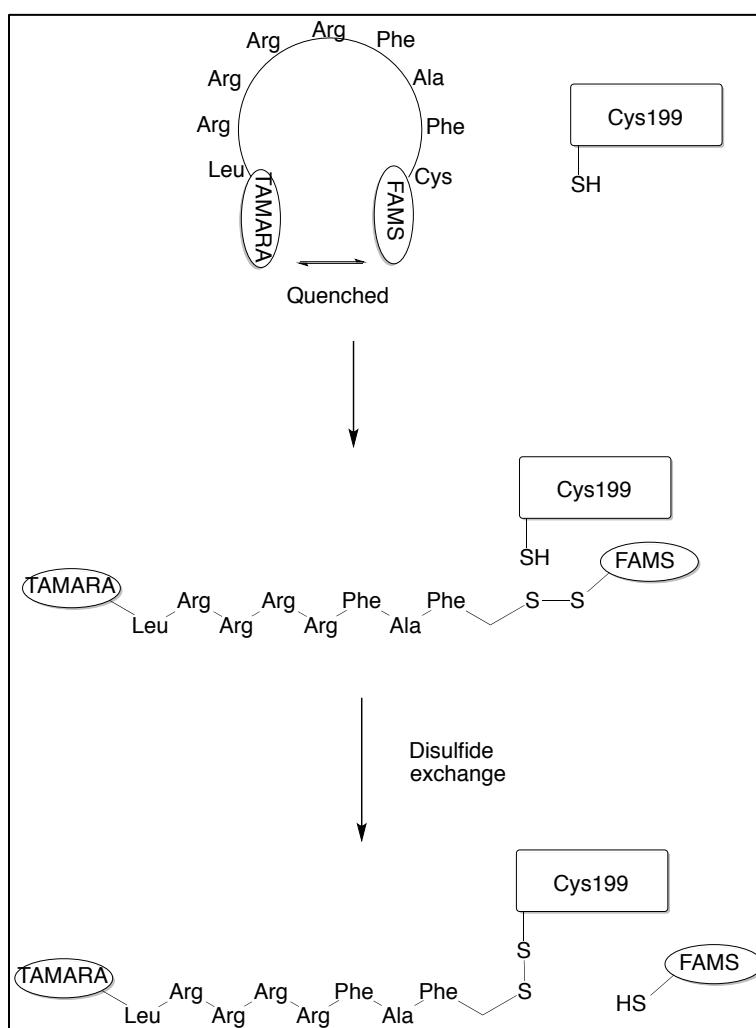


Figure 11: Mechanism-based quenched fluorescent probe of PKA

1.3: Activity-Based Protein Profiling

Genomic analysis relies almost exclusively on manipulating gene expression (RNA-interference, knock-out/down, etc.) in order to determine a protein's function and importance in a disease state. This approach is usually coupled with a generic proteomics approach (mass spectrometry, blotting techniques etc.) to correlate protein levels with genomic analysis. Activity-based protein profiling (ABPP) has arisen out of a necessity to determine, in addition to total protein amounts (proteomics), protein function in complex biological mixtures.^{15,59} The successful design and implementation of a covalent ABP is a critical step to begin the process of characterizing the active site, and activity (not always the same) of specific proteins and/or families of proteins (discussed in section 1.2).

1.3.2: ABPP Applications

ABPP applications include, but are not limited to, molecular target identification, drug discovery, off-target analysis, and active site characterization.^{14,15,60} Molecular target identification is dominated by gel electrophoresis ABPP techniques.¹⁵ Healthy and disease state samples are compared for aberrantly active (or inactivated) protein levels. The resulting differences can be attributed to the disease state and warrants further examination.^{15,61} Drug discovery efforts can be enhanced with an ABP.⁶² By competition with potential drug candidates, a subsequent decrease in probe labeling is noted and can be interpreted in a number of different ways. Additionally, if a family selective ABP is being utilized, off-target binding analyses can be conducted by this competitive labeling experiment.^{18,20} By serendipity an ABP may identify a novel protein that shares the mechanism of action of the target enzyme. This can enable the identification and subsequent classification of new or old proteins with previously unknown function(s).^{15,20}

1.3.3: Historical Perspective of ABPP Development

ABPP at its onset was primarily focused on protease and protease-like enzyme families.^{11,18,21} This is due to the catalytic mechanism of these enzymes being well defined which allows for a more straight-forward probe design. The serine hydrolases have seen significant progress in ABP development and implementation in ABPP. Serine hydrolases encompass a number of different proteins, which include lipases, proteases, esterases, and peptidases. Despite the differing substrate specificity, the diverse proteins converge on a shared active site mechanism of action. This catalytic mechanism utilizes a serine residue that is made nucleophilic in the active site for subsequent attack on the carbonyl carbon of the substrate to form a tetrahedral intermediate. Water then hydrolyzes the following acyl-enzyme intermediate to regenerate the serine and eject the product. Targeting the transition state of an enzyme is an effective strategy to produce inhibitors. The fluorophosphonate, and aryl phosphonate electrophiles have been shown to be effective reactive moieties for ABPP of the serine hydrolases.^{18,63-67}

An effective example of ABPP applied to the serine hydrolases is from the Jessani group using the phosphonate electrophiles as transition state mimetics that also form a covalent bond. Their work led to the identification of the integral membrane protein KIA1361 as an important biological target in aggressive cancers.⁶⁸ These probes have been conclusively demonstrated to selectively react with the active form of the enzyme and not physiologically relevant inactive forms; this makes them effective tools for ABPP. Certain other groups have developed similar probes and have used them extensively in ABPP applications that examine the cancer phenotype.^{15,69}

In a similar setting, the cysteine proteases have garnered remarkable success in ABP development and applications in ABPP.^{13,19,20} However, the subtle differences in the active site, the differing mechanism of action, the nature of the nucleophile (serine OH as compared to the cysteine SH), and hard-soft acid base interactions allow for orthogonal targeting by electrophiles. Of particular interest is the fluorophosphonate electrophile: it does not inactivate the cysteine proteases. Many other cysteine selective electrophiles do covalently label the cysteine proteases with varying efficiency and selectivity. The acyloxymethyl ketone (AOMK) electrophile synthesis and application has been optimized and tailored to the cysteine protease family.²⁰ AOMK has also demonstrated intrinsic selectivity for the cysteine proteases while generally not reacting with less potent nucleophiles.⁷⁰ The solid phase synthesis of AOMK containing peptides/small molecules has been disclosed and has since spurred a large increase in ABPP of the cysteine proteases.^{19,20}

Many more enzyme classes have been targeted with varying degrees of success; however, as our understanding of enzyme catalysis and active site dynamics increases, so has the pool of potential targets for ABP development increased.^{17,71,72} Not only can we target new catalytic mechanisms but new classes of enzymes. It is indeed important that more ABPs be developed to target and characterize more disease states. The kinome has proved a bountiful source of therapeutic targets but has mostly evaded wide spread irreversible inhibitor development and thus the potential for ABP development.^{17,23}

1.3.4: ABPP and the Kinome

There is a current need for ABPs for the kinome. Many kinases are implicated in various disease states, however their immediate function is difficult to elucidate without such probes.^{59,73-}

⁷⁵ Currently there are few examples of selective kinase activity-based probes that target RSK,

BTK, and FGFR (Figure 12),^{26,31,76,77} all of which target the conserved cysteine in the nucleotide-binding site.¹⁷ There are also examples of non-selective ABPs, where, simply put, a known irreversible inhibitor has been outfitted with a tag and electrophile.⁷⁸ While these approaches have yielded successful ABPs, there are many kinases with a cysteine in the ATP-binding pocket (approximately 200), and the ATP-binding site is conserved among many enzymes and enzyme classes.^{26,73} This has made it difficult to achieve the level of selectivity required for selective enzyme activity-based protein profiling (ABPP) since more proteins than those in the kinome utilize ATP; a significant portion of the proteome has a nucleotide binding site.¹⁷

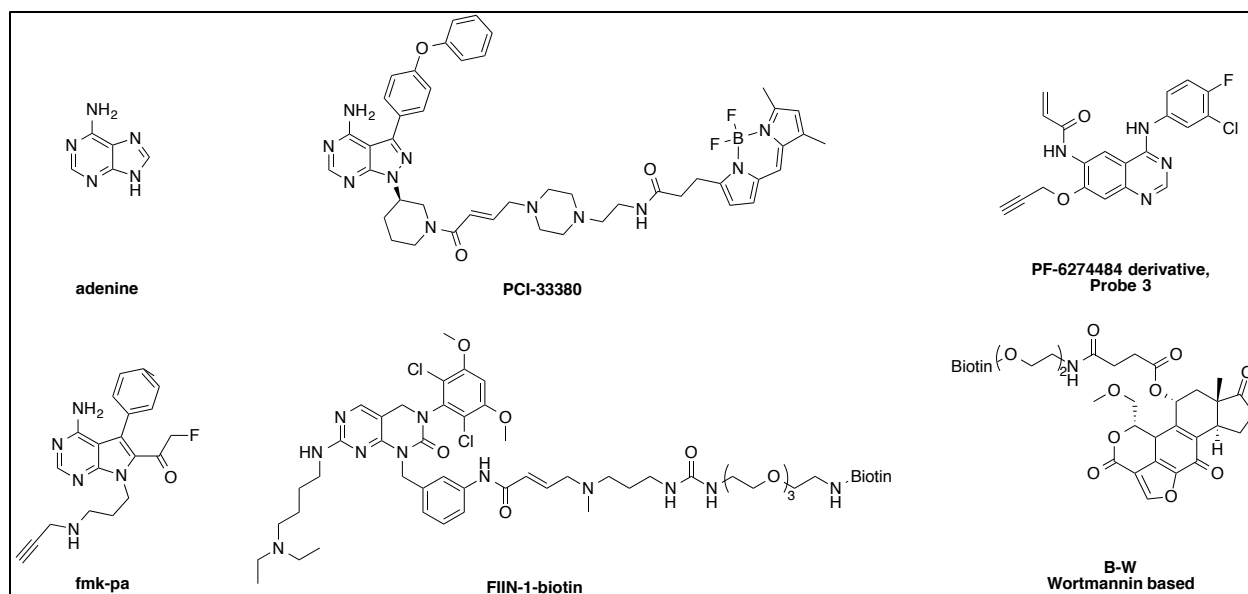


Figure 12: Adenine base and representative activity-based probes for the kinome.

It is generally assumed that if Type I inhibitors, ATP-competitive, can bind to a kinase nucleotide binding site, it is in its active conformation and therefore with the appropriate placement of a tag can be an ABP.^{17,59,60,71} As a result, the ABPs available for the kinases rely on this mechanism of action to inactivate in an activity-dependent manner. There have been a number of examples of how one might discover irreversible inhibitors that behave in this manner, and while they may produce ABPs Type I in nature, they are unable to, or currently are not being used to, examine other mechanisms of action.⁷³

There is another binding site that has similar activity dynamics in the kinome, and in some cases is more sensitive to active site dynamics; this site is the substrate-binding site.³³ In addition to providing the scaffold for proper orientation of a substrate for phosphoryl transfer, the substrate-binding site is sensitive to many post-translational modifications that do not always affect the nucleotide binding site. For example, PKAC α is regulated by an endogenous inhibitor peptide that does not prevent binding of ATP; therefore, a (theoretical) Type I ABP would not account for such a regulatory mechanism. To date, there currently is no other general strategy to

develop, or singular example of, an ABP that does not rely on an ATP competitive mechanism in the kinome. Therefore, the development of a general strategy to produce ABPs for the kinome that relies on the substrate-binding site would have significant impact on the field.

1.4: General Hypothesis

The above is the summary knowledge gained towards the development of Type IV covalent inactivators of PKA α and their applications. Using this and the vast literature on PKA (see chapter 2), we hypothesize that an activity-based probe can be effectively developed for the prototype kinase that utilizes a binding pocket other than the ATP-binding pocket. But utilizing a high affinity pseudosubstrate peptide with a known binding site (active-site directed) and mechanism of action, we can effectively target Cys199 of PKA in an irreversible and selective manner to produce an activity-based probe for activity-based protein profiling. We additionally suggest that this approach can be generalized, by nature of its application to the prototype kinase and existence of similar cysteines in other kinases, for activity-based protein profiling of the kinome. This hypothesis was tested by synthesizing a number of peptidomimetic compounds based on a structure-based design approach and their mechanism of action was investigated by both various inhibition and gel electrophoresis assays (see section 3.12).

Chapter 2: cAMP-Dependent Protein Kinase

2.1: cAMP-dependent Protein Kinase

Phosphorylation is an important regulatory post-translational modification in eukaryotes. Phosphorylation is often responsible for regulating the dynamics of the cellular environment; at the same time it is often reversible by enzymes known as phosphatases. Phosphorylation is the transfer of a phosphate group to a substrate. Enzymatic proteins that catalyze the transfer of a phosphate group are known as kinases. Common substrates include serine, threonine, and tyrosine. Eukaryotic protein kinases (EPKs) make up a superfamily of homologous proteins. The EPK homology region is defined by the catalytic (or kinase) domain; this domain is approximately 250 amino acids. The catalytic domain is responsible for the catalytic activity and is where the phospho transfer takes place. Kinases generally utilize ATP or GTP as their phosphate source and catalyze the transfer of the terminal gamma phosphate to the substrate.⁷⁹ The phosphate transfer process can be viewed as a general three-step mechanism. The first two of which are not necessarily in this order: 1) the nucleotide binds to the nucleotide binding pocket of the catalytic domain; 2) a substrate binds in the substrate-binding pocket of the catalytic domain; 3) there is a transfer of the gamma-phosphate to the substrate.⁷⁹ The first two steps may not necessarily occur in that sequence and may occur in a different sequence *in vivo*.^{80,81} It was previously believed that a divalent cation, such as Mg^{2+} , was required for the phosphate transfer step. This has recently been shown to not be the case in terms of phosphate transfer alone (for PKA α), the divalent cation plays a larger role in release of ADP which is the rate limiting step in catalysis turnover.⁸⁰ Taylor and colleagues have demonstrated phosphoryl transfer in the absence of divalent metal cations.⁸⁰

The kinase superfamily is referred to as the kinome and accounts for ~2% of the human genome. The kinases are broken up into eight broad classes based on the homology of their catalytic domains: AGC; CAMK; CMGC; TK; TKL; STE; RGC; and CK1. PKA is a member of the AGC kinase family, the AGC kinases are serine/threonine specific kinases. Because the cAMP-dependent protein kinase (PKA) was the first crystallized, and its core residues (40-300) are highly conserved, it is the prototype kinase.⁸² PKA is undoubtedly the most studied and perhaps well understood of the protein kinases. The catalytic subunit α of PKA (PKAC α) was the first kinase crystal structure to be solved; this protein continues to be the template to which we base general kinase structure and function on.^{42,83} This structure also contributed to the initiation of a new chapter in eukaryote protein kinase (EPK) drug discovery, structure-based drug design.⁸⁴

2.2: Structure of PKA.

Specific regions of PKA are often referred to when discussing inhibition strategies, and these regions often serve as the template for the modeling of other kinases. The main portions of the kinase that are involved with substrate, inhibitor, or regulatory function and/or binding are the nucleotide binding loop (51-56), hinge region (120-126), catalytic loop (162-173), E-helix (140-159), 3rd beta strand (67-75), C-helix (85-97), activation loop (184-208), and the P+1 loop (211-214). These regions are highlighted in Figure 13 below with the crystal structure of PKAC α , which contains the catalytic subunit with ATP, and the inhibitor peptide PKI(5-24) (PDBID: 1ATP). Type IV inhibitors bind to the substrate-binding pocket (occupied by substrate, white in Figure 13) made up by the activation loop (magenta) and the catalytic loop (teal). It is important to note that affects made outside of the pocket (such as post-translational modifications) can greatly affect the characteristics of the substrate-binding site. Cysteine-199,

the cysteine which we focus on for this thesis, is located on the activation loop. Cysteines in the activation loop are very common and their location is often conserved. For example, the human kinome contains 99 kinases that share a cysteine in the same spot as PKA α (to be discussed later). Many more cysteines exist throughout the activation loop and their presence is an indication of their potential to be targeted (see Chapter 3 Figure 69 for complete human kinome activation loop sequence alignment with cysteine highlights).

The activation loop (or T-loop) is characterized by a conserved DFG (aspartic acid-phenylalanine-glycine) start sequence and ends at the APE (alanine-phenylalanine-glutamic acid) motif. This region is highly conserved in eukaryote protein kinases (EPKs) and is heavily involved in the catalytic activity of EPKs. For most EPKs the activation loop is disordered when the kinase is not phosphorylated at the appropriate residues (Thr 197 for PKA). This disordered nature of the region reduces affinity of substrates and, in result, the kinase catalytic activity is severely diminished or completely abolished. Therefore, the nature of the activation loop and by extension the substrate-binding pocket is an important regulatory factory in the kinome (see section 2.3 on PKA regulation below).

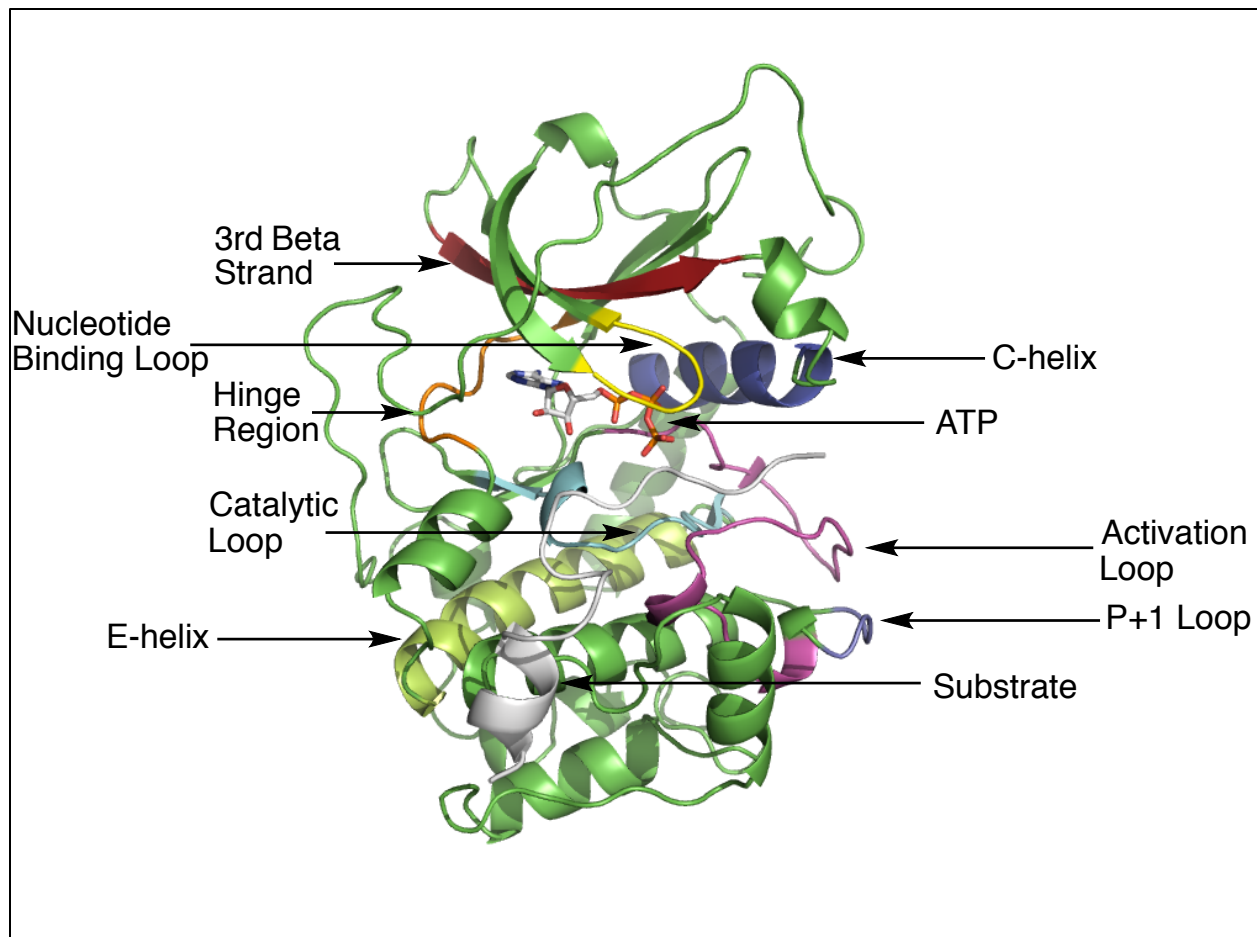


Figure 13: Major regions interacting with the active-site. Image generated on pymol.

2.3: Expression and Regulation of PKA.

PKA consists of multiple subunits and splice variants produced in most mammalian cell and tissue types. There are three catalytic subunits denoted alpha, beta, and gamma (PKA α , PKA β , PKA γ). The alpha and beta are the two major isoforms found in humans. The gamma subunit is primarily expressed in the prostate. In addition to the catalytic subunits are regulatory subunits; these regulatory subunits also have multiple isoforms: Ia, Ib, IIa, and IIb. The regulatory subunits all have cAMP binding domains (CBDs), and have high affinity for the second messenger. However, the different regulatory isoforms have different affinities for cAMP.^{42,85,86} This allows for greater regulation of cAMP signaling, by having different amounts

of PKA activated at different thresholds of cAMP (discussed below). However, the main focus will remain on the alpha subunit, PKAC α .

Despite the localized expression of the catalytic subunit isoforms, their regulatory mechanisms are essentially the same. PKA is regulated by multiple endogenous regulatory mechanisms, many of which are conserved or very similar within the kinome.⁸⁴ Upon transcription, PKA is autophosphorylated on Ser 338 and then rapidly phosphorylated on Thr 197 by PDK1.⁸⁷ However, these phosphorylations are considered silent when left as is, in that they are not dephosphorylated by known phosphatases.³⁸ Additionally, the phosphorylation occurs immediately during (auto) and upon transcription (PDK1).⁸⁷ However, it has been demonstrated that oxidation of Cys199 by glutathione, a physiologically relevant post-translational modification, renders the pThr 197 and pSer 338 residues susceptible to phosphatase activity.³⁸ Whether or not this is a physiologically relevant event remains to be conclusively determined. What is clear is that phosphorylation at Thr 197 causes an ordering of the activation loop (and by extension the substrate-binding pocket as a whole), which increases substrate-binding resulting in increased catalytic activity.⁸⁷ Of particular note is that the inhibitor peptide (PKI, IP20) binds to the dephosphorylated isoform with ~9 fold less affinity than for the phosphorylated isoform (6.4 vs 54 nM).⁸⁷

Once translated, PKAC α forms the inactive holoenzyme by binding as a heterotetramer with two regulatory subunits. These regulatory subunits bind with high affinity to the substrate-binding site and occlude substrates from binding; therefore, inhibiting the catalytic activity of PKAC α .⁸⁸⁻⁹² However, the second messenger cAMP binds to the regulatory subunits cooperatively and with high affinity, which causes the release of the free, catalytically active, enzyme.⁹²

The free PKAC α may still remain inactive because it can bind to the endogenous inhibitor peptide, the heat-stable protein kinase inhibitor (PKI).^{93,94} PKI binds selectively and with very high affinity to the free catalytic subunits of PKA. In addition to substrate competitive regulation, cysteine 199 can be oxidized with glutathione, which inhibits activity. The specific residue interactions between the pseudosubstrate inhibitor PKI and the catalytic subunit are detailed in a 2-D representation below.

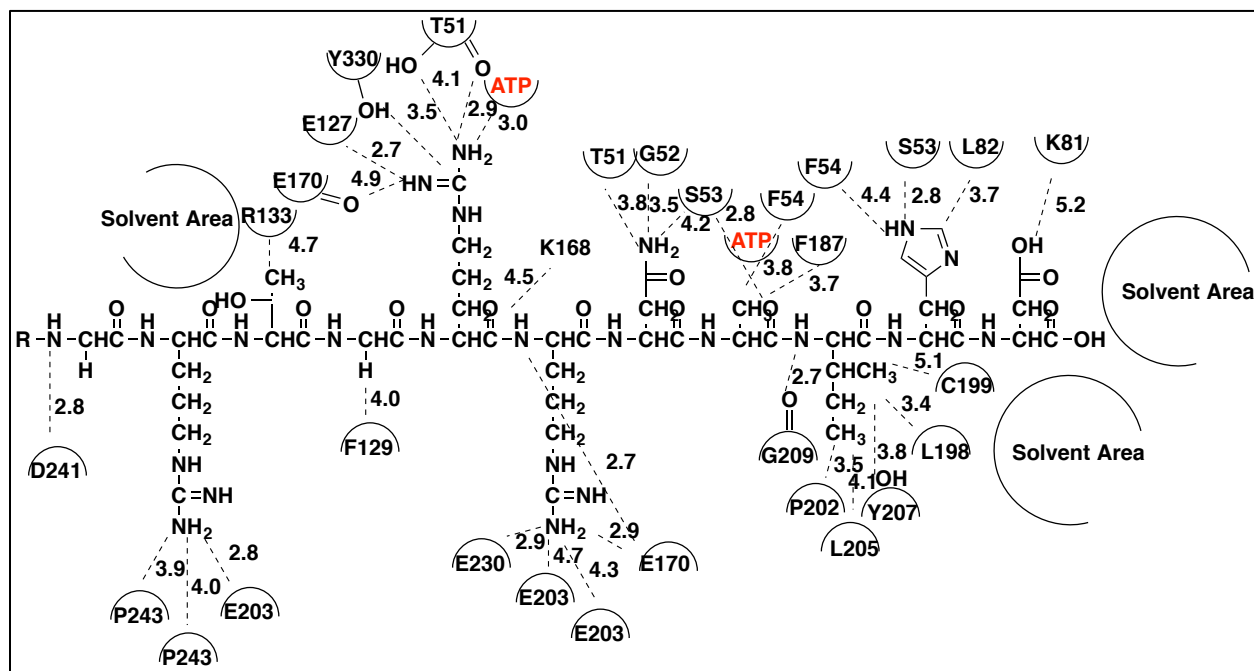


Figure 14. PKI(14-24) 2-D representation of intermolecular interactions with PKAC α .

In addition to the regulatory mechanisms described above, the functional effect of PKA is also spatially and temporally regulated by A-Kinase anchoring proteins (AKAPs), of which there are more than fifty (when splice variants are considered).⁹⁵ The regulatory subunits bind to the AKAPs, which are clustered, and upon stimulation with cAMP, catalytically active PKAC α is released in a localized fashion. The original AKAPs were isolated as contaminants when attempting to purify regulatory subunit.⁹⁵ It is clear that PKA functional activity is not only regulated in a dynamic nature but it is tissue specific (see Table below for a list of AKAPs and their tissue expression). It is because of this dynamic activity that current methods to detect PKA activity *in vivo* do not necessarily reflect the function of PKA in that state and no one method available can decipher all the data.

Table 3. Selection of known A-Kinase Anchoring Proteins (AKAPs).^{95,96}

AKAP	Tissue Expression
D-AKAP1	Ubiquitous
AKAP-KL	Kidney, lung, thymus, cerebellum, heart
AKAP110	Testis
AKAP79	Ubiquitous
mAKAP	Heart, brain, skeletal muscle
AKAP18 α	Heart, brain, lung, pancreas, kidney
AKAP18 β	Kidney, brain
AKAP18 γ	Heart, brain, placenta, lung, pancreas
AKAP18 δ	Heart, kidney inner medulla
AKAP95	Nuclear matrix
AKAP350	Ubiquitous
Isoform Yotiao	Brain, heart, placenta, skeletal muscle, pancreas, testis
D-AKAP2	Ubiquitous
AKAP220	Testis, brain, kidney
Gravin	All tissues except liver

AKAP-Lbc	Ubiquitous
AKAP28	Lung
GSKIP	Ubiquitous
MyRIP	Ubiquitous
Rab32	Ubiquitous
SKIP	Heart, brain, ovary, spleen
BIG2	Placenta, lung, heart, brain, kidney, pancreas
Ezrin	Blood cells, placenta, secretory epithelia, brain
WAVE-1	Brain, platelets, liver
MAP2	Brain, ovaries
Neurobeachin	Ubiquitous
MTG8	Brain, lymphocytes
Myosin VIIA	Ubiquitous
MTG16b	Ubiquitous
Synemin	Muscle
PAP7	Ubiquitous
Myospryn	Skeletal and heart muscle
SFRS17A	Ubiquitous
Merlin	CNS
Moesin	Blood
AKAP85	Lymphocytes, epithelial cells
Pericentrin	Ubiquitous
RSK1	Ubiquitous

The second messenger cAMP is generated from ATP by adenylate cyclases (ACs), whose activity can be increased by extracellular signals. Levels of cAMP are regulated by extracellular signals that can activate ACs through G-protein coupled receptors (GPCRs) and phosphodiesterases (PDEs) that catalyze the breakdown of cAMP.⁹⁷ GPCRs can be coupled to a variety of G protein complexes which in turn can positively or negatively effect AC activity. For example, the G_{α_s} protein increases AC activity and the G_{α_i} inhibits AC activity. In a healthy physiological state, PKA acts as the main intracellular target of cAMP. Once cAMP is generated,

it binds to the regulatory subunits that inhibit PKA and causes the release of catalytically active PKA α .⁹⁷

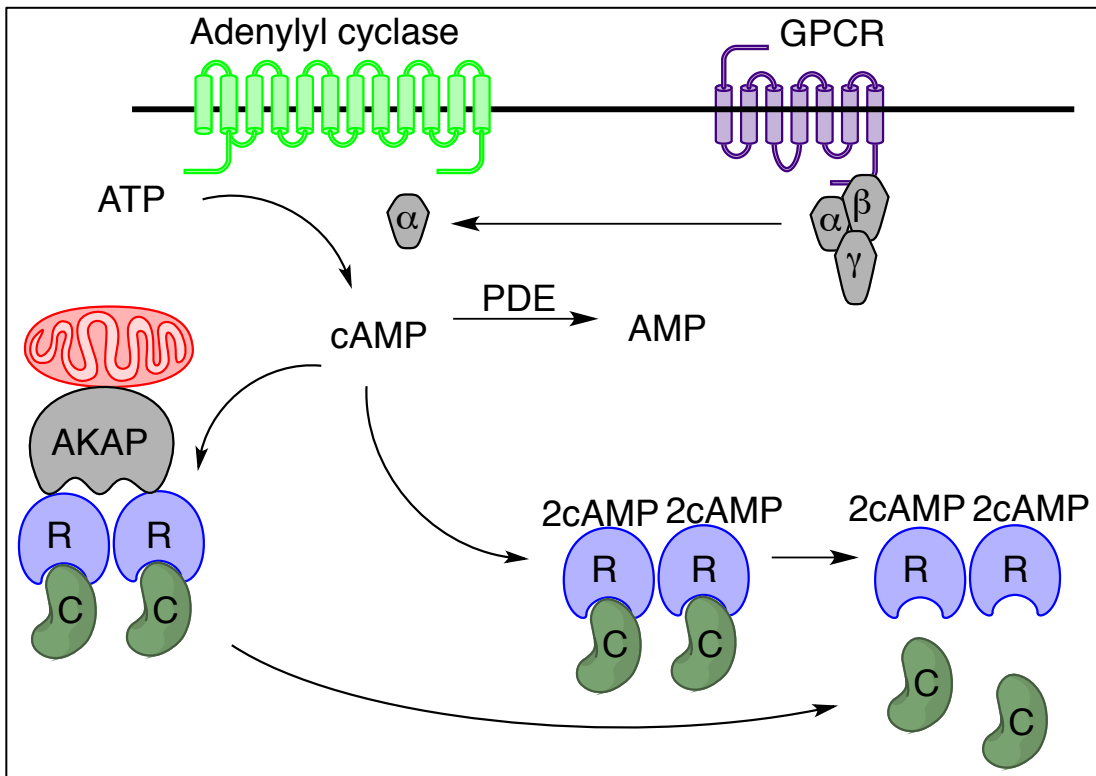


Figure 15. Schematic representation of cAMP-dependent activation of PKA.

2.4.1: PKA activity.

PKA is ubiquitously expressed and is responsible for the regulation of multiple proteins and transcription factors via phosphorylation of many Ser/Thr residues that directly result in increased cAMP levels (often resultant from GPCR stimulation).⁶ The consensus sequence for phosphorylation by PKA α is RRXS.⁶ A brief sample of various protein substrates is listed

below in Table 4.⁹⁸ Taylor and colleagues have performed a quantitative mass spectrometry based proteomic analysis to identify many proteins whose expression is effected by directly altered by PKA.⁶

Table 4. Selected substrates of PKA α .

PKA Substrates
Muscle Glycogen Synthase
Phosphorylase Kinase α
Protein Phosphatase 1
CREB
Liver Tyrosine Hydroxylase
Phopholamban
USP20
PKA α (auto)
CDC25B
ABL1
NFKB1
CLDN3
RORA

Table 5. Proteins whose expression is increased (green) or decreased (red) directly by PKA activity.

PKA-Dependent Protein Expression
Isocitrate dehydrogenase (NAD) subunit γ
glutathione reductase
glyoxylate reductase 1 homologue
mortality factor 4-like protein 2
isoform 4 of E3 ubiquitin-protein ligase
nuclear autoantigenic sperm protein isoform 1
isoform 1 of Rab GDP dissociation inhibitor β
GTP-binding nuclear protein Ran
prostaglandin E synthase 3
translin-associated protein X
F-actin-capping protein subunit $\alpha 2$
(Rpsa-ps7) similar to 40S ribosomal protein SA
scavenger mRNA-decapping enzyme
exosome complex exonuclease RRP41
isoform 2 of phosphoglycerate mutase family member 5
(gm4492) similar to gag
isoform 2 of acidic leucine-rich nuclear phosphoprotein 32 family member E
peptidyl-prolyl cis-trans isomerase
Annexin A5
sinalosome complex subunit 4
leucine-rich repeat containing protein 59
isoform 1 of 36biquitin carboxyl-terminal hydrolase isozyme L5
Tnp1 transportin-1

The different holoenzymes play a role in PKA's normal function as well. Type I holoenzymes (defined by which regulatory subunit the catalytic subunit is bound, for Type I it is RI) are typically found in the cytosol and Type 2 are generally localized to the membrane. The dynamics of PKA signaling modulate cell cycle entry in multiple systems. PKA has also been identified as a regulator of deubiquitinase (DUB) activity for GPCRs, thus playing a role in receptor desensitization. PKA has also been demonstrated to have an important role in the regulation and development of Schwann cell (SC) growth and proliferation.⁸⁸

PKA signaling is closely tied to β -adrenergic stimulation. Upon stimulation of a positively coupled to cAMP GPCR, cAMP is generated and causes the release of free, catalytically active PKA α . A brief illustration of PKA's role in heart muscle contractility and energy production in the tissue is shown below in Figure 16.⁹⁸ When this signaling is perturbed, various disease states can result.^{96,98}

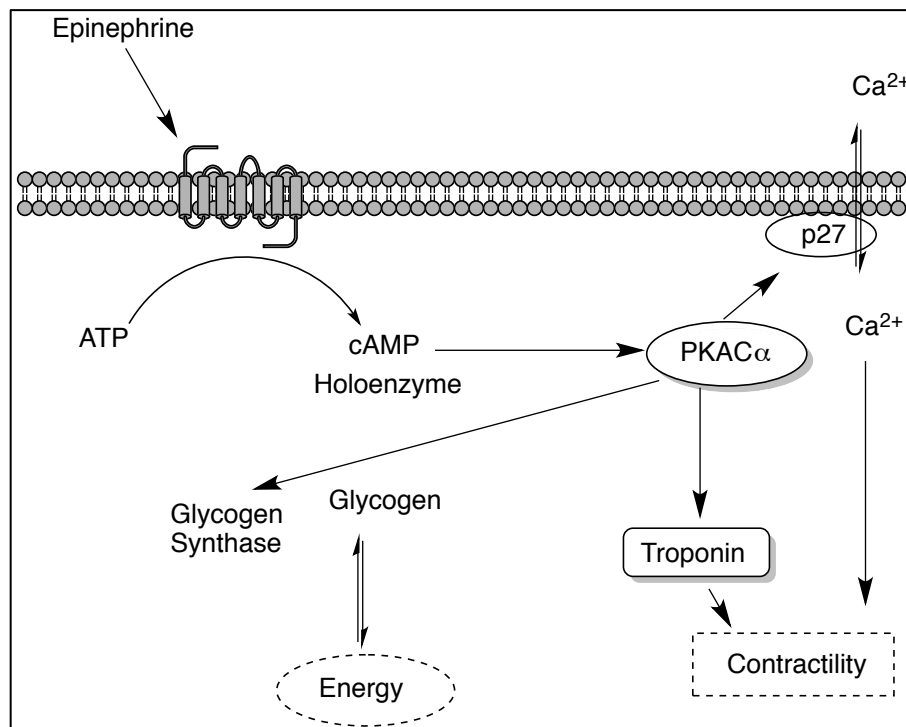


Figure 16. PKA's role in heart contractility and energy consumption.

2.4.2: Aberrant PKA activity.

Aberrant PKA activity has been implicated in a number of cancers, with opposing effects of both increasing and decreasing cell proliferation.^{99,100} For example, it has been shown that an increase in the expression of regulatory subunit IA, which results in a decrease of PKA catalytic subunit activity, causes increased cell proliferation in human melanoma cells.^{101,102} Conversely, the cAMP response element modulator (CREB) is activated by PKA. Studies have shown that increased levels of PKA increase CREB activity and contribute to cell proliferation in various cancers.¹⁰³ It has also been demonstrated that certain forms of cancer excrete PKA α , known as extracellular protein kinase (ECPKA); the activity and amount of ECPKA strongly correlates

with tumor size.¹⁰⁴ This is a particularly interesting observation for PKA in that a probe that selectively detects ECPKA, such as the one discussed in this thesis, could be a valuable tool in the clinic as a detection method for a tumor biomarker.

Aberrant PKA activity has been identified and implicated the PKA pathway as a therapeutic target in Cushing's disease.¹⁰⁵ This example is another prominent illustration of the normal PKA catalytic activity being influenced by alterations in its regulatory subunit binding.¹⁰⁵ The reduced affinity of catalytic subunit for the regulatory subunit, and therefore its ability to form the inactive holoenzyme, cause an increased basal level of PKA α activity.¹⁰⁵

PKA activity is, not surprisingly, implicated in a number of other endocrine disorders as well.^{97,105} Instead of normal stimulation of GPCRs by endogenous hormones, mutations and/or regulatory perturbations that increase basal levels of PKA activity lead to related disease states. Aberrant PKA activity has been implicated in the endocrine disorders hyperthyroidism and acromegaly.¹⁰⁶⁻¹⁰⁹ Because PKA plays such a central role to cAMP signaling and protein expression, its involvement in various disease states is vast and diverse; therefore, methods to detect PKA activity have often been sought.

2.5: Current methods to detect PKA and PKA α activity.

There are numerous antibodies commercially available for Western blot detection of many aspects of PKA, including both catalytic subunits (generally nonspecific splice variant detection), and the regulatory subunits. Some of these antibodies are non-selective, that is they detect all forms of PKA. There are also phosphorylation specific antibodies which only detect catalytic subunits of PKA that have been phosphorylated at Thr 197. These phospho specific antibodies are one current technology used to quantify active amounts of PKA. However, these antibodies are unable to take into account the other mechanism of regulation that PKA is subject to. Another common practice is to measure a specific substrate, or even total phosphorylation events that could be attributed to PKA. For example, there are CREB phosphorylation specific antibodies and by quantifying the levels of phosphorylation, it is reasoned that increased (or decreased phosphorylation) is an indicator of PKA activity. Additionally, a common antibody recognizes the substrate consensus sequence of PKA (RRXS/T) in its phosphorylated form RRXpS/T and by quantifying global detection of phosphorylation (or in some cases visualization) can be interpreted to be an indicator of PKA activity. These methods tend to fall short of truly accurate active levels of PKA and better reflect situational specific increases in a particular event correlated to PKA activity.

There are a variety of sophisticated kits and detailed methods to analyze substrate turnover in complex biological mixtures and isolated protein solutions for both well and lesser equipped laboratories. Genomic sequencing is a stand by for most biology labs, however this does not address the phenotype. Substrate turnover is another common method, but this generally cannot be used *in vivo* nor can it account for pathway redundancies, e.g., a secondary enzyme causing additional activity due to overlapping consensus sequences (see discussion of consensus

sequence antibody for PKA activity above). When substrate is used *in vitro* it is very effective. Multiple detection methods can be employed to detect substrate turnover with isolated enzyme including, but not limited to, radiometric analysis, UV detections, fluorescence polarization, fluorescence-resonance energy transfer (FRET), thin-layer chromatography, and blotting techniques. We utilized a commercially available FRET based assay to determine out PKA activity *in vitro* and will be our procedures discussed in detail in the experimental section.

There are a number of examples of a substrate-based probes to measure phosphate transfer at the source, both in whole cell and isolated enzyme assays. These probes utilize substrates demonstrated to be selectively phosphorylated by PKA α (kemptide for example), and a fluorophore whose emission is shifted when bound to and phosphorylated by PKA α . Lawrence and colleagues developed such a probe utilizing a coumarin derivative tag and a quencher dye for detection. When the probe is phosphorylated by PKA it causes a sharp increase in the coumarin fluorophore's emission spectra allowing for selective detection. Through numerous peptide syntheses and various dyes, they optimized the substrate properties for maximum signal with minimal background. This is also detectable and quantifiable in real time so it has been used to characterize the location of PKA that is in the process of, or has very recently, phosphorylated the substrate based probe. This allows quantification of the relative amounts of PKA in mitochondrial microenvironments.¹¹⁰

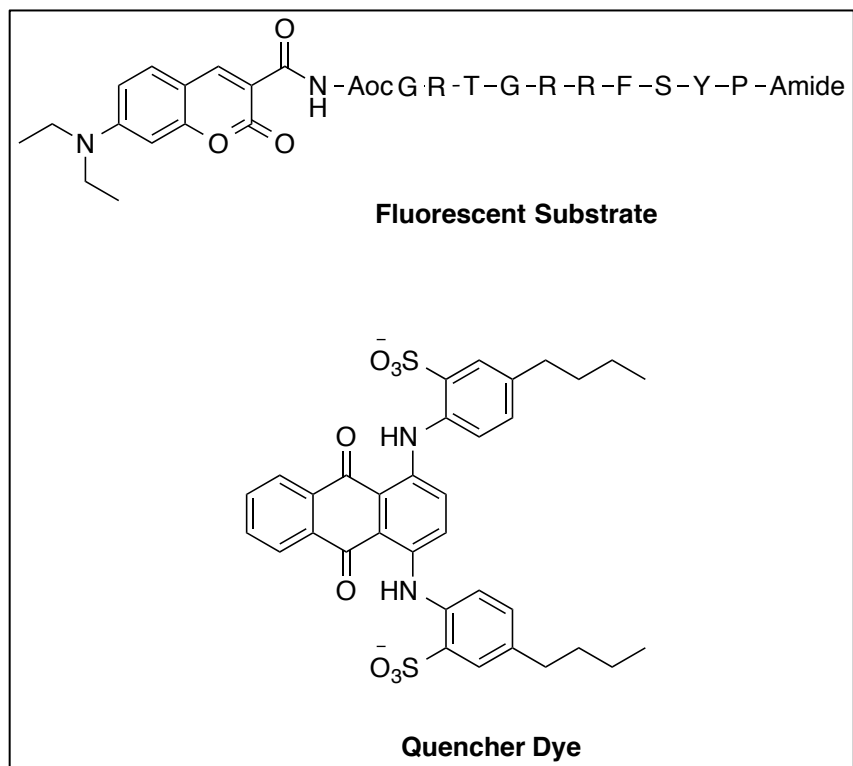


Figure 17. Substrate-based probe of PKA α catalytic activity.

Lawrence et al have also described a unique probe for detecting intracellular levels of PKA. They utilize a portion of PKI as an active site directed scaffold. However, instead of targeting Cys199 in the substrate-binding pocket, they target a non active-site cysteine (Cys 343) that does not inhibit the enzyme. Once their probe has bound, they expose it to UV light and a photoreactive moiety causes the release of PKI and only the labeled portion of the probe covalently bound to the auxiliary cysteine remains. Here they report that their probe identifies free and catalytically active enzyme yet does not inhibit it and thus they can tag it and follow its activity as a result of various stimuli.¹¹¹

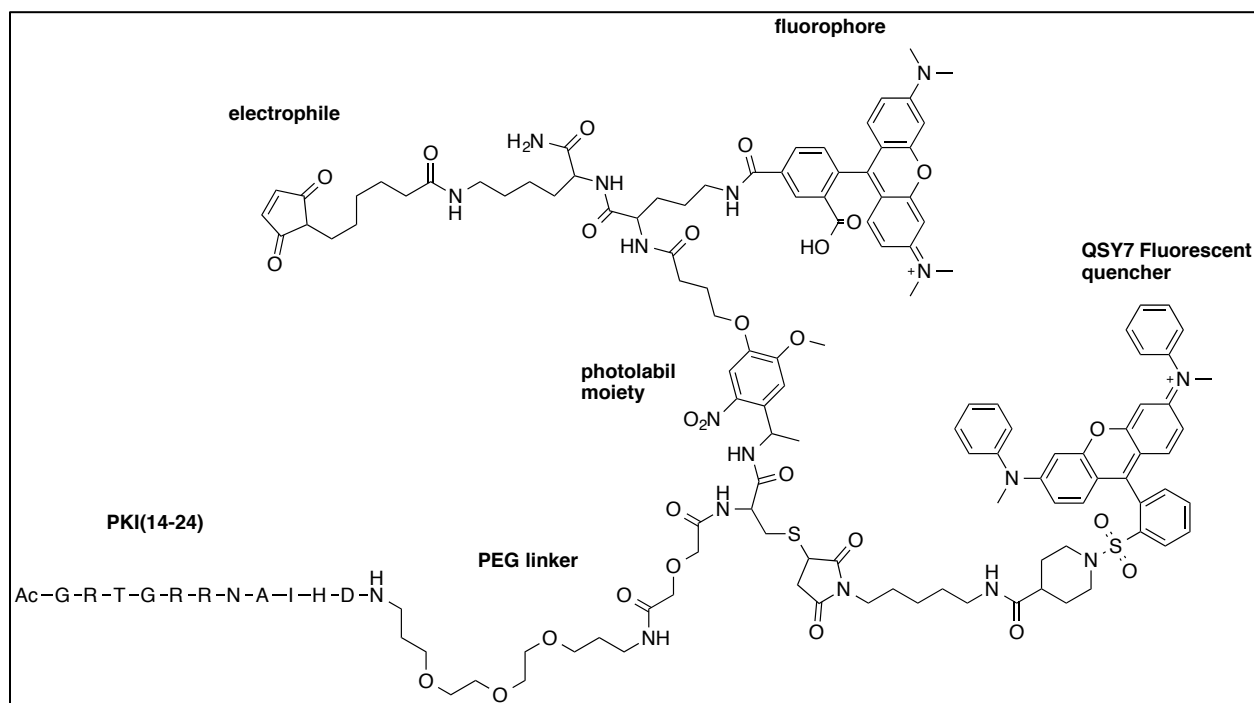


Figure 18. Active-site directed probe with electrophile directed towards Cys343.

Another group has developed an affinity assay based on the PKI scaffold.⁹³ In essence, this is the purpose of our probe but as applied in a reversible situation. PKI's mechanism of action is well documented and therefore this report concludes that it can be used to selectively detect and measure amounts of free and catalytically active amounts of PKA α . They utilize residues 5-24 of PKI and express it linked to glutathione *S*-transferase (GST, with a Gly₅ linker): GST-PKI(5-24). Upon generation of GST-PKI(5-24), they immobilized it onto solid glutathione beads for use in affinity purification. They were able to pull down catalytically active PKA and perform a number of activity-based experiments. An interesting outcome was the confirmation of H89 (a high affinity ATP competitive inhibitor of PKA) reducing affinity of PKI for the catalytic

subunit. However, they go on to note that the assay simply evaluates relative degrees of PKI affinity and does not quantify PKAC α activity itself.⁹³

Imperiali and Shults have developed a generalizable strategy to apply to numerous protein kinases and display the utility of their approach on PKAC α . They append a Sox residue to the C-terminal a PKA substrate (Ac-Leu-Arg-Arg-Ala-Ser-Leu-Pro-Sox-NH₂). When the substrate is unphosphorylated, the affinity for Mg²⁺ of the substrate (has an engineered β turn for Mg²⁺ binding and is the lynch pin for the technique) is minimal, but upon phosphorylation the affinity increase dramatically. This increased binding of Mg²⁺ causes a detectable fluorescence signal to be generated by the Sox residue.¹¹²

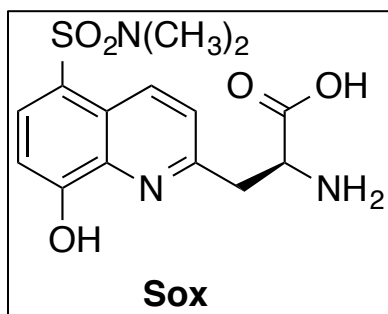


Figure 19. Sox residue used for selective detection of Mg²⁺ binding which was correlated to phosphorylation of substrate.

Uri and coworkers have developed an easily accessible assay that utilizes thin-layer chromatography to detect PKA substrate turnover activity.¹¹³ They appended 5-TAMRA (a common fluorophore) to kemptide (a commonly used and commercially available PKA

substrate) and developed TLC conditions sufficient to separate the phosphorylated and non phosphorylated substrates, thereby allowing for selective detection and quantification.¹¹³ While this assay is generally only applicable in situations with isolated enzyme, its simplicity and accessibility make it noteworthy.

The mechanism based fluorescence reporter mentioned in the irreversible Type IV inhibitors section of Chapter 1 (Figure 11) can also be included here in the review of methods to detect PKAC α activity.⁵⁸ Tung and colleagues' mechanism based fluorescence reporter selectively reacts with Cys199 in the activation loop. Until this selective interaction occurs, the probe they developed remains quenched. In experiments they conducted in fetal bovine serum spiked with PKAC α , they noted significant increase in fluorescence intensity in a dose dependent manner with increasing PKAC α concentration.⁵⁸

PKA activity is an important indicator of cellular homeostasis and, as such, probes that accurately detect the activity of PKAC α *in vivo* would have diverse applications in a variety of diseased and non-diseased systems. Here we report the efforts and resulting data towards the production of an ABP for the cAMP-Dependent Protein Kinase A (PKA). PKA is the prototype kinase, therefore the strategy described in the following text may serve as a general strategy to target other kinases with a similar cysteine in the activation loop.

Chapter 3: Development of ABPs for PKAC α

Chapter 2 details the dynamic regulatory mechanism associated with PKAC α catalytic activity. These mechanisms reinforce the high degree of sensitivity associated with the substrate-binding pocket. Therefore, a probe that is selective for the active conformation of the substrate-binding pocket would have significant advantages in terms of monitoring more accurately the levels of active protein available in the cell. Below is detailed the rationale for selection of the peptide scaffold as the recognition sequence and the subsequent structure-based design used to implement it an effort to produce an ABP.

3.1: Background on the heat-stable protein kinase inhibitor (PKI)

The heat-stable protein kinase inhibitor (PKI) is endogenously expressed as a 76 amino acid protein (7,989 Da). It was identified by Edwin G. Krebs et al. in 1971.¹¹⁴ They detailed many characteristics of PKI; most notably, it was shown to be an efficacious inhibitor of PKAC α .¹¹⁴ Many groups have performed subsequent structure-activity relationship studies on the peptide scaffold to determine the amino acids critical for binding, selectivity, and effective inhibition. Below is a brief summary of the data obtained in the context of PKI as a selective, active-site directed, peptide inhibitor.

The expression of PKI has been shown to vary greatly between tissue types. A study done on various rabbit tissues revealed that brain tissue had the highest levels of endogenous PKI. Cardiac muscle and skeletal muscle had roughly equivalent amounts of PKI, at about 1/3 that of the brain. The liver, kidney, and thymus only had a fraction of PKI as compared to brain and muscle tissues.¹¹⁵ These amounts were reported as units/g and generally only serve as relative amounts for these purposes.

Multiple truncations of the full length PKI have been found to retain significant inhibition activity against PKAC α . Many of the initial structure-activity relationship studies relied on isolating endogenous sources of PKI and truncating it with different proteolytic enzymes. Also, a few synthetic peptides are included (discussed in next paragraph).¹¹⁴⁻¹¹⁸ Some notable fragments that were identified are listed in Table 6 below. While these studies effectively demonstrated that it is possible for fragments of the full-length heat-stable protein kinase inhibitor to inhibit the catalytic activity, the peptides were limited to truncations made by their proteolytic enzymes and therefore the studies were not exhaustive.

Table 6. Fragments of PKI and the corresponding K_i values for PKAC α .

Sequence	K_i
TTYADFIASGRTGRRNAIHD	0.3 nM
TTYADFIASGRTGRRNAIHD - NH ₂	2.3 nM
TTYADFIASGRTGRRNAI - NH ₂	3.1 nM
TYADFIASGRTGRRNAI - NH ₂	1.7 nM
FIASGRTGRRNAIHD - NH ₂	73 nM
IASGRTGRRNAIHD - NH ₂	115 nM
GRTGRRNAIHD - NH ₂	57 nM
GKTGRRNAIHD - NH ₂	370 nM
ADFIASGRTGRRNAI - NH ₂	90 nM
DFIASGRTGRRNAI - NH ₂	97 nM

The next round of structure-activity relationship studies performed on PKI brought in a number of synthetic peptides. Among these is the primary example of the minimum sequence required for maximum inhibition, PKI(14-22)-Amide, with a K_i of 36 nM along with valuable structure-activity relationship data. PKI(14-22)-Amide, surprisingly, has an even lower K_i than PKI(14-24)-Amide (57 nM).^{94,117,119} This is one of the major reasons PKI(14-22) was selected as the “full length” ABP recognition sequence.

Table 7. Structure-activity relationship analysis by amino acid substitution.

PKI(14-22)	K_i
GRTGRRNAI - NH ₂	36 nM
GRTGRRAAI - NH ₂	550 nM
GRTGRRGAI - NH ₂	110 nM
GRTLRRNAI - NH ₂	390 nM
GRAGRRNAI - NH ₂	140 nM
GRTGRRNAL - NH ₂	180 nM
GRTGRRNAG - NH ₂	1400 nM

3.2: PKI Selectivity.

Full length PKI is regarded as being very selective for PKAC α in complex biological mixtures.^{116,120} The selectivity of PKI(14-22)-Amide has been examined on a number of isolated enzymes; however, a full panel of kinase inhibition has not been published.^{116,119,121} Proteome selectivity of a derivative of PKI(14-22) is briefly addressed by an affinity pull-down experiment performed with murine tissue lysates. One enzyme that in particular continues to be part of the equation when considering PKI's *in vivo* activity is the cGMP-dependent protein kinase, PKG. The activation loop sequences of these two kinases have high similarity, and as a result the shorter PKI sequences have activity against PKA and PKG.^{118,119}

Table 8. Sequence alignment of DFG---APE regions of PKA and PKG.

	Activation Loop Sequence alignment
PKA	DFGFAKRVKG-- RTWTLCGTPEYLAPE
PKG	DFGFAKKIGFGKKTWTFCGTPEYVAPE

Table 9. Representative PKI fragments and their corresponding affinity for PKG.^{119,121}

PKI Fragments	PKA K_i	PKG K_i	PKG/PKA
TYADFIASGRTGRRNAI - NH ₂	1.7 nM	37820 nM	22247
GRTGRRNAI - NH ₂	36 nM	8000 nM	222

Additionally, various derivatives of the PKI inhibitor peptide have been produced to attenuate its activity profile. One research team has attached the DPTsh1 shuttling peptide to PKI(5-24)-Amide to produce a selective, cell permeable, peptide-based, inhibitor of PKA α .¹²² Various lengths of the inhibitor peptide PKI are commercially available from many vendors. Additionally, these peptides are available with various N-terminal modifications; one of which is the addition of a myristyl group, which has been demonstrated to make the peptide cell permeable while maintaining affinity (our lab determined the IC₅₀ of commercial Myr-PKI(14-22)-Amide to be 47.9 nM).¹²⁰

3.3.1: Inhibitor rationale: Structure-based design of PKI-based compounds.

The multiple crystal structures of PKA α have played vital roles in deciphering the complex regulatory mechanisms that attenuate its catalytic activity. The first crystal structure of PKA α was the first of any protein kinase and thus provided valuable data concerning the makeup of the active site.⁸³ Prior to this crystal structure, the use of active-site directed probes and subsequent analysis was the main method to determine the residues that make up the binding site (classical). Additionally, the first crystal structure was published as a His₆ tagged recombinant protein bound to both ATP and a portion of the heat stable protein kinase inhibitor PKI(5-24). This particular crystal structure clearly illustrates the proximity of Cys199 to the P+1 and P+2 positions of the inhibitor peptide.

PKI-Ile22 occupies the hydrophobic site at the P+1 position, this position has been demonstrated to have significant effect on the binding affinity of the peptide inhibitor (see Table 4, above). From the crystal structure the distance was measured from the alpha carbon on the C-terminal end of the peptide to estimate where the electrophilic carbon of an electrophile, such as a chloromethyl ketone, would reside. It was determined to be 7.3 Å for an Ile22 based electrophile. At the P+2 position is a histidine residue that has numerous interactions with surrounding residues (the specifics of which are detailed in Figure 14). From the crystal structure (1ATP) the distance was from the alpha carbon on the C-terminus side of His23 to estimate where an electrophile, like glycine halomethyl ketone, would reside; it was determined to be 8.3 Å (Figure 20 below).

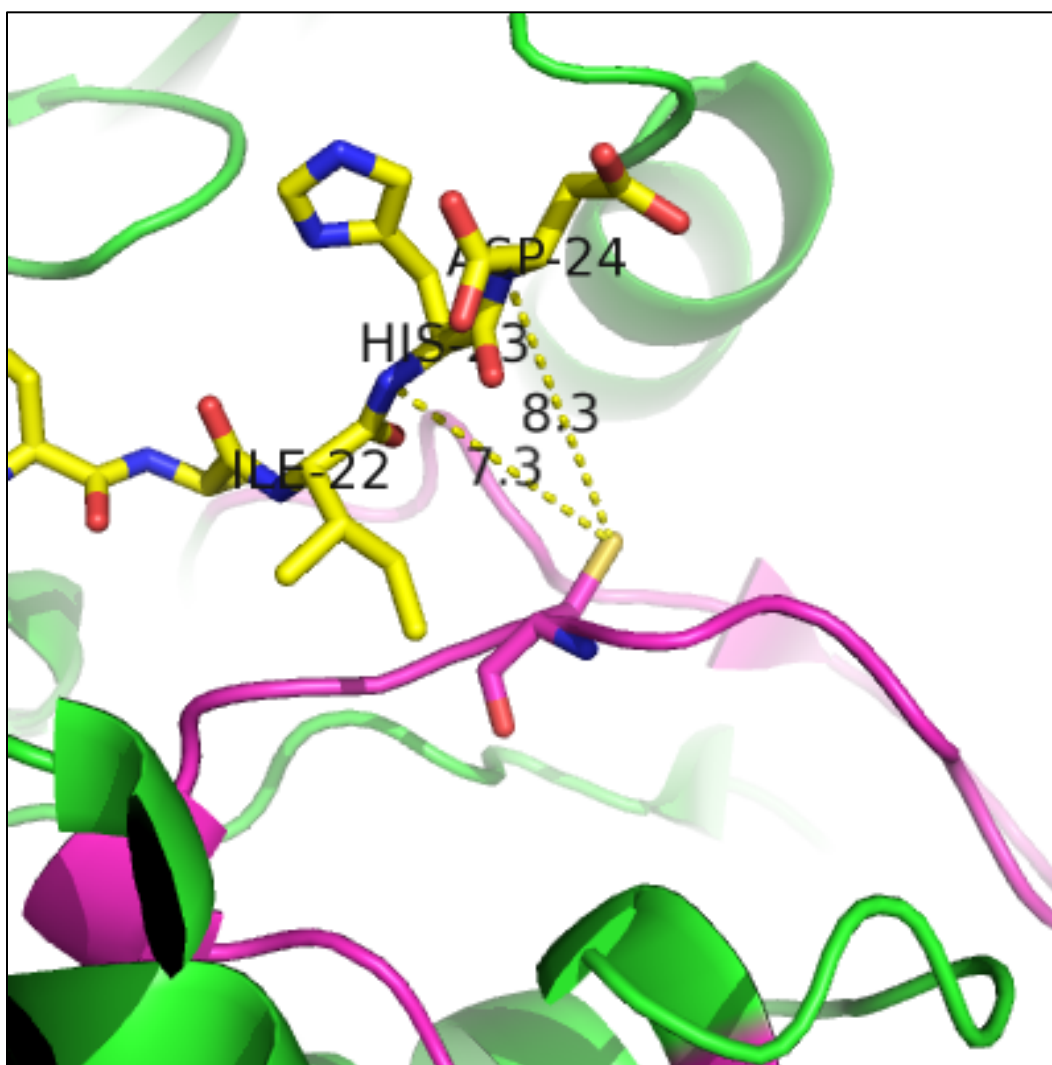


Figure 20. Distance analysis of relevant alpha carbons to the side chain of Cys199.

3.3.2 Activity-Based Probe Rational: Selecting PKI as the active-site recognition sequence.

Numerous inhibitors that target the ATP-binding site have been developed. Most of these, however, show little selectivity for PKA α . This is mostly due to the conserved nature of the nucleotide-binding site among many proteins in mammalian cells. Additionally, inhibitors of this nature must have high affinity to compete with millimolar concentrations of intracellular ATP if

they are to make the transfer from the lab to the clinic. While there have been some covalent inhibitors produced for other kinases that target the ATP-binding site, PKA does not have an appropriately placed cysteine necessary to be a target of this strategy.

PKI has been demonstrated to be highly selective for PKA *in vivo*. In addition to its high selectivity, PKI (and many of its fragments) have high affinity for PKAC α based on the available information and, perhaps most importantly, the mechanism of action of pseudosubstrate inhibitors. More specifically, by binding with the substrate-binding pocket of PKAC α , PKI binds competitively with a number of endogenous regulatory mechanisms (reviewed in Chapter 2.3). Therefore, PKI presented itself as an ideal candidate as the recognition scaffold for the generation of an activity-based probe of PKAC α .

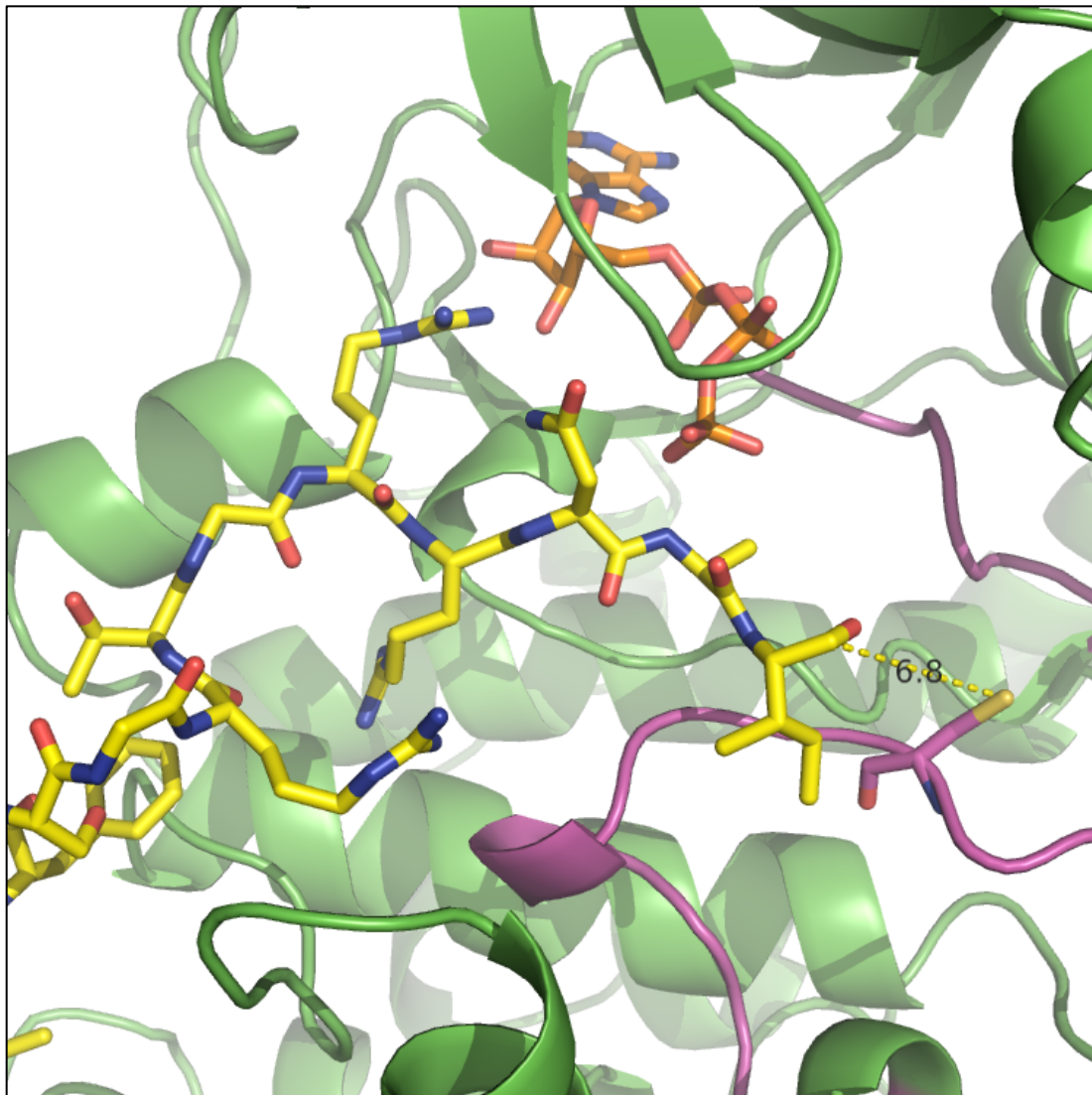


Figure 21. View of critical amino acids in PKI for affinity for PKAC α .

3.4: Single Amino Acid Analogues

3.4.1: Rational and design of single amino acid analogues.

The distance between the carbonyl carbon of the P + 1 Ile22 and Cys199 in the cocrystal structure 1ATP is 6.8 Å, the C-terminal α -carbon distance is 7.3 Å and the C-terminal α -carbon at the P+2 position is 8.3 Å. The objective was to selectively react with this cysteine in the activation loop by utilizing endogenous binding mechanisms and a known binding mechanism of action. The project began by preparing a library of single amino acid analogues to capitalize on the hydrophobic binding pocket at the P+1 binding site of PKI, and its close proximity to the cysteine. It was hypothesized that the single amino acid, isoleucine, would maintain affinity for the hydrophobic binding pocket such that it would position itself appropriately for an appropriate cysteine selective electrophile. Also, this binding mechanism should be predictive of the full length peptide, thus providing valuable data pertaining to its activity-based mechanism of action and ability to inhibit the enzyme by alkylating Cys199.

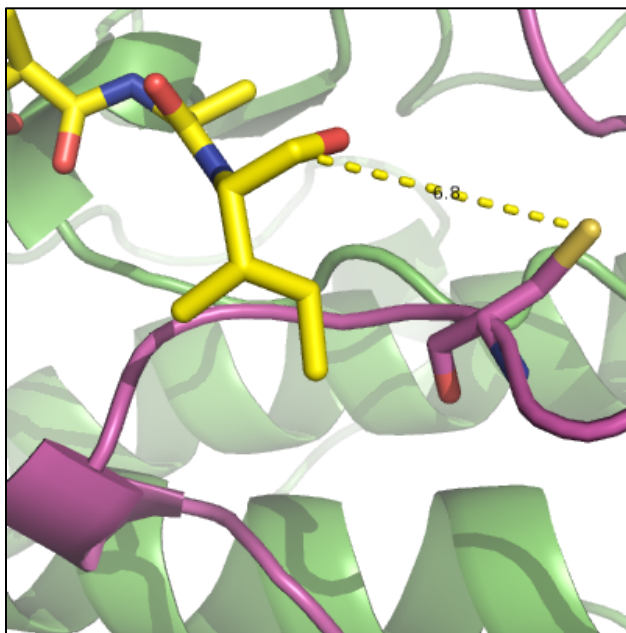


Figure 22. Close up on Ile22 and proximity to Cys199.

The first round of single amino acid analogues were centered around isoleucine, phenylalanine, and glycine. It was hypothesized that the isoleucine would bind in a similar manner to the isoleucine in PKI (Figure 23), the phenylalanine may be either able to increase hydrophobic interactions or be too large and thus provide important selectivity data, and the glycine would serve as a control for the backbone and/or amide in conjunction with the vinyl ketone to demonstrate the added binding interactions of the side chains.

3.4.2: Preparation of the single amino acid analogues.

The initial electrophile selected was the vinyl ketone electrophile, this is a particularly electrophilic moiety. Also, a vinyl ketone ensures labeling at the desired nucleophilic cysteine if the binding hypothesis holds true. Analogues were prepared in a short two-step synthesis.

Starting with the commercially available *t*-butyl carbamate (Boc) protected amino acids, a standard coupling was performed with *N*-(3-dimethylaminopropyl)-*N'*-ethylcarbodiimide (EDCI) hydrochloride, 1-hydroxybenzotriazole (HOBt) hydrate, 4-methylmorpholine as the base, *N,O*-dimethylhydroxylamine hydrochloride, and dichloromethane as the solvent at ambient temperature for 16 hr to generate the Weinreb amide leaving group. The Weinreb amide is a suitable leaving group for the subsequent Grignard reaction with vinylmagnesium bromide in ether at 0 °C to produce the Boc protected amino acids with a vinyl ketone electrophile at the C-terminal position. A control ethyl compound was synthesized by taking compound **2** and reducing the vinyl group with Pd/C and hydrogen gas at 1 atm for 16 hr.

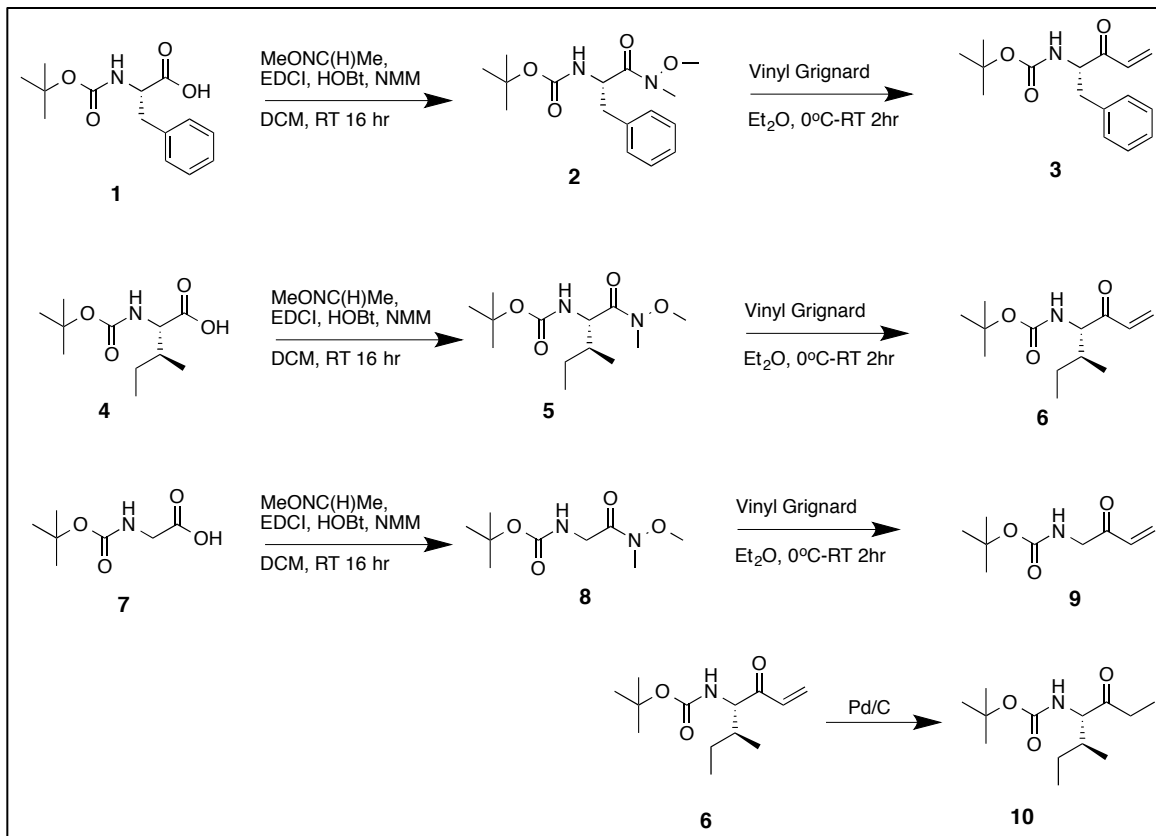


Figure 23. Synthesis of Boc vinylketone amino acid derivatives.

The propargyloxycarbonyl (Poc) protected amino acids were synthesized in anticipation of the utilization of ‘click’ chemistry for selective detection.³⁴ The free base amino acids were commercially available. To prepare the Poc protected amino acids, propargyl chloroformate was incubated with the desired amino acid and sodium hydroxide as the base. Then a standard coupling was performed with *N*-(3-dimethylaminopropyl)-*N'*-ethylcarbodiimide (EDCI) hydrochloride, 1-hydroxybenzotriazole (HOBT) hydrate, 4-methylmorpholine as the base, *N,O*-dimethylhydroxylamine hydrochloride, and dichloromethane as the solvent at ambient

temperature for 16 hr to generate the Weinreb amide leaving group. Followed by a Grignard reaction with vinylmagnesium bromide in ether at 0 °C to produce the Poc protected amino acids with a vinyl ketone electrophile at the C-terminal position.

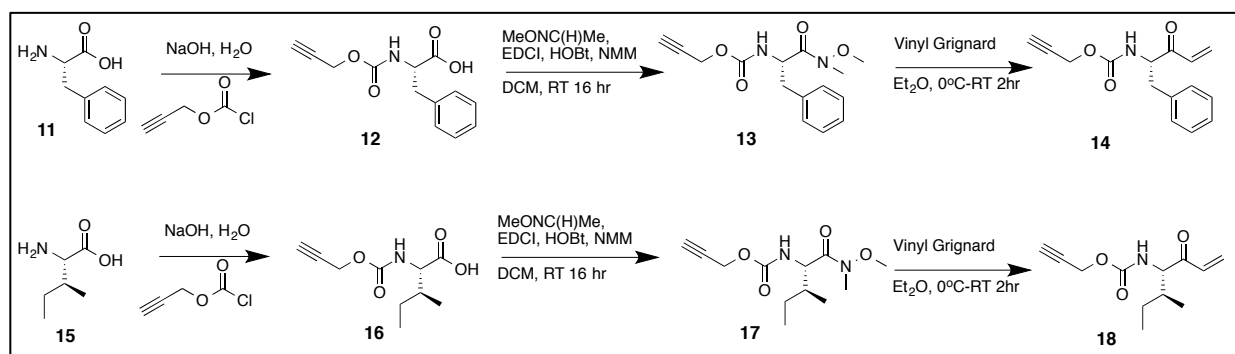


Figure 24. Synthesis of Poc vinylketone amino acid derivatives.

An additional set of single amino acid analogues was synthesized to explore other electrophilic moieties with the goal of identifying the most suitable electrophile appropriate for selective labeling of activation segment cysteine while exploring various distances of the electrophilic group. Beginning with the commercially available Boc-protected isoleucine a standard coupling was performed with *N*-(3-dimethylaminopropyl)-*N'*-ethylcarbodiimide (EDCI) hydrochloride, 1-hydroxybenzotriazole (HOBT) hydrate, 4-methylmorpholine as the base, ethanolamine, and dichloromethane (DCM) as the solvent at ambient temperature for 16 hr. The resultant alcohol was exposed to Appel reaction conditions to substitute the alcohol with a halide. A halide source (I_2 , CBr_4 , or CCl_4), triphenylphosphine, imidazole, and DCM and the solvent at 0 °C for 4 hr yielded the alkyl halide electrophilic analogues **22-24**.

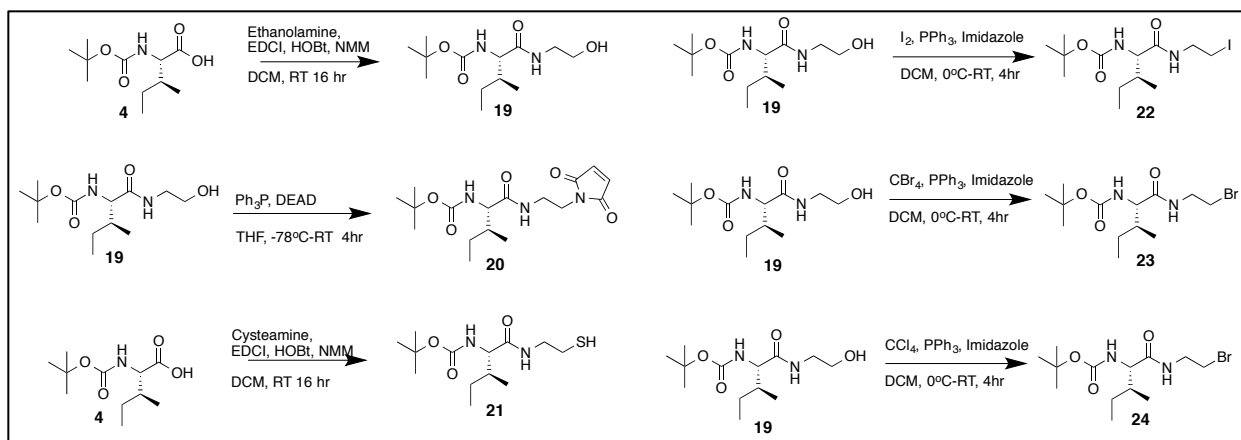


Figure 25. Synthesis of various amino acid—electrophile derivatives.

To produce a sulfur analogue for generating a disulfide bond with Cys199 and the Boc-protected isoleucine, a standard coupling was performed with *N*-(3-dimethylaminopropyl)-*N'*-ethylcarbodiimide (EDCI) hydrochloride, 1-hydroxybenzotriazole (HOBt) hydrate, 4-methylmorpholine as the base, cysteamine, and dichloromethane (DCM) as the solvent at ambient temperature for 16 hr.

To produce a maleimide analogue for covalent attachment with Cys199 and the electrophilic maleimide group on the Boc protected isoleucine. A standard coupling was performed with *N*-(3-dimethylaminopropyl)-*N'*-ethylcarbodiimide (EDCI) hydrochloride, 1-hydroxybenzotriazole (HOBt) hydrate, 4-methylmorpholine as the base, ethanolamine, and dichloromethane (DCM) as the solvent at ambient temperature for 16 hr. The resultant alcohol was purified on silica and then made into an electrophilic group with triphenylphosphine, diethyl azodicarboxylate (DEAD), and tetrahydrofuran (THF) as the solvent at -78 °C for 4 hr for the S_N2 reaction with commercially available maleimide to produce **20**.

3.4.3 Evaluation of single amino acid analogues as PKAC α and AKT inhibitors.

The first set of single amino acid analogue compounds with the vinyl ketone was tested for their inhibitory properties in a biochemical fluorescence resonance energy transfer (FRET) assay (Z'-LYTE kinase assay, Ser/Thr kit 1 and 6, Invitrogen, assays were run as published in reference 34)³⁴ using commercially available recombinant PKAC α and AKT1 (Invitrogen, P2999). This assay utilizes proprietary peptides that serve as substrates for the target enzyme and are labeled with coumarin and fluorescein at opposite ends for FRET action. The kinase (PKAC α or AKT1) transfers a phosphate to the substrate from ATP. The reaction is halted and the FRET signal measured. The detectable FRET signal is only from phosphorylated substrate where the coumarin and fluorescein are still connected by the substrate scaffold. Unphosphorylated peptide is cleaved by a proprietary protease provided in the kit. The proteolytic action prevents FRET from occurring with the unphosphorylated substrate. Therefore, a decrease in FRET signaling is indicative of decreased enzymatic action. The compounds added that decrease FRET signaling can be interpreted as inhibitors of PKAC α or AKT1. However, whether these are ATP or substrate competitive inhibitors is, generally, not discernable from these data.

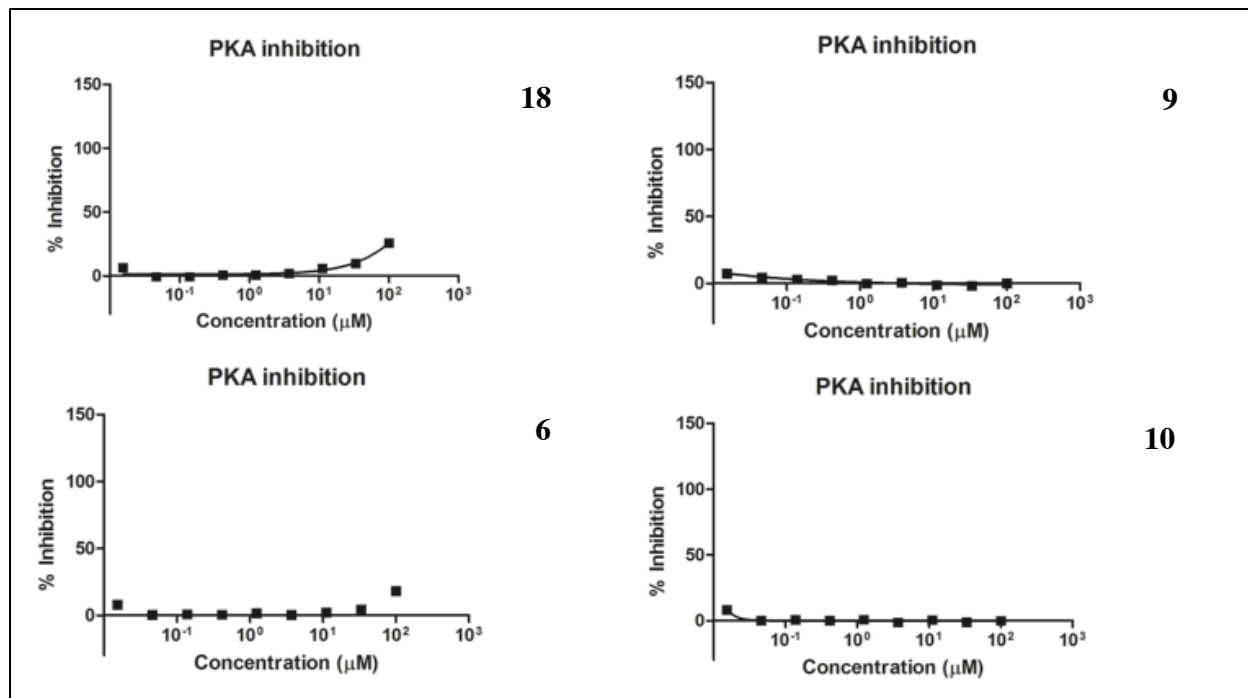


Figure 26. PKAC α inhibition graphs.

Table 10. PKAC α IC $_{50}$'s by Z'Lyte Assay

Compound	PKAC α IC $_{50}$ (μM)
3	56.2 ^a
6	>100
9	>100
10	>100
18	>100

Table 10. a: value obtained from reference 24.³⁴

3.4.4: Results of Single Amino Acid Analogues

The four compounds were tested against PKAC α in triplicate. These compounds did not show any inhibition at concentrations up to 100 μ M. This observation could be attributed to a number of factors. It is possible the vinyl ketone Michael acceptor is too reactive and is essentially used up non-specifically before it can alkylate a residue that inhibits the enzyme. It is also possible that the cysteine is not as accessible when the full length peptide is not present and therefore the electrophile cannot reach the cysteine, although previous attempts with single amino acid analogues by other groups were successful (see Chapter 1). Another possibility that more closely matches previously published results is that the reactivity of Cys199 towards external electrophiles is significantly reduced in the presence of ATP (at various physiologically relevant concentrations, see chapter 1 Type IV inhibitors of PKAC α , section 1.3); therefore, the inhibitory effect seen by alkylation of Cys199 would not have occurred and the amino acids alone would not have sufficient binding affinity to inhibit activity.

Three of the single amino acid analogues were also tested against AKT1 in triplicate using the Z'Lyte assay. The purpose of testing against AKT1, another AGC kinase, was to provide valuable selectivity data. AKT1's hydrophobic pocket at the P+1 position has been demonstrated to be better suited for aromatic moieties and it was hypothesized that we could obtain selectivity both for and against AKT1 via this mechanism. AKT1 was selected due to both its similar consensus sequence with PKAC α (RXRXXSF and RRXS respectively) and its availability in our lab. The results are displayed below.

Compound	AKT1 IC ₅₀ (μM)	95% Confidence Int	PKACα IC ₅₀ (μM)
3	0.58 ^a	.46-.75	56.2 ^a
6	1.56	1.36-1.78	>100
9	12.32	9.89-15.35	>100
10	-	-	>100
14	2.44	1.23-2.76	-
18	-	-	>100

Table 11. Summary information of AKT1 and PKACα inhibition.

Table 11. a: value obtained from reference 24.³⁴

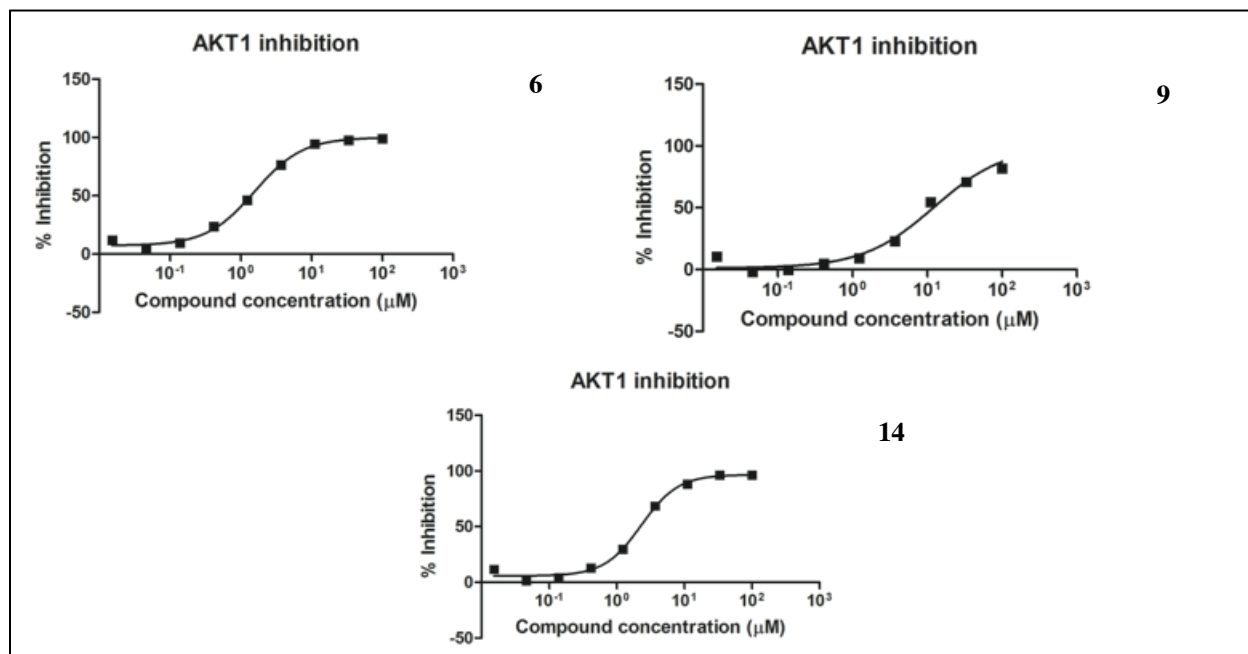


Figure 27. AKT1 inhibition.

In all cases, compounds that were tested against both enzymes (**3**, **6**, **9**) indicated they were more potent inhibitors of AKT1 than PKAC α . Compounds **3**, **14**, **9**, and **6** had 0.58, 2.44, 12.32, and 1.56 mM activity, respectively. It was not unexpected that the phenylalanine analogues would have better activity than the glycine analogues. This is particularly true when considering that the available data for TPCK, a phenylalanine based chloromethyl ketone commercially available and commonly used as a protease inhibitor, was demonstrated to have selectivity for AGC kinase cysteines in the activation loop that have a phenylalanine hydrophobic pocket adjacent to the cysteine of interest.³⁵

3.4.5: Discussion of the Single Amino Acid Analogue Results

After review of the data and available literature it was determined that, first, the single amino acid residues would not provide the desired properties to reliably target Cys199. Second, the single amino acid analogues would not provide the selectivity required for activity-based protein profiling on either a family or target selective scale (for the kinome). Third, that the vinyl ketone is too reactive of an electrophile to be reliably used and stored under mild conditions for extended periods of time (a logistical consideration). Lastly, it appears reactivity of Cys199 is not as robust as indicated with pure enzyme and it is necessary to increase the amount of time the electrophile is in proximity of the thiol side chain for adequate alkylation to occur. Therefore, a new hypothesis was needed to address issues of reactivity, selectivity, and binding action.

3.5 Production and Evaluation of Longer Peptide Probes

By returning to the original structure-based design approach of PKI complexed with PKAC α it was concluded that there are a minimum number of amino acids from the inhibitor peptide required for the preparation of an activity based probe with the necessary properties. It

was also hypothesized that there was a need for more stable electrophiles and that, despite their weaker reactivity, the appropriate placement by the PKI scaffold would be enough for sufficient labeling at Cys199. Additionally, new assays were required to address the need to determine if labeling was occurring in addition to the inhibitory properties. Therefore the Z'Lyte assay was no longer sufficient for the purposes of characterization (as a stand alone indicator), and a new method to assist in determining the mechanism of action was required.

3.5.1 Experimental design.

It was decided that gel electrophoresis techniques would allow for a more mechanistic characterization of new probes (as compared to the FRET assay). The initial experiments focused on fluorescence detection techniques using compounds tagged with rhodamine and different electrophiles. To perform these experiments, sufficient amounts of probe and a large scale source of protein were required. As a result, manual solid phase peptide synthesis to produce the peptide scaffold for the probe, solution phase organic synthesis to produce large quantities of a reactive rhodamine derivative, solution phase organic synthesis to produce the electrophiles, and recombinant protein expression for the preparation of PKA α presented themselves as solutions to the problem.

The general strategy selected for the production of probe involved a combination of synthetic steps that took place both on solid phase and in the solution phase with a (necessary) two-phase purification work up. The peptide was to be synthesized on a super acid-sensitive resin. The final N-terminal deprotection was to be done on the resin, then a tag could be placed on the N-terminus while still on solid phase using basic S_N2 conditions. The use of a super acid-sensitive resin is critical to the successful synthesis of these probes. The super acid-sensitive resin allows for orthogonal deprotection from the resin while maintaining the side chain

protecting groups on the amino acids. The side chain protecting groups prevent undesired coupling at later stages in the synthesis, not just for the Fmoc-based solid phase synthesis.

The 2-chlorotriyl chloride (2-CTC) resin was selected to be the solid support system for our Fmoc-based peptide chemistry. The 2-CTC resin has a number of desirable properties. It has been proven effective in Fmoc-based peptide syntheses.¹²³ The cleaved alcohol resin can be regenerated with thionylchloride to produce the original 2-CTC species, if desired.¹²⁴ It is not patent protected and is generally cheaply commercially available from multiple vendors in various preparations. Perhaps most importantly, it is super acid-sensitive, which means we can use a <3% TFA solution in dichloromethane to remove the peptide from the resin.¹²³ These weakly acidic conditions will preserve the side chains of the amino acids necessary as part of the PKI scaffold and allow for subsequent orthogonal chemistry.

The fluorescent tag rhodamine was selected for the development of the first round of peptide-based probes. Many derivatives of rhodamine are available, as it is a common fluorophore. However, we needed relatively large quantities of a reactive rhodamine derivative to synthesize our probes and commercially available analogues were generally cost prohibitive. Therefore, the synthesis began with the generic rhodamine B which is very economical. For a linker, N-methylamino butyric acid was coupled. This route was adapted from a previously reported synthesis and improved upon it to prepare our rhodamine-NHS ester in large quantities.^{125,126}

The electrophile was reevaluated and based on available data it was determined to move forward with the chloromethyl ketone. The chloromethyl ketone has a variety of pros and cons for its usage in ABPP. Very much in its favor is its selectivity for cysteine over other amino acids. It is also relatively small and can be incorporated into various scaffolds. Conversely, its

synthesis it difficult and requires the use of a potentially explosive diazomethane intermediate. As a result the first priority was to identify a different route to the chloromethyl ketone that did not require diazomethane.

3.5.2 Preparation of the Chloromethyl Ketone

In an attempt to avoid using diazomethane as the intermediate to the production of chloromethyl ketone, a new synthetic route was explored that would allow the production of glycine chloromethyl ketone without the need for the specialized equipment to produce diazomethane. The initial starting materials benzylamine and epichlorohydrin are commercially available. Mixing benzylamine and epichlorohydrin in cyclohexane at ambient temperature for 16 hrs produces **25**. Followed by addition of the Boc protecting group, this is important if one desires to acid deprotect in the end and produce the stable HCl salt. The Boc group was added using Boc anhydride in dichloromethane at ambient temperature for 16 hr to produce **26**. The alcohol was oxidized to a ketone by Swern oxidation conditions to produce the doubly protected chloromethyl ketone (**27**). Finally the benzyl group was removed with Pd(OH)/C in ethanol (Pd/C was not effective at removing this group), and hydrogen at 1 atm for 16 hr. While this did produce the desired chloromethyl ketone in quantities to move forward, we would need large quantities and the yield was relatively poor at this time (conditions were not optimized).

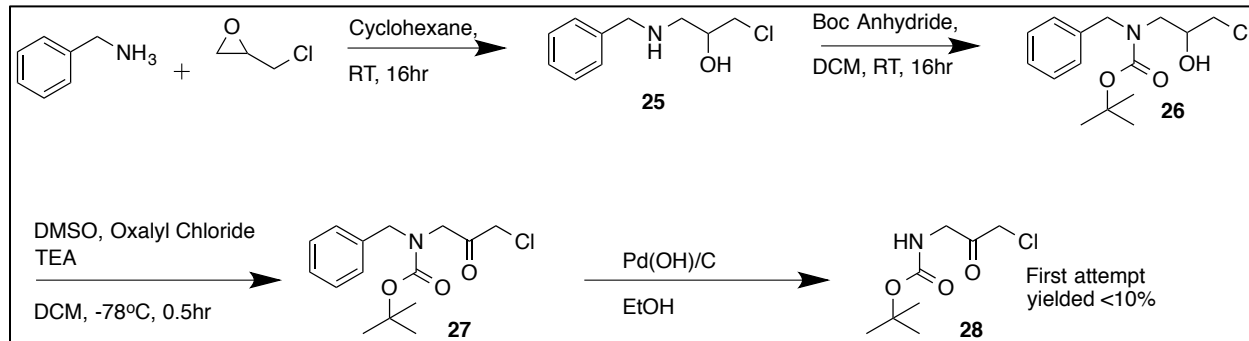


Figure 28. Alternative route to glycine chloromethyl ketone.

As a result, the use of diazomethane chemistry to produce the selected chloromethyl ketone moiety for incorporation into our probe was necessary. To produce the diazomethane intermediate, the mixed anhydride of the Boc-protected amino acid must be produced.¹²⁷ This is done by incubating the Boc-protected amino acid with isobutyl chloroformate in tetrahydrofuran with *N*-methylmorpholine as the base at -20 °C for 0.5 hr. Diazomethane is prepared from a stable, commercially available, derivative: Diazald. Diazald is broken down into diazomethane with KOH, the resulting diazomethane is then distilled with ether into a separate flask and kept cool in an ice bath. The diazomethane ether solution is poured directly into the mixed aldehyde produced in the previous steps and allowed to react for 4 hr, while the remaining diazomethane is quenched. The Boc protected amino acid with the diazomethane moiety is stable enough for purification. This product is treated with 4 N HCl in dioxane and monitored by TLC until completion. The resulting HCl salt can be crashed out by triturating with ether allowing for easy isolation without the need for column chromatography (Figure 29).¹²⁷

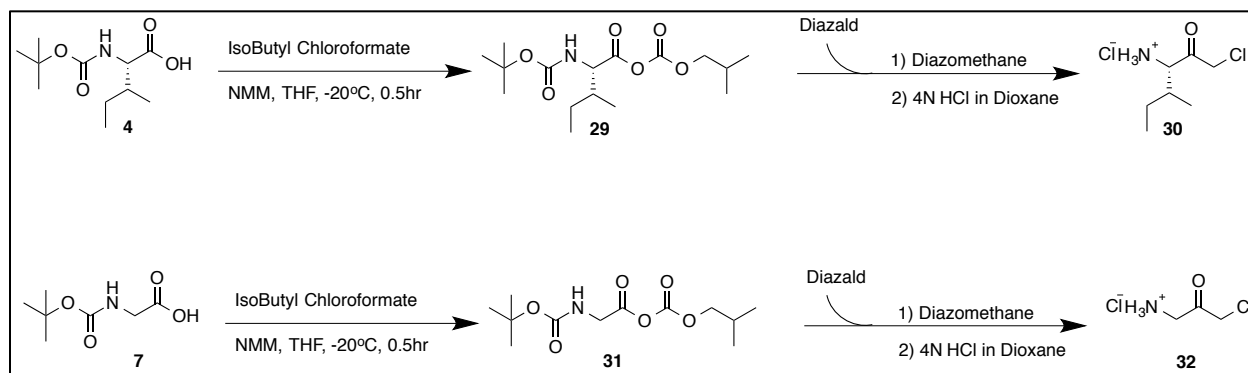


Figure 29. Diazomethane route to chloromethyl ketone formation.

3.5.3: Preparation of Rhodamine-NHS Ester.

The need for an abundant source of fluorophore led to an extensive search of the literature for a method to rapidly access large quantities of a reactive rhodamine derivative. What was found was a derivative of rhodamine B that would provide a linker and the ability to make the NHS ester for nucleophilic substitution onto the N-terminal of the peptide.^{125,126} Starting with rhodamine B, a standard coupling was performed with *N*-(3-dimethylaminopropyl)-*N'*-ethylcarbodiimide (EDCI), *N*-hydroxysuccinimide, and dichloromethane (DCM) as the solvent at ambient temperature for 16 hr. The resulting NHS ester **35** is ideal for the S_N2 chemistry we employed to attach the *N*-methylamino butyric acid. The secondary amine is critical for the rhodamine to maintain its fluorescent characteristics; if it were not a secondary amine it would be subject to intramolecular lactam formation and subsequent quenching of the fluorescent

character. The resulting acid **34** is then exposed to a second round of standard coupling conditions, although this time with *N,N'*-dicyclohexylcarbodiimide (DCC), *N*-hydroxysuccinimide, and dichloromethane (DCM) as the solvent at ambient temperature for 16 hr. The final product was crashed out of solution with ether and collected as a viscous resin.

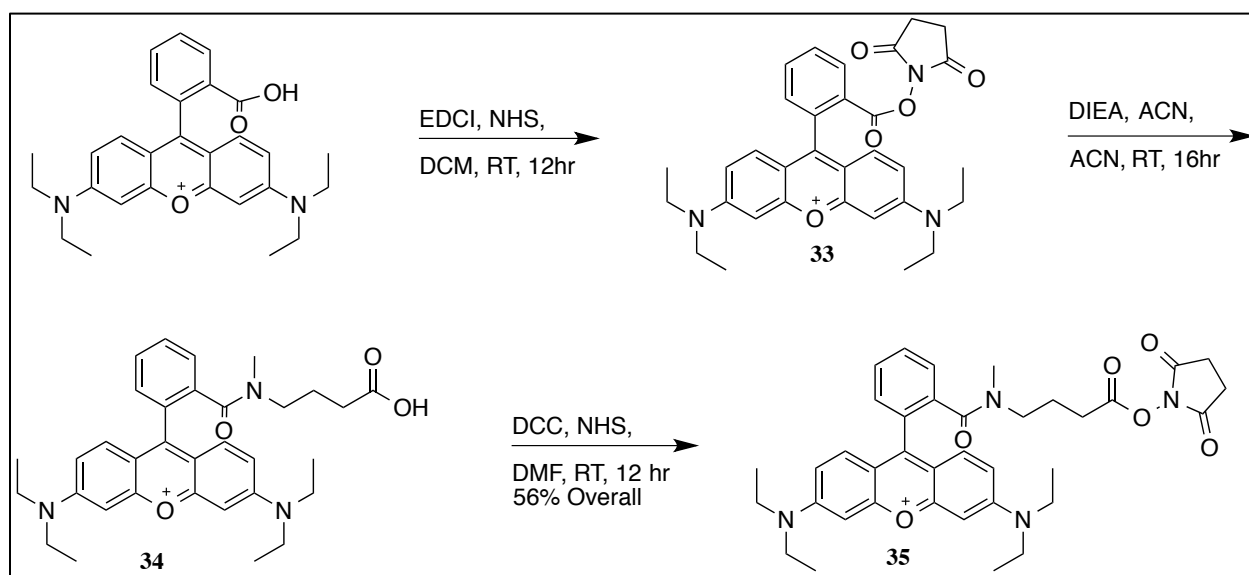


Figure 30. Synthesis of Rhodamine-NHS ester.

3.5.4: Preparation of Peptide Scaffold.

The traditional approach to large scale peptide synthesis relies on the use of solid-phase Fmoc based chemistry.¹²³ The super acid sensitive 2-chlorotrityl chloride (2-CTC) resin was selected as the solid phase support system. It was hypothesized that incorporating the amino acids ¹⁸RRNA²¹ onto the single amino acid Ile(22) (RRNAI) would be adequate for demonstrating the feasibility of the probe and testing against the initial activity-based experiments. Additionally, the consensus sequence for PKACa is RRXS; thus, by incorporating more of the PKI scaffold, the probe now contains the consensus sequence.^{42,55,128} The 2-CTC resin was first swelled with DCM for 5 minutes, then DMF for 5 minutes. Fmoc-Ile-OH was added with triethylamine as the base and allowed to react for 1 hr. Once the first amino acid is loaded onto the resin, iterative fmoc based chemistry can be used to add the additional amino acids. All amino acids were purchased from ChemImpex as Fmoc-protected derivatives. The Fmoc is removed with a 20% piperidine solution. There is a subsequent coupling with the next amino acid in the sequence. This is followed by another deprotection in 20% piperidine. These steps are repeated until the desired peptide is produced.

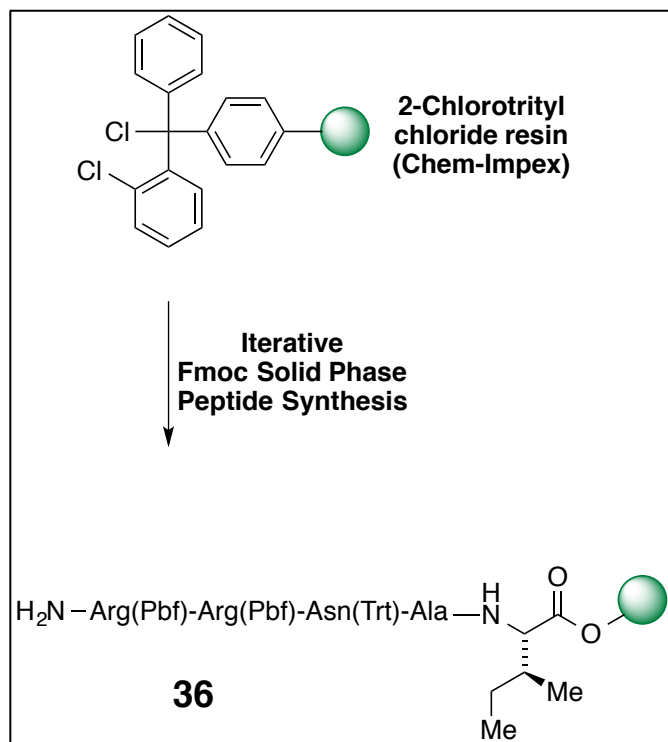


Figure 31. Solid phase synthesis of the pentapeptide.

3.5.5: Assembly of the PentaPeptide Probe.

The glycine chloromethyl ketone was synthesized in the same manner as described above (Scheme 5). The glycine was hypothesized to allow for the greatest maneuverability of the electrophile to accommodate the trajectory of the thiol group on Cys199, while not interfering with the positioning of the important PKI-Ile22 side chain.

The order in which the pieces of the probe are assembled is critical to the successful synthesis. While the peptide is still on the resin it was treated with a solution of Rhodamine-NHS

ester and triethylamine (TEA) in dimethylformamide (DMF). The reaction was stirred for 3 hr, washed with DMF five times, then DCM five times.

The resin-bound product was taken directly to the next step. By attaching the rhodamine while on solid phase the N-terminus is effectively capped, which is essentially for subsequent reactions, and allows for easy work up. Rhodamine-PKI(18-22)-OH was then cleaved from the resin with a 2% TFA in DCM (this preserves the side chain protecting groups). The solvent was removed under vacuum (Scheme 8) and the product was characterized by MALDI mass spectrometry and taken directly to the next step.

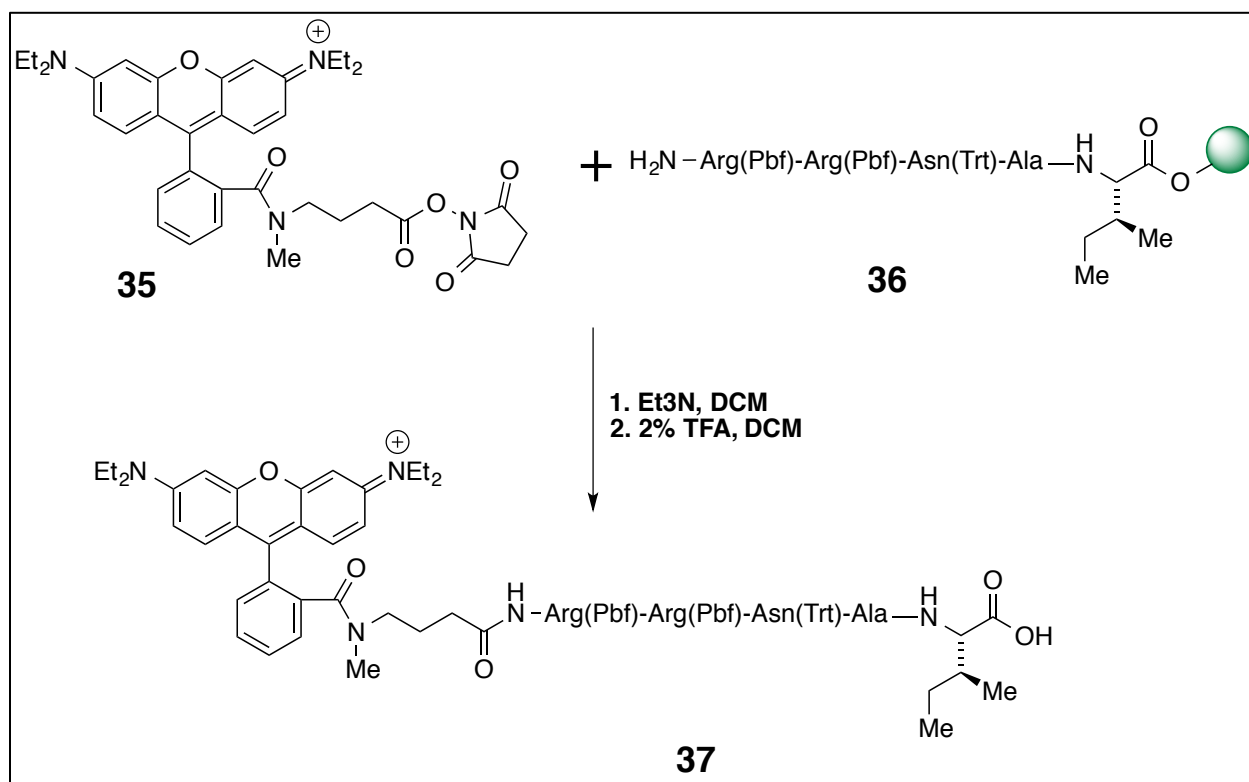


Figure 32. Solid phase addition of rhodamine tag and soft cleavage.

The next reaction is the coupling of the glycine chloromethyl ketone **32**, the peptide is preincubated with (benzotriazol-1-yloxy)tripyrrolidinophosphonium hexafluorophosphate (PyBOP), and diisopropylethylamine (DIEA) in DCM. Then, the glycine chloromethyl ketone was added to the solution. The reaction was stirred for 16 h. Solvent was removed and the purified on a silica gel flash column, 0-30% over 10 minutes MeOH/DCM. The probe is then globally deprotected with 95:2.5:2.5 TFA:TIS:H₂O (5 mL) for 1 hr, and triturated with ether to afford crude product. This product was then purified on HPLC (95:5 to 75:25 H₂O:ACN over 20 minutes). The two-stage purification has proven to be a necessary extra step for the successful isolation of the final product (Scheme 9). Attempts to circumvent the silica column have resulted in the inability to isolate final product with sufficient purity to conduct research.

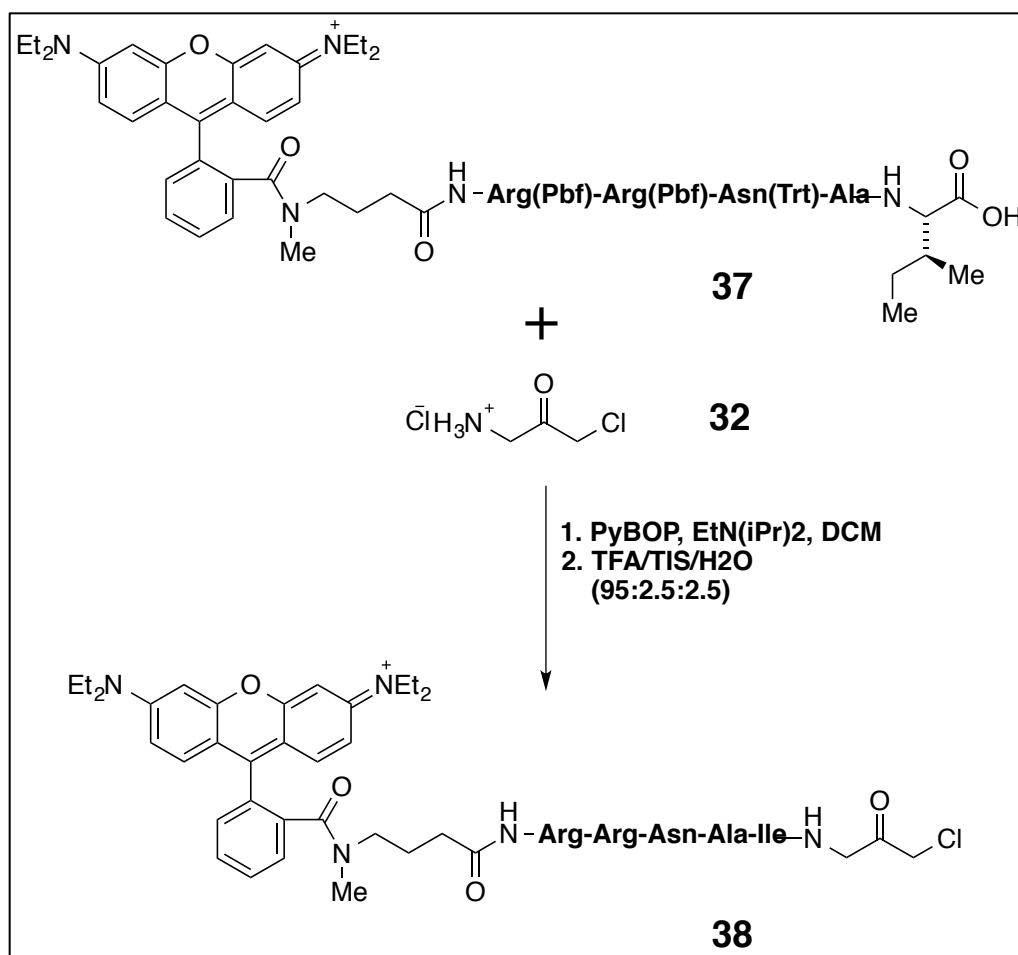


Figure 33. Coupling of the electrophile to **37** to generate **38**.

3.6: First Protein Production Experiments

The initial experiments utilized PKAC α protein prepared using the previously reported procedure by Taylor et al.¹²⁹ The PKAC α plasmid is available from Addgene (Plasmid #14921), The C199A mutant was prepared with a QIAquick exchange kit. PKAC α is particularly suited for expression in bacteria due to its ability to autophosphorylate. Upon transcription PKAC α

undergoes cis phosphorylation at Ser338.¹³⁰ It does undergo autophosphorylation at Thr197; however, this is a much slower reaction and does not result in complete conversion to the fully phosphorylated protein.¹³¹

In mammalian cells, phosphorylation at Thr197 occurs rapidly and irreversibly by PDK1.^{38,130} Competent *E. coli* cells were transformed with the wt or mutant PKAC α plasmid and grown for 16 hr at 37 °C with ampicillin selection and moderate shaking in a test tube. An aliquot was taken into a 1 L Erlenmeyer flask with ampicillin selection and auto-induction media and grown at 37 °C for 16 hr with moderate shaking. Following growth, cells were spun down at 6000 rpm for 10 min, and lysed into buffer (25 mM Tris, pH 8, 300 mM NaCl, and 10 mM imidazole) at ambient temperature. Cellular debris was removed by centrifugation at 20,000 rpm for 30 min and the soluble fraction was decanted onto a nickel column. Following sample loading, the nickel column was washed with 5 column volumes of a non-eluting buffer that prevents nonspecific binding to the nickel (25 mM Tris, pH 8, 300 mM NaCl, and 10 mM imidazole). Isolated PKAC α protein is then eluted with 100 mM imidazole and concentration determined by absorption at 280 nm on a spectrophotometer. Purity was analyzed by Coomassie stain (Figure 34 below).

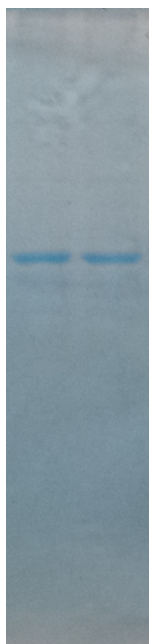


Figure 34. Coomassie stain of purified recombinant PKA C α .

3.6.1 Validation of Rhodamine

Prior to completion of the fully assembled pentapeptide probe it was necessary to determine whether or not the rhodamine analog synthesized could be detected on a GE Typhoon gel imaging instrument. Recombinant PKA C α was incubated with 25 equivalents of Rhodamine-NHS (**35**) for 1 hr at ambient temperature. To the solution was then added a denaturing sample buffer and incubated at 100 °C for 5 minutes before being run on a 10% SDS page gel at 170 V for 1 hr. The gel was imaged on a GE Typhoon gel imager set for detection of the similar TAMARA fluorophore.

As was anticipated, there was robust labeling of all contents of the protein solution. The NHS ester (**35**) is a nonspecific electrophile and will robustly react with all available nucleophiles in solution, if allowed to react for sufficient time in suitable conditions.

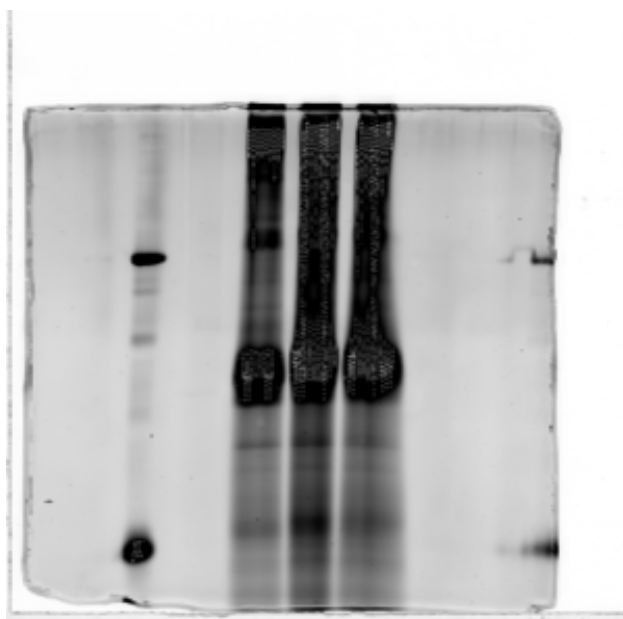


Figure 35. Evaluation of **35**.

3.6.2: Discussion of Rhodamine-NHS Labeling Experiment.

There is significant labeling in the higher molecular weight regions mostly due to how the sample was denatured. The initial experiments did not contain a disulfide reducing agent, such as betameracптоethanol (BME), which was omitted to ensure that there was no reversal of any labeling reactions that may have occurred. This lack of disulfide reducing agent allowed significant intermolecular disulfides to persist during the gel electrophoresis and imaging steps. The described experiment provided the necessary proof for utilizing the rhodamine derivative synthesized in the lab.

3.7: Biological Characterization of the pentapeptide (38) as a probe for PKAC α .

It was decided to examine the new probe for both its ability to inhibit wt PKAC α in the Z'Lyte kinase assay and its ability to label the protein as wt, mutant, and in complex biological mixtures. All gels were cast in house and made to contain 10% acrylamide, following the exact procedure detailed in the experimental. HCT-116 cell lysates are known to overexpress AKT (Cys310 known to be nucleophilic see Chapter 1, section 1.3), these were procured in and supplied by Dr. Richard G Moran's lab in the pharmacology and toxicology Department of VCU.

Multiple gel electrophoresis experiments were conducted to characterize the pentapeptide probe and its interactions with various substances. The first gel electrophoresis experiment shown below examined the labeling of the pentapeptide probe with wt recombinant protein, C199A mutant, the HCT-116 cell lysates, and the HCT-116 cell lysates spiked with wt recombinant protein. The ladder was purchased from Biorad and run at 1:100 dilution for fluorescence experiments and at 1x for colorimetric experiments. For lanes containing wt protein recombinant PKAC α was incubated in phosphate buffer (25 mM PO₄ pH 7.2) with different concentrations of probe for 1 hr at ambient temperature. The samples were quenched with a denaturing sample buffer with bromophenol blue marker and incubated at 100 °C for 5 min. The resulting solution was loaded onto the gel and run at a constant 170 V for 1 hr. The C199A mutant was incubated in the same manner and conditions as the wild type protein. The HCT-116 cell lysates were incubated in identical conditions. The additional HCT-116 cell lysate lanes were spiked with recombinant PKAC α prior to incubation with probe. Then, all lanes were imaged on a typhoon imager.

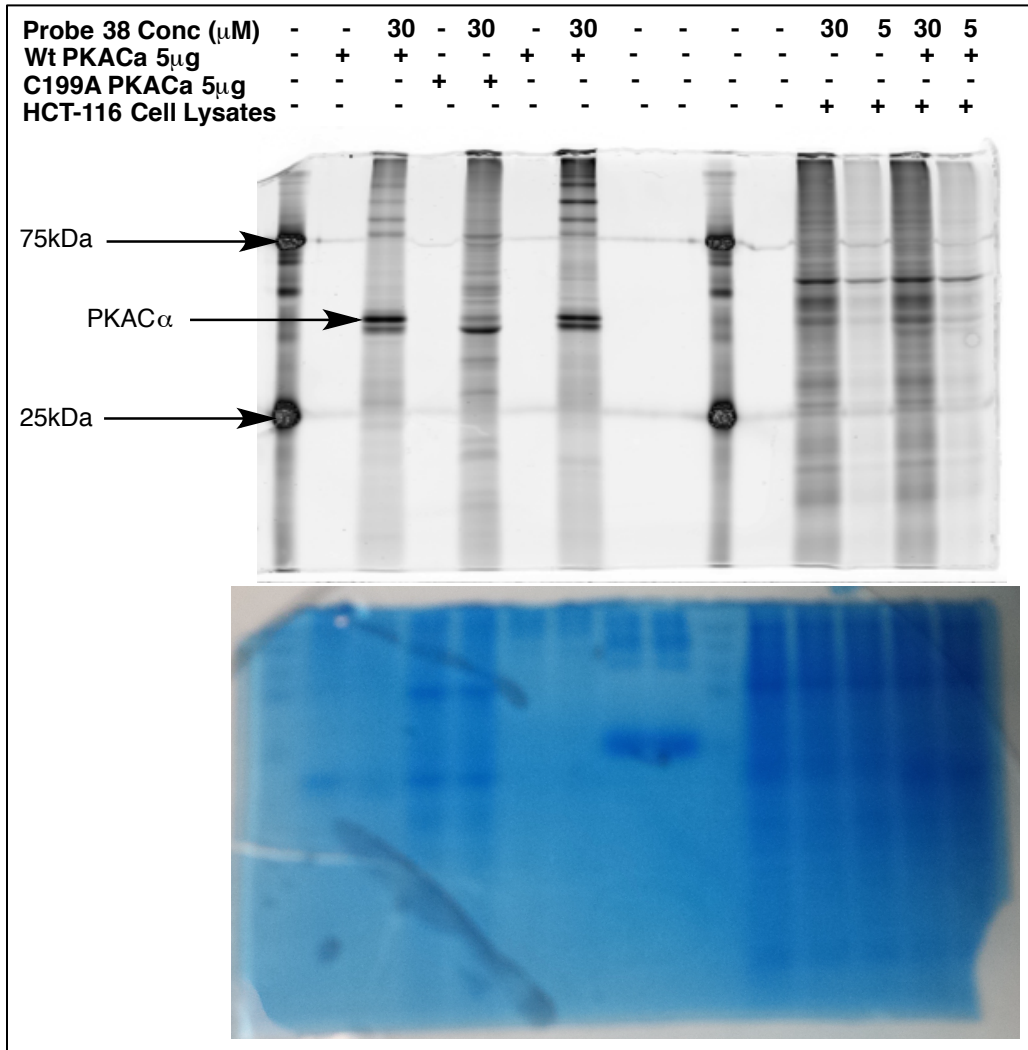


Figure 36. Examination of Probe **38** with wt PKAC α (lanes 2, 3, 6, and 8), C199A (lanes 4 and 5), and HCT-116 cell lysates (lanes 11-15).

3.7.1: Discussion of Figure 36.

This gel (Figure 36) demonstrates a number of positive characteristics of the probe and provides significant data with which to move forward. Due to the nature of how gels work, it can be concluded that the probe does in fact covalently label the protein in an irreversible manner. The labeling by the probe was robust and easily detected. The probe did not label non-selectively in the HCT-116 cell lysates, meaning that there is not aberrant labeling throughout the lane. What is particularly interesting is the location of the single band in lanes 13 and 15, which contain 30 mM of probe **38** and 16 μ g of lysates. This band strongly correlates with the molecular weight of AKT1, and matches some of this lab's previous results.³⁴ It is also important to note that the cysteine in AKT1 was found to be nucleophilic (see chapter 1, section 1.3). Probe **38** displays remarkable selectivity in a complex biological mixture. Additionally, high selectivity for the upper band was retained in extreme excess of recombinant protein, it is possible that bio reagents (such as ATP) in the lysate are inhibiting labeling of PKA α . The probe did however label the C199A mutant of PKA α , which was unexpected in that the probe was designed to only react with Cys199. It may be possible that the probe is alkylating another residue. There is precedent with Lysine-72 being alkylated by a fluorosulphone analog, by Taylor et al.¹³² However, Lys72 is not located in the substrate-binding site. There is another cysteine residue. However, it is not located near the substrate-binding site either.

3.7.2: Activity-based ATP effects on labeling.

To further examine the characteristics observed in the gel above and to test the hypothesis that ATP may be inhibiting labeling, another gel (Figure 29) was run. Only recombinant PKA α was run on this gel and various biologically relevant conditions were examined. Physiologically relevant levels of magnesium chloride were examined: the Mg²⁺ cation is required for efficient

catalytic activity and substrate turnover.^{80,82,93} ATP was examined at 1 equivalent to the enzyme (~5.8 μM). These conditions were introduced prior to incubation with the probe. Additionally, fluoresceine-maleimide and Rhodamine NHS-ester were utilized as well. The incubation conditions for each of the probes were identical and are as follows. Recombinant PKAC α was incubated in phosphate buffer (25 mM PO₄ pH 7.2) with different concentrations of probe and physiologically relevant substances for 1 hr at ambient temperature. The samples were quenched with a denaturing sample buffer with bromophenol blue marker and incubated at 100 °C for 5 minutes. The resulting solution was loaded onto the gel and run at a constant 170 V for 1 hr.

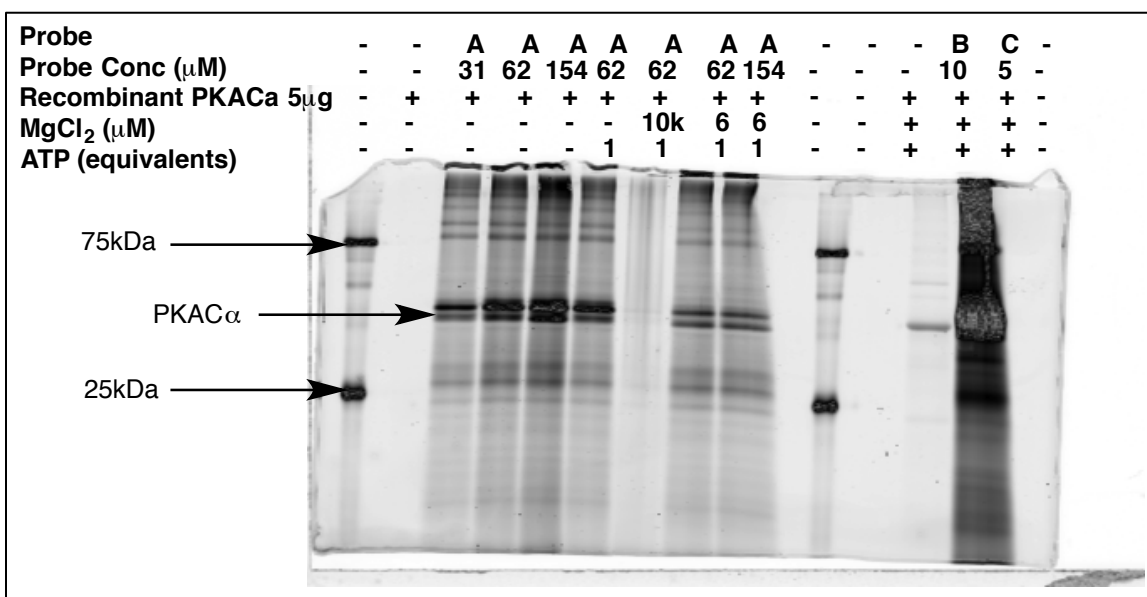


Figure 37. Examination of A = 38, B = fluoresceine-maleimide, and C = 35.

3.7.3: Results and Discussion of Figure 37.

As was demonstrated in the previous experiment, robust labeling occurs when recombinant protein and probe are incubated together without any other additives. However, when ATP is introduced (1 equivalent) to the incubation conditions, a slight reduction in labeling

is noted (lane 6). Upon addition of 10 mM MgCl_2 , labeling is completely abolished (lane 7). Addition of 1 equivalent of MgCl_2 causes a reduction in labeling (lanes 8 and 9). Fluoresceine-Maleimide and Rhodamine-NHS both label robustly; however, fluoresceine-maleimide appears to only label one band of PKAC α (lane 13). The rhodamine-NHS labels nonspecifically (lane 14).

Both a divalent metal ion (such as Mg^{2+}) and ATP are required for efficient phosphate transfer to a substrate (it will occur in the absence of, but not efficiently).⁸⁰ The addition of 1 equivalent of ATP incurred a minor reduction in labeling efficiency by the probe. This is an unfortunate observation in that physiologically relevant concentrations of ATP are significantly higher than those examined in the gel (3-10 mM).¹³³ Also, addition of the MgCl_2 salt at 10 mM concentration completely abolished labeling (this is the salt concentration used in the inhibition assays to be discussed below). While robust labeling is observed, the probe will not label in active-like conditions, which excludes it from being classified as an activity-based probe for PKAC α ; however, selective labeling of what appears to be AKT in the cell lysates is a positive result.

3.7.4: Inhibition of PKAC α with RAC-1-280.

To determine whether or not the probe was an effective inhibitor of wt PKAC α , the Z'Lyte kinase inhibition assay kit was utilized. The IC_{50} of probe **38** was determined to be 6.9 μM . While the IC_{50} was higher than would be expected for a covalent inhibitor, it is clear from the gel experiments labeling is most likely inhibited in conditions that would allow for phosphoryl transfer. It may be that the same protective features the previous Type IV irreversible inhibitors (see Chapter 1, section 1.3) encountered with ATP in the inhibition assay are at work.

As well as from MgCl_2 , the inhibition assay conditions are run at 10 mM MgCl_2 (Invitrogen Z'LYTE manufacturer protocol). This concentration of MgCl_2 was shown to completely abolish labeling. Therefore, the IC_{50} may only be indicative of the reversible peptide. The intention was that this data, in conjunction with the mechanistic data gleaned from the *in vitro* gel experiments, would validate the probe. The IC_{50} data plus the lack of selectivity for PKAC α in a complex biological mixture leads to a hypothesis that more of the inhibitor peptide sequence PKI was needed to obtain selectivity for PKAC α and to produce an activity-based probe.

3.7.5: DFG Sequence Alignment.

To determine the broad applicability of the method to the kinome, a sequence alignment was performed on the eukaryote protein kinome. It was determined that 99 human protein kinases share a similar cysteine in the activation loop. Among them is AKT1 (discussed in Chapter 1, section 1.3), and the homologous PKG (from the same family of AGC kinases). The results of the alignment are shown in the experimental (Chapter 4, Figure 69). The cysteine that corresponds to the position in PKAC α is highlighted in a red box. Other cysteines in the activation loop are highlighted in orange text and present potential targets by a similar strategy; that is a substrate based small molecule/peptide with an appropriately placed electrophile could have the potential to react with these cysteines in an activity-dependent manner. The alignment and analysis was performed with ClustalX 2.1 and the kinome fasta file was obtained from kinase.com.

3.7.6: Discussion of the Pentapeptide Experiments.

The pentapeptide analogue (Rh-PKI(18-22)-G-(CMK)) provided significant strides in the production of active-site directed probes for the lab and established protocols for labeling and imaging various samples. The rhodamine derivative synthesized was proven effective at labeling and detection. The synthesis that was modified to obtain large quantities of the rhodamine-NHS proved to be easily replicated and to have agreeable yields. The glycine chloromethyl ketone moiety was shown to effectively label recombinant PKAC α . The synthesis of the entire probe was a significant step as well and the two-stage purification was shown to be necessary and this synthesis is easily applied to other peptides and compatible electrophiles. This is the synthetic method that was carried forward to the remaining probes. The probe also displayed remarkable selectivity in HCT-116 cell lysates, albeit not for PKAC α , but it is important to note that the chloromethyl ketone moiety will readily react with free sulfurs and the level of selectivity observed is a significant result. Additionally, the band that is labeled occurs at a molecular weight consistent with the molecular weight of AKT, which has a nucleophilic cysteine (Cys310) that has been demonstrated to react with various electrophiles (see chapter 1, section 1.3).

The characterization of (Rh-PKI(18-22)-G-(CMK)) also revealed a number of negative attributes. Labeling can easily be abolished with physiologically relevant concentrations of MgCl₂. ATP appears to have a protective effect on (Rh-PKI(18-22)-G-(CMK)) labeling of wt PKAC α . (Rh-PKI(18-22)-G-(CMK)) does not label PKAC α in HCT-116 cell lysates (to a detectable level), even when the sample was spiked with excess PKAC α . The IC₅₀ determined by the Z'Lyte kinase assay was indicative of reversible kinetics (high IC₅₀ and a hill slope of 1). The

data would suggest that, despite (Rh-PKI(18-22)-G-(CMK)) being an active-site directed probe, it is not an activity-based probe in that it actually is prohibited from labeling in conditions conducive to catalytic activity.

It was decided at this point to synthesize a larger portion of PKI in order to gain affinity for the catalytic subunit and subsequently increase labeling. PKI(14-22)-Amide has been shown to retain suitable affinity for PKAC α (K_i 36 nM) while being synthetically accessible at 9 amino acids in length. Therefore, the next analogue synthesized was Rh-PKI(14-22)-Gly-(CMK)

3.8: Preparation of PKI(14-22)Gly-CMK

The same order of operations was utilized to complete the synthesis of PKI(14-22)Gly-CMK. The 2-CTC resin proved to be a valuable resin for this synthetic route and resin preloaded with Ile was purchased from ChemImpex. The same batch of glycine chloromethyl ketone produced utilizing the diazomethane intermediate was used. The synthetic route we chose to make our rhodamine NHS ester provided us a route that enabled large scale production; therefore, we did not have to synthesize more for the production of this probe as the previous batch was sufficient. An additional step was added to the peptide synthesis, an acetyl capping step to cap off any uncoupled N-termini after each coupling step.

Schemes 10 and 11 depict the production of the PKI(14-22)-GlyCMK probe. Briefly, 2-chlorotrityl chloride (2-CTC) resin preloaded with Ile was purchased from ChemImpex (200-400 mesh, Catalog #03472). Peptide couplings were carried out manually via standard Fmoc amino acid protection chemistry. Amino acids were activated and added to resin with (benzotriazol-1-yloxy)tripyrrrolidinophosphonium hexafluorophosphate (PyBOP) and diisopropylethylamine (DIEA). The resin was swelled with DCM (5 min) then DMF (5 min). All amino acids were added by the general procedure that follows (with the exception of Arg, which underwent double

couplings): Fmoc deprotection (20% piperidine in DMF, 3 x 5 min), wash with DMF 3x, amino acid coupling (PyBOP, DIEA 0.1 M in DMF, 1 hr, 2x for Arg), wash with DMF 3x, acetyl cap (pyridine:acetic anhydride 20:20, 0.15 M in DMF, 30 min). After the final deprotection (Gly 14) with 20% piperidine in DMF, the resin-bound product was taken directly to the next step.

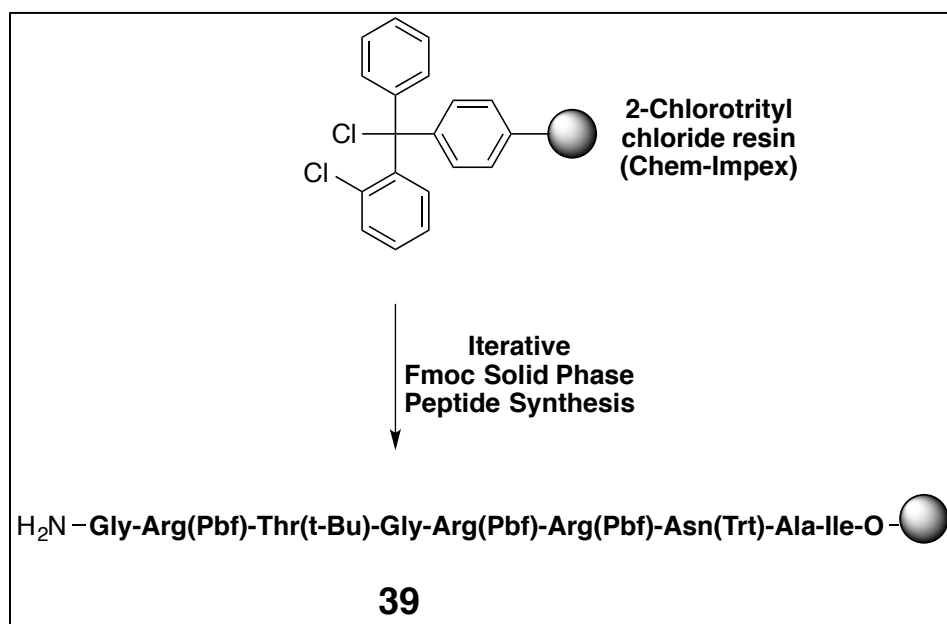


Figure 38. Iterative solid phase synthesis of **39**.

While the peptide is still on the resin it was treated with a solution of RhodamineNHS ester and triethylamine (TEA) in dimethylformamide (DMF). The reaction was stirred for 3 h, washed with DMF 5x, then DCM 5x. The resin-bound product was taken directly to the next step. By attaching the rhodamine while on the solid phase the N-terminus is capped, which is essential for subsequent reactions, and allows for easy work up. Rhodamine-PKI(18-22)-OH was then cleaved from the resin with a weakly acidic solution of TFA in DCM (2% v/v). The solvent was removed under vacuum and product taken directly to the next step. The next reaction is the

coupling of the glycine chloromethyl ketone **32**, where the peptide is preincubated with (Benzotriazol-1-yloxy)tripyrrolidinophosphonium hexafluorophosphate (PyBOP) and diisopropylethylamine (DIEA) in DCM. Then the glycine chloromethyl ketone was added to the solution. The reaction was stirred for 16 hr. Solvent was removed and the purified on a silica gel flash column, 0-30% over 10 minutes MeOH/DCM. The probe is then globally deprotected followed by trituration with ether to afford crude product. Product purified on HPLC.

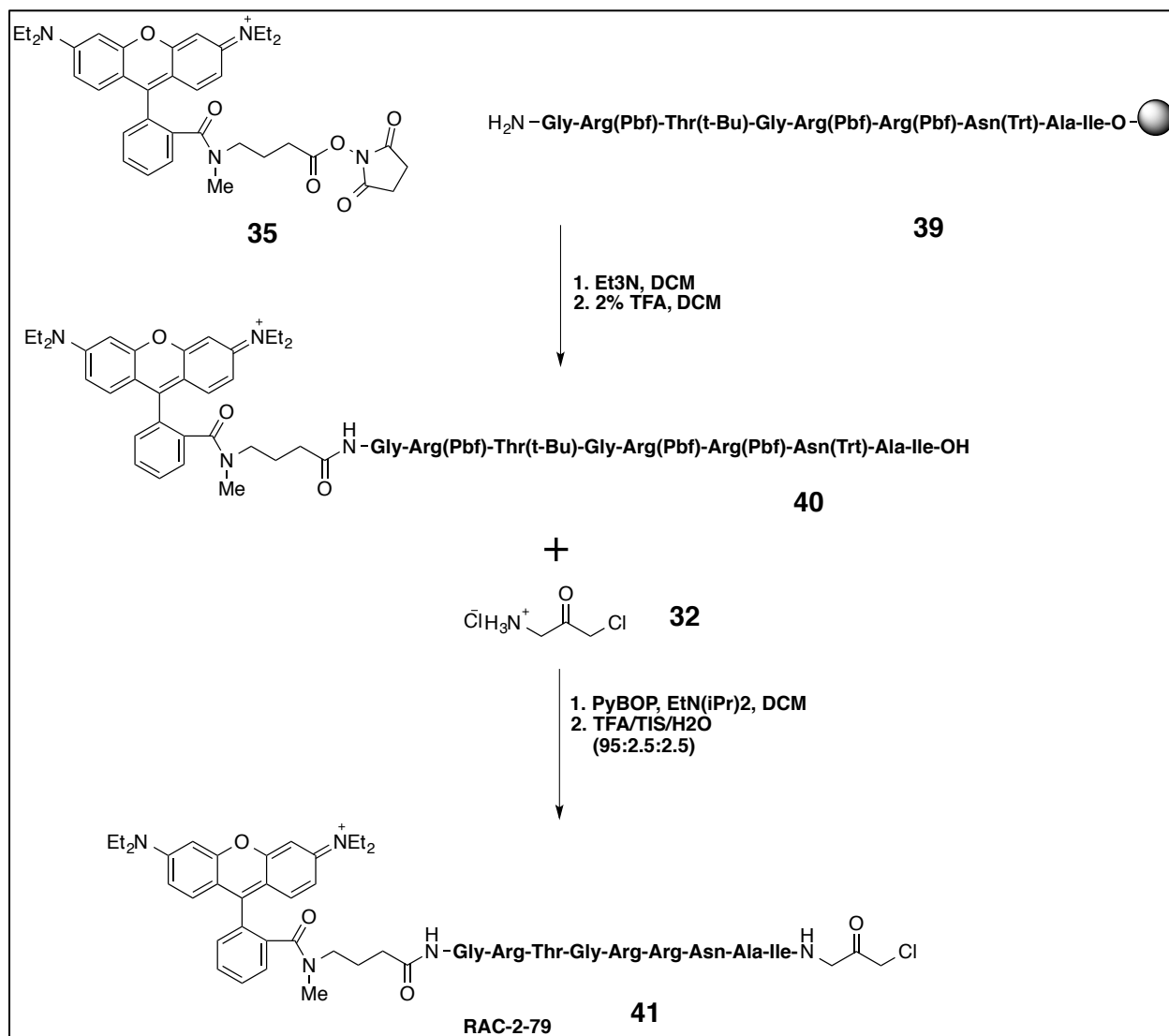


Figure 39. Mixed solid phase and solution phase chemical assembly of **41**.

3.9: Biological Characterization of Rh-PKI(14-22)-G-(CMK).

In a similar setup, the longer length probe was examined for its ability to label PKA α . The limit of detection for protein amounts was examined. The saturability of labeling was examined with non-covalent Myr-PKI(14-22)-Amide, which examines a number of characteristics and will be discussed after in section 3.9.2. The labeling of the cysteine to alanine mutant (C199A) examined the residue being labeled. Oxidation of the cysteine was attempted in order to mimic the endogenous regulatory mechanism of glutathiolation. Labeling under different pH conditions examined the differences in the two bands. The Coomassie stained gels and fluorescent gels of applicable experiments underwent secondary analysis due to their overlap and the predominant band species was determined and examined. Additionally, the protein production was modified to better represent physiological conditions (see section 3.9.11). All gels were cast in house and made to contain 10% acrylamide, the exact procedure is detailed in Chapter 4, the biological experimental section.

3.9.1: Protein—Probe Limit of Detection.

Many gel electrophoresis experiments were conducted with the nonapeptide-based probe. The first, of note, is detailed below where the limit of detection of protein in the presence of excess probe was examined. Protein concentration was determined by absorbance at 280 nM and diluted such that it was 1 mg/mL in phosphate buffer (25 mM PO₄ pH 7.2). The probe was made as a 10 mM stock in DMSO and diluted accordingly for appropriate final concentrations in the gel experiments. The gel was cast as 1.5 mm thick and the wells were a total volume of 20 μ L. The samples were quenched with a denaturing sample buffer (made in-house and described in the experimental) and incubated at 100 °C for 5 minutes. The denaturing sample buffer did not contain a disulfide reducing agent (such as betamercaptoethanol, BME).

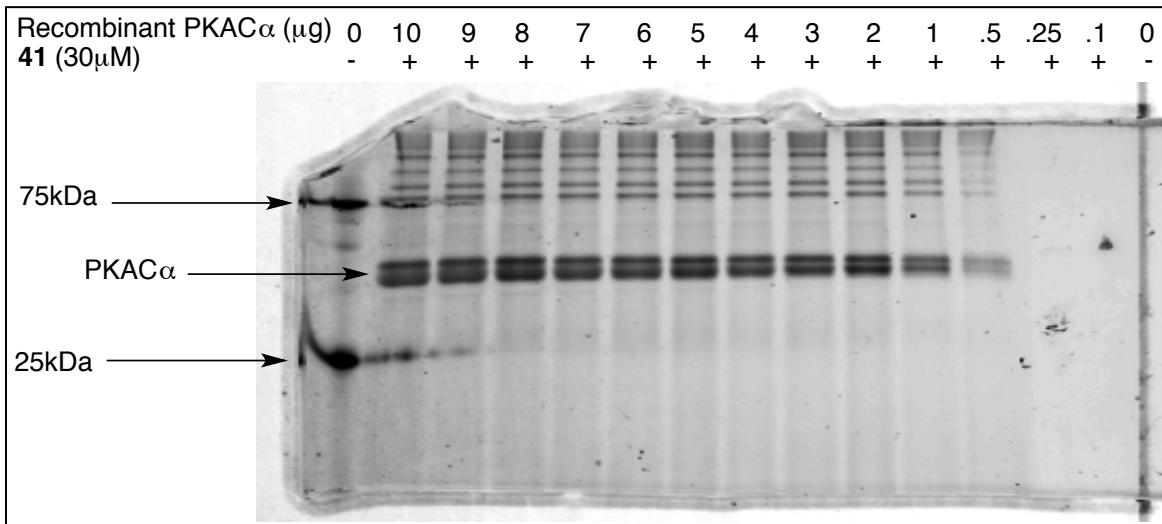


Figure 40. Protein concentration detection analysis.

3.9.2: Results and Discussion of Figure 40.

The Rh-PKI(14-22)-G-(CMK) probe displays robust labeling of isolated recombinant PKAC α at varying amounts. The last prominent labeling signal is observed at 2 μ g of recombinant protein; 1 μ g and less does not provide as potent signal. The lack of disulfide reducing agent is apparent in the upper portions of the gel (indicating higher molecular weight); these are most likely intermolecular disulfide bonds. The double banding of recombinant PKAC α is observed again. The extended length of the peptide recognition scaffold did not provide the level of selectivity desired for single band images at all observable protein concentrations. It is clear that optimization is necessary moving forward for a gel image that consists of only one band.

3.9.3: Mutant labeling experiments.

In order to fully characterize the mechanism of action of the Rh-PKI(14-22)-G-(CMK) probe, additional gels were run to examine the effects of other changes. In Figure 41 below, the labeling characteristics of the probe were examined against the cysteine mutant of PKA α (C199A) and limit of detection experiments were included with a lower concentration of probe. Both protein concentrations were determined by absorbance at 280 nm and diluted such that it was 1 mg/mL in phosphate buffer (25 mM PO₄ pH 7.2). The probe was made as a 10 mM stock in DMSO and diluted accordingly for appropriate final concentrations in the gel experiments. The gel was cast as 1.5 mm thick and the wells were a total volume of 20 μ L. The samples were quenched with a denaturing sample buffer (made in house and detailed in the biological experimental section) and incubated at 100°C for 5 minutes. This time the denaturing sample buffer did contain a disulfide reducing agent (betamercaptoethanol, BME). Coomassie staining was performed with blue G250 in a H₂O/MeOH/AcOH solution, and destained with a H₂O/MeOH/AcOH solution.

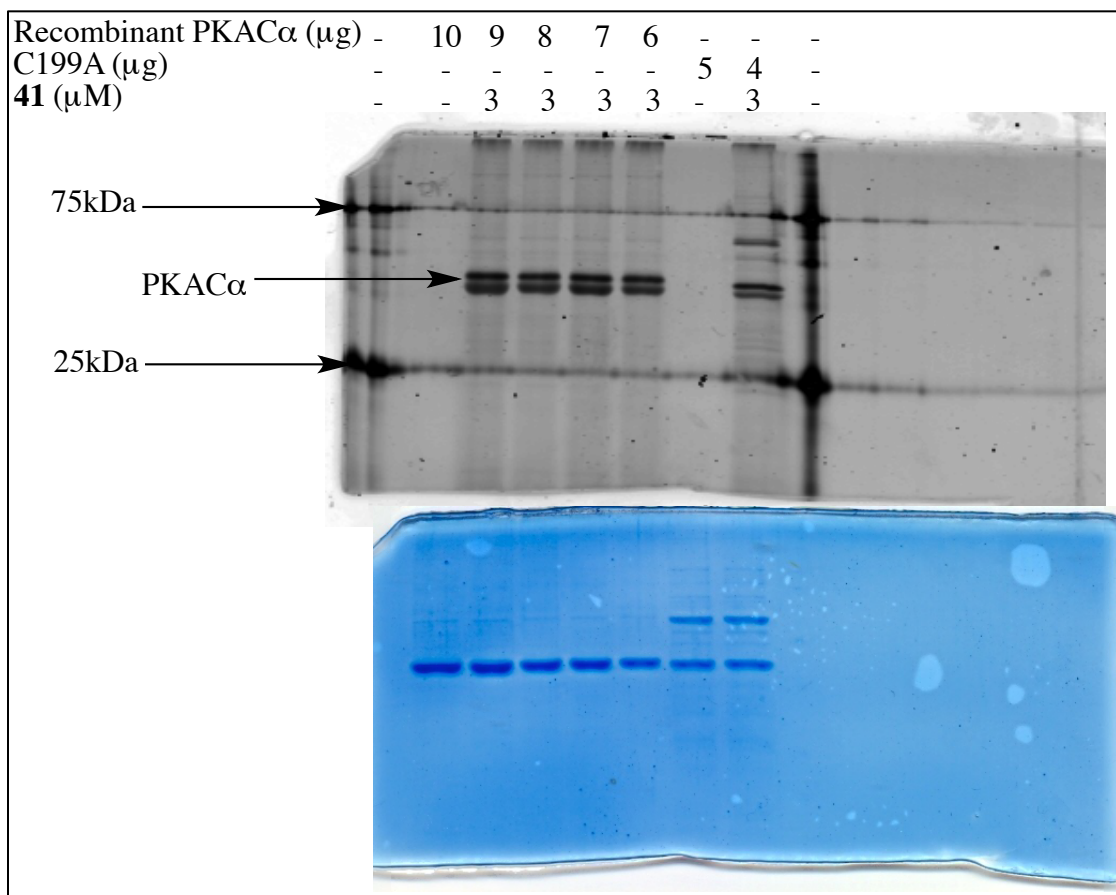


Figure 41. Labeling analysis with wild-type and C199A PKAC α .

3.9.4: Results and Discussion of Figure 41.

The Rh-PKI(14-22)-G-(CMK) probe displays robust labeling of isolated recombinant PKAC α at the reduced concentration (3 μ M). However, robust labeling occurred with the C199A mutant. It is possible that labeling is occurring at a different residue, e.g., Lysine-72 is in proximity and has been shown to react with nucleophiles placed in close proximity; this is, however, unlikely because lysine-72 resides more in the nucleotide-binding site than the substrate-binding pocket. There is another lysine residue more appropriately placed, Lysine-83, and may be a target of an appropriately placed electrophile. The distance from the alpha-carbon at the P+2 position is 5.6 Å to Lys83 and it is 8.3 Å to Cys199. This observation is interesting

and not necessarily an exclusion for qualification of an activity-based probe. The C199A mutant does retain activity and such a probe would still label in an activity-dependent manner. What is fortunate from this experiment, however, is the high molecular weight impurity in the C199A samples. These two spots give points of reference for alignment, and as a result a secondary analysis was performed by overlapping the Coomassie stained gel and the fluorescent image, detailed below.

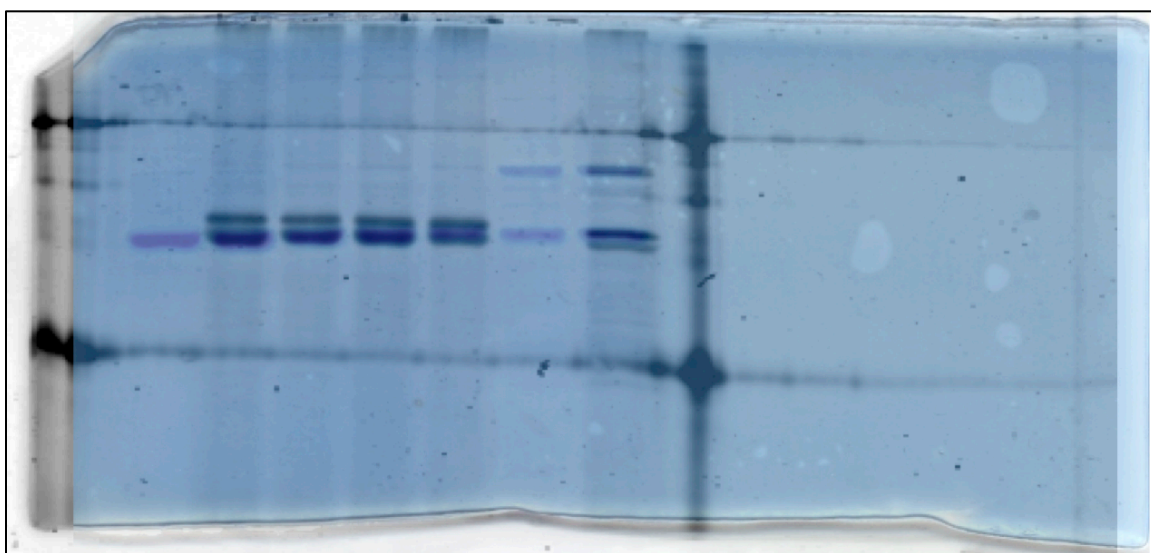


Figure 42. Coomassie and fluorescence image overlap from Figure 41.

3.9.5: Saturability with Myr-PKI(14-22)-Amide.

To further characterize the mechanism of action of the Rh-PKI(14-22)-G-(CMK) probe additional gels were run to examine the effects of competition with a known inhibitor with a known mechanism of action. In Figure 44 below, the labeling characteristics of the probe were examined against the wild-type recombinant PKAC α and increasing concentrations of the reversible inhibitor Myr-PKI(14-22)-Amide ($IC_{50} = 49.9$ nM). Protein concentrations were determined by absorbance at 280 nm and diluted such that it was 1 mg/mL in phosphate buffer (25 mM PO₄ pH 7.2). The probe was made as a 10 mM stock in DMSO and diluted accordingly for appropriate final concentrations in the gel experiments. The gel was cast as 1.5 mm thick and the wells were a total volume of 20 μ L. The samples were prepared for gel electrophoresis as above and Coomassie stain performed as above.

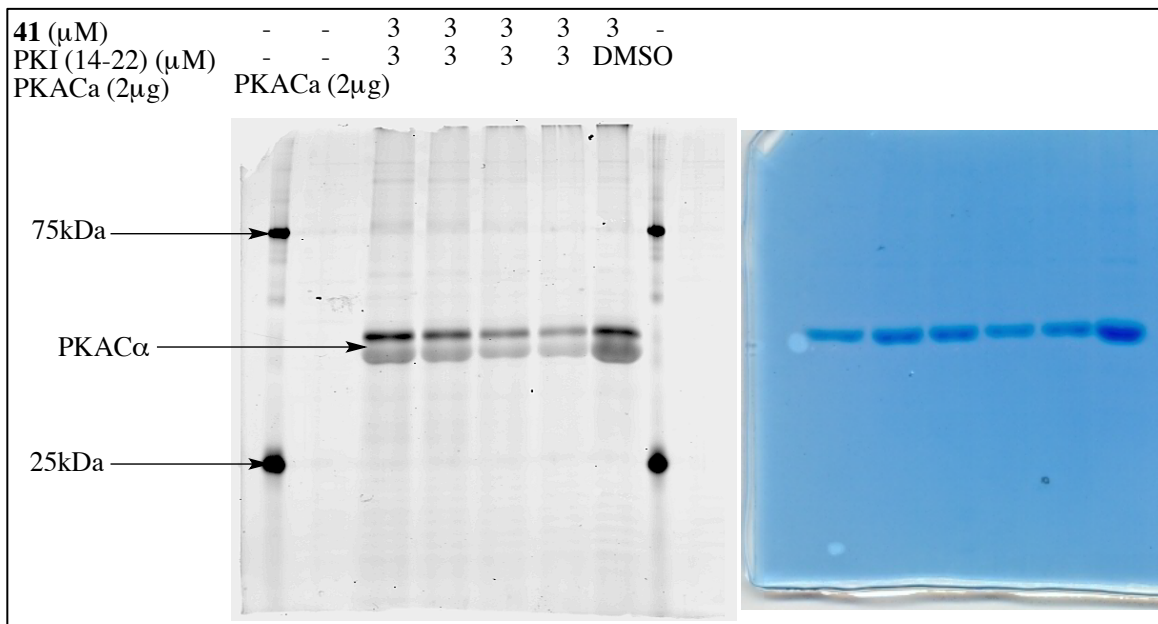


Figure 43. Saturability of labeling.

3.9.6: Results and discussion of the saturability experiment.

The labeling lane (lane 3), which lacks any inhibitor, displays robust labeling. Increasing the concentration of Myr-PKI(14-22)-Amide, an active-site directed reversible inhibitor, reduces labeling in a dose dependent manner. DMSO did not inhibit labeling; therefore, the decrease in labeling can be attributed to Myr-PKI(14-22)-Amide. The Coomassie stain gel image matches the fluorescence image. The dose dependent decrease in signal appears to be linear for both bands (upper and lower), indicating the labeling of each band is occurring in the active site.

3.9.7 Cysteine oxidation with glutathione.

The mechanism of action of the Rh-PKI(14-22)-G-(CMK) probe must be further characterized to understand what is happening on a molecular level; therefore, additional gels were run to examine the effects of cysteine oxidation with glutathione. In Figure 44 below, the labeling characteristics of the probe were examined against the wild-type recombinant PKAC α and with oxidative conditions to mimic the endogenous regulatory mechanism of glutathiolaytion at Cys199. PKAC α concentration was determined as described above. The probe was made as a 10 mM stock solution in DMSO and diluted accordingly for appropriate final concentrations in the gel experiments. The gel was cast as 1.5 mm thick and the wells were a total volume of 20 μ L. Prior to incubation with probe, the appropriate lanes were incubated for 1 hr with relevant reagents (diamide, glutathione (GSH), and diamide with GSH). Then the samples were incubated with probe for an additional 1 hr. The samples were prepared for gel electrophoresis as described above, imaging and staining was performed as described above.

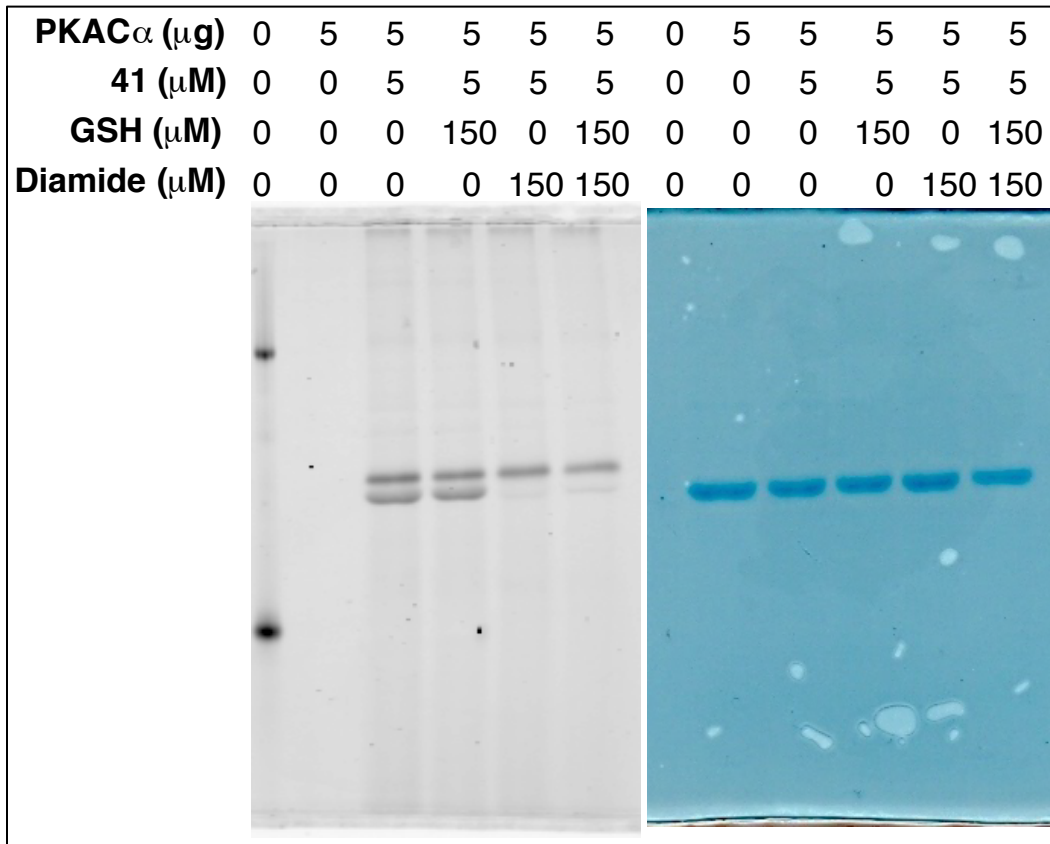


Figure 44. Examination of the effects of cysteine oxidation on labeling.

3.9.8: Results and discussion of the cysteine oxidation experiment (Figure 44).

The control labeling lane (lane 3) displays robust labeling. GSH alone has no observable impact on labeling of wild-type recombinant PKAC α . When diamide is introduced, the bottom band was selectively knocked out. When diamide and GSH are both introduced, again the bottom

band was selectively knocked out. The Coomassie image matches the fluorescent image and indicates equal protein loading. The selective knockout of labeling for the bottom band is an interesting result that has a number of possible explanations. The unphosphorylated form of the protein at Thr197 has a disordered activation loop. Therefore, it is possible that Cys199 is more easily accessible when the activation loop is disordered and, as a result, oxidizes much easier than the ordered species. It is also possible that oxidation at Cys199 was incomplete. However, the methods to perform this oxidation were previously reported by Taylor et al.³⁷ Another possibility is that oxidation is occurring but it is not inhibiting labeling: i.e., that it is labeling two different residues one for each band. This last hypothesis was further examined in the next discussed gel.

3.9.9: Labeling analysis in different pH conditions.

The residue(s) that the Rh-PKI(14-22)-G-(CMK) probe is alkylating must be further characterized to understand what is happening on a molecular level; therefore, additional gels were run to examine the effects of pH changes to labeling. In Figure 45 below, the labeling characteristics of the probe were examined against the wild-type recombinant PKAC α and with phosphate buffer solutions of increasing acidity. The PKAC α concentration was determined and adjusted appropriately as described above. The probe was made as a 10 mM stock solution in DMSO and diluted accordingly for appropriate final concentrations in the gel experiments. The gel was cast as 1.5 mm thick and the wells were a total volume of 20 μ L. Then the samples were incubated with probe for 1 hr. The individual samples were prepared for gel electrophoresis as described above. Imaging and staining was conducted as described above.

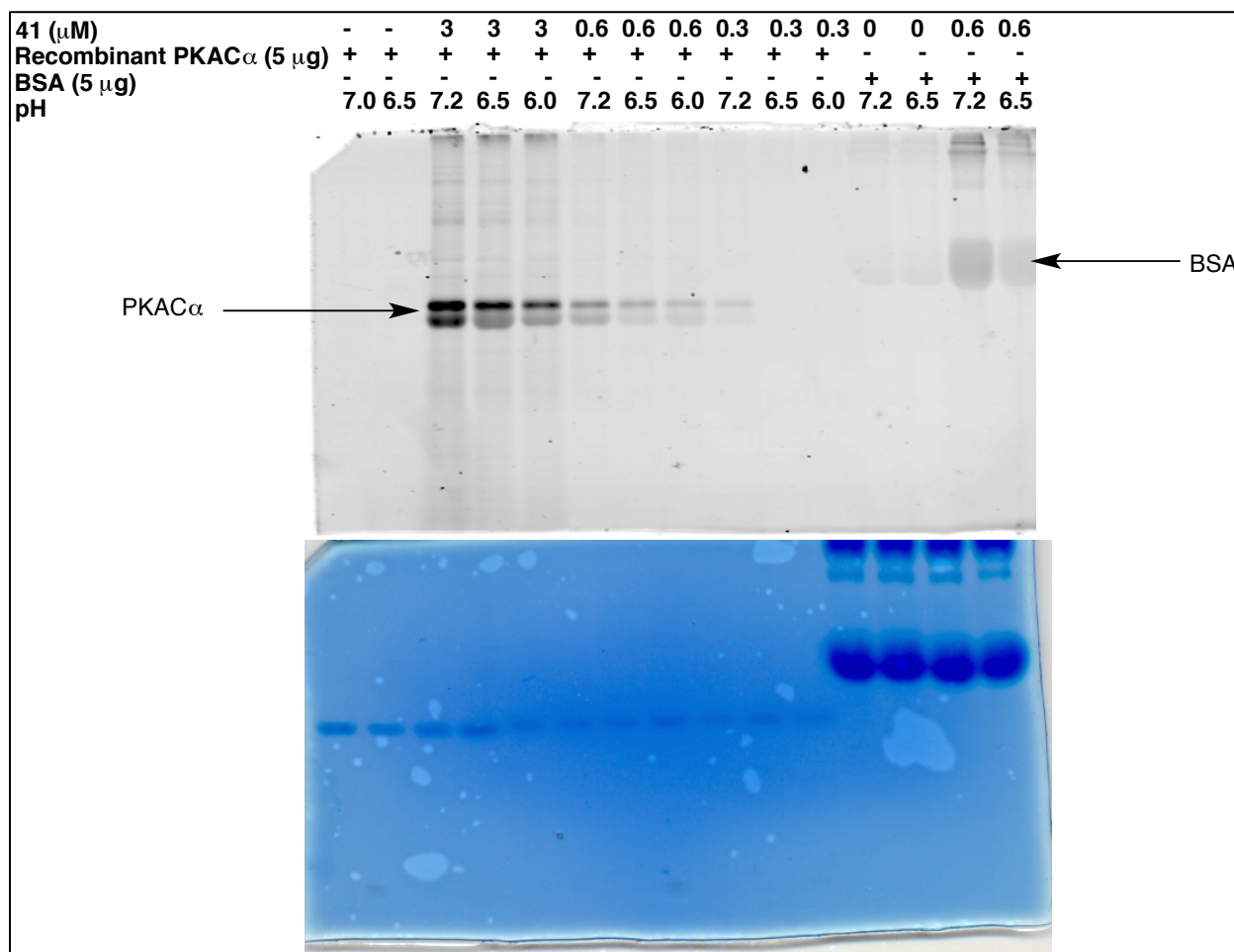


Figure 45. Analysis of pH effects on labeling.

3.9.10: Results and Discussion of Figure 45.

The Rh-PKI(14-22)-G-(CMK) probe displays robust labeling of isolated recombinant PKAC α at the standard buffer pH of 7.2. However, the labeling subsequently reduces with the corresponding reduction in pH. The reduction in labeling is noted for both band species in a similar fashion for each decrease in pH. At a concentration of 300 nM of probe, only the labeling

at pH 7.2 is detectable. A similar reduction of labeling is observed with the off target bovine serum albumin (BSA). Because the labeling is affected by pH changes for both bands in a similar manner, the data suggest that the two bands are labeled at the same residue, as their isoelectric points respond at the same rate to pH changes. This reduces the likelihood (the possibility mentioned in the cysteine oxidation gel discussed above) that two different residues were being labeled. Fortunately, with the BSA producing two spots, points of reference for alignment were available and as a result a secondary analysis was performed by overlapping the Coomassie stained gel and the fluorescent image, detailed below.

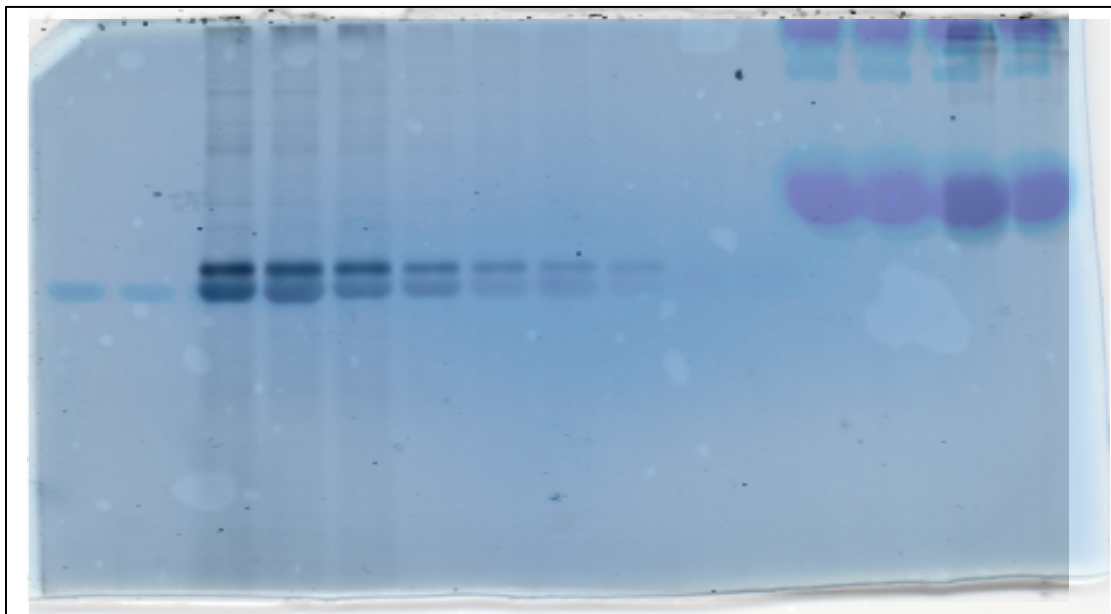


Figure 46. Overlap of fluorescence and Coomassie gel images from Figure 46.

3.9.11: Analysis of PDK1 phosphorylation on PKAC α and labeling.

To examine the effect of phosphorylation of Thr197 on labeling with Rh-PKI(14-22)-G-(CMK) recombinant PKAC α was phosphorylated *in vitro*. To promote phosphorylation at Thr197, the enzyme that performs this catalytic action *in vivo* (3-phosphoinositide-dependent protein kinase 1, PDK1) was purchased from Invitrogen. Recombinant PKAC α was diluted and mixed with appropriate amounts of PDK1. In Figure 47, the labeling characteristics of the probe were examined against the wild-type recombinant PKAC α and with recombinant PKAC α that was treated with PDK1. Both protein solution concentrations were determined as described above. The probe was made as a 10 mM stock solution in DMSO and diluted accordingly for appropriate final concentrations in the gel experiments. The gel was cast as 1.5 mm thick and the wells were a total volume of 20 μ L. Then the samples were incubated with probe for 1 hr. The samples were prepared for gel electrophoresis as described above. Imaging and staining was performed as described above.

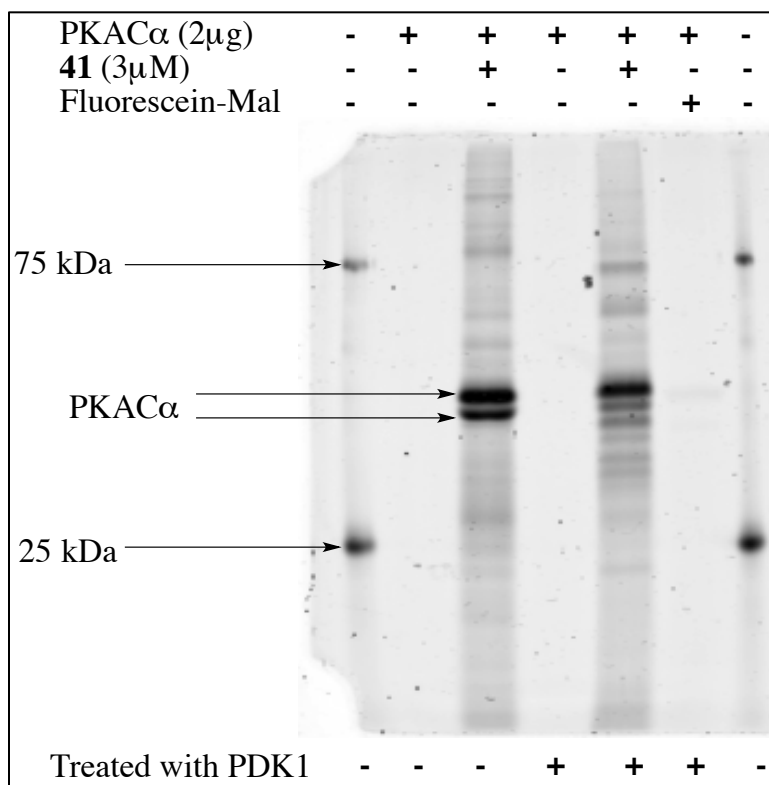


Figure 47. PKAC α treated with PDK1 analyzed with **41**.

3.9.12 Results and Discussion of Figure 47.

Probe **41** again displayed robust labeling of isolated recombinant PKAC α at the standard buffer pH of 7.2. Rh-PKI(14-22)-G-(CMK) revealed that by treatment of PKAC α with PDK1, a single band can be produced in the gel. This confirmed the hypothesis of the two bands differing by a phosphate moiety. However, the method by which we produced the protein was inefficient (only made 100 μ g on the first run) and relies on outside sources of PDK1, which proved cost

inefficient. Therefore, it was determined that a method to produce large enough quantities for activity-based experiments of PKAC α was necessary. Additionally, probe **41** did not display the selective qualities necessary for the activity-based probe and it was determined that the chloromethyl ketone moiety remained too reactive. As a result, a switch to an electrophile with a reduced reactivity profile was selected.

3.9.13: Discussion of the Biological Characterization of 41.

The nonapeptide analogue **41** enabled extensive characterization of the interactions between the specifically placed chloromethyl ketone moiety and different isoforms of PKAC α . The probe demonstrated selectivity for pThr197 PKAC α over Thr197 PKAC α . The labeling was saturable as was demonstrated with Myr-PKI(14-22)-Amide. The probe did not respond to the C199A mutant, as was expected. The probe did not respond to the glutathiolation experiments, as was also expected. It is possible that it is labeling another amino acid. The phosphorylation of Thr197 was successful and produced enough to confirm the hypothesis.

Based upon these observations, it was decided to synthesize a different derivative of PKI in order to gain selectivity for the catalytic subunit and ideally increase specific labeling at Cys199 in an activity-dependent manner. PKI(14-22) has already demonstrated itself to be a good length and so it was decided not to change the recognition scaffold. It was, instead, decided to change the reactivity of the electrophile. The hypothesis was that, by reducing the reactivity of the electrophile, selective labeling would be achieved in both isolated and complex biological mixtures.

3.10: The fluoromethyl ketone electrophile

The fluoromethyl ketone moiety is less reactive than the chloromethyl ketone. Its synthesis is a little more complicated in that the free base of glycine fluoromethyl ketone, for example, is not stable and therefore a multistep synthesis is necessary.^{134,135} A multistep synthesis for the production of glycine fluoromethyl ketone has been published and the results were reproduced in this lab.¹³⁵ The scheme is depicted below with the yields obtained in this lab, all spectral data matched the previously reported values and are detailed in the experimental section. The protected glycine fluoromethyl ketone was used in the same capacity as the glycine chloromethyl ketone in terms of appending to the peptide scaffold.

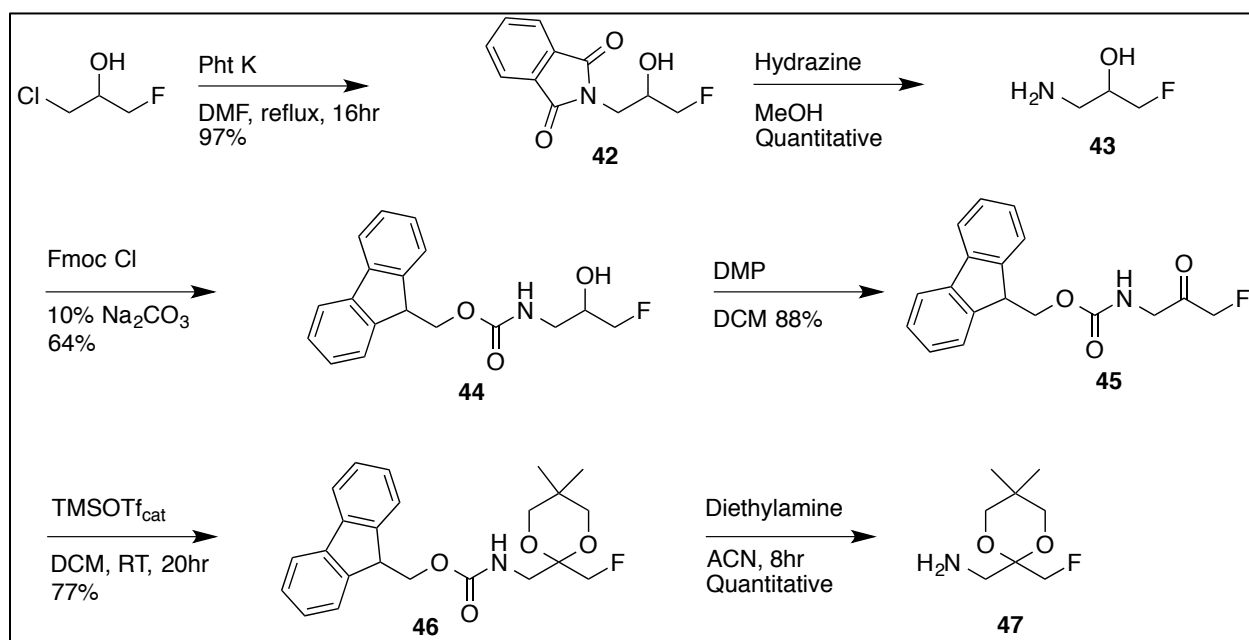


Figure 48. Synthesis of fluoromethyl ketone.

The chemistry scheme in Figures 49-50 depict the production of the PKI(14-22)-G-(FMK) probe. Briefly, 2-Chlorotrityl Chloride (2-CTC) resin preloaded with Ile was purchased

from ChemImpex (200-400 mesh, Catalog #03472). Peptide couplings were carried out manually via standard fmoc amino acid protection chemistry. Amino acids were activated and added to resin with (benzotriazol-1-yloxy)tripyrrolidinophosphonium hexafluorophosphate (PyBOP) and diisopropylethylamin (DIEA). The resin was swelled with DCM (5 min) then DMF (5 min). All amino acids were added by the general procedure that follows (with the exception of Arg, which underwent double couplings): Fmoc deprotection (20% piperidine in DMF, 3 x 5 min), wash with DMF 3x, amino acid coupling (PyBOP, DIEA 0.1 M in DMF, 1 hr, 2x for Arg), wash with DMF 3x, acetyl cap (pyridine:acetic anhydride 20:20, 0.15 M in DMF, 30 min). After the final deprotection (Gly 14) with 20% piperidine in DMF, the resin-bound product was taken directly to the next step.

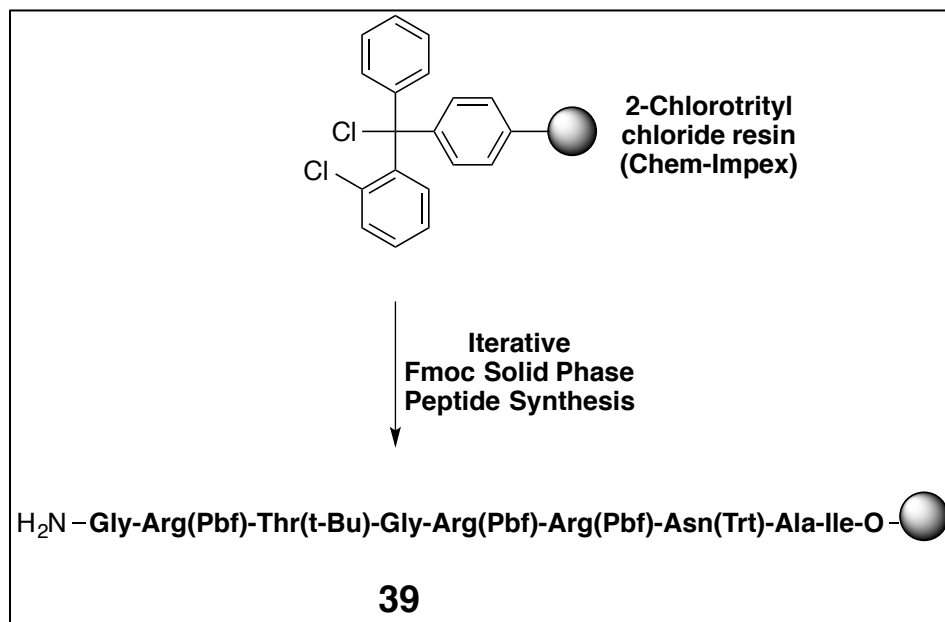


Figure 49. Production of peptide on resin.

While the peptide is still on the resin it was treated with a solution of Rhodamine-NHS ester and triethylamine (TEA) in dimethylformamide (DMF). The reaction was stirred for 3 h, washed with DMF 5x, then DCM 5x. The resin-bound product was taken directly to the next step. Rhodamine-PKI(14-22)-OH was then cleaved from the resin with a 2% TFA in DCM. The solvent was then removed under vacuum. Product taken directly to the next step.

The subsequent reaction is the addition of the electrophile by coupling of the glycine fluoromethyl ketone **47**. Briefly, the peptide is preincubated with (Benzotriazol-1-yloxy)tripyrrolidinophosphonium hexafluorophosphate (PyBOP), and diisopropylethylamine (DIEA) in DCM. Then the glycine fluoromethyl ketone was added to the solution. The reaction was stirred for 16 h. Solvent was removed and purified on a silica gel flash column, 0-30% over 10 minutes MeOH/DCM. The probe is then globally deprotected with 95:2.5:2.5 TFA:TIS:H₂O (5 mL) for 1 hr, then triturated with ether to afford crude product. The crude product was purified on HPLC (95:5 to 75:25 H₂O:ACN over 20 minutes).

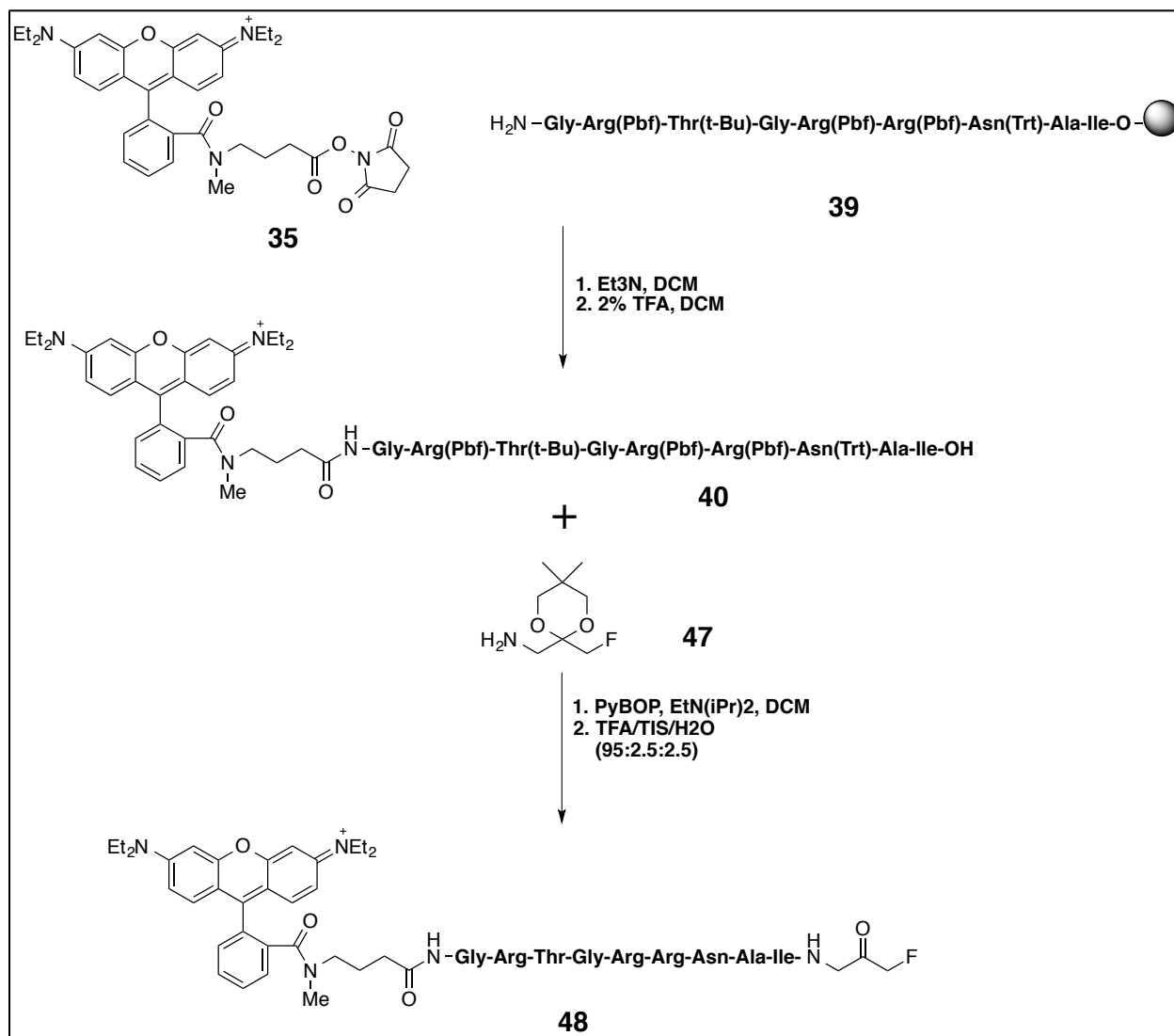


Figure 50. Assembly of Rh-PKI(14-22)-G-(FMK).

3.11: Expression of Phosphorylated PKAC α

To adequately examine a probe for activity-based protein profiling (ABPP), relatively large quantities of isolated protein are required for activity-based experiments. Previously, it was determined that in order to examine the physiologically relevant form of PKAC α (phosphorylated at Thr197) we needed to devise a method that would produce pThr197 PKAC α as the only species (at least by probe detection limits). The PDK1 plasmid was a generous gift from Justin Rettenmaier at the University of California, San Francisco. However, useful quantities could not be isolated from *E. coli* due to poor solubility and low expression levels. Therefore, the initial method of mixing the isolated proteins would not work when attempting to produce in-house PDK1.

3.11.1: Crude lysate mixture method.

The next experiment to produce pThr197 PKAC α involved the generation of PDK1 lysates, without purifying, as the source of PDK1. Briefly, competent *E. coli* cells were transformed with the PDK1 plasmid and grown for 16 hr at 37 °C with ampicillin and moderate shaking in a test tube. An aliquot was taken into a 1 L Erlenmeyer flask with ampicillin selection and auto-induction media and grown at 37 °C for 16 hr with moderate shaking. Following growth, cells were spun down at 6000 rpm for 10 min, and lysed into MOPS buffer (50 mM MOPS, pH 7.4, 100 mM NaCl, 10 mM BME, 10 mM MgCl₂, and 1 mM ATP) at ambient temperature. Cellular debris was removed by centrifugation at 20,000 rpm for 30 min. The supernatant was taken onto the next step without further purification.

Simultaneously, competent *E. coli* cells were transformed with the wt-PKAC α plasmid and grown for 16 hr at 37 °C with ampicillin and moderate shaking in a test tube. An aliquot was taken into a 1 L Erlenmeyer flask with ampicillin selection and auto-induction media and grown

at 37°C for 16 hr with moderate shaking. Following growth, cells were spun down at 6000 rpm for 10 min, and lysed into buffer (25 mM tris, pH 8, 300 mM NaCl, and 10 mM imidazole) at ambient temperature. Cellular debris was removed by centrifugation at 20,000 rpm for 30 min and the soluble fraction was decanted onto a nickel column. Following sample loading, the nickel column was washed with 5 column volumes of a non-eluting buffer (25 mM tris, pH 8, 300 mM NaCl, and 10 mM imidazole). Isolated PKAC α protein is then eluted with 100 mM imidazole and concentration determined by absorption at 280 nm on a spectrophotometer.

The purified PKAC α was then added directly to the lysates which were made from the PDK1 transformed *E. coli* cells and lysed into MOPS buffer. The solution was allowed to react for 90 minutes at ambient temperature. Then the solution was buffer exchanged into buffer for the nickel column (25 mM tris, pH 8, 300 mM NaCl, and 10 mM imidazole), and decanted onto a nickel column. The same procedure was followed for purifying PKAC α as stated above.

3.11.2: Gel of Pure PKAC α treated with PDK1 lysates.

In Figure 51, below, the labeling characteristics of the probe were examined against the wild-type recombinant PKAC α that was treated with PDK1 lysates. The final PKAC α solution concentration was determined by absorbance at 280 nm and diluted to 1 mg/mL in phosphate buffer (25 mM PO₄ pH 7.2). Appropriate amounts of protein were added to reaction vessels (epindorf tubes). The probe was made as a 10 mM stock solution in DMSO and diluted accordingly for appropriate final concentrations in the gel experiments. The gel was cast as 1.5 mm thick and the wells were a total volume of 20 μ L. The samples were incubated with probe for 1 hr. The samples were prepared for gel electrophoresis as described above. Fluorescence imaging and Coomassie staining were performed as described above.

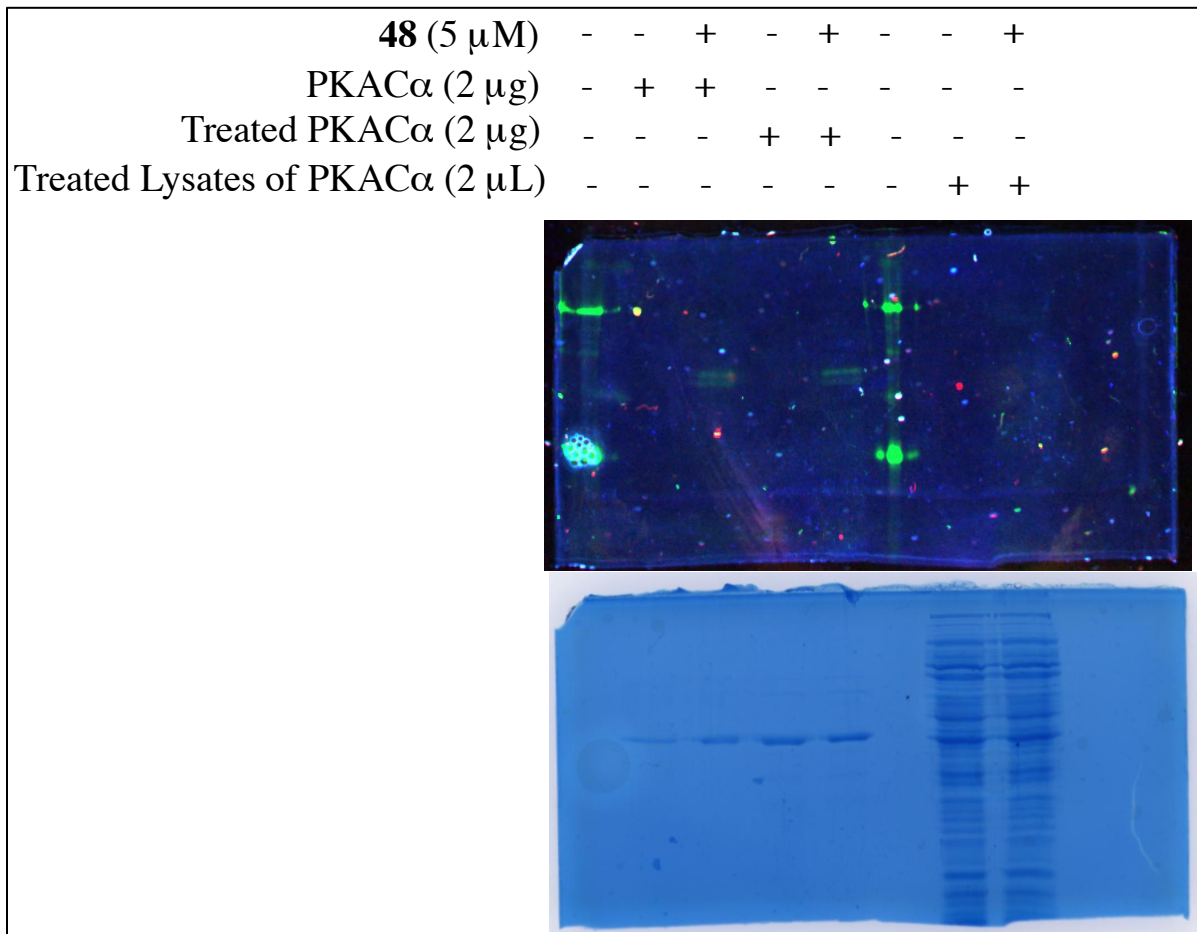


Figure 51. Examination of labeling on treated PKAC α .

3.11.3: Results and Discussion of Figure 51.

The Rh-PKI(14-22)-G-(CMK) probe again displayed robust labeling of isolated recombinant PKAC α at the standard buffer pH of 7.2. Additionally, Rh-PKI(14-22)-G-(CMK) labeled the treated with lysates PKAC α in a similar way to the treated with commercial PDK1. This confirmed the hypothesis of treating with PDK1 to obtain the phosphorylated species as the predominant form. Unfortunately, it is a rather crude method for producing the protein and the results were not immediately reproducible. Therefore, it was necessary to explore an alternative route of producing PKAC α pThr197.

3.11.4 Co-expression of PKAC α and PDK1.

To co-express the two proteins they must each be selected for in the bacterial growth media. Therefore, the original plasmid PDK1 had to be switched to a compatible vector. The PDK1 plasmid was isolated with a QIAprep Spin Mini Prep Kit (procedure in the experimental section). A pRSF Duet Plasmid (Kan resistant) was isolated from an overnight culture with the same kit. The PDK1 plasmid was digested with BglIII and NdeI restriction enzymes and the pRSF Duet plasmid with Bam HI and NdeI. The resulting solutions were run on agarose gel (cast in house, see experimental) and the appropriate bands were imaged with ethidium bromide and excised with a scalpel (Figure 40 below). They were ligated together with a DNA ligase enzyme. The resulting solution was used to transform competent *E. coli* cells (detailed in experimental). After subsequent incubation, the new plasmid was isolated with a QIA Spin Mini Prep Kit and then transfected into cells already expressing PKAC α . The same process was done with cells expressing the mutant C199A PKAC α .

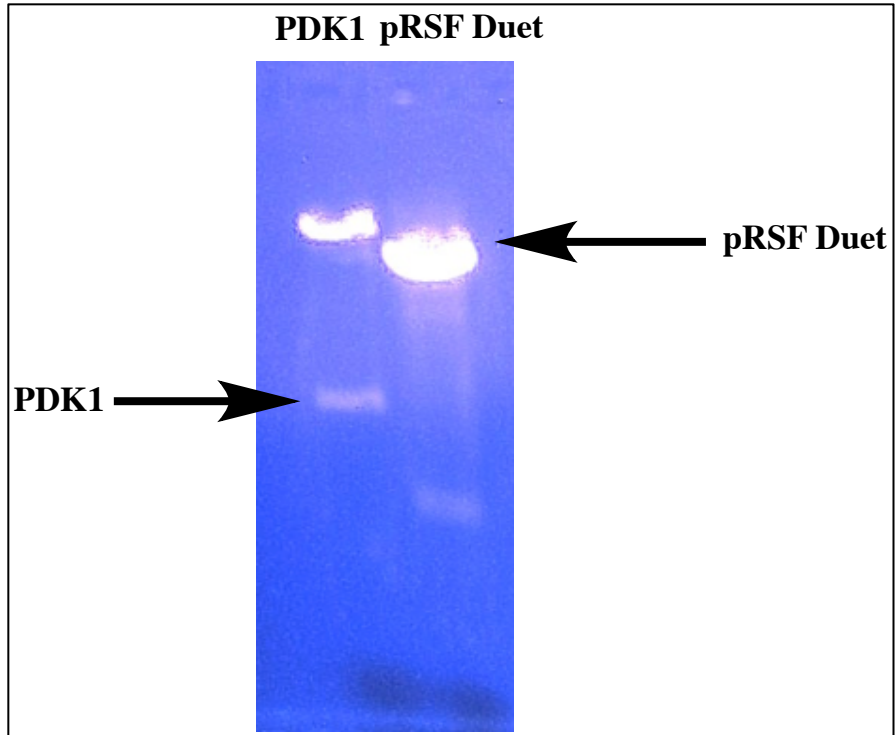


Figure 52. Agarose gel electrophoresis of PDK1 plasmid and pRSF duet.

3.11.5: Labeling of coexpressed PKAC α and PDK1.

In Figure 53, below, the labeling characteristics of the probe were examined against the wild-type, and C199A, recombinant PKAC α that was coexpressed with PDK1. The final PKAC α solution concentration was determined by absorbance at 280 nm and diluted to 1 mg/mL in phosphate buffer (25 mM PO₄ pH 7.2). The probe was made as a 10 mM stock solution in DMSO and diluted accordingly for appropriate final concentrations in the gel experiments. The gel was cast as 1.5 mm thick and the wells were a total volume of 20 μ L. Then the samples were incubated with probe for 1 hr. The samples were quenched with a denaturing sample buffer (made in house and detailed in the biological experimental section) and incubated at 100°C for 5 minutes. The denaturing sample buffer contained a disulfide reducing agent (betamercaptoethanol, BME). Fluorescent images were taken on an Amersham 600 Imager. Coomassie staining was performed with blue G250 in a H₂O/MeOH/AcOH solution, and destained with a H₂O/MeOH/AcOH solution. Images of the Coomassie stained gel were taken on an Amersham 600 Imager.

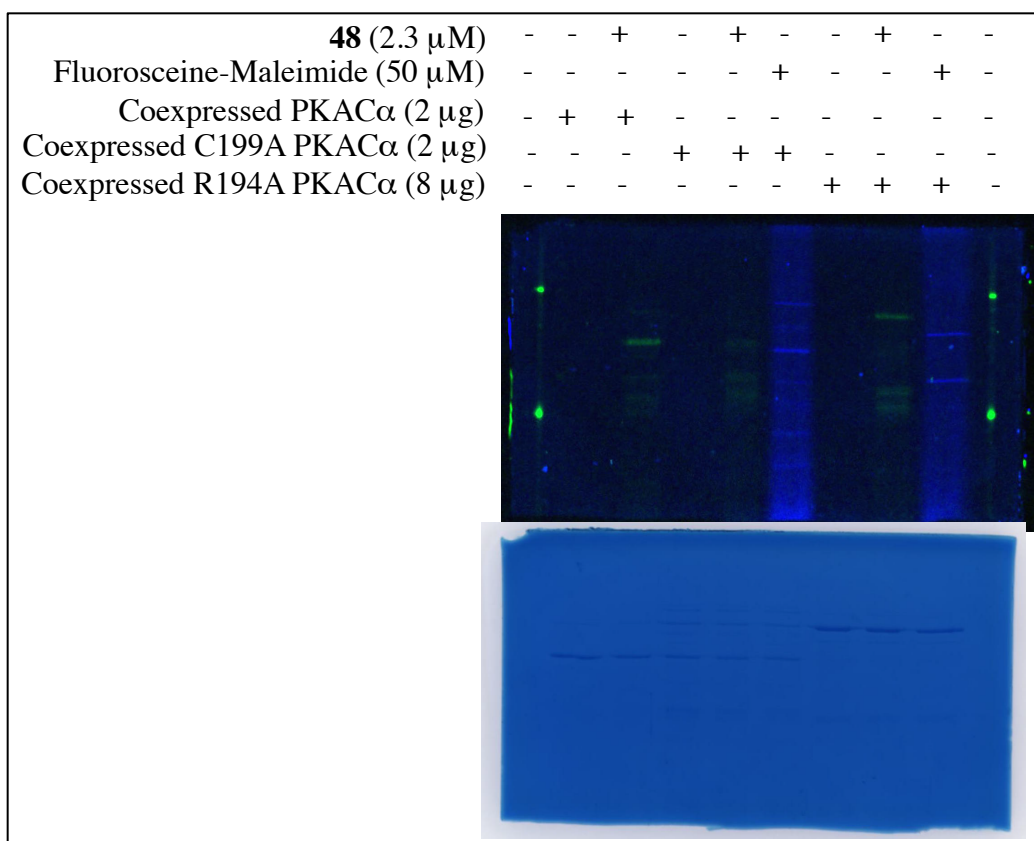


Figure 53. Examination of coexpressed PKAC α and PDK1 labeling with **48**.

3.11.6: Results and Discussion of Figure 53.

The Rh-PKI(14-22)-G-(CMK) probe again displayed robust labeling of isolated recombinant PKAC α at the standard buffer pH of 7.2. This time only one band is observed. This confirmed the utility of the coexpression platform. However, it is now abundantly clear that the conditions for expression can be tuned with the isolated PKAC α to promote phosphorylation.^{42,83,129-131} In effect, a method was developed to easily produce large quantities of PKAC α phosphorylated at Thr197 without the close monitoring of conditions.

3.12: Biological Characterization of 48.

In a similar setup to the chloromethyl ketone derivative, the fluoromethyl ketone probe was examined for its ability to label PKAC α . Saturability of labeling was examined with non-covalent Myr-PKI(14-22)-Amide. The labeling of the cysteine to alanine mutant (C199A) was examined to examine the residue being labeled. Oxidation of the cysteine was attempted to mimic the endogenous regulatory mechanism of glutathiolation. Labeling with increasing concentrations of ATP and MgCl₂ was examined as was labeling in many complex biological mixtures such as: MCF7 cells, MDA-MB-231 cells, bovine heart tissue lysates, mouse heart tissue lysates, and *E. coli* lysates. All gels were cast in house and made to contain 10% acrylamide, the exact procedure is detailed in the biological experimental section.

3.12.1: Activity-Based Experiment: Probe labeling saturation.

To analyze the labeling characteristics of the Rh-PKI(14-22)-G-(FMK) (**48**) probe saturation gels were run to examine the effects of competition with a known inhibitor with a known mechanism of action. In Figure 54 below, labeling of PKAC α with probe **48** was competed off with incrementally increasing concentrations of commercially available Myr-PKI(14-22)-Amide (IC₅₀ = 49.9 nM) . Protein concentration and probe concentrations were prepared and determined as described above. The samples were prepared for gel electrophoresis as described above. Fluorescence imaging and Coomassie staining were performed as described above.

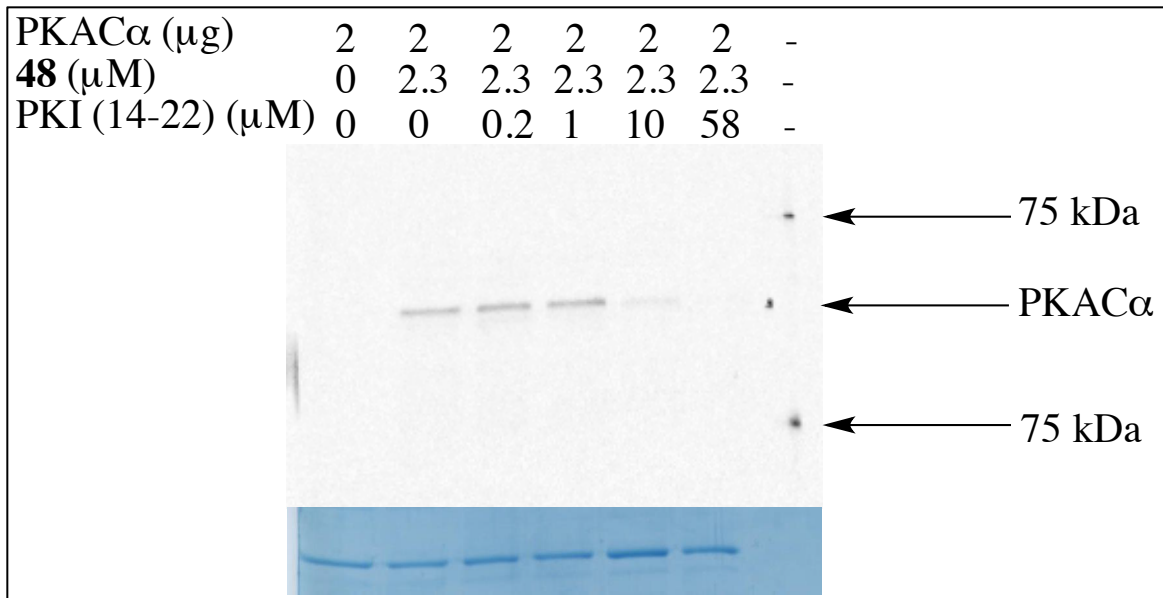


Figure 54. Saturability of labeling of probe **48**.

Compound **48** displayed robust labeling of isolated enzyme. The labeling was reduced in a dose dependent manner by competition with Myr-PKI(14-24)-Amide. As increasing amount of reversible inhibitor are added, non specific labeling is not observed. The Coomassie stain gel image matches the fluorescence image.

3.12.2: Activity-Based Experiment: Cysteine Oxidation.

In Figure 55 below, the labeling characteristics of the probe were examined against the wild-type recombinant PKAC α and with oxidative conditions to mimic the endogenous regulatory mechanism of glutathiolaytion at Cys199. Prior to incubation with probe, the appropriate lanes were incubated for 1 and 4 hr with Ellman's reagent (a generic cysteine oxidizer). Then the samples were incubated with probe for an additional 1 hr. The gel cast, detection, staining, and imaging were the same as above.

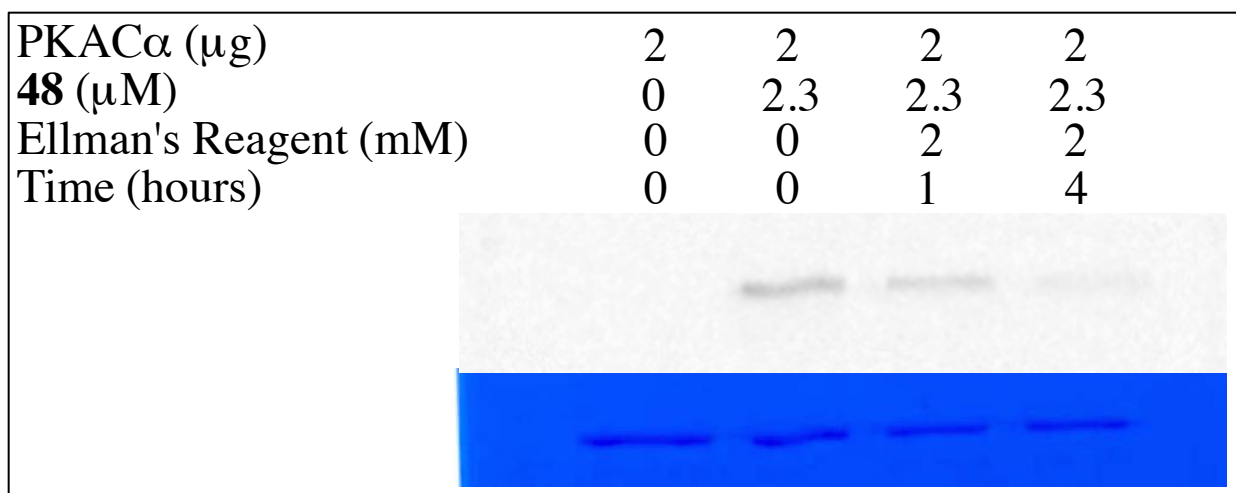


Figure 55. Cysteine oxidation effect on labeling by Ellman's reagent.

Probe **48** displayed robust labeling in the control lane (lane 2). Ellman's reagent (2 mM) inhibited labeling over the course of 4 hr. The activation loop cysteine is held in conformation when Thr197 is phosphorylated and as a result the oxidation at Cys199 takes longer to occur.

3.12.3: Selectivity Experiment: C199A Mutant.

To analyze the effects of probe **48** on labeling the C199A mutant of PKAC α and further confirm the mechanism of labeling, the gel below was run (Figure 56) where conditions were the same as above. Imaging, detection, and staining were repeated same as above.

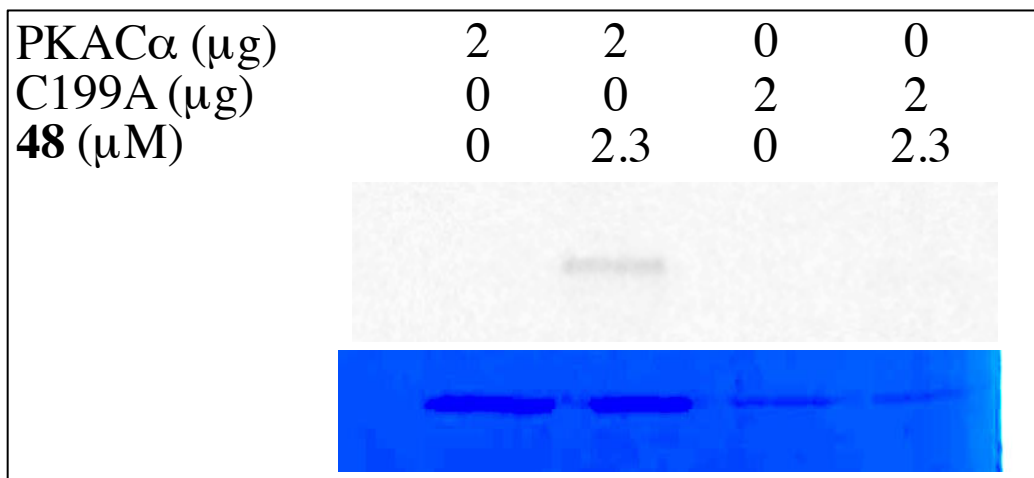


Figure 56. Selectivity labeling experiment with wild-type and mutant PKAC α .

Probe **48** displayed selectivity for the wild-type PKAC α over the C199A mutant. Robust labeling was detected in the control lane (lane 2), and no detectable labeling occurred in lane 4 which contains the C199A mutant.

3.12.4: Activity-Based: Effects of ATP and MgCl₂ on Labeling Efficiency.

Previous results from this lab indicated that these probes have decreased labeling efficiency in physiological conditions. To examine this hypothesis, probe **48** was incubated with wild-type PKAC α with increasing concentrations of ATP and in the buffer used for the Z'LYTE kinase assay (high MgCl₂ concentration 10 mM, buffer B).¹³³

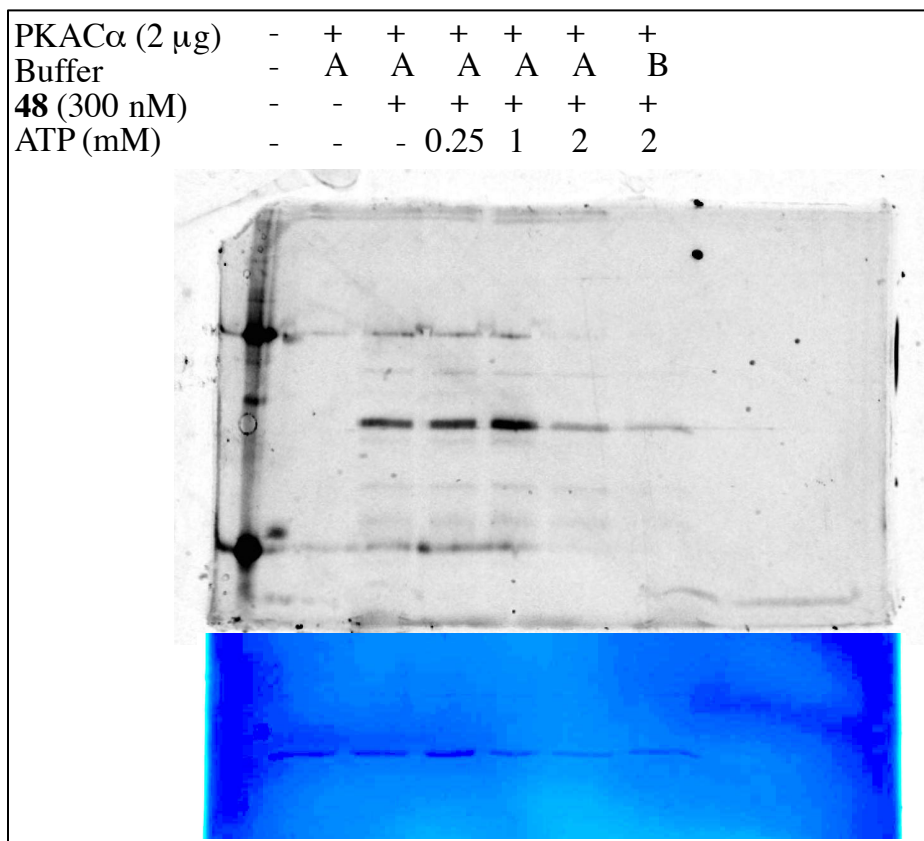


Figure 57. Labeling in the presence of ATP and MgCl₂.

Probe **48** displays positive labeling characteristics with low levels of ATP (0.25 – 1 mM) in lanes 4 and 5. However, when the concentration is increased to 2 mM, labeling is decreased, but not abolished, which is a significant first for these types of probes. The effect of the kinase buffer B did not affect labeling in a significant manner.

3.12.5: Additional investigation into Cys199 labeling mechanism of action.

Trypsin digest mass spectrometry was utilized to confirm the location of binding of probe **48** to PKAC α . Briefly, unmodified or treated PKAC α was buffer exchanged into a lysis buffer ((25 mM Tris pH 7.6, 1 mM EDTA, 150 mM NaCl, 1% Triton X-100, 0.1% SDS, and 10 mM DTT). The protein solution was mixed with trypsin at a ratio of 20:1 protein to protease. The resulting solution was incubated at 37 °C for 24 hr (in a sealed eppendorf tube). The sample was analyzed by MALDI mass spectrometry with CHCA matrix (Sigma) on a Voyager DE-Pro™ MALDI TOF Mass Spectrometer.

Table 12: Trypsin Digest Mass Spec Results

PKAC α Trypsin Fragment: TWpTL R GTPEYLAPEIILSK		
	Mass Calculated	Mass Found
Untreated	2215.0893	2215.6430
Treated with RAC-2-116	2609.2960	2609.5996

Table 12: Mass found was the PKAC α sequence + Probe Fragment (NAIG) + Na⁺. Exact mass of probe fragment (NAIG) was calculated to be 371.2169.

3.12.6: Examination in Complex Biological Mixture: MCF7 Lysates.

Once the labeling mechanism of action had been extensively characterized and shown to display characteristics consistent with an activity-based probe, selectivity in complex biological mixtures was the necessary next step. MCF7 cells (a breast cancer cell line) were grown in T75 flasks with RPMI buffer and 10% FBS (no antibiotic). Once confluent, the cells were collected by centrifugation and the RPMI media exchanged with phosphate buffer. Cells were lysed with a Dounce homogenizer and debris removed by centrifugation. Concentrations were determined by Bradford assay (detailed procedure and results in experimental).

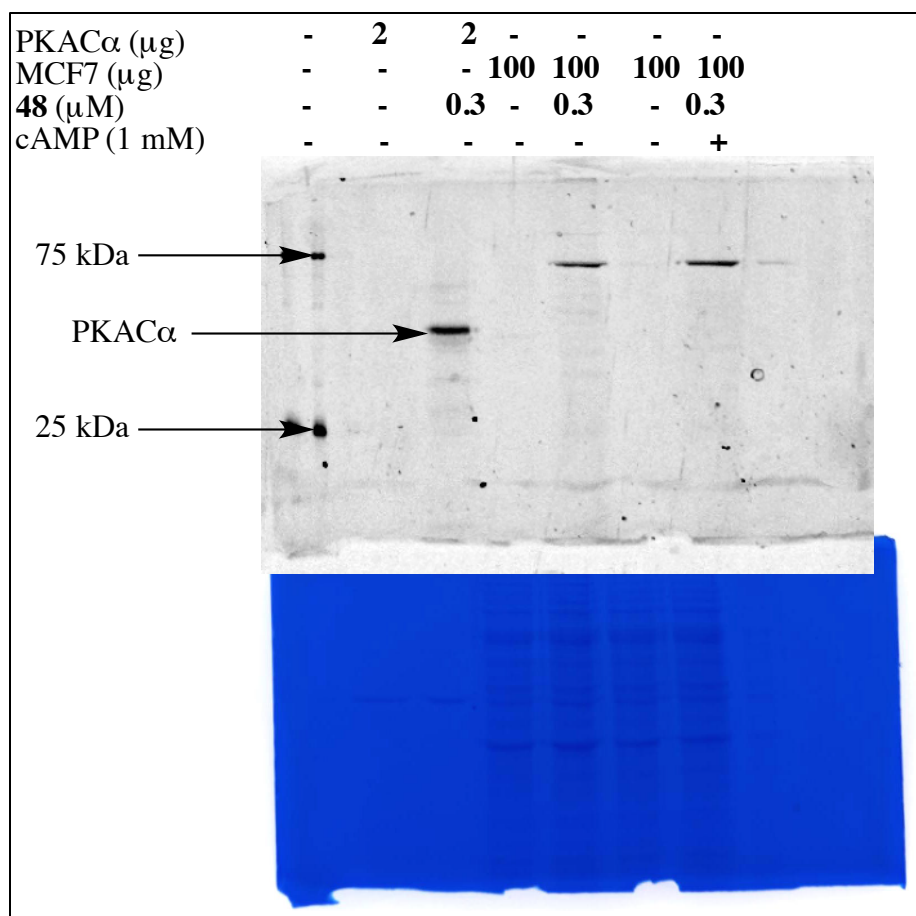


Figure 58. Labeling in MCF7 cell lysates.

Probe **48** displayed robust labeling of the control PKAC α lane (lane 3). The cell lysates were treated with/without probe and with/without cAMP to ensure release of the catalytic subunit from the holoenzyme. A single band was observed in both MCF7 cell lanes (lanes 5 and 7); however, the molecular weight does not match that of PKAC α and more closely matches the homologous PKG (~76 kDa).

3.12.7: Examination in Complex Biological Mixture: MDA-MB-231 Lysates.

The MCF7 cells were revealed to have very little total amounts of PKA.¹³⁶ MDA-MB-231 cancer cells do have large quantities of PKA (contained in the holoenzyme).¹³⁶ Therefore, MDA-MB-231 cells were examined with probe **48**. MDA-MB-231 cells (another breast cancer cell line) were grown in T75 flasks with RPMI buffer, 1% ampicillin, and 10% FBS. Once confluent, the cells were collected by centrifugation and the RPMI media exchanged with phosphate buffer with 1x Rouché Protease inhibitor cocktail. Cells were lysed with a Dounce homogenizer and debris removed by centrifugation. Concentration determined by Bradford assay (detailed procedure and results in experimental).

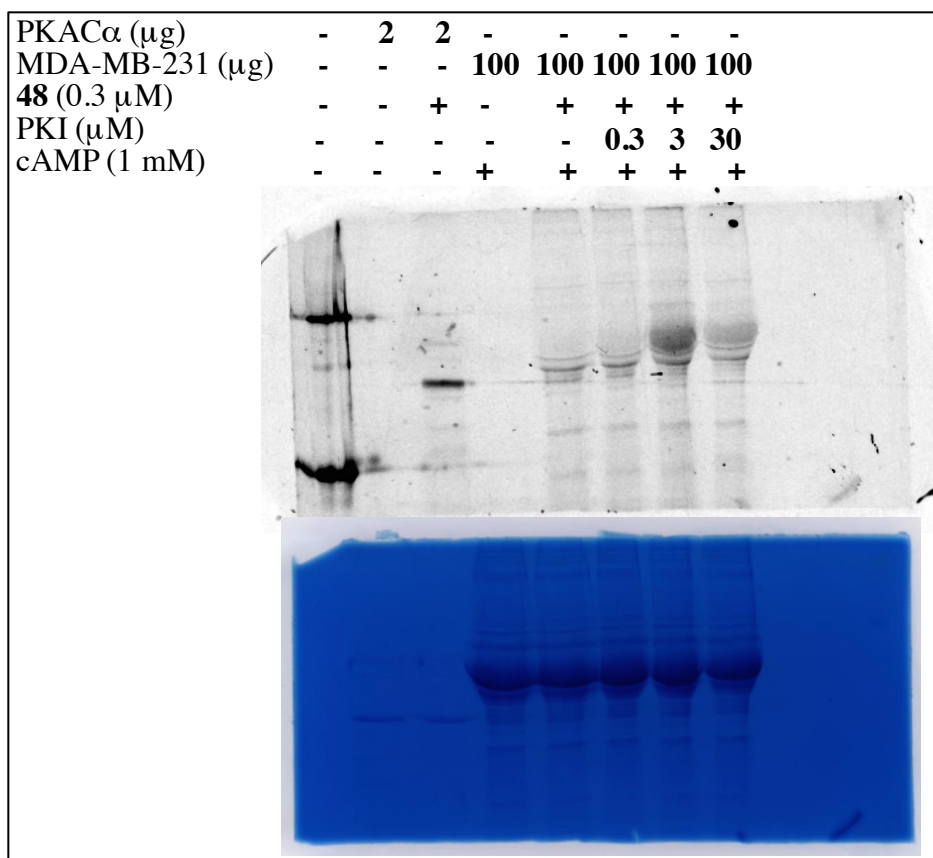


Figure 59. Examination of MDA-MB-231 Lysates with compound **48**.

Probe **48** effectively labels recombinant PKAC α in the control lane (lane 3). There is selective labeling in the lysates. The band does not correspond with the molecular weight of PKAC α . Myr-PKI(14-22)-Amide does not competitively knock out labeling at equivalents up to 50x.

3.12.7: Examination in Complex Biological Mixture: Bovine heart lysates.

Early work with PKAC α was performed with tissue samples.^{44,114} Specifically, bovine heart was used extensively. Testing the hypothesis that PKA is not abundant enough in the samples for adequate labeling, bovine heart tissue was examined. Briefly, bovine heart tissue was cut into equal parts of 10 g pieces. One piece was incubated with protease inhibitor and the lysates were produced with a tissue homogenizer. The debris was removed by sequential centrifugation. Lysate concentrations were determined by Bradford assay and probe incubation performed as previously described. A PKAC α pThr197 specific antibody was used for Western blot (detailed procedure available in experimental).

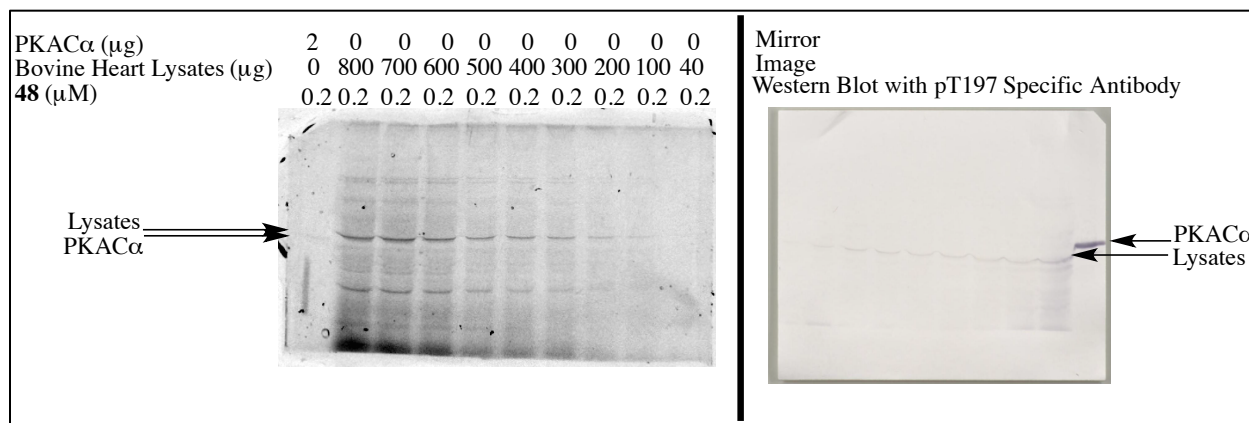


Figure 60. Examination of bovine heart lysates with compound **48**.

The dense nature of these tissues allowed for the facile production of concentrated lysates. A significant load of lysates was analyzed and probe **48** did display selective labeling. However, the band is similar to that observed in the MDA-MB-231 lysates and does not correspond with PKAC α . Moreover, the antibody detection indicates the band being observed by fluorescence is not that being labeled by antibody.

3.12.9: Examination in Complex Biological Mixture: Mouse heart lysates.

To examine the possibility of species variance in PKAC α production and labeling, mouse heart lysates were prepared in the same manner as above. Protein concentration determined by Bradford, and antibody detection with a PKAC α pThr197 antibody, all as described above.

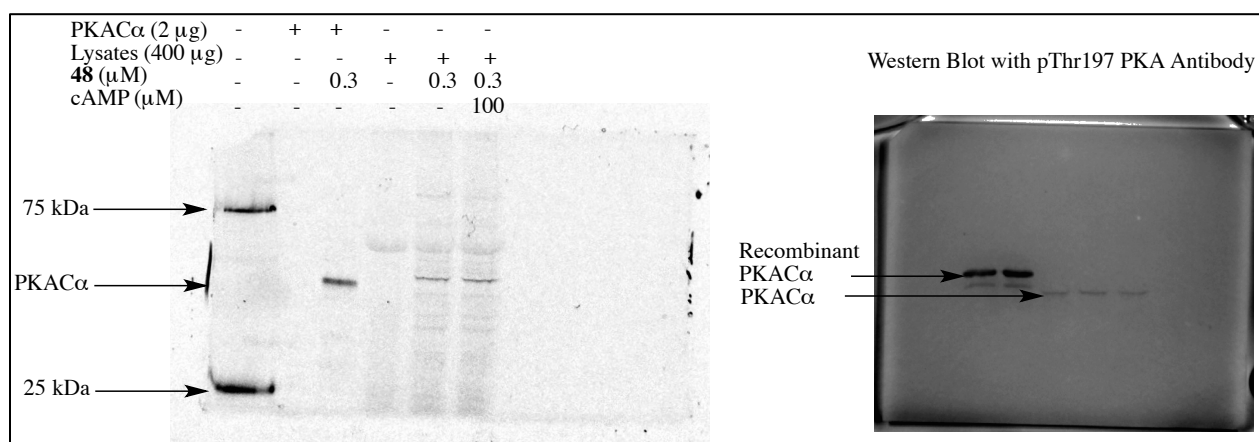


Figure 61. Examination of mouse heart lysates with compound **48**.

A similar labeling profile was noted in the mouse heart lysates as with the bovine heart lysates. That is, heavy lysate loads were found in each lane with selective labeling of one band that does not correspond with the expected molecular weight. The antibody reveals a similar result as that of bovine: the band labeled is not the band that corresponds with PKAC α .

3.12.10: Discussion of Biological Characterization of Probe 48.

The fluoromethyl ketone probe was examined extensively by multiple mechanisms and variables. The saturability of labeling by competition with Myr-PKI(14-22)-Amide was examined. The labeling was reduced with increasing concentrations of the reversible inhibitor in a dose dependent manner. Cysteine oxidation's effect on labeling with the use of Ellman's reagent to oxidize Cys199 was examined.¹³⁷ Upon treatment with Ellman's reagent for 4 hrs labeling was effectively abolished. Rh-PKI(14-22)-G(FMK) (**48**) did not detectably label the C199A mutant of PKA α . The trypsin digest mass spec indicated that a residue in the activation loop is being modified. The IC₅₀ of the probe was determined to be 11 nM (as determined by Invitrogen). These results were very favorable for a selective probe that labels the catalytic subunit in an activity-dependent manner. As a result, the probe was examined in a number of biological systems.

The first system examined was MCF7 cell lysates. The procedure for growing up these cells and producing lysates is detailed in the experimental. The MCF7 cell line is a breast cancer cell line. When we examined the labeling in these lysates, the probe displayed remarkable selectivity. However, this singular band did not correspond with PKA α and as a result we set out to examine a different biological system with potentially greater amounts of PKA.

Cell lysates were reexamined to test the hypothesis that there was not enough PKA for labeling. The MDA-MB-231 cell line was selected due to it having demonstrated robust production of PKA. The growing conditions were similar to the MCF7 cell line but with protease inhibitor in the lysate solution, which may have influenced the labeling. However, the band does not match PKA α in molecular weight, nor is it labeled by antibody.

Bovine heart was readily available from the local butcher, and early PKA work in the literature dealt with PKA isolated from bovine hearts (Chapter 2). The tissue was marinated in protease inhibitor and homogenized. The debris was removed by sequential centrifugation and concentration determined by Bradford assay. A detailed work up is described in the experimental section. While selective labeling occurred again, the molecular weight again did not match that would be expected from PKA, it was slightly higher. The Western blot with anti-PKAC α confirmed that the labeled band does not correspond with the PKA identified with antibody, and does seem to be the same band labeled in the MDA-MB-231 lysates.

We reexamined the labeling of the probe in mouse heart lysates. The mouse hearts were a generous gift from Dr. Jolene Windle. The tissue was marinated in protease inhibitor and homogenized. The debris was removed by sequential centrifugation and concentration determined by Bradford assay. A detailed work up is described in the experimental section. Again, selective labeling was observed on a band not consistent with the molecular weight of PKAC α but similar to that observed in bovine heart and MDA-MB-231 cell lysates (3 species covered). In an effort to determine the identity of the labeled peptide, biotinylated analogues were synthesized for pull-down experiments.

3.13: Development of a Biotinylated Peptide Probe.

To determine the identity of the fluorescently labeled protein, biotinylated analogues were designed for pull-down experiments. The full length probe was assembled in the same fashion as Rh-PKI(14-22)-G-FMK and the scheme is depicted below (a detailed procedure is available in the experimental section). Biotin-NHS was synthesized according to a previously described route and the spectral data matched previously reported values.¹³⁸ The synthetic scheme is depicted below.

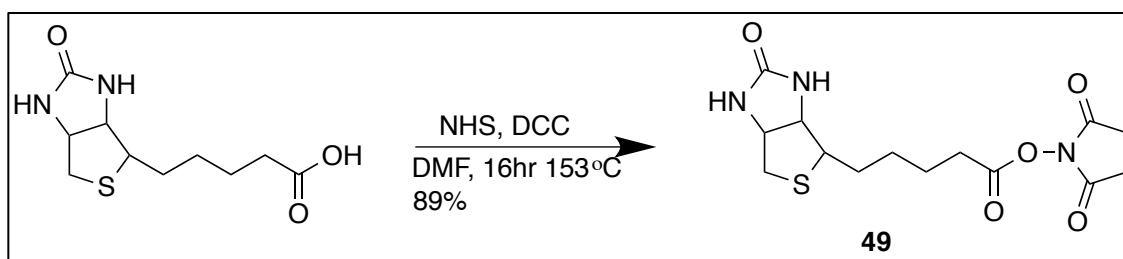


Figure 62. Synthesis of Biotin-NHS.

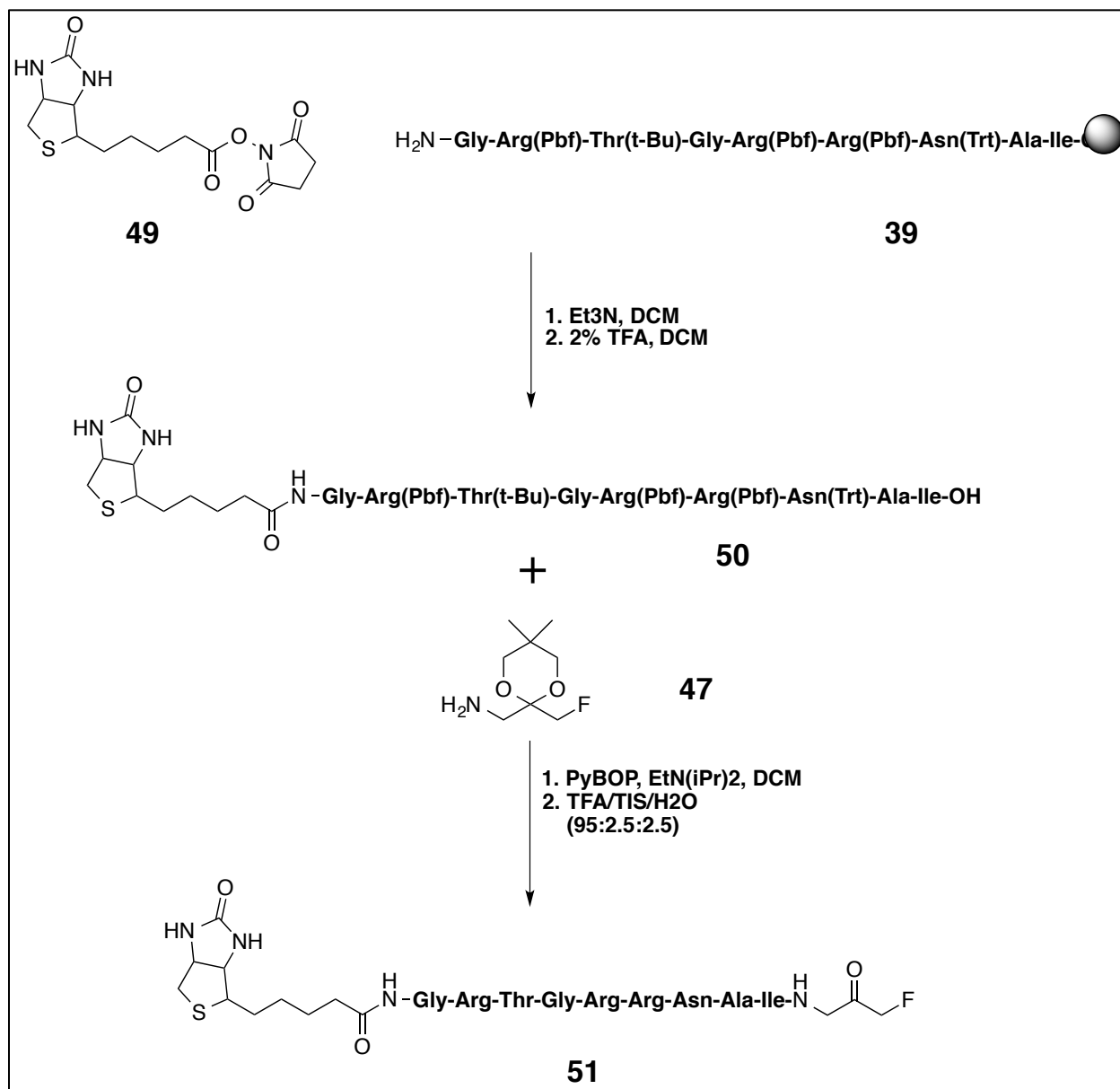


Figure 63. Synthesis of Biotin-PKI(14-22)-G-(FMK).

3.13.1: Biological Characterization of 51, Biotin-PKI(14-22)-G-(FMK).

The biotinylated probe did not detectably label recombinant PKAC α in conditions that paralleled that of the fluorescently labeled probe (300 nM). Later experiments show minimal labeling and will be discussed in a later section. The hypothesis at the time was that there was a difference between PKAC α produced recombinantly and endogenously expressed PKAC α . As a result, the pull-down experiment was performed and the results are detailed below.

Briefly, mouse heart lysates were passed through a streptavidin column to remove endogenously biotinylated proteins from the untreated lysates. Then the eluent was diluted 10 fold into phosphate buffer and incubated with 300 nM of biotin-PKI(14-22)-G-(FMK) for 1 hr. The solution was then incubated with the column for 1 hr and subsequently eluted with a biotin solution. A detailed procedure is available in the experimental.

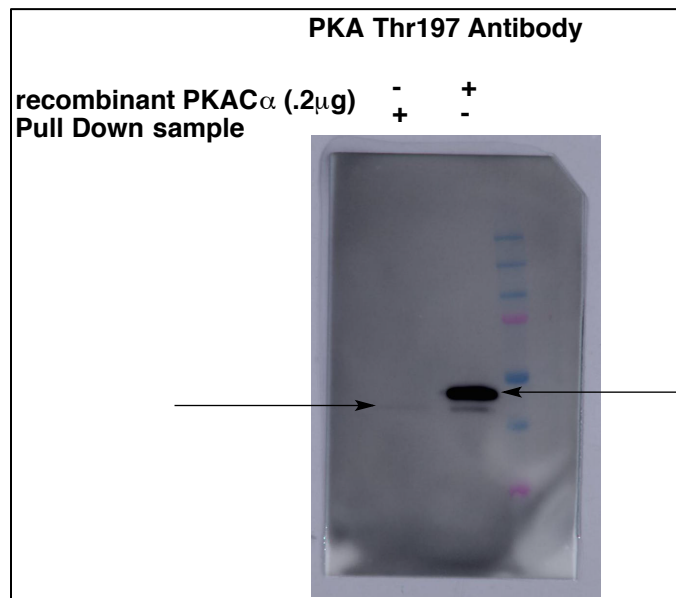


Figure 64. Western blot of the pull-down sample with pThr197 antibody.

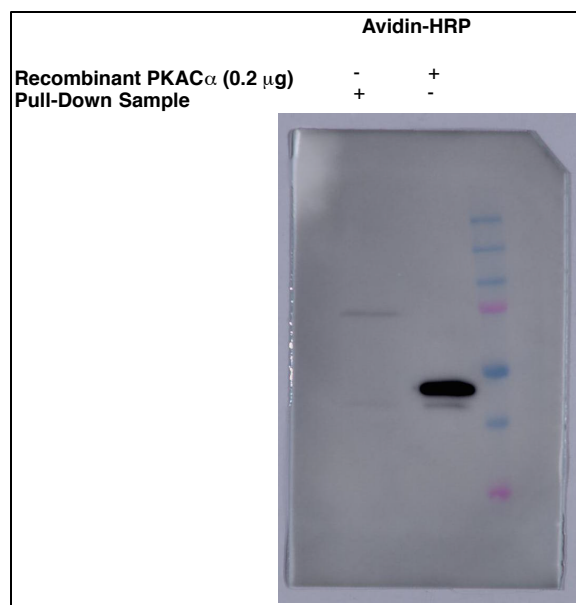


Figure 65. Western blot of the pull-down sample with streptavidin-HRP.

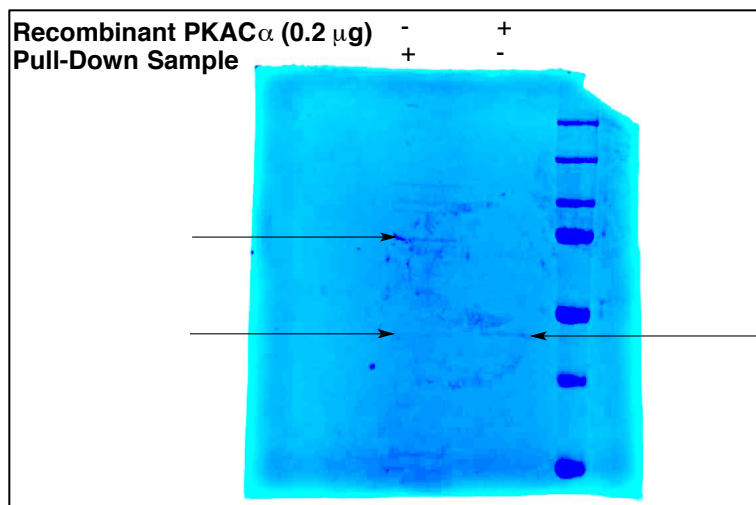


Figure 66. Coomassie stain of pull-down sample, major bands highlighted.

3.13.2: Results and Discussion of the Biological Characterization of 51.

The IC₅₀ of biotin-PKI(14-22)-G-(FMK) was determined to be 149 nM (by Invitrogen). The results of the pull-down experiment reveal that PKAC α was pulled down. But, in addition another prominent protein with a much higher molecular weight was observed. The streptavidin-hrp blot indicates a relative larger quantity of the higher molecular weight protein. Similarly, the Coomassie stain image appears to indicate that the higher molecular weight protein is present in larger quantities (reminiscent of the results obtained when examining the MCF7 cell line). When the IC₅₀ is considered along with the pull-down results, it is reasonable to assume the probe does not covalently interact with PKAC α on a level of selectivity necessary for ABPP of PKA. It was hypothesized that the linker was not long enough and so another analogue was designed to extend the linker between biotin and the recognition scaffold.

3.13.3: Addition of a linker.

The 8-(Fmoc-amino)octanoic acid (AOC) linker is solid-phase chemistry compatible and has been utilized in similar probes as a linker. The synthesis was carried out on a peptide synthesizer and assembly of the probe was similar to that of the previous probes. A detailed procedure is available in the experimental section. The probe was analyzed under similar conditions; however, labeling was demonstrated at relatively high concentrations.

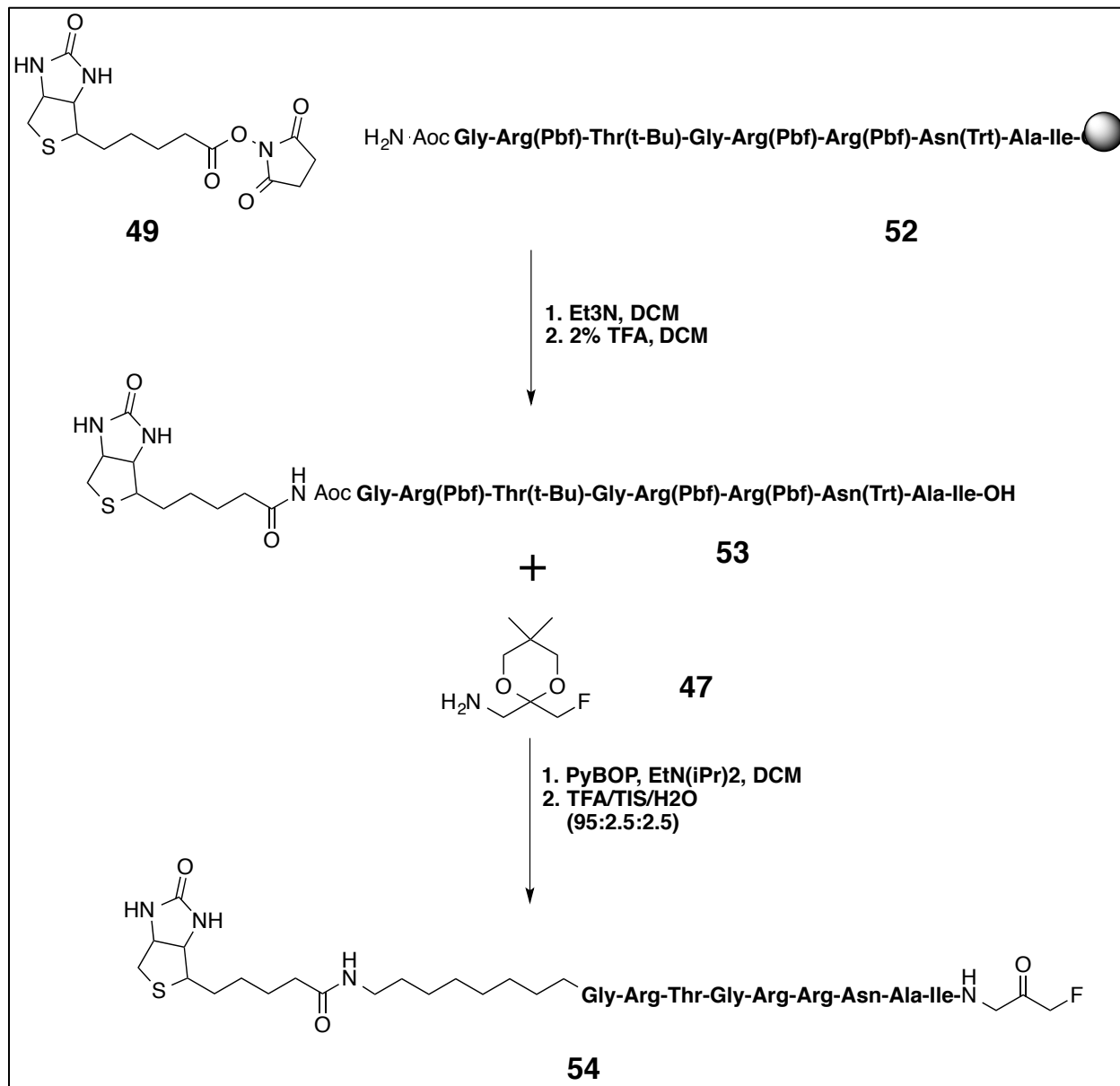


Figure 67. Synthesis of Biotin-Aoc-PKI(14-22)-G-(FMK).

3.13.4: Biological Characterization of Compound 54.

To examine the labeling efficiency of the new probe and test the limits of detection. The probe was incubated with recombinant PKAC α and detected by streptavidin-HRP ECL substrate on an Amersham 600 imager (detailed experimental available in Chapter 4).

PKAC α (2 μ g)	-	+	+	+	+	+	+	+
51 (μ M)	-	-	0.5	1	2	-	-	-
54 (μ M)	-	-	-	-	-	0.5	1	2

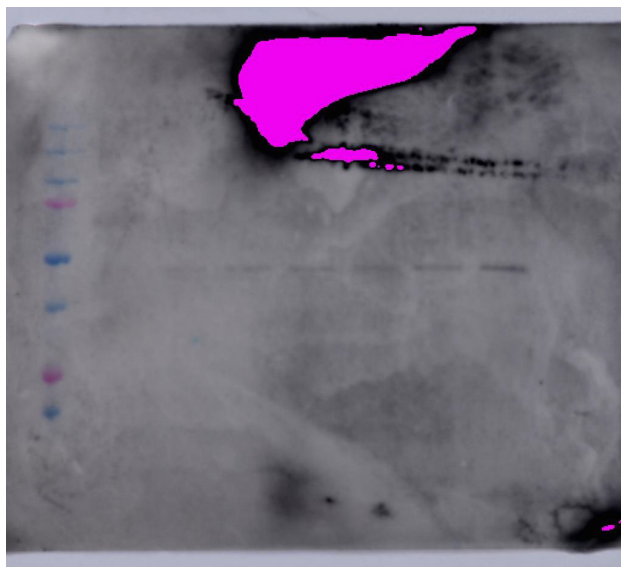


Figure 68. Detection of recombinant PKAC α labeled with **51** (lanes 3-5) and **54** (lanes 6-8).

3.13.5: Results and Discussion of the Biotinylated Derivatives.

The IC₅₀ of the biotin-AOC-PKI(14-22)-(FMK) probe against PKAC α was determined to be 14.1 nM (by Invitrogen). This confirmed the hypothesis that the linker length was not long enough. Without the linker, the IC₅₀ was 149 nM. The IC₅₀ is also indicative of increased binding over the reversible inhibitor (IC₅₀ = 49 nM, determined by Invitrogen). However, labeling of recombinant protein remained an issue: even at high concentrations, only trace labeling was

detectable. No labeling was detected in MDA-MB-231 lysates (only endogenous biotinylated peptides were shown by Western blot), and no labeling of commercial bovine PKAC α was observed. The biotinylated peptide-based probes did not label in a manner consistent with the fluorescently labeled probes. This suggests that the rhodamine is influencing the position of the electrophile such that labeling is occurring more robustly than non-interfering tags.

3.14: Results, Discussion, and Future Directions.

The active site of protein kinases has been shown to be influenced by certain post-translational modifications, as was suggested by others.^{40,128,137,139-141} While this work did not produce an activity-based probe suitable for activity-based protein profiling of PKAC α in complex biological mixtures, it did produce probes capable of investigating the active-site of PKAC α , as demonstrated by the selectivity for pThr197 and sensitivity to cysteine oxidation. Additionally, the probes are capable of assessing those post-translational modifications in a concerted, *in vitro*, manner without the use of multiple proteomic techniques. The reactivity of Cys199 has not been systematically studied, although, these probes are capable of such characterization. In addition, ABPs may have been developed for proteins of interest by probe **38** and probes **48** and **51** (as evidenced by their proteome wide selectivity and interactions with a PKI fragment) and further investigations into these ABPs is warranted. This represents a large step forward in the characterization of active site substrate-binding dynamics in the kinome.

A sequence alignment of the human kinome revealed that a total of ninety-nine kinases carry a cysteine in the position similar to PKAC α -C199 (see Figure 69). These kinases are mainly clustered in the AGC family and the CaMK family. Access to the cysteine in these kinases is restricted by selectivity filters in the P+1 binding site and the substrate-binding groove, allowing selective targeting of each cysteine and kinase with a high affinity peptide scaffold.

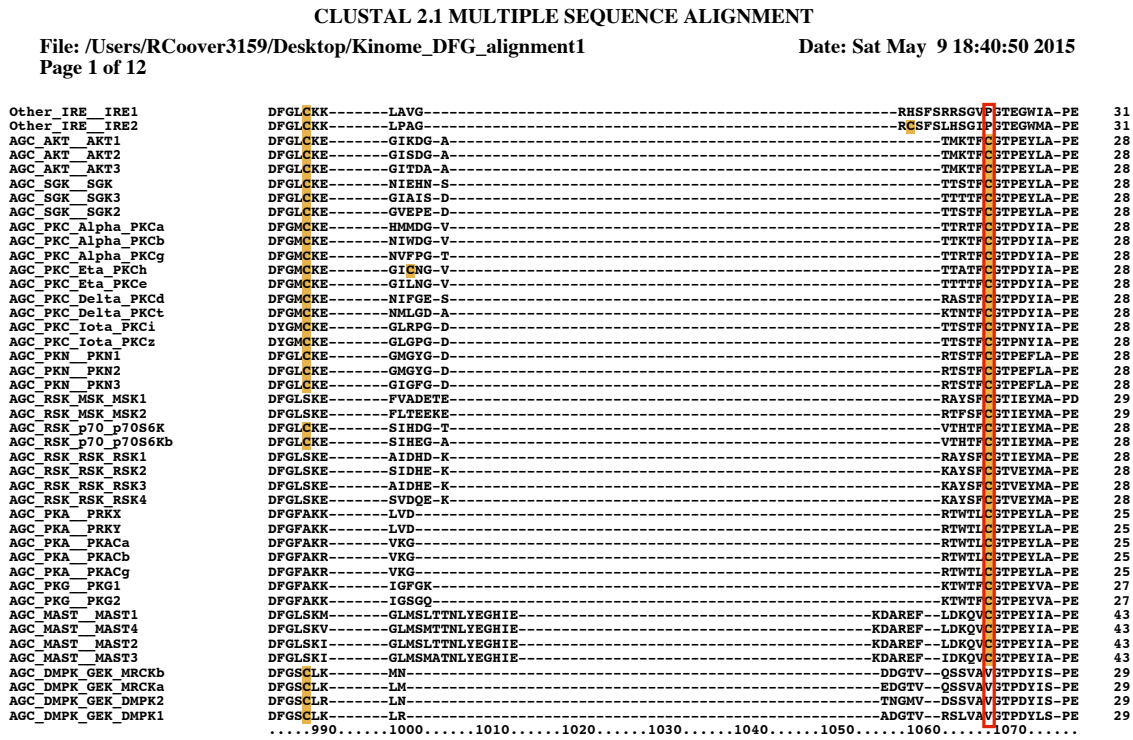
High affinity inhibitory peptides are known for several of the kinases in Figure 69, including AKT, PKG, AMPK, CaMKI, CHK2, and multiple isoforms of PKC. The activation loop cysteines in several of these kinases, including AKT1-C310, RSK1-C220, S6K1-C254, and MSK1-C214, have been shown to react with electrophiles. The flexible, efficient, and modular synthetic method presented here will allow the incorporation of a variety of electrophiles and detection tags into these peptides to prepare additional substrate competitive inhibitor probes for the kinases in Figure 69.

While an ABP probe was not developed for PKAC α specifically, a general strategy for developing substrate competitive inhibitor probes for kinases that targets the activation loop was developed and implemented. Work to further enhance peptide-based probe labeling and selectivity for PKAC α (modification of the electrophile reactivity and position) in complex biological mixtures, and the use of it to study PKAC α activity in diverse biological systems is currently underway in our lab.

Chapter 4. Experimentals

4.1 ClustalX Sequence Alignment

Kinome activation loop (DFG-APE) sequence alignment:



CLUSTAL 2.1 MULTIPLE SEQUENCE ALIGNMENT

File: /Users/RCoover3159/Desktop/Kinome_DFG_alignment1
Page 3 of 12

Date: Sat May 9 18:40:50 2015

CAMK_MAPKAPK_MNK_MNK2	DFDLGSG-----IKLNGD C SPIS-----	-----TP-----ELLT F CSAEYMA-PE	35
CAMK_RSKb_MSKb_Domain2_MSK1	DFGFARL-----KPPD-----	-----NQ-----PLKTF C TLHYAA-PE	28
CAMK_RSKb_MSKb_Domain2_MSK2	DFGFARL-----RPQSP-----	-----GV-----PMQTF C TLQYAA-PE	29
CAMK_RSKb_RSKb_Domain2_RSK2	DFGFAPQ-----LRAE-----	-----NG-----LLMTP C TANFVA-PE	28
CAMK_RSKb_RSKb_Domain2_RSK3	DFGFAPQ-----LRAE-----	-----NG-----LLMTP C TANFVA-PE	28
CAMK_RSKb_RSKb_Domain2_RSK1	DFGFAPQ-----LRAG-----	-----NG-----LLMTP C TANFVA-PE	28
CAMK_RSKb_RSKb_Domain2_RSK4	DFGFAPQ-----LRGE-----	-----NG-----LLLTP C TANFVA-PE	28
CAMK_PKD_PKD1	DFGFARI-----IGE-----	-----KS-----FRRSV V TPPAYLA-PE	27
CAMK_PKD_PKD3	DFGFARI-----IGE-----	-----KS-----FRRSV V TPPAYLA-PE	27
CAMK_PKD_PKD2	DFGFARI-----IGE-----	-----KS-----FRRSV V TPPAYLA-PE	27
CAMK_RAD53_CHK2	DFGHSKI-----LGE-----	-----TS-----LMRTL C STPYLA-PE	27
CAMK_CAMK_Unique_STK33	DFGLAVK-----KQSRs-----	-----EA-----MLQAT C STPYMA-PE	29
CAMK_CAMKL_AMPK_AMPKa1	DFGLSNM-----M-----	-----SDGE-----FLRTS C SPNYAA-PE	27
CAMK_CAMKL_AMPK_AMPKa2	DFGLSNM-----M-----	-----SDGE-----FLRTS C SPNYTA-PE	27
CAMK_CAMKL_BRSK_BRSK2	DFGMASL-----Q-----	-----VGDS-----LLET S CSPHYA C -PE	27
CAMK_CAMKL_BRSK_BRSK1	DFGMASL-----Q-----	-----VGDS-----LLET S CSPHYA C -PE	27
CAMK_CAMKL_MARK_MARK2	DFGFSNE-----F-----	-----TFGN-----KLD T CSPPYAA-PE	27
CAMK_CAMKL_MARK_MARK1	DFGFSNE-----F-----	-----TVGN-----KLD T CSPPYAA-PE	27
CAMK_CAMKL_MARK_MARK3	DFGFSNE-----F-----	-----TVGG-----KLD T CSPPYAA-PE	27
CAMK_CAMKL_MARK_MARK4	DFGFSNE-----F-----	-----TLGS-----KLD T CSPPYAA-PE	27
CAMK_CAMKL_QIK_QIK	DFGFGNF-----F-----	-----KSGE-----LLAT W CSPPYAA-PE	27
CAMK_CAMKL_QIK_SIK	DFGFGNF-----Y-----	-----KSGE-----PLST W CSPPYAA-PE	27
CAMK_CAMKL_QIK_QSK	DFGFSNL-----F-----	-----TPGQ-----LLK T W C SPPYAA-PE	27
CAMK_CAMKL_NuaK_NuaK1	DFGLSNL-----Y-----	-----QKDK-----FLQ T CSPPLYAS-PE	27
CAMK_CAMKL_NuaK_NuaK2	DFGLSNL-----Y-----	-----HQGK-----FLQ T CSPPLYAS-PE	27
CAMK_CAMKL_MELK_MELK	DFGL C AK-----P-----	-----KGNKDY-----HLQ T C C SLAYAA-PE	29
CAMK_CAMKL_NIM1_NIM1	DFGFSTV-----S-----	-----KKGE-----MLN T CSPPYAA-PE	27
CAMK_CAMKL_SNRK_SNRK	DFGFSNK-----P-----	-----QPKK-----KLT S CSLAYSA-PE	27
CAMK_CAMKL_HUNK_HUNK	DFGLSN C -----AG-----	-----ILGYSD-----P F ST C SPAYAA-PE	30
CAMK_TSSK_TSSK	DFGFGR-----	-----QAGHPD-----LST T C C SAAYAS-PE	28
CAMK_TSSK_TSSK3	DFGFAPV-----	-----LPKSHRE-----LSQ T C C STAYAA-PE	29
CAMK_TSSK_TSSK2	DFGFAPV-----	-----LRDSNGRII-----LSK T C C SAAYAA-PE	32
CAMK_TSSK_TSSK1	DFSFAPV-----	-----LRD S NGRMA-----LSK T C C SPAYAA-PE	32
CAMK_TSSK_TSSK4	DFGFAPV-----	-----YRQV N FSH-----LSQ T C C SPAYA C -PE	43
CAMK_PIM_PIM3	DFGSGAL-----LK-----	-----DT-----VYTD F C TRVYSP-PE	26
CAMK_PIM_PIM1	DFGSGAL-----LK-----	-----DT-----VYTD F C TRVYSP-PE	26
CAMK_PIM_PIM2	DFGSGAL-----LH-----	-----DE-----PYTD F C TRVYSP-PE	26
CAMK_CAMKL_PASK_PASK	DFGSAAY-----LER-----	-----GK-----LFY T C C IEYA-PE	27
Other_CAMKK_Meta_CAMKK2	DFGVSNE-----FK-----	-----GSDA-----LLSN V TPAFMA-PE	28
Other_CAMKK_Meta_CAMKK1	DFGVSNQ-----FE-----	-----GNDA-----QLS T A C TPAFMA-PE	28
CAMK_CAMKL_LKB_LKB1	DLGVAEA-----LHP-----	-----FAADD-----T C RT S C C SPAFOP-PE	30
CAMK_CAMKL_CHK1_CHK1	DFGLATV-----FRY-----	-----NNRER-----LLNK M C TLPYVA-PE	30
Other_AUR_AurC	DFGWSVH-----TLP-----	-----ERK T M C TLDYL P -PE	26
990.....1000.....1010.....1020.....1030.....1040.....1050.....1060.....1070.....		



CLUSTAL 2.1 MULTIPLE SEQUENCE ALIGNMENT

File: /Users/RCoover3159/Desktop/Kinome_DFG_alignment1
 Page 4 of 12

Date: Sat May 9 18:40:50 2015

Other_AUR_AurB	DFGWSVH-----APSL-----	RRKTMCTLDYLP-PE	26
Other_AUR_AurA	DFGWSVH-----APSS-----	RRRTLCTLDYLP-PE	26
Other_PLK_PLK3	DFGLAAR-----LEPPE-----	Q--RKKTICTPNYVA-PE	28
Other_PLK_PLK2	DFGLAAR-----LEPLE-----	H--RRRTICTPNYLS-PE	28
Other_PLK_PLK1	DFGLATK-----VEYDG-----	E--RKKTLCTPNYIA-PE	28
Other_PLK_PLK4	DFGLATQ-----LKMPE-----	E--KHYTLCTPNYIS-PE	28
CAMK_DAPK_DAPK1	DFGLARK-----IDFGNEF-----	-----KNIFCTPEFVA-PE	27
CAMK_DAPK_DAPK3	DFGLARK-----IEAGNEF-----	-----KNIFCTPEFVA-PE	27
CAMK_DAPK_DAPK2	DFGLAHE-----IEDGVVF-----	-----KNIFCTPEFVA-PE	27
CAMK_DAPK_DRAK1	DFGLSRI-----LKNSEEL-----	-----REIMCTPEYVA-PE	27
CAMK_DAPK_DRAK2	DFGMSRK-----IGHAACL-----	-----REIMCTPEYLA-PE	27
CAMK_MLCK_caMLCK	DFGLARR-----YKPREKL-----	-----KVNCTPEFLA-PE	27
CAMK_MLCK_SgK085	DFGLARR-----YKPREKL-----	-----KVNCTPEFLA-PE	27
CAMK_MLCK_skMLCK	DFGLARR-----YNPNEKL-----	-----KVNCTPEFLS-PE	27
CAMK_MLCK_smMLCK	DFGLARR-----LENAGSL-----	-----KVLCTPEFVA-PE	27
CAMK_MLCK_TTN	EFGQARQ-----LKFQDNF-----	-----RLLCTAPEYVA-PE	27
CAMK_Trio_Trio	DFGDAVQ-----LNTTYII-----	-----HQLLNPEFAA-PE	27
CAMK_Trio_Trad	DLEDVQV-----ISGHPHI-----	-----HLLLNPEFAA-PE	27
CAMK_Trio_SPEG	DFGNAQE-----LTPGEPO-----	-----YQVCTPEFVA-PE	27
CAMK_Trio_Obscn	DFGFAQN-----ITPAELO-----	-----FSQGSPEFVS-PE	27
CAMK_Trio_Domain2_SPEG	DFGSAQP-----YNPQALRP-----	-----LGRKCTLEFMA-PE	29
CAMK_Trio_Domain2_Obscn	DLGNAQS-----LSQEKVLP-----	-----SDKKDYLETMA-PE	29
CMGC_CDK_CDC2_CDK2	DFGLARA-----FG-----	VP-VRT--YTHEVTLWYRA-PE	28
CMGC_CDK_CDC2_CDK3	DFGLARA-----FG-----	VP-LRT--YTHEVTLWYRA-PE	28
CMGC_CDK_CDC2_CDK2	DFGLARA-----FG-----	IP-IRV--YTHEVTLWYRS-PE	28
CMGC_CDK_CDK5_CDK5	DFGLARA-----FG-----	IP-VRC--YSAEVTWYRP-PD	28
CMGC_CDK_TAIRE_PCTAIRE1	DFGLARA-----KS-----	IP-TKT--YSNEVTWYRP-PD	28
CMGC_CDK_TAIRE_PCTAIRE2	DFGLARA-----KS-----	VP-TKT--YSNEVTWYRP-PD	28
CMGC_CDK_TAIRE_PCTAIRE3	DFGLARA-----KS-----	VP-TKT--YSNEVTWYRP-PD	28
CMGC_CDK_TAIRE_PFTAIRE1	DFGLARA-----KS-----	VP-SHT--YSNEVTWYRP-PD	28
CMGC_CDK_TAIRE_PFTAIRE2	DFGLARA-----KS-----	IP-SQT--YSSEVTWYRP-PD	28
CMGC_CDK_CDK4_CDK4	DFGLARI-----YS-----	Y--QMA--LTPVVTWYRA-PE	27
CMGC_CDK_CDK4_CDK6	DFGLARI-----YS-----	F--QMA--LTSVVTWYRA-PE	27
CMGC_CDK_CDK10_CDK10	DFGLARA-----YG-----	VP-VKP--MTPKVTWYRA-PE	28
CMGC_CDK_PITSLRE_PITSLRE	DFGLARE-----YG-----	SP-LKA--YTPVVTWYRA-PE	28
CMGC_CDK_CDK7_CDK7	DFGLAKS-----FG-----	SP-NRA--YTHVVTWYRA-PE	28
CMGC_CDK_CCRK	DFGLARV-----FS-----	PDGSRLL--YTHVVTWYRA-PE	29
CMGC_CDK_CDK7_CHEP	DFGLARL-----YS-----	SEESRP--YTHVVTWYRP-PE	29
CMGC_CDK_CDK7_CDK7	DFGLARL-----YN-----	SEESRP--YTHVVTWYRP-PE	29
CMGC_CDK_CDK9_CDK9	DFGLARA-----FSL-----	AKNSQPN--RYTNVTWYRP-PE	32
CMGC_CDK_CDK8_CDK8	DMGFARL-----FN-----	-----SPLKPLA-DLDPVVTWYRA-PE	31
CMGC_CDK_CDK8_CDK11	DMGFARL-----FN-----	-----SPLKPLA-DLDPVVTWYRA-PE	31
CMGC_MAPK_ERK_Erk1	DFGLAR-----I-AD-----	-----PEHDHTG-FLTEVVTWYRA-PE	31



CLUSTAL 2.1 MULTIPLE SEQUENCE ALIGNMENT

File: /Users/RCoover3159/Desktop/Kinome_DFG_alignment1
Page 5 of 12

Date: Sat May 9 18:40:50 2015

CMGC_MAPK_ERK_Erk2	DFGLAR-----V-AD-----	-----PDHDTG--FLTEYVTRWYRA-PE	31
CMGC_MAPK_ERK_Erk5	DFGMARG-----L-ET-----	-----SPAHQY--FMTEYVTRWYRA-PE	32
CMGC_MAPK_nmo_NLK	DFGLAR-----L-V-----	-----EELDES--HMTQEVVTRWYRA-PE	29
CMGC_MAPK_JNK_JNK1	DFGLAR-----L-V-----	-----TAGTSF--MMPYVTRWYRA-PE	27
CMGC_MAPK_JNK_JNK3	DFGLAR-----L-V-----	-----TAGTSF--MMPYVTRWYRA-PE	27
CMGC_MAPK_JNK_JNK2	DFGLAR-----L-V-----	-----TAGTSF--MMPYVTRWYRA-PE	27
CMGC_MAPK_p38_p38a	DFGLAR-----L-V-----	-----TAGTSF--MMPYVTRWYRA-PE	27
CMGC_MAPK_p38_p38b	DFGLAR-----L-V-----	-----TAGTSF--MMPYVTRWYRA-PE	27
CMGC_MAPK_p38_p38g	DFGLAR-----L-V-----	-----TAGTSF--MMPYVTRWYRA-PE	27
CMGC_MAPK_p38_p38d	DFGLAR-----L-V-----	-----TAGTSF--MMPYVTRWYRA-PE	27
CMGC_MAPK_Erk7_Erk7	DFGLARS-----LGDL-----	-----PEGPED--AVTEYVTRWYRA-PE	33
CMGC_MAPK_ERK_Erk3	DFGLAR-----IMD-----	-----PHYSHG--HLEGLVTRWYRA-PR	31
CMGC_MAPK_ERK_Erk4	DFGLAR-----IVD-----	-----QHYSHG--YLEGLVTRWYRA-PR	31
CMGC_RCK_MAK	DFGLAR-----IVD-----	-----ELRSQP--PYTDVSTRWYRA-PE	27
CMGC_RCK_ICK	DFGLAR-----IVD-----	-----EIRSKP--PYTDVSTRWYRA-PE	27
CMGC_RCK_MOK	DFGSR-----SVYSKO--PYTEYSTRWYRA-PE	27	
CMGC_CDKL_CDKL2	DFGFART-----LAA-----	-----P-GEV--YTDVTRWYRA-PE	28
CMGC_CDKL_CDKL3	DFGFART-----LAA-----	-----P-GDI--YTDVTRWYRA-PE	28
CMGC_CDKL_CDKL1	DFGFARL-----LTG-----	-----P-SDV--YTDVTRWYRA-PE	28
CMGC_CDKL_CDKL4	DFGFAQI-----LI-----	-----P-GDA--YTDVTRWYRA-PE	27
CMGC_CDKL_CDKL5	DFGFARN-----LSEG-----	-----N-NAN--YTEYTRWYRA-PE	29
CMGC_GSK_GSK3A	DFGSAKO-----LVR-----	-----GEP--NVSYSRYRA-PE	27
CMGC_GSK_GSK3B	DFGSAKO-----LVR-----	-----GEP--NVSYSRYRA-PE	27
CMGC_CLK_CLK1	DFGSATY-----DDEH-----	-----HSTLVSTRHYRA-PE	25
CMGC_CLK_CLK4	DFGSATY-----DDEH-----	-----HSTLVSTRHYRA-PE	25
CMGC_CLK_CLK2	DFGSATF-----DHEH-----	-----HSTLVSTRHYRA-PE	25
CMGC_CLK_CLK3	DFGSATF-----DHEH-----	-----HSTLVSTRHYRA-PE	25
CMGC_SRPK_SRPK2	DLGNACW-----VHKH-----	-----FTEDVTRQYRA-VE	25
CMGC_SRPK_MSSK1	DLGNACW-----VHKH-----	-----FTEDVTRQYRA-VE	25
CMGC_SRPK_SRPK1	DLGNACW-----VHKH-----	-----FTEDVTRQYRA-VE	25
CMGC_DYRK_Dyrk1_DYRK1B	DFGSSCO-----LGQR-----	-----IYQVDSRFYRA-PE	25
CMGC_DYRK_Dyrk1_DYRK1A	DFGSSCO-----LGQR-----	-----IYQVDSRFYRA-PE	25
CMGC_DYRK_Dyrk2_DYRK2	DFGSSCY-----EHQR-----	-----VYTVDSRFYRA-PE	25
CMGC_DYRK_Dyrk2_DYRK3	DFGSSCF-----EYQK-----	-----LYTVDSRFYRA-PE	25
CMGC_DYRK_Dyrk2_DYRK4	DFGSSCY-----EHQK-----	-----VYTVDSRFYRA-PE	25
CMGC_DYRK_HIPK_HIPK1	DFGSASH-----VSKA-----	-----V--GSTYDSRYRA-PE	26
CMGC_DYRK_HIPK_HIPK2	DFGSASH-----VSKA-----	-----V--GSTYDSRYRA-PE	26
CMGC_DYRK_HIPK_HIPK3	DFGSASH-----VSKT-----	-----V--GSTYDSRYRA-PE	26
CMGC_DYRK_HIPK_HIPK4	DFGSASI-----FSEVR-----	-----YV--KEPYDSRFYRA-PE	28
CMGC_DYRK_PRP4_PRP4	DFGSASH-----VADN-----	-----D--ITPYDSRFYRA-PE	26
Other_CK2_CK2a1	DWGLAEF-----YH-----	-----PGQEYN--VTVASRYFKG-PE	27
Other_CK2_CK2a2	DWGLAEF-----YH-----	-----PAQEYN--VTVASRYFKG-PE	27
Other_NKF1_SgK069	DFGHTRP-----RG-----	-----TLRLA--GPIPYTAPELCA-PP	30
990.....1000.....1010.....1020.....1030.....1040.....1050.....1060.....1070.....		



CLUSTAL 2.1 MULTIPLE SEQUENCE ALIGNMENT

File: /Users/RCoover3159/Desktop/Kinome_DFG_alignment1
Page 6 of 12

Date: Sat May 9 18:40:50 2015

Other_NKF1_SgK110	DLGLTRP-----EG-----	SPTPAP--PVPLFAPPPELCL--LL	30
Other_NKF1_SBK	DFGMTRR-----VG-----	ERVKRV--SGTIFVTAPEVCO--AG	30
Other_IKK_IKka	DLGYAKD-----VDQGS-----	LCTSFVSTLQYLA--PE	27
Other_IKK_IKkb	DLGYAKE-----LDQGS-----	LCTSFVSTLQYLA--PE	27
Other_IKK_IKKe	DFGAARE-----LDDDE-----	KFVSVVSTEEYLH--PD	27
Other_IKK_TBK1	DFGAARE-----LEDDE-----	QFVSLVSTEEYLH--PD	27
STE_STE11_MAP3K2	DFGASKR-----LQTI-----	LSGTG---MKSVDTPYWM--PE	31
STE_STE11_MAP3K3	DFGASKR-----LQTI-----	MSGTG---MRSVDTPYWM--PE	31
STE_STE11_MAP3K8	DFGQARR-----LAWAG-----	LNQTHS--DMLKSMSTPYWMA--PE	34
STE_STE11_MAP3K5	DFGTSKR-----LAGIN-----	PC-----TETFDTLQYMA--PE	28
STE_STE11_MAP3K7	DFGTSKR-----LAGVN-----	PC-----TETFDTLQYMA--PE	28
STE_STE11_MAP3K6	DFGTSKR-----LAGIT-----	PC-----TETFDTLQYMA--PE	28
STE_STE11_MAP3K4	DFGQSVK-----LKNNNA-----	QTMFG---EVNSTLSTAYMA--PE	32
STE_STE11_MAP3K1	DFGAAAR-----LASKG-----	TGAG---EPGGQLSTIAFMA--PE	32
STE_STE20_FRAY_OSRI1	DFGVSAF-----LATGG-----	DITR--NKVRKTFVTPYWMA--PE	33
STE_STE20_FRAY_STLK3	DFGVSAF-----LATGG-----	DVTR--NKVRKTFVTPYWMA--PE	33
STE_STE20_STLK_STLK5	GLRSNLS-----MISHG-----	QRQRVVDHFFPKYSKVLFWLS--PE	35
STE_STE20_STLK_STLK6	GLSRLHS-----LVKHG-----	QRIRAVIDFFPQPSVQVWLS--PE	35
STE_STE20_KHS_KHS1	DFGVAAK-----ITAT-----	IAK-----RKSFTDTPYWMA--PE	28
STE_STE20_KHS_KHS2	DFGVSAQ-----ITAT-----	IAK-----RKSFTDTPYWMA--PE	28
STE_STE20_KHS_GCK	DFGVSGE-----LTAS-----	VAK-----RRSFTDTPYWMA--PE	28
STE_STE20_KHS_HPK1	DFGISAQ-----IGAT-----	LAR-----RLSFTDTPYWMA--PE	28
STE_STE20_MSN_ZC1/HGK	DFGVSAQ-----LDRT-----	VGR-----RNTFDTPYWMA--PE	28
STE_STE20_MSN_ZC3/MINK	DFGVSAQ-----LDRT-----	VGR-----RNTFDTPYWMA--PE	28
STE_STE20_MSN_ZC2/TNIK	DFGVSAQ-----LDRT-----	VGR-----RNTFDTPYWMA--PE	28
STE_STE20_MSN_ZC4/NRK	DFGVSAQ-----VSRT-----	NGR-----RNSFTDTPYWMA--PE	28
STE_STE20_MinaC_MYO3B	DFGVSAQ-----LTSI-----	RIR-----RNSVSTPPFMA--PE	28
STE_STE20_MinaC_MYO3A	DFGVSAQ-----LTSI-----	RIR-----RNSVSTPPFMA--PE	28
STE_STE20_MST_MST1	DFGVAGO-----LTDI-----	MAK-----RNTVSTPPFMA--PE	28
STE_STE20_MST_MST2	DFGVAGO-----LTDI-----	MAK-----RNTVSTPPFMA--PE	28
STE_STE20_YSK_MST3	DFGVAGO-----LTDI-----	QIK-----RNTVSTPPFMA--PE	28
STE_STE20_YSK_YSK1	DFGVAGO-----LTDI-----	QIK-----RNTVSTPPFMA--PE	28
STE_STE20_YSK_MST4	DFGVAGO-----LTDI-----	QIK-----RNTVSTPPFMA--PE	28
STE_STE20_SLK_SLK	DFGVSAK-----NTRT-----	IQR-----RDSFTDTPYWMA--PE	28
STE_STE20_SLK_LOK	DFGVSAK-----NLKT-----	LQK-----RDSFTDTPYWMA--PE	28
STE_STE20_TAO_TAO2	DFGSASI-----MAP-----	ANSFVSTPYWMA--PE	24
STE_STE20_TAO_TAO1	DFGSASM-----ASF-----	ANSFVSTPYWMA--PE	24
STE_STE20_TAO_TAO3	DFGSASM-----ASF-----	ANSFVSTPYWMA--PE	24
STE_STE20_PAKA_PAK1	DFGFCAQ-----ITPE-----	QSK-----RSTMVSTPYWMA--PE	28
STE_STE20_PAKA_PAK3	DFGFCAQ-----ITPE-----	QSK-----RSTMVSTPYWMA--PE	28
STE_STE20_PAKA_PAK2	DFGFCAQ-----ITPE-----	QSK-----RSTMVSTPYWMA--PE	28
STE_STE20_PAKB_PAK4	DFGFCAQ-----VSKE-----	VPR-----RKSLVSTPYWMA--PE	28
STE_STE20_PAKB_PAK5	DFGFCAQ-----VSKE-----	VPK-----RKSLVSTPYWMA--PE	28



CLUSTAL 2.1 MULTIPLE SEQUENCE ALIGNMENT

File: /Users/RCoover3159/Desktop/Kinome_DFG_alignment1
Page 7 of 12

Date: Sat May 9 18:40:50 2015

```

STE STE20_PAKB_PAK6      DFGFCAQ-----ISKD-----VPK-----RKSLVPTPYWMA-PE 28
STE STE7_MAP2K1         DFGVSGQ-----LIDSM-----ANS-----FVTRSYMS-PE 26
STE STE7_MAP2K2         DFGVSGQ-----LIDSM-----ANS-----FVTRSYMA-PE 26
STE STE7_MAP2K5         DFGVSTQ-----LVNSI-----AKT-----YVFTNAYMA-PE 26
STE STE7_MAP2K6         DFGISGY-----LVDSV-----AKTI-----DAGCKPYMA-PE 27
STE STE7_MAP2K3         DFGISGY-----LVDSV-----AKTM-----DAGCKPYMA-PE 27
STE STE7_MAP2K4         DFGISGQ-----LVDSI-----AKTR-----DAGCRPYMA-PE 27
STE STE7_MAP2K7         DFGISGR-----LVDSK-----AKTR-----SAGAAAYMA-PE 27
Other_NKF4_CLI1K1      DFGLSKV-----GAGLAPR-----G-----KEGNQDNKNVNVNK-----YMLSSAGSDPYMA-PE 45
Other_NKF4_CLI1K1      DFGLSKV-----CS-----G-----ASGQNPPEPVSUNK-----FLLSTACSTDPYMA-PE 39
Other_ULK_ULK1         DFGFARY-----LQSN-----MMAATLQSSPMYMA-PE 27
Other_ULK_ULK2         DFGFARY-----LHSN-----MMAATLQSSPMYMA-PE 27
Other_ULK_ULK3         DFGFAQH-----MSPW-----DEKHVLRGSPLYMA-PE 27
Other_ULK_ULK4         NFCLAKV-----EGENLEEFALVAA-----EEGGDNGENVLKK-----SMKSRVKGSPVYTA-PE 51
Other_ULK_Fused        DFGFARA-----MSTN-----T-----MVLTSIKGTPLYMS-PE 28
Other_NEK_NEK1         DFGIARV-----LNSTVE-----LARTCTGTPPYLS-PE 28
Other_NEK_NEK5         DFGIARV-----LNNMSE-----LARTCTGTPPYLS-PE 28
Other_NEK_NEK3         DFGSARL-----LSNPM-----FACTVPTPYVP-PE 28
Other_NEK_NEK4         DLGIARV-----LENHCD-----MASTLCTPPYMS-PE 28
Other_NEK_NEK2         DFGIARI-----LNHDT-----FAKTFVTPPYMS-PE 28
Other_NEK_NEK9         DYGLAKK-----LNSEYS-----MAETLVTPPYMS-PE 28
Other_NEK_NEK8         DFGISKI-----LSSK-----S-----TPCYIS-PE 20
Other_NEK_NEK6         DLGLGRF-----FSSETT-----AAHSLVTPPYMS-PE 28
Other_NEK_NEK7         DLGLGRF-----FSSKTT-----AAHSLVTPPYMS-PE 28
Other_NEK_NEK11        DFGVSRV-----LMGSCD-----LATTLCSTPHYMS-PE 28
Other_NEK_NEK10        DFGLAKQ-----KQENSK-----LT-SVVPTILYSC-PE 27
Other_TLK_TLK1         DFGLSKI-----MDDDSYG-----VDGMDLTSQCASTYWLP-PE 34
Other_TLK_TLK2         DFGLSKI-----MDDDSYMS-----VDGMELTSQCASTYWLP-PE 35
CAMK_Trbl_Trbl        SLEDTHI-----MKGED-----DALSDKHGCPAYVS-PE 28
CAMK_Trbl_Trbl        SLEDAYI-----LRGDD-----DSLSDKHGCPAYVS-PE 28
CAMK_Trbl_Trbl        NLEDSGV-----LTGPD-----DSLWDKHCAPAYVG-PE 28
CAMK_CAMK-Unique_SgK495 NFCLGKH-----LVSEG-----DLLKDKRGSPAYIS-PD 28
Other_NKF3_SgK223      NFLKAKQ-----KPG-C-----TPNLQQRKQSARLA-PE 27
Other_NKF3_SgK269      NFSQAKQ-----KS-H-----LVDPEILRQSARLA-PE 26
Other_NAK_AAK1         DFGSATN-----KQNP-----QTEGVNAVEDEIKKVTLSYRA-PE 36
Other_NAK_BIKE         DFGSATN-----KFLNP-----QKDGNNVVEEIKKVTLSYRA-PE 36
Other_NAK_GAK          DFGSATN-----ISHIPDYS-----W-----SAQRRLVEEITERCTPMYRT-PE 40
Other_PEK_PEK_PEK      DFGLVV-----AMDQDEEQT-----VLTMPAYARHTGCVFKLYMS-PE 40
Other_PEK_PEK          DFGLVV-----SLKND-----GKTRTKLRLYMS-PE 27
Other_PEK_GC2_GC2      DFGLATDHLAFSADSKDDQDQDGD-----LIKSDPS-GHLTGMVFLALYVS-PE 46
Other_WEE_Wee1        D-EDDW--ASNKVMFKIGDLGH-----V-----TRISSPQVEGDSRFLA-NE 39
Other_WEE_Wee1B       ENEADWF--LSANVMYKIGDLGH-----A-----TSINKPKVEGDSRFLA-NE 41
Other_WEE_MY1         D---FG-----LLVELGTAG-----AGEVQEGDPRYMA-PE 27
.....990.....1000.....1010.....1020.....1030.....1040.....1050.....1060.....1070.....

```



CLUSTAL 2.1 MULTIPLE SEQUENCE ALIGNMENT

File: /Users/RCoover3159/Desktop/Kinome_DFG_alignment1
Page 8 of 12

Date: Sat May 9 18:40:50 2015

TKL_STKR_Type1_ALK1	DLGLAVM-----HSQ---GSD-----	-----YLDIGNNFRVETKRYMA-PE	32
TKL_STKR_Type1_ALK2	DLGLAVM-----HSQ---STN-----	-----QLDVGNNFRVETKRYMA-PE	32
TKL_STKR_Type1_ALK4	DLGLAVR-----HDA---VTD-----	-----TIDIPNQRVETKRYMA-PE	32
TKL_STKR_Type1_TGFbr1	DLGLAVR-----HDS---ATD-----	-----TIDIAPNHRVETKRYMA-PE	32
TKL_STKR_Type1_ALK7	DLGLAVK-----HDS---TLN-----	-----TIDIPQNKVETKRYMA-PE	32
TKL_STKR_Type1_BMPRIa	DLGLAVK-----FNS---DTN-----	-----EVDVPLNTRVETKRYMA-PE	32
TKL_STKR_Type1_BMPRIb	DLGLAVK-----FIS---DTN-----	-----EVDIPFNTRVETKRYMP-PE	32
TKL_STKR_Type2_ACTR2	DFGLALK-----FEA---GKS-----	-----AGD---THGQVETRYMA-PE	30
TKL_STKR_Type2_ACTR2B	DFGLAVR-----FEP---GKP-----	-----PGD---THGQVETRYMA-PE	30
TKL_STKR_Type2_TGFbr2	DFGLSLR-----LDP---TFS-----	-----VDDLANSQVETARYMA-PE	32
TKL_STKR_Type2_MISR2	DLGLALV-----LPG---LTPPPAW-----	-----TPTPOGPAIMEVETORYMA-PE	40
TKL_STKR_Type2_BMPR2	DFGLSMR-----LTGNRLVRP-----	-----G---EEDNAISEVETIRYMA-PE	36
RGC_RGC_ANPa	DYGLSEF-----R---DLD-----	-----PEQGHVYAKKLWTA-PE	28
RGC_RGC_ANPb	DYGLASF-----RS---TAE-----	-----PDDSHALYAKKLWTA-PE	29
RGC_RGC_HSER	DFGNSI-----LP---PK-----	-----KDLWTA-PE	19
RGC_RGC_CYGD	DHGHGRL-----LE---AQR-----	-----VLPPEPRAEDQLWTA-PE	29
RGC_RGC_CYGF	DIGFNDI-----LE---MLR-----	-----LSEESSMEELLWTA-PE	29
TK_Abl_ABL	DFGLSRL-----MT---GDT-----	-----YT-AHAGA-KFPVKWTA-PE	29
TK_Abl_ARG	DFGLSRL-----MT---GDT-----	-----YT-AHAGA-KFPVKWTA-PE	29
TK_Tec_BTK	DFGLSRY-----VL---DDE-----	-----YT-SSVGS-KFPVKWSP-PE	29
TK_Tec_BMX	DFGMTRY-----VL---DDO-----	-----YV-SSVGT-KFPVKWSA-PE	29
TK_Tec_TEC	DFGMARY-----FL---DDO-----	-----YT-SSSGA-KFPVKWCP-PE	29
TK_Tec_TXK	DFGMTRY-----VL---DDE-----	-----YV-SSFGA-KFPVKWSP-PE	29
TK_Tec_ITK	DFGMTRF-----VL---DDO-----	-----YT-SSTGT-KFPVKWAS-PE	29
TK_Src_HCK	DFGLARV-----IE---DNE-----	-----YT-AREGA-KFPVKWTA-PE	29
TK_Src_LYN	DFGLARV-----IE---DNE-----	-----YT-AREGA-KFPVKWTA-PE	29
TK_Src_LCK	DFGLARL-----IE---DNE-----	-----YT-AREGA-KFPVKWTA-PE	29
TK_Src_BLK	DFGLARI-----ID---S-E-----	-----YT-ARQGA-KFPVKWTA-PE	28
TK_Src_SRC	DFGLARL-----IE---DNE-----	-----YT-ARQGA-KFPVKWTA-PE	29
TK_Src_YES	DFGLARL-----IE---DNE-----	-----YT-ARQGA-KFPVKWTA-PE	29
TK_Src_FYN	DFGLARL-----IE---DNE-----	-----YT-ARQGA-KFPVKWTA-PE	29
TK_Src_FGR	DFGLARL-----IK---DDE-----	-----YN-PCQGS-KFPVKWTA-PE	29
TK_Src_FRK	DFGLARV-----FKV---DNEDI-----	-----YE-SRHEI-KLPVKWTA-PE	32
TK_Src_BRK	DFGLARL-----IK---EDV-----	-----Y-LSHDH-KLPVKWTA-PE	28
TK_Src_SRM	DFGLARL-----LK---DDI-----	-----YS-PSSSS-KLPVKWTA-PE	29
TK_Csk_CSK	DFGLTKE-----AS---STQ-----	-----DT-G---KLPVKWTA-PE	25
TK_Csk_CTK	DFGLAKA-----ER---KGL-----	-----DS-S---KLPVKWTA-PE	25
TK_Fer_FER	DFGMSRQ-----ED---GGV-----	-----YS-SSG-LKLPVKWTA-PE	29
TK_Fer_FES	DFGMSRE-----EA---DGV-----	-----YA-ASGGS-KLPVKWTA-PE	30
TK_FGFR_FGFR2	DFGLARD-----INN---IDY-----	-----YK-KTTNG-KLPVKWMA-PE	30
TK_FGFR_FGFR3	DFGLARD-----VHN---LDY-----	-----YK-KTTNG-KLPVKWMA-PE	30
TK_FGFR_FGFR1	DFGLARD-----IHH---IDY-----	-----YK-KTTNG-KLPVKWMA-PE	30
TK_FGFR_FGFR4	DFGLARG-----VHH---IDY-----	-----YK-KTSNG-KLPVKWMA-PE	30



CLUSTAL 2.1 MULTIPLE SEQUENCE ALIGNMENT

File: /Users/RCoover3159/Desktop/Kinome_DFG_alignment1
Page 9 of 12

Date: Sat May 9 18:40:50 2015

TK_Ret_RET	DFGLSRD-----VYE--EDS-----	YV-KRSQG-RLPVKWMA-IE	30
TK_VEGFR_KDR	DFGLARD-----IYK--DPD-----	YV-RKGDARLPVKWMA-PE	30
TK_VEGFR_FLT1	DFGLARD-----IYK--NPD-----	YV-RKGDTRLPVKWMA-PE	30
TK_VEGFR_FLT4	DFGLARD-----IYK--DPD-----	YV-RKGSARLPVKWMA-PE	30
TK_PDGFPR_FMS	DFGLARD-----IMN--DSN-----	YI-VKGNARLPVKWMA-PE	30
TK_PDGFPR_KIT	DFGLARD-----IKN--DSN-----	YV-VKGNARLPVKWMA-PE	30
TK_PDGFPR_PDGFra	DFGLARD-----IMH--DSN-----	YV-SKGSARLPVKWMA-PE	30
TK_PDGFPR_PDGFrb	DFGLARD-----IMR--DSN-----	YI-SKGSARLPVKWMA-PE	30
TK_PDGFPR_FLT3	DFGLARD-----IMS--DSN-----	YV-VKGNARLPVKWMA-PE	30
TK_Tie_TIE2	DFGLSR-----G--QEV-----	YV-KKTMGRLPVPRWMA-IE	27
TK_Tie_TIE1	DFGLSR-----G--EEV-----	YV-KKTMGRLPVPRWMA-IE	27
TK_Alk_ALK	DFGMARD-----IYR--ASY-----	Y--RKGGARLPVKWMP-PE	30
TK_Alk_LTK	DFGMARD-----IYR--ASY-----	Y--RRGDRALPVKWMP-PE	30
TK_Sev_ROS	DFGLARD-----IYK--NDY-----	Y--RKRGEGLPVRWMA-PE	30
TK_InsR_INSR	DFGMTRD-----IYE--TDY-----	Y--RKGGKGLPVRWMA-PE	30
TK_InsR_IGF1R	DFGMTRD-----IYE--TDY-----	Y--RKGGKGLPVRWMS-PE	30
TK_InsR_IRR	DFGMTRD-----IYE--TDY-----	Y--RKGGKGLPVRWMA-PE	30
TK_DDR_DDR1	DFGMSRN-----LYA--GDY-----	Y--RVGGARLPVRWMA-WE	30
TK_DDR_DDR2	DFGMSRN-----LYS--GDY-----	Y--RIGGRALPVRWMS-WE	30
TK_Trk_TRKB	DFGMSRD-----VYS--TDY-----	Y--RVGGHTLPVRWMP-PE	30
TK_Trk_TRKC	DFGMSRD-----VYS--TDY-----	Y--RVGGHTLPVRWMP-PE	30
TK_Trk_TRKA	DFGMSRD-----IYS--TDY-----	Y--RVGGHTLPVRWMP-PE	30
TK_Musk_MUSK	DFGLSRN-----IYS--ADY-----	Y--KANENDALPVRWMP-PE	30
TK_Ror_ROR1	DLGLSRE-----IYS--ADY-----	Y--RVQSKSLPVRWMP-PE	30
TK_Ror_ROR2	DLGLFRE-----VYA--ADY-----	Y--KLLGNSLPVRWMA-PE	30
TK_CCK4_CCK4	ALGLSKD-----VYN--SEY-----	Y--HFR-QAVPLRWS-PE	29
TK_Axl_AXL	DFGLSKK-----IYN--GDY-----	Y--RQRIARLPVKWIA-IE	30
TK_Axl_MER	DFGLSKK-----IYS--GDY-----	Y--RQRIARLPVKWIA-IE	30
TK_Axl_TYRO3	DFGLSRK-----IYS--GDY-----	Y--RQCASKLPVKWLA-LE	30
TK_Met_MET	DFGLARD-----MYD--KEY-----	YSVHNKTKALPVKWMA-LE	32
TK_Met RON	DFGLARD-----ILD--REY-----	YSVQQRHARLPVKWMA-LE	32
TK_Ryk_RYK	DNALSRD-----LFP--MDY-----	H--LGDNERPVRWMA-LE	30
TK_Ack_ACK	DFGLMRA-----LPQN--DDH-----	Y--VMQEHKLPFANCA-PE	31
TK_Ack_TNK1	DFGLVRP-----LGGA--RGR-----	Y--VMGGERLPYTCA-PE	31
TK_EGFR_EGFR	DFGLARL-----LGAE--EKE-----	Y--HAE-GGKLPVKWMA-LE	30
TK_EGFR_HER2/ErbB2	DFGLARL-----LDID--ETE-----	Y--HAD-GGKLPVKWMA-LE	30
TK_EGFR_HER4/ErbB4	DFGLARL-----LEGD--EKE-----	Y--HAD-GGKLPVKWMA-LE	30
TK_EGFR_HER3/ErbB3	DFGVADL-----LPFD--DKQ-----	L--LYS-EAKLPVKWMA-LE	30
TK_Syk_SYK	DFGLSKA-----LRAD--ENV-----	Y--KAOHTGLPVRWYA-PE	31
TK_Syk_ZAP70	DFGLSKA-----LGAD--DSY-----	Y--TARSAGLPVKWYA-PE	31
TK_Eph_EphA3	DFGLSRV-----LEDDP-EAA-----	Y--TTR-GGKLPVRWTS-PE	31
TK_Eph_EphA5	DFGLSRV-----LEDDP-EAA-----	Y--TTR-GGKLPVRWTS-PE	31
TK_Eph_EphA4	DFGMSRV-----LEDDP-EAA-----	Y--TTR-GGKLPVRWTS-PE	31
990.....1000.....1010.....1020.....1030.....1040.....1050.....1060.....1070.....		



CLUSTAL 2.1 MULTIPLE SEQUENCE ALIGNMENT

File: /Users/RCoover3159/Desktop/Kinome_DFG_alignment1
Page 10 of 12

Date: Sat May 9 18:40:50 2015

TK_Eph_EphA6	DFGLSRV-----LEDDP-EAA-----	-----Y--TTT-GGKIPIRWTA-PE	31
TK_Eph_EphA7	DFGLSRV-----IEDDP-EAV-----	-----Y--TTT-GGKIPVRWTA-PE	31
TK_Eph_EphB1	DFGLSRV-----LQDDTSDPT-----	-----Y--TSSLGGKIPVRWTA-PE	33
TK_Eph_EphB2	DFGLSRF-----LEDDTSDPT-----	-----Y--TSALGGKIPIRWTA-PE	33
TK_Eph_EphB3	DFGLSRF-----LEDDPSDPT-----	-----Y--TSSLGGKIPIRWTA-PE	33
TK_Eph_EphB4	DFGLSRF-----LEENSSDPT-----	-----Y--TSSLGGKIPIRWTA-PE	33
TK_Eph_EphA8	DFGLSRV-----LEDDP-DAA-----	-----Y--TTT-GGKIPIRWTA-PE	31
TK_Eph_EphA2	DFGLSRV-----LEDDP-EAT-----	-----Y--TTS-GGKIPIRWTA-PE	31
TK_Eph_EphA1	DFGLTRL-----LDD-FDGT-----	-----Y--ETQ-GGKIPIRWTA-PE	30
TK_Eph_EphB6	RLGHS-----	-----PQ-GPS-LLRWAA-PE	19
TK_Eph_EphA10	GFGRGP-----RDRS-EAV-----	-----Y--TTM-SGRSPALWAA-PE	29
TK_Fak_FAK	DFGLSRV-----MED--STY-----	-----Y--KAS-KGLPIKWWA-PE	29
TK_Fak_PYK2	DFGLSRV-----IED--EDY-----	-----Y--KAS-VTLPIKWWA-PE	29
TK_JakA_JAK1	DFGLTKA-----IET--DKE-----	-----YYTVKDDR-DSPVFWYA-PE	31
TK_JakA_TYK2	DFGLAKA-----VPE--GHE-----	-----YYRVREDG-DSPVFWYA-PE	31
TK_JakA_JAK2	DFGLTKV-----LPQ--DKE-----	-----YYKVKEPG-ESPFWYA-PE	31
TK_JakA_JAK3	DFGLAKL-----LPL--DKD-----	-----YYVREPG-ESPFWYA-PE	31
TK_Lmr_LMR1	DYGLARL-----KVR--EDY-----	-----FVTADQLVPLRWTA-PE	30
TK_Lmr_LMR3	DYGLAHS-----NYK--EDV-----	-----YLTPERLHPLRWAA-PE	30
TK_Lmr_LMR2	DYGIIFS-----RYK--EDY-----	-----IETDKKFPPLRWTA-PE	30
TK_JakB_Domain2_JAK1	DPGIPIT-----VLS-----	-----RQEC--VERIPWTA-PE	24
TK_JakB_Domain2_TYK2	DPGVGLG-----ALS-----	-----REER--VERIPWLA-PE	24
TK_JakB_Domain2_JAK2	DPGISIT-----VLP-----	-----KDIL--VERIPWVP-PE	24
TK_JakB_Domain2_JAK3	DPGVSPA-----VLS-----	-----LEML--DRIPWVA-PE	24
TKL_LISK_LIMK_LIMK2	DFGLSRL-----IVEERKRAPMEKATTKK	-----RTLKKNDRKKRYTVGNPYWMA-PE	48
TKL_LISK_LIMK_LIMK1	DFGLARL-----MVDKKTQP_EGL	-----RSLKKPDRKKRYTVGNPYWMA-PE	42
TKL_LISK_TESK_TESK1	DFGLAEK-----IPVYREGA-----	-----RKEPLAVGSPFWMA-PE	32
TKL_LISK_TESK_TESK2	DFGLAEK-----IPDVSMOS-----	-----EK--LAVGSPFWMA-PE	30
TKL_MLK_HH498_HH498	DFGESRF-----LQSLD-ED-----	-----NNTKQFNLRWMA-PE	29
TKL_MLK_TAK1_TAK1	DFGTACD-----IQT-----	-----HMTNKGSAWMA-PE	25
TKL_MLK_LZK_DLK	DFGTSKE-----LSD--KS-----	-----TKMSFATYAWMA-PE	27
TKL_MLK_LZK_LZK	DFGTSKE-----LSD--KS-----	-----TKMSFATYAWMA-PE	27
TKL_MLK_MLK_MLK1	DFGLARE-----WH--RT-----	-----TKMSAATYAWMA-PE	26
TKL_MLK_MLK_MLK3	DFGLARE-----WH--RT-----	-----TKMSAATYAWMA-PE	26
TKL_MLK_MLK_MLK4	DFGLARE-----WH--RT-----	-----TKMSAATYAWMA-PE	26
TKL_MLK_MLK_MLK2	DFGLARE-----WH--RT-----	-----TKMSAATYAWMA-PE	26
TKL_MLK_MLK_ZAK	DFGASRF-----HN--RT-----	-----TMSLVTTFPWWMA-PE	26
TKL_RAF_BRAF	DFGLATV-----KSRWSSGH-----	-----QEQISSLWMA-PE	30
TKL_RAF_RAF1	DFGLATV-----KSRWSSGQ-----	-----QVEQISSLWMA-PE	30
TKL_RAF_ARAF	DFGLATV-----KTRWSSGQ-----	-----PLEQISSLWMA-PE	30
TKL_RAF_KSR1	LFGISGV-----VREGRRRE-----	-----QLKSHDWLWMA-PE	30
TKL_RAF_KSR2	LFSGISV-----LQAGRRED-----	-----KLRIONWLCYLA-PE	30
TKL_RIPK_ANKRD3	DFGLAKC-----NGLS-H-----	-----SHDLSMDGLFC-TIAYLP-PE	31



CLUSTAL 2.1 MULTIPLE SEQUENCE ALIGNMENT

File: /Users/RCoover3159/Desktop/Kinome_DFG_alignment1
Page 11 of 12

Date: Sat May 9 18:40:50 2015

TKL_RIPK_SgK288	DFGLSKW-----MEQSTR-----	-----MQYIERSALRQ-----MLSYIP-PE	32
TKL_RIPK_RIPK2	DFGLSKW-----RMSLSL-----	-----QSRSSKSAPEGTIIYMP-PE	33
TKL_RIPK_RIPK3	DFGLSTF-----QGGG-----	-----QSGTSGSEFGTTLGYLA-PE	30
TKL_RIPK_RIPK1	DLGLASF-----KMWSKLN-----EE-	-----HNELREVDGTAKKNGTLYYMA-PE	41
TKL_IRAK_IRAK1	DFGLARF-----SRFAG-SSP-----	-----SQSSMVARTQVRRTLAYLP-EE	37
TKL_IRAK_IRAK3	DFPMAHF-----R--S--HLE-----	-----HQSCINIMTSSSSKHLWYMP-EE	34
TKL_IRAK_IRAK2	HP-MAHL-----CP-----VNR-----	-----RSKYTMKTHLLRCSAAYLP-ED	33
TKL_IRAK_IRAK4	DFGLARA-----S-----	-----EKFAQVMTSRINVTAYMA-PE	30
Other_NRBP_NRBP1	VAPDTIN-----NH-----	-----VKTREEDLNLHFFA-PE	26
Other_NRBP_NRBP2	ALPDDLRL-----SP-----	-----IRAEREERLNLHFFP-PE	26
Other_Wnk_Wnk1	DLGLATL-----KR-----	-----ASFAKSVIETPEFMA-PE	26
Other_Wnk_Wnk3	DLGLATL-----MR-----	-----TSFAKSVIETPEFMA-PE	26
Other_Wnk_Wnk2	DLGLATL-----KR-----	-----ASFAKSVIETPEFMA-PE	26
Other_Wnk_Wnk4	DLGLATL-----KR-----	-----ASFAKSVIETPEFMA-PE	26
CK1_CK1_CK1a	DFGLAKK-----YRDN-----	-----RTRQHIPYREDKNIETARYAS-IN	35
CK1_CK1_CK1a2	DFGLAKK-----YRDN-----	-----RTRQHIPYREDKNIETARYAS-IN	35
CK1_CK1_CK1d	DFGLAKK-----YRDA-----	-----RTRQHIPYRENKNIETARYAS-IN	35
CK1_CK1_CK1e	DFGLAKK-----YRDA-----	-----RTRQHIPYRENKNIETARYAS-IN	35
CK1_CK1_CK1g3	DFGLAKE-----YIDP-----	-----ETKKHIPYREKSLIETARYMS-IN	35
CK1_CK1_CK1g1	DFGLAKE-----YIDP-----	-----ETKKHIPYREKSLIETARYMS-IN	35
CK1_CK1_CK1g2	DFGLAKE-----YIDP-----	-----ETKKHIPYREKSLIETARYMS-IN	35
CK1_TTBK_TTBK2	DFGLARQ-----FTN-----	-----SGGDVRRPPRAVAGFRSTVRYAS-IN	34
CK1_TTBK_TTBK1	DFGLARQ-----YTN-----	-----TTGDVRRPPRAVAGFRSTVRYAS-VN	34
CK1_VRK_VRK1	DYGLAYR-----YCP-----	-----GVHKEVKEDPKRKHGTIEFTS-ID	35
CK1_VRK_VRK2	DYGLAYR-----YCP-----	-----GNHKQYQENPKRKHGTIEFTS-ID	35
CK1_VRK_VRK3	GYGFAPR-----YCP-----	-----GKHVAVVEGSRSPHETDLEFIS-MD	35
Other_NRF5_SgK307	NLEYMLE-----SEDR-----	-----GVQRDLTRVPLP-----LQLYNMAA-PE	33
Other_NRF5_SgK424	-----	-----	-----
Other_NAK_NPSK1	SMNQAEIH-----VEGSR-----	-----QALTLQDNAAQRTISYRA-PE	34
Other_PEK_HRI	DFGLACT-----DILQKNTDWTN-----	-----RNGKRTPTHTSRVETCLYAS-PE	40
Other_TTK_TTK	DFGLIANG-----MQPDTTS-----	-----VVKDSQVETVNYMP-PE	30
STE_Ste-Unique_COT	DFGLSVO-----MTED-----	-----VYFPKDLRSTETIYMS-PE	28
STE_Ste-Unique_NIK	DFGHAVC-----LQPDGLG-----	-----KSLLTGDYIIPSTETHMA-PE	33
Other_CDC7_CDC7	NFNHSSISHESPAVKLMQSKTVDVLSRKLATKKKAISTKMNSAVMRKTASSCPASLTCDCYATDKVCSICLSRRQVAPRAETPFGRA-PE	-----	93
TK_TK-Unique_SuTK106	-LGLAYE-----VYTRG-----	-----AISSTQIPLKWL-PE	27
TKL_LRRK_LRRK2	DYGLAQY-----CORMG-----	-----IKTSEETPFGRA-PE	26
Other_Other-Unique_SgK496	DLGFCRP-----	-----EAMMGGSIETPIHMA-PE	25
Other_MOS_MOS	DFGSEK-----LEDLLCFQTP-----	-----SYPIETTYTHRA-PE	31
Other_TBCK_TBCK	KFGLYH-----MTAHG-----	-----DDVDFPIVPSYLA-PE	27
TKL_LRRK_LRRK1	DYGLSRQ-----SFHEG-----	-----ALGVEETPGYQA-PE	26
Other_Other-Unique_KIS	DFGLSPK-----EGN-----	-----QDVKXIDTDGYRA-PE	25
TKL_TKL-Unique_MLKL	ELRKTQTS-----MSLG-----	-----TTREKTRVKSTAYLS-PQ	30
Other_Bud32_PRPK	DFGLS-----FIS-----	-----ALPEDKQVDLYVL-EK	23
.....990.....1000.....1010.....1020.....1030.....1040.....1050.....1060.....1070.....			



CLUSTAL 2.1 MULTIPLE SEQUENCE ALIGNMENT

File: /Users/RCoover3159/Desktop/Kinome_DFG_alignment1
Page 12 of 12

Date: Sat May 9 18:40:50 2015

```

Other_NKF2_PINK1      DFGCLADESIGLQLPFSS-----WYVDRGNGCLMA-PE 34
Other_TOPK_PBK       DVGVSLP-----LDEN-----MTVTDPEACYLITPEWKP-KE 31
AGC_MAST_MASTL      DFGLSK-----VT-----LNRDINMDILTT-PS 23
Other_Other-Unique_RNaseL  DFDKS-----IKWAGDPQ 13
TKL_MLK_ILK_ILK     DVKFSFQ-----CPGRMYAPAWVA-PE 21
Other_Other-Unique_SgK071  DLSSNVL-----MTDKAKWN-----IRAEDPFRKSWMA-PE 31
STE_STE-Unique_Domain2_GCN2  DISLSKR-----LAD-----ICKELVFGTRVRFSD 26
Other_SCY1_SCYL2     DFCVSSST-----NPSEQE-----PKFPCREWDFMLPSLGLPNPE 34
Other_SCY1_SCYL1     DYMYSAQ-----GNGGG-----PPRKGTFLEQYDF-PE 28
Other_SCY1_SCYL3     --GMET-----VCKVSDATPEFLRSIQ 20
Other_Other-Unique_SgK196  QYLLTSN-----FS-----ILANDLDALPLVNHSSG 26
Other_VPS15_PIK3R4   DFASFKPTYLPEDNPADFNFFDTSRRR-----TCYIAPERFVDDGMFAALEYMRDPS 54
Other_BUB_BUB1       DLGQSID-----MKLFPKG-----TIFTAKCETSQFQC-VE 30
Other_BUB_BUBR1      DFSYSVD-----LRVQLD-----VFTLSCFRTVQILEGQK 30
Other_Other-Unique_SgK493  DLDDAR-----VEETP-----CAGSDCILEFPARNF 27
Other_Other-Unique_SgK396  DFDFTKS-----VSQR-----ASVNMVGDLSLMS-PE 27
Other_Slob_Slob      DLENS-----LLGLFSFYRSYFSQFR 21
Other_Haspin_Haspin  -YTLNGK-----SSTIP-----SGLQVSDIDYTL SRL 27
.....990.....1000.....1010.....1020.....1030.....1040.....1050.....1060.....1070.....

```

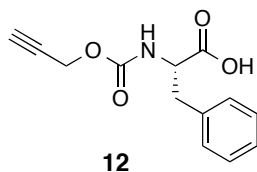


Figure 69. Human kinome DFG-APE sequence alignment.

4.2 General Chemical Methods:

Chemical reagents and solvents were purchased from Sigma-Aldrich (MO, USA), Alfa-Aesar (MA, USA), Fisher Scientific (PA, USA). Amino acids and coupling reagents were purchased from Chem-Impex. Analytical Thin Layer Chromatography (TLC) was performed using silica gel GHLF plates (Analtech Inc., DE, USA). Flash Chromatography was performed on TELEDYN ISCO CombiFlash® Rf instrument using RediSep Rf Normal-phase Flash Columns (4g, 12g, 24g, or 40g). ¹H NMR and ¹³C NMR were recorded on a Bruker Topspin 400MHz using Chloroform-d and deuterated DMSO. All chemical shifts are reported as δ in units of parts per million (ppm) relative to chloroform and DMSO residual peaks at 7.26 and 2.50 respectively (¹H) and 77.16 and 39.52 respectively (¹³C). The multiplicity (s = singlet, d = doublet, dd = doublet of doublets, t = triplet, q = quartet, m = multiplet), coupling constants(s) (Hz). Electrospray ionization (ESI) mass spectra were obtained from Perkin Elmer Flexar UPLC/AxION2 TOF Mass Spectrometer. Matrix-Assisted Laser Desorption/Ionization (MALDI) spectra were obtained from Voyager DE-Pro™ MALDI TOF Mass Spectrometer.

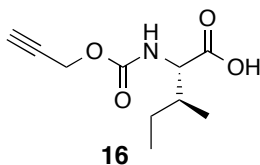
4.2.1



((prop-2-yn-1-yloxy)carbonyl)-*L*-phenylalanine (**12**). To a vial add 8 mL H₂O, 467.52 mg NaOH, and 660.8 mg phenylalanine (freebase form). To the solution add 0.39 mL propargylcarbamate. Allow to react for 16 hr at ambient temperature. Wash with 2 N

HCl/EtOAc, collect organic layer. (438 mg, 43.8%). R_f (90:10 DCM:MeOH)= 0.47. Crude product taken forward to Weinreb Amide formation.

4.2.2



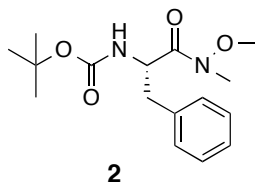
((prop-2-yn-1-yloxy)carbonyl)-*L*-isoleucine (**16**). To a vial add 8 mL H₂O, 467.52 mg NaOH, and 616 mg isoleucine (freebase form). To the solution add 0.39 mL propargylcarbamate. Allow to react for 16 hr at ambient temperature. Wash with 2 N HCl/EtOAc, collect organic layer. (463 mg, 46.3%). R_f (90:10 EtOAc:Hexanes)= 0.44. Crude product taken forward to Weinreb Amide formation.

4.3 General Procedure for the Formation of Weinreb Amide Intermediates.

To a vial was added 1 equivalent of amino acid (Boc or Poc protected). To the vial was added DCM (.25 M final concentration of amino acid). To the solution was added *N*-(3-Dimethylaminopropyl)-*N'*-ethylcarbodiimide (EDCI, 1.2 equivalents), 1-Hydroxybenzotriazole (HOBT) hydrate (1 equivalent), and 4-methylmorpholine (4 equivalents). This solution was allowed to react for 15 minutes at ambient T. To the solution was then added *N,O*-Dimethylhydroxylamine hydrochloride (1.1 equivalents) and allowed to react for 16 hr. The reaction solution was washed with 1N HCl once, then with saturated NaCO₃, then the organic solvent was collected and solvent removed in vacuo. The crude product was purified by flash

chromatography on silica by CombiFlash instrument (0-100% EtOAc:Hexanes over 20 column volumes).

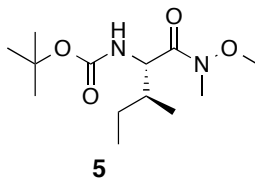
4.3.1



tert-butyl (*S*)-1-(1-(methoxy(methyl)amino)-1-oxo-3-phenylpropan-2-yl)carbamate (**2**). (2g, 87%)

^1H NMR (400 MHz, CDCl_3) δ 7.28 (m, 2H) 7.22 (d, $J=7.2$, 1H), 7.17 (d, $J=7.6$, 2H), 5.14 (br, 1H), 4.95 (br, 1H), 3.65 (s, 3H), 3.16 (s, 3H), 3.05 (dd, $J_1=6.2$, $J_2=13.5$, 1H), 2.89 (m, 1H), 1.39 (s, 9H).

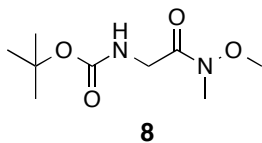
4.3.2



tert-butyl ((*2S,3S*)-1-(methoxy(methyl)amino)-3-methyl-1-oxopentan-2-yl)carbamate (**5**). (574

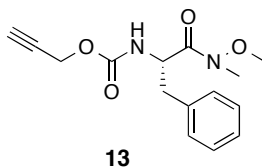
mg 67%) ^1H NMR (400 MHz, CDCl_3) δ 5.2 (s, 1H), 4.6 (s, 1H), 3.7 (s, 3H), 3.2 (s, 3H), 2.1 (s, 1H), 1.7 (m, 1H), 1.5 (m 1H), 1.4 (s, 9H), 1.0 (m, 1H), 1.9 (m, 6H).

4.3.3



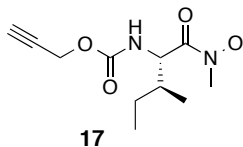
tert-butyl (2-(methoxy(methyl)amino)-2-oxoethyl)carbamate (**8**). (302 mg, 77%) ^1H NMR (400 MHz, CDCl_3) δ 5.2 (s, 1H), 4.0 (s, 2H), 3.6 (s, 3H), 3.1 (s, 3H), 1.4 (s, 9H).

4.3.4



prop-2-yn-1-yl(*S*)-(1-(methoxy(methyl)amino)-1-oxo-3-phenylpropan-2-yl)carbamate (**13**). (0.312 g, 61% yield). ^1H NMR (400MHz, CD_3OD) δ 7.23-7.29 (m, 5H), 4.89 (m, 1H), 4.60 (s, 2H), 3.73 (s, 3H), 3.17 (s, 3H), 3.04 (dd, $J_1=5.9$, $J_2=13.3$, 1H), 2.86 (m, 2H).

4.3.5

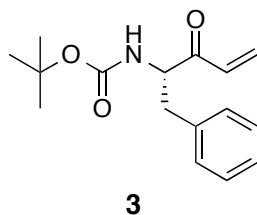


((prop-2-yn-1-yloxy)carbonyl)-*L*-isoleucine (**17**). (480 mg, 94%) ^1H NMR (400 MHz, CDCl_3) δ 5.3 (d, 1H, $J=9$), 4.6 (m, 3H), 3.7 (s, 3H), 3.1 (s, 3H), 2.4 (s, 1H), 2.0 (s, 1H), 1.7 (m, 1H), 1.5 (m, 1H), 1.0 (m, 1H), 0.9 (m, 6H).

4.4 General Procedure for Grignard Reactions with Weinreb Amides.

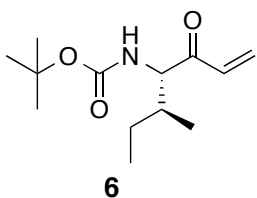
The appropriate Weinreb amide (above) (1 equivalent) was dissolved in anhydrous THF (.3 M). The solution was then cooled to $-40\text{ }^\circ\text{C}$ in a dry ice/ACN bath and purged with argon before 1M vinyl magnesium bromide in Ether (5 equivalents) was added dropwise (over 5 minutes). After 3h stirring at $-40\text{ }^\circ\text{C}$, the reaction mixture was poured into cold 3N HCl, and extracted three times with ethyl acetate. The combined organic layers were dried over anhydrous sodium sulphate and concentrated *in vacuo*. The crude product was purified over silica gel chromatography to obtain the desired product.

4.4.1



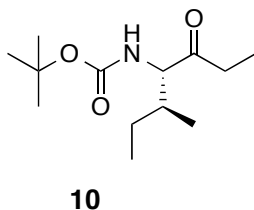
tert-butyl (*S*)-(3-oxo-1-phenylpent-4-en-2-yl)carbamate (**3**). (156 mg, 67%) ^1H NMR (400MHz, CDCl_3) δ 7.25 (m, 3H) 7.10 (d, $J=7.4$, 2H), 6.41 (m, 2H), 5.83 (d, $J=10.4$, 1H), 5.22 (m, 1H), 4.86 (q, $J=9$, 1H), 3.14 (dd, $J_1=6.4$, $J_2=13.8$, 1H), 2.98 (dd, $J_1=8.0$, $J_2=15.4$, 1H), 1.42 (s, 9H). ^{13}C NMR (100MHz, CDCl_3) δ 197.9, 155.2, 136.0, 133.5, 130.2, 129.6, 128.6, 127.1, 79.9, 58.3, 38.2, 28.4. HRMS (ESI) $\text{C}_{16}\text{H}_{21}\text{NO}_3$ m/z [$\text{M}+\text{Na}^+$] found 298.1415, expected 298.1419.

4.4.2



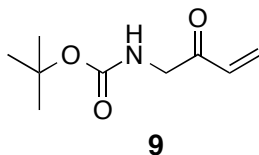
tert-butyl ((*4S,5S*)-5-methyl-3-oxohept-1-en-4-yl)carbamate (**6**). (34 mg, 45%) ^1H NMR (400MHz, CDCl_3) δ 6.4 (m, 2H), 5.8 (d, 1H, $J=10.32$), 5.1 (s, 1H), 4.5 (m, 1H), 1.8 (m, 1H), 1.5 (s, 1H), 1.3 (m, 2H), 1.4 (s, 9H), 1 (m, 3H), 0.8 (m, 3H). ^{13}C NMR (100MHz, CDCl_3) δ 199.2, 155.9, 134.2, 129.7, 79.7, 61.9, 37.8, 28.4, 24.3, 16.3, 11.7.

4.4.3



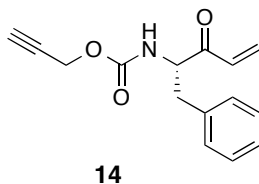
tert-butyl ((3*S*,4*S*)-3-methyl-5-oxoheptan-4-yl)carbamate (**10**). To a solution of **6** was added Pd/C (0.1 mol%) with H₂(g) at ATM and ambient temperature for 16 hr. The solution was filtered through celite and solvent removed in vacuo. (22 mg, Quantitative) ¹H NMR (400MHz, CDCl₃) δ 5.0 (s, 1H), 4.2 (s, 1H), 2.4 (m, 1H), 1.8 (s, 1H), 1.4 (s, 3H), 1.3 (s, 9H), 1.0 (m, 3H), 0.9 (d, 3H, J=6.8), 0.8 (m, 3H). ¹³C NMR (100MHz, CDCl₃) δ 210.5, 155.9, 79.6, 63.6, 37.2, 34.3, 28.3, 24.2, 16.1, 11.6, 7.5.

4.4.4



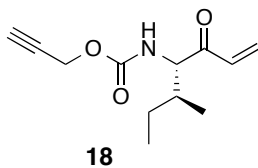
tert-butyl (2-oxobut-3-en-1-yl)carbamate (**9**). (34 mg, 45%) ¹H NMR (400MHz, CDCl₃) δ 6.3 (m, 2H), 5.9 (d, 1H J=8.2), 5.2 (s, 1H), 4.2 (s, 2H), 1.4 (s, 9H). ¹³C NMR (100MHz, CDCl₃) δ 205.3, 155.4, 79.6, 62.9, 36.4, 34.1, 28.3.

4.4.5



prop-2-yn-1-yl (*S*)-(3-oxo-1-phenylpent-4-en-2-yl)carbamate (**14**). (135.7 mg, 38%) ¹H NMR (400MHz, CD₃OD) δ 7.22-7.28 (m, 5H), 6.61 (dd, J₁=10.1, J₂=12.4, 1H), 6.36 (d, J=17.4, 1H), 5.87 (d, J=11.4, 1H), 4.72 (m, 1H), 4.60 (s, 2H), 3.24 (dd, J₁=5.5, J₂=13.9, 1H), 2.87 (m, 2H).

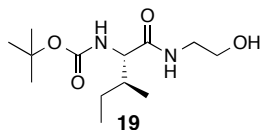
4.4.6



prop-2-yn-1-yl ((*4S,5S*)-5-methyl-3-oxohept-1-en-4-yl)carbamate (**18**). (50.86 mg, 33%) R_f (50:50 Hexanes:EtOAc) = 0.68. ¹H NMR (400MHz, CDCl₃) δ 6.4 (m, 1H), 6.3 (m, 1H), 5.8 (d, 1H, J=10.28), 5.4 (s, 1H), 4.6 (m, 3H), 2.4 (s, 1H), 2.0 (m, 1H), 1.3 (m, 2H), 1.2 (m, 1H), 0.9 (d, 3H, J=6.8), 0.8 (m, 3H). ¹³C NMR (100MHz, CDCl₃) δ 198.3, 155.5, 133.9, 130.0, 78.1, 74.7, 62.4, 52.8, 37.6, 24.2, 16.1, 11.6.

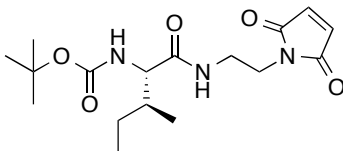
4.5 Synthesis of Remaining Single Amino Acid Analogues

4.5.1



tert-butyl ((2*S*,3*S*)-1-((2-hydroxyethyl)amino)-3-methyl-1-oxopentan-2-yl)carbamate (**19**). (936 mg, 93.6%). To a dry reaction vessel add 841.9 mg of Boc-Ile-OH and 18.2 mL of anhydrous DCM. To the solution at .85 mL NMM, 906.7 mg EDCI, 590.5 mg HOBt, and was allowed to equilibrate for 15 minutes. To the reaction solution was added ethanolamine (0.26 mL) dropwise over 1 minute. Solution allowed to react for 16 hr at ambient temperature. The crude product was purified over silica gel chromatography to obtain the desired product. ¹H NMR (400MHz, CDCl₃) δ 6.8 (s, 1H), 5.2 (s, 1H), 3.9 (t 1H, J1=7.08, J2=8.28), 3.7 (s, 2H), 3.4 (m, 2H) 3.3 (s, 1H), 1.8 (s, 1H), 1.5 (s, 1H), 1.4 (s, 9H), 1.1 (m, 1H), 0.9 (m, 6H).

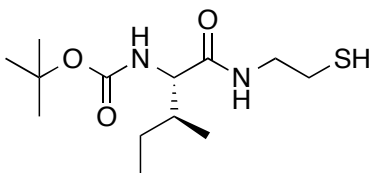
4.5.2



tert-butyl((2*S*,3*S*)-1-((2-(2,5-dioxo-2,5-dihydro-1*H*-pyrrol-1-yl)ethyl)amino)-3-methyl-1-oxopentan-2-yl)carbamate (**20**). (93.33 mg, 31%). To a dry reaction vessel, add anhydrous THF,

flush with argon, and cool to -78°C under argon. To the THF slowly add triphenyl phosphine Ph_3P and allow to equilibrate for 5 minutes. To the solution, slowly add diethyl azodicarboxylate (DEAD) and allow to equilibrate for 5 minutes. To the solution, add **19** and allow to equilibrate for 5 minutes. To the solution, add maleimide, stir, allow to reach ambient temperature, and let react for 16 hrs. Solvent removed in vacuo. The crude product was purified over silica gel chromatography to obtain the desired product. ^1H NMR (400MHz, CDCl_3) δ 6.6 (s, 2H), 6.2 (s, 1H), 4.8 (m, 1H), 4.2 (s, 1H), 3.8 (m, 2H), 3.6 (m, 2H), 3.4 (s, 2H), 1.8 (s, 1H), 1.5 (s, 2H), 1.4 (s, 9H), 0.8 (m, 6H). ^{13}C NMR (100MHz, CDCl_3) δ 174.3, 171.0, 168.9, 134.4, 72.3, 67.1, 58.2, 38.1, 36.5, 24.7, 14.7, 11.5.

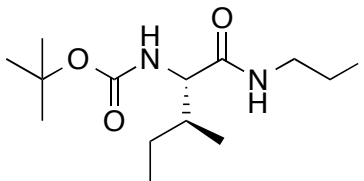
4.5.3



tert-butyl ((2*S*,3*S*)-1-((2-mercaptoethyl)amino)-3-methyl-1-oxopentan-2-yl)carbamate (**21**). (102.93 mg, 51%). To a dry reaction vessel add 159.6 mg of Boc-Ile-OH and 3.45 mL of anhydrous DCM. To the solution add 17 mL NMM, 172.5 mg EDCI, 112.1 mg HOBt, and was allowed to equilibrate for 15 minutes. To the reaction solution was added cysteinamine (058.6 mg) slowly. Solution allowed to react for 16 hr at ambient temperature. The reaction mixture was poured into cold 1N HCl, and extracted three times with ethyl acetate. The combined organic layers were dried over anhydrous sodium sulphate and concentrated *in vacuo*. The crude product was purified over silica gel chromatography to obtain the desired product. ^1H NMR (400MHz,

CDCl₃) δ 6.3 (s, 1H), 4.9 (s, 1H), 3.8 (t, 1H J1=6.48, J2=8.52), 3.4 (m, 2H), 2.6 (m, 2H), 1.8 (s, 1H), 1.4 (s, 9H), 0.8 (m, 6H). ¹³C NMR (100MHz, CDCl₃) δ 201.3, 171.8, 155.7, 65.2, 42.3, 39.3, 37.2, 28.3, 24.5, 15.8, 11.4.

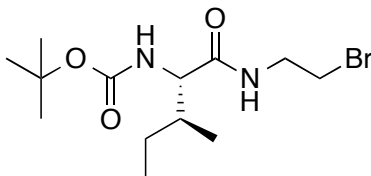
4.5.4



tert-butyl ((2*S*,3*S*)-1-((2-iodoethyl)amino)-3-methyl-1-oxopentan-2-yl)carbamate (**22**).

Procedure adapted from Helmboldt, H. et al.¹⁴² (37 mg, 27%) To a dry reaction vessel add anhydrous DCM (1 mL), flush with argon, and cool to 0°C under argon. To the DCM slowly add triphenyl phosphine (Ph₃P, 99.6 mg) and allow to equilibrate for 5 minutes. To the solution slowly add imidazole (25.9 mg) and allow to equilibrate for 5 minutes. To the solution slowly add I₂ allow to equilibrate for 15 minutes. To the solution add **19**, stir, allow to reach ambient temperature, and let react for 4 hrs. Solvent removed in vacuo. Taken back up in non polar solvent and passed through celite. The crude product was purified over silica gel chromatography to obtain the desired product. ¹H NMR (400MHz, CDCl₃) δ 6.4 (s, 1H), 5.0 (s, 1H), 3.9 (t, 1H J1=2.4, J2=6.4), 3.6 (m, 1H), 3.5 (m, 1H), 3.2 (m, 2H), 1.8 (s, 1H), 1.4 (s, 9H), 0.8 (m, 6H). ¹³C NMR (100MHz, CDCl₃) δ 171.7, 155.8, 80.1, 59.5, 41.8, 37.0, 28.3, 24.8, 15.7, 11.4, 4.6.

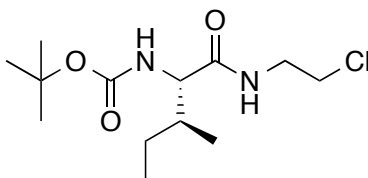
4.5.5



tert-butyl ((2*S*,3*S*)-1-((2-bromoethyl)amino)-3-methyl-1-oxopentan-2-yl)carbamate (**23**).

Procedure adapted from Bora, I. et al.¹⁴³ (47.65 mg, 51%). To a dry reaction vessel add 0.5 mL of DCM. To the DCM add 77.18 mg of **19**. To the solution add 102.8 mg of CBr₄. Cool to 0°C. To the solution slowly add 81.3 mg of Ph₃P over 20 minutes. Allow to react for 4hr. Pour solution into excess hexanes and filter out the salt precipitate. Remove solvent in vacuo. The crude product was purified over silica gel chromatography to obtain the desired product. ¹H NMR (400MHz, CDCl₃) δ 6.7 (s, 1H), 5.1 (s, 1H), 4.0 (t, 1H J1=2.4, J2=6.4), 3.7 (m, 1H), 3.6 (m, 1H), 3.4 (m, 2H), 1.9 (s, 1H), 1.5 (s, 9H), 0.9 (m, 6H). ¹³C NMR (100MHz, CDCl₃) δ 171.7, 155.8, 80.1, 59.5, 41.1, 37.1, 31.9, 28.3, 24.8, 15.7, 11.4.

4.5.6

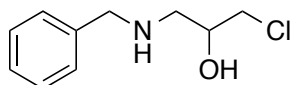


tert-butyl ((2*S*,3*S*)-1-((2-chloroethyl)amino)-3-methyl-1-oxopentan-2-yl)carbamate (24).

Procedure adapted from Bora, I. et al.¹⁴³ (55.72 mg, 68%). To a dry reaction vessel add 0.5 mL of DCM. To the DCM add 77.18 mg of **19**. To the solution add 47.7 mg of CCl₄. Cool to 0°C. To the solution slowly add 81.3 mg of Ph₃P over 20 minutes. Allow to react for 4hr. Pour solution into excess hexanes and filter out the salt precipitate. Remove solvent in vacuo. The crude product was purified over silica gel chromatography to obtain the desired product. ¹H NMR (400MHz, CDCl₃) δ 6.6 (s, 1H), 5.0 (s, 1H), 4.0 (t, 1H J1=2.4, J2=6.4), 3.7 (m, 1H), 3.6 (m, 1H), 3.4 (m, 2H), 1.9 (s, 1H), 1.5 (s, 9H), 0.9 (m, 6H). ¹³C NMR (100MHz, CDCl₃) δ 171.7, 155.8, 80.1, 59.4, 43.6, 41.1, 37.1, 28.3, 24.8, 15.7, 11.4.

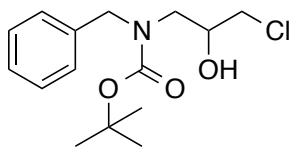
4.6 Alternative Route to Chloromethyl Ketone.

4.6.1



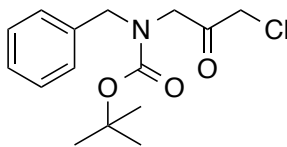
1-(benzylamino)-3-chloropropan-2-ol (**25**). Procedure adapted from patent US6362188.¹⁴⁴ (1.75g, 88%) To a solution of benzylamine (1.08927g) in cyclohexane (1M, 10.17 mL) was added epichlorohydrin (1 equivalent, 0.82 mL). The solution was allowed to react and precipitate collected by vacuum filtration and wash with cold cyclohexane. Product taken directly to next step.

4.6.2



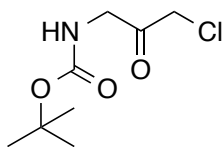
tert-butyl benzyl(3-chloro-2-hydroxypropyl)carbamate (**26**). Procedure adapted from Org. Lett 2010, 12, 2746-2749.¹⁴⁵ (358.2 mg, 45%). To a solution of **25** in DCM (0.25M) was added 1 equivalent of Boc anhydride. The solution was allowed to react for 30 minutes and then the solvent was removed in vacuo. The crude product was purified over silica gel chromatography to obtain the desired product as a white crystalline solid. Spectral data matched previously reported.¹⁴⁶

4.6.3



tert-butyl benzyl(3-chloro-2-oxopropyl)carbamate (**27**). Procedure adapted from JOC 2001, 66, 8661.¹⁴⁶ (98 mg, quantitative). Swern oxidation: to a dry vial add anhydrous DCM (3.3 mL) at -78°C. To the DCM add oxalyl chloride (0.03 mL). Separately prepare a solution of DMSO in DCM (1 mL). Add the DMSO solution to the oxalyl chloride solution slowly over 10 minutes. Prepare a third solution of **26** in DCM (1 mL). Add the alcohol containing solution to the mother liquor dropwise over 10 minutes, stir for 20 minutes. Prepare a solution of excess TEA (4.5 equivalents) in DCM, and add dropwise. Stir for 30 minutes. Wash with H₂O and extract with DCM 3X. Collect organic layers and remove solvent in vacuo to produce product of sufficient purity to move forward (one spot by TLC, R_F = .77 in 70:30 EtOAc:Hexanes). ¹H NMR (400MHz, CDCl₃) δ 7.2 (m, 5H), 4.5 (s, 1H), 4.5 (s, 1H), 4.1 (s, 1H), 4.08 (s, 1H), 4.0 (s, 1H), 3.9 (s, 1H), 1.4 (s, 9H).¹⁴⁶

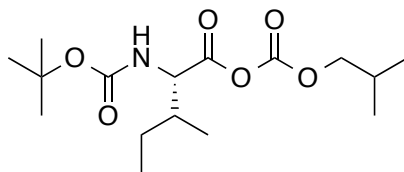
4.6.4



tert-butyl (3-chloro-2-oxopropyl)carbamate (**28**). First attempt with Pd/C at atmospheric pressure (H₂) and ambient temperature did not produce any effect. The addition of PdOH/C (25% w/w) did produce multiple spots. Only a small fraction was able to be recovered as pure product after celite and silica column workup (~10%).

4.7 Diazomethane route to Chloromethyl ketones

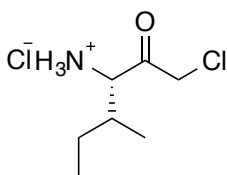
4.7.1



(2*S*,3*S*)-2-((*tert*-butoxycarbonyl)amino)-3-methylpentanoic (isobutyl carbonic) anhydride (**29**). Procedure adapted from J. Med. Chem 1995, 38, 1015-1021.¹²⁷ To a dry round bottom flask was added 12.5 mL of anhydrous THF. To the THF was added Boc-Ile-OH (1.15645g) and 1

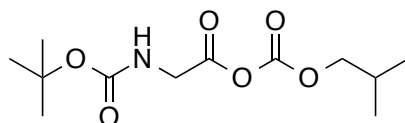
equivalent of NMM (0.55 mL). To the solution was added isobutylchloroformate (0.78 mL). Crude used in next step.

4.7.2



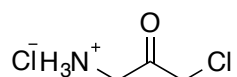
(3*S*,4*S*)-1-chloro-4-methyl-2-oxohexan-3-aminium chloride (**30**). To the solution of **29** prepared in the previous step was added a solution of diazomethane in ether (formed *in situ* with a minidiazald kit according to manufacturers instructions). The solution was allowed to react for 5 hr and allowed to reach ambient temperature. Then the remaining diazomethane was quenched with glacial acetic acid (~1 mL until no more bubbling occurred). The diazo intermediate was isolated by silica chromatography and then treated with 4 equivalents of HCl (4N in dioxane) and allowed to react for 5 hrs. ~75% solvent removed under vacuum and the remaining was triturated with ether to crash out the product. ¹H NMR (400MHz, CD₃OD) δ 4.6 (s, 2H), 4.4 (s, 1H), 3.3 (s, 3H), 2.2 (m, 1H), 1.4 (m, 1H), 1.3 (m, 1H), 1.2 (d, 3H, J=6.88), 1.0 (m, 3H).

4.7.3



2-((*tert*-butoxycarbonyl)amino)acetic (isobutyl carbonic) anhydride (**31**). Procedure adapted from J. Med. Chem 1995, 38, 1015-1021.¹²⁷ To a dry round bottom flask was added 12.5 mL of anhydrous THF. To the THF was added Boc-Gly-OH (0.87590g) and 1 equivalent of NMM (0.55 mL). To the solution was added isobutylchloroformate (0.78 mL). Crude used in next step.

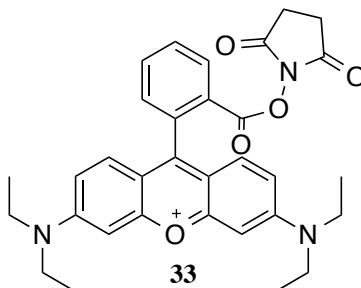
4.7.4



3-chloro-2-oxopropan-1-aminium chloride (**32**). To the solution of **31** prepared in the previous step was added a solution of diazomethane in ether (formed *in situ* with a minidiazald kit according to manufacturers instructions). The solution was allowed to react for 5 hr and allowed to reach ambient temperature. Then the remaining diazomethane was quenched with glacial acetic acid (~1 mL until no more bubbling occurred). The diazo intermediate was isolated by silica chromatography and then treated with 4 equivalents of HCl (4N in dioxane) and allowed to react for 5 hrs. ~75% solvent removed under vacuum and the remaining was triturated with ether to crash out the product. ¹H NMR (400MHz, CD₃OD) δ 4.6 (s, 2H), 4.2 (s, 2H), 3.3 (s, 3H).

4.8 Synthesis of Rhodamine derivatives

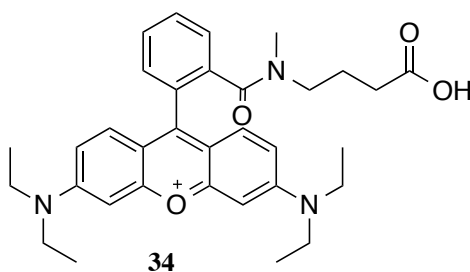
4.8.1



3,6-bis(diethylamino)-9-(2-(((2,5-dioxopyrrolidin-1-yl)oxy)carbonyl)phenyl)xanthylium

(33): To a solution of rhodamine B (5.0 g, 10.44 mmol) and EDC (3.0 g, 15.66 mmol) in DCM (250 mL) was added N-hydroxysuccinimide (1.3 g, 11.48 mmol). The reaction was stirred at ambient temperature for 12 hr. Solvent was removed and the product was purified via flash chromatography (silica DMC:MeOH 9:1). Yield 75.4% (4.3 g, 7.9 mmol). Analytical data (^1H NMR, ^{13}C NMR, mass spec) matched the previously reported data.¹²⁵

4.8.2

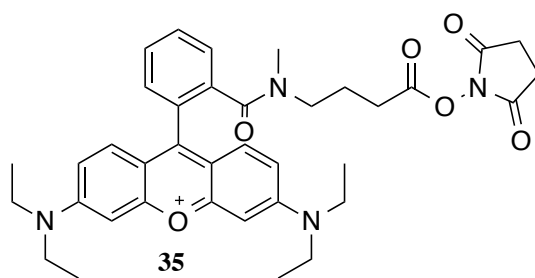


9-(2-((3-carboxypropyl)(methyl)carbamoyl)phenyl)-3,6-bis(diethylamino)xanthylium (34):

To a solution of **33** (2.9 g, 5.29 mmol) and DIEA (2.7 g, 21.16 mmol) in I (52.9 mL) was added 4-methylaminebutyric acid hydrochloride (1.2 g, 7.94 mmol). The reaction was stirred at ambient

temperature for 16 hr. Solvent was removed under vacuum and product was isolated by extraction (H₂O/CHCl₃). The organic layers were combined, dried, and taken directly to next step. Yield 87.5%. MS (MALDI) C₃₂H₄₀N₃O₄ calculated 542.3013 found 542.5626. Analytical data (¹H NMR, mass spec) matched the previously reported data.¹²⁶

4.8.3



3,6-bis(diethylamino)-9-(2-((4-((2,5-dioxopyrrolidin-1-yl)oxy)-4-oxobutyl)(methyl)carbamoyl)phenyl)xanthylum (35): To a solution of **34** (2.2 g, 4.00 mmol) and DCC (1.1 g, 5.2 mmol) in DMF (35 mL) was added N-Hydroxysuccinimide (0.5 g, 4.00 mmol). The reaction was stirred at ambient temperature for 16 hr. The filtrate was collected then triturated with diethyl ether, centrifuged, and solvent decant. The product, collected in the bottom of the centrifuge tube as an oil, was taken to next step. Yield 85.6%. MS (MALDI) C₃₇H₄₃N₄O₆ calculated 639.3177 found 639.8263. ¹H-NMR (400 MHz, CD₃Cl): δ 7.98 (s, 1H), 7.65 (m, 2H), 7.52 (m, 1H), 7.34 (m, 1H), 7.22 (d, 1H J = 9.5 Hz), 6.94 (d, 2H J = 9.6 Hz), 6.76 (s, 2H), 3.61 (m, 8H), 3.27 (t, 2H J = 7.0 Hz), 2.92 (s, 3H) 2.85 (m, 6H), 2.17 (t, 2H J = 7.0 Hz), 1.29 (t, 12H J = 7.0 Hz); ¹³C NMR (125 MHz, CDCl₃): δ 172.27, 169.21, 168.51, 167.77, 162.51, 157.61,

155.66, 136.16, 131.93, 130.03, 127.37, 114.04, 96.47, 53.85, 46.12, 42.22, 37.76, 36.45, 31.36, 27.90, 25.60, 21.39, 18.61, 17.31, 12.60.

4.9 General Protocol for Probe Assembly.

First Phase.

1. Prepare the peptide on the synthesizer or manually (ensure removal of the the last Fmoc).
2. Prepare an appropriately sized solid-phase extraction (SPE) column with a stopcock (the white end piece that fits on those plastic SPE columns nicely). If you are only using a portion of your peptide (which I recommend but it is not necessary you can use all that you've made) use one of the smaller SPE columns, however I prefer the ones that can hold >15 mL.
3. Add a stir bar.
4. Transfer the amount of peptide (still on resin) you wish to carry forward through the synthesis (example: if you have 1 mol of peptide *on resin* and it's in 1 mL of a mixture (mix thoroughly), if you transfer 0.5 mL you will have transferred 0.5 moles).
5. Wash with DMF 5 times for 3 minutes each (use volumes appropriate to your SPE column, I use ~ 5mL usually, with the stir bar on) to ensure no residual deprotection agent.
6. To the SPE column add 5 mL of DMF.
7. To the mixture add 10 equivalents of triethylamine.
8. To the mixture add 5 equivalents of your tag (in this case biotin-NHS).
9. Allow to react for 5 hours (you can let it go overnight but at your own peril as it is generally completed after 5 hours and the resin is sensitive).
10. Wash with DMF 5 times for 3 minutes each.

11. Wash with DCM 5 times for 3 minutes each (this removes all the DMF).

This completes the first phase of your probe synthesis. Next will be the soft cleavage from the resin.

Second Phase.

1. Still in your SPE column. Treat your resin with 2% TFA in DCM for 2 minutes (2.5 mL, there should be a visible reaction). Collect the flow through. Repeat one additional time to ensure cleavage.
2. The resin should have turned black (or very dark in any case). If it is not, repeat step 1 from phase 2.
3. Remove deprotection cocktail under vacuum.
4. Weigh your sample (determine how many moles you have as well).

You have now produced a tagged portion of your peptide with a free C-terminal acid. Next you will couple your electrophile.

Third Phase.

1. Take your peptide starting material up in DCM (5 mL).
2. To the solution add 20 equivalents of diisopropylethylamine.

3. To the solution add 3 equivalents of EDCI.
4. To the solution add 2 equivalents of HOBt.
5. Allow to solution to react for 15 minutes at RT.
6. To the solution add 4 equivalents of your electrophile (in this case it's the HCl salt of Ile-chloromethyl ketone).
7. Allow to react for at least 4 hours.
8. Monitor reaction by TLC in DCM:MeOH 90:10 until no change is observed.
9. Remove solvent under vacuum.
10. Run on combiflash. The default time for the column you select should be fine, the columns have approximate weight ranges for your reference. Use DCM:MeOH gradient 0-30% MeOH over the course of the gradient. Do not exceed 30% MeOH if you can avoid it.
11. You will have to check your fractions by MALDI to find your peptide (the MALDI matrix solution is slightly acidic and may deprotect some of your peptide, watch for deprotection peaks as well).
12. Collect appropriate fractions and remove solvent under vacuum.

You now have produced TAG-Peptide(protected)-Electrophile. Next is global deprotection and purification.

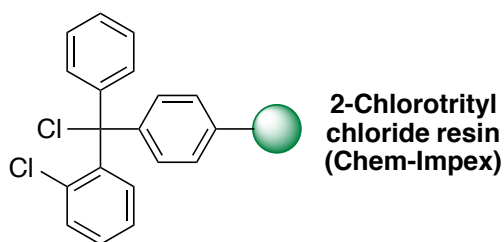
Fourth Phase.

1. Weigh your sample.

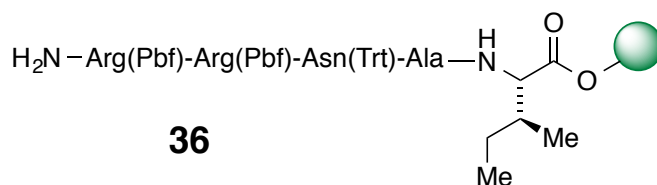
2. Prepare the deprotection cocktail: 95:2.5:2.5 TFA:TIS:H₂O (10 mL is plenty for any size application 0.2 mmol or less)
3. To your sample add the deprotection cocktail.
4. Stir for 4 hours.
5. Triturate with ether (abundant precipitate should form).
6. Spin down for 10 minutes on the Genevac (no vacuum!).
7. Decant off solution (save it until you confirm you have your product).
8. Dry the solid precipitate under vacuum.
9. Confirm by MALDI that you have successfully synthesized the probe before attempting to purify it.
10. Take up your sample in as little DMSO as possible. Use the best DMSO you can find as water and other contaminants will react with your electrophile. I keep a bottle in the biolab, with the gel reagents, for such purposes you can use this but do not contaminate it lest you plan to order more and wait.
11. The methods I have prepared on the HPLC will work for your biotinylated peptide (look for “Prep Scale” Methods, “after deprotection” “isohold” in the methods section of the HPLC software).
12. When considering how much to inject, it helps if you work out the math at how much you could *possibly* recover per injection volume and the resolution you are obtaining (if your product is more pure upfront this is easy). In short though, more is generally better and you will just have to feel it out as it is a new compound.
13. Determine/confirm where the compound elutes by MALDI.
14. Collect the appropriate fraction(s).

15. Remove sample under vacuum (Genevac allows for the most hands free approach, set to HPLC and confirm that it is still running every so often).
16. Weigh your sample (and calculate the moles, it is a salt).
17. If you have enough; produce a 10 mM stock solution of your peptide and freeze it as soon as possible.

4.9.1



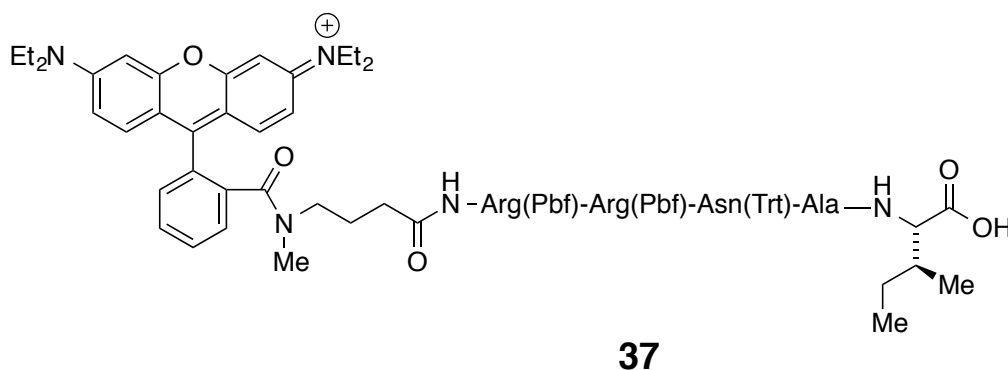
↓
**Iterative
Fmoc Solid Phase
Peptide Synthesis**



PKI(14-22)-2-Cl-trityl Resin Synthesis. 2-Chlorotrityl Chloride (2-CTC) resin preloaded with Ile was purchased from ChemImpex (200-400 mesh, Catalog #03472). Peptide couplings were carried out manually via standard Fmoc amino acid protection chemistry. Amino acids were

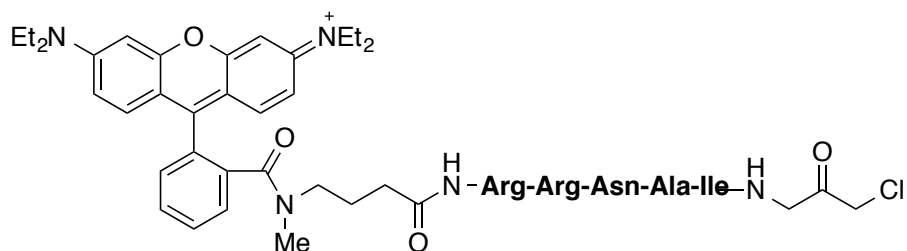
activated and added to resin with (Benzotriazol-1-yloxy)tripyrrolidinophosphonium hexafluorophosphate (PyBOP) and diisopropylethylamin (DIEA). The resin was swelled with DCM (5 min) then DMF (5 min). All amino acids were added by the general procedure that follows (with the exception of Arg, which underwent double couplings): Fmoc deprotection (20% piperidine in DMF, 3 x 5 min), wash with DMF 3x, amino acid coupling (PyBOP, DIEA 0.1 M in DMF, 1 hr, X2 for Arg), wash with DMF 3x. After the final deprotection (Arg 22) with 20% piperidine in DMF, the resin-bound product was taken directly to the next step.

4.9.2



Rhodamine-PKI(18-22)-2-Cl-trityl Resin Synthesis. To the peptide on resin was added **35** (6 eq) and TEA (10 eq) in DMF (0.05 M of **35**). The reaction was stirred for 3 h, washed with DMF 5x, then DCM 5x. The resin-bound product was taken directly to the next step. The Rhodamine-peptide bound to resin was cleaved under soft conditions with 2% TFA in DCM. Solvent removed in vacuo. MS (MALDI) C₁₀₃H₁₃₂N₁₅O₁₆S₂ calculated 1898.9418, found 1898.6289.

4.9.3



38

38. Rhodamine-PKI(18-22)-OH (0.05 mmol, **37**) was taken up in DCM (5 mL). PyBOP (0.065 mmol), DIEA (0.2 mmol), and chloromethyl ketone **32** (0.065 mmol) were added to the solution. The reaction was stirred for 16 h. Solvent was removed and the purified on a silica gel gravity column, washed with DCM, and eluted with 20% MeOH/DCM. The solid was then globally debrotected with 95:2.5:2.5 TFA:TIS:H₂O (5 mL) for 1 hr. Then triturated with ether to afford the crude product. Product purified on HPLC (95:5 to 75:25 H₂O:ACN over 20 minutes). MS (MALDI) C₆₁H₉₂ClN₁₆O₁₀ calculated 1243.6871, found 1244.1763.

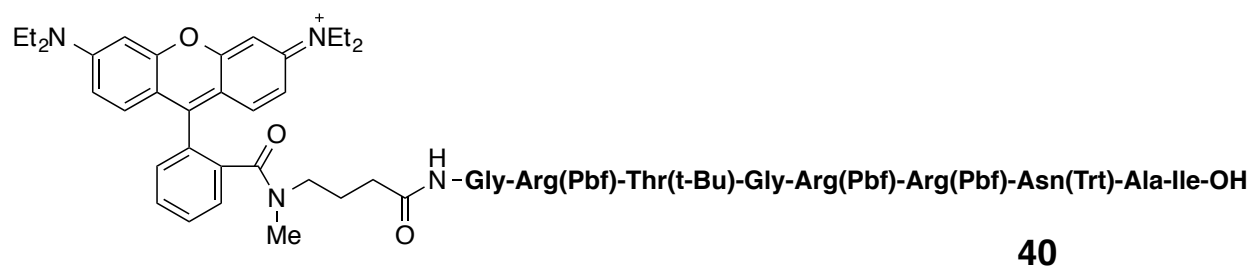
4.9.4



39

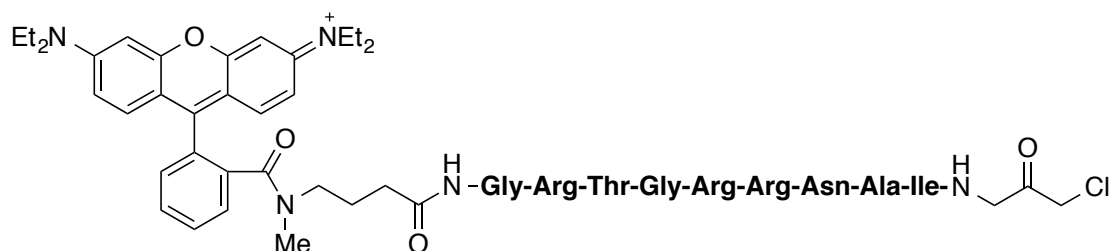
PKI(14-22)-2-Cl-trityl Resin Synthesis (39). 2-Chlorotrityl Chloride (2-CTC) resin preloaded with Ile was purchased from ChemImpex (200-400 mesh, Catalog #03472). Peptide couplings were carried out manually via standard Fmoc amino acid protection chemistry. Amino acids were activated and added to resin with (Benzotriazol-1-yloxy)tripyrrolidinophosphonium hexafluorophosphate (PyBOP) and diisopropylethylamin (DIEA). The resin was swelled with DCM (5 min) then DMF (5 min). All amino acids were added by the general procedure that follows (with the exception of Arg, which underwent double couplings): Fmoc deprotection (20% piperidine in DMF, 3 x 5 min), wash with DMF 3x, amino acid coupling (PyBOP, DIEA 0.1 M in DMF, 1 hr, X2 for Arg), wash with DMF 3x, acetyl cap (pyridine:acetic anhydride 20:20, 0.15 M in DMF, 30 min). After the final deprotection (Gly 14) with 20% piperidine in DMF, the resin-bound product was taken directly to the next step.

4.9.5



40. To the peptide on resin (**39**) was added **35** (6 eq) and TEA (10 eq) in DMF (0.05 M of **35**). The reaction was stirred for 3 h, washed with DMF 5x, then DCM 5x. The resin-bound product was taken directly to the next step. The Rhodamine-peptide bound to resin was cleaved under soft conditions with 2% TFA in DCM. Solvent removed in vacuo. MS (MALDI) $C_{134}H_{181}N_{22}O_{24}S_3$ calculated 2578.2781, found 2578.9558.

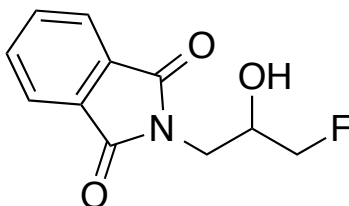
4.9.6



41. Rhodamine-PKI(14-22)-OH (0.05 mmol, **40**) was taken up in DCM (5 mL). PyBOP (0.065 mmol), DIEA (0.2 mmol), and chloromethyl ketone **32** (0.065 mmol) were added to the solution. The reaction was stirred for 16 h. Solvent was removed and the purified on a silica gel gravity column, washed with DCM, and eluted with 20% MeOH/DCM. The solid was then globally deprotected with 95:2.5:2.5 TFA:TIS:H₂O (5 mL) for 1 hr. Then triturated with ether to afford the crude product. Product purified on HPLC (95:5 to 75:25 H₂O:ACN over 20 minutes). MS (MALDI) C₇₅H₁₁₈ClN₂₃O₁₅ calculated 1615.8850 , [C₇₅H₁₁₈ClN₂₃O₁₅ + Na] calculated 1638.8748 found 1638.7704.

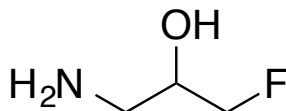
4.10 Synthesis of Fluoromethyl Ketone

4.10.1



2-(3-fluoro-2-hydroxypropyl)isoindoline-1,3-dione (**42**). Procedure adapted from ChemBioChem 2012, 13, 80-84.¹³⁵ (1.34465g, 60%). To a round bottom flask add 10 mL DMF and 1.7596g of potassium phthalamide. To the mixture add 1-chloro-3-fluoro-2-propanol (0.87 mL). Reflux for 16 hr. Triturate with ether, collect precipitate. The crude product was purified over silica gel chromatography to obtain the desired product. ¹H NMR (400MHz, CDCl₃) δ 7.8 (m, 2H), 7.7 (m, 2H), 4.5 (m, 1H), 4.4 (m, 1H) 4.1 (m, 1H), 3.8 (m, 1.5H), 3.1 (s, 0.5H), 2.9 (s, 1H), 2.8 (s, 1H), 2.0 (s, 0.5H), 1.2 (m, 1H). HRMS (ESI) [C₁₁H₁₀FNO₃+H] calculated 224.0645, found 224.0716.

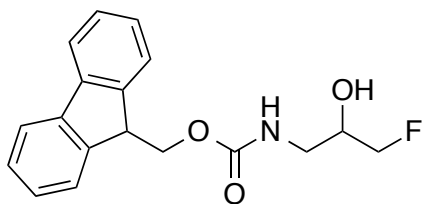
4.10.2



1-amino-3-fluoropropan-2-ol (**43**). Procedure adapted from ChemBioChem 2012, 13, 80-84.¹³⁵

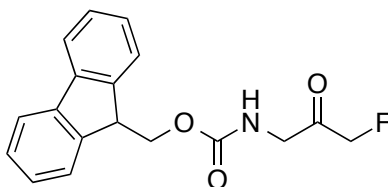
To a solution of **42** (1.12g, 5 mmol) in MeOH (100 mL) was added hydrazine hydrate (0.23mL, 0.95 equiv to **42**) and the reaction mixture was stirred at ambient temperature for 20h, during which time a precipitate formed. Conc. aq. HCl (1mL of a 37% soln, 2 equiv to **42**) was added and the mass was stirred 3 hours. The precipitate was then filtered out. The MeOH was removed in vacuo. Then 30 mL of water was added and then cooled to 0°C. Crude solution taken forward to next step.

4.10.3



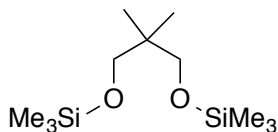
(9*H*-fluoren-9-yl)methyl (3-fluoro-2-hydroxypropyl)carbamate (**44**). Procedure adapted from ChemBioChem 2012, 13, 80-84.¹³⁵ To the solution of **43** generated previously was added 10% Na₂CO₃ (30 mL). To the solution was added 1.102g fmoc-chloride dissolved in 50 mL dioxane. Solution allowed to reach 16 hr. Dioxane was removed under vacuum and crude product was extracted with EtOAc. The organic layer was washed with saturated NaCl solution and solvent removed in vacuo. The crude product was purified over silica gel chromatography to obtain the desired product. ¹H NMR (400MHz, CDCl₃) δ 7.8 (d, 2H J=7.52), 7.6 (m, 2H), 7.4 (m, 2H), 7.3 (m, 2H), 4.4 (m, 2H), 4.1 (m, 1H), 2.9 (s, 4H), 1.3 (s, 2H). HRMS (ESI) [C₁₈H₁₈FNO₃ +Na] calculated 315.1271, 338.1161 (Na adduct) found 338.1172.

4.10.4



(9*H*-fluoren-9-yl)methyl (3-fluoro-2-oxopropyl)carbamate (**45**). Procedure adapted from ChemBioChem 2012, 13, 80-84.¹³⁵ **44** (81.33 mg, 0.26 mmol) was taken up in DCM (5 mL). To the solution was added DMP (275.69 mg, 0.65 mmol). Reaction monitored by TLC to completion. Solvent removed *in vacuo*. The crude product was purified over silica gel chromatography to obtain the desired product. ¹H NMR (400MHz, CDCl₃) δ 7.8 (d, 2H J=7.52), 7.6 (m, 2H), 7.4 (m, 2H), 7.3 (m, 2H), 5.4 (s, 1H), 5.0 (s, 1H), 4.9 (s, 1H), 4.4 (m, 2H), 4.3 (s, 2H), 4.2 (m, 1H), 1.2 (s, 1H). ¹³C NMR (125 MHz, CDCl₃): δ 202.2, 156.3, 143.9, 141.4, 127.9, 127.2, 125.0, 120.1, 84.1, 67.2, 48.2, 47.3. HRMS (ESI) [C₁₈H₁₆FNO₃+Na] calculated 313.1114, 336.1012 (Na adduct) found 336.1017.

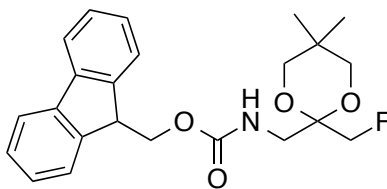
4.10.5



2,2,5,5,8,8-hexamethyl-3,7-dioxa-2,8-disilanonane. To a round bottom flask was added 32 mL diethylether. To the diethylether was added 2,2-dimethylpropane-1,3-diol (1g, 9.6 mmol). To the solution was added 3.35 mL TEA (24 mmol). To the solution was added TMSCl over 5 minutes and allowed to react for 16 hr at ambient temperature. White precipitate filtered off. Ether layer

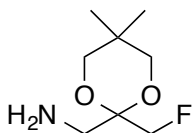
washed with water. Solvent removed in vacuo to afford pure product as a clear liquid. ^1H NMR (400MHz, CDCl_3) δ 3.2 (s, 4H), 0.7 (s, 6H), 0.0 (s, 18H). ^{13}C NMR (125 MHz, CDCl_3): δ 68.5, 37.7, 22.0, 0.2.

4.10.6



(9H-fluoren-9-yl)methyl ((2-(fluoromethyl)-5,5-dimethyl-1,3-dioxan-2-yl)methyl)carbamate (**46**). Procedure adapted from ChemBioChem 2012, 13, 80-84.¹³⁵ **45** (61.24 mg, 0.20 mmol) was taken up in DCM (7 mL). To the solution was added THS protected diol from previous step (69.58 mg, 0.28 mmol). Solution cooled to 0°C. To the reaction was added TMSOTf (catalytic, 0.02 mmol). Reaction allowed to reach ambient temperature and equilibrate for 16 hr. Solvent removed *in vacuo*. The crude product was purified over silica gel chromatography to obtain the desired product. ^1H NMR (400MHz, CDCl_3) matched previously reported data.¹³⁵ δ 7.8 (d, 2H $J=7.52$), 7.6 (m, 2H), 7.4 (m, 2H), 7.3 (m, 2H), 5.4 (s, 1H), 5.0 (s, 1H), 4.9 (s, 1H), 4.4 (m, 2H), 4.3 (s, 2H), 4.2 (m, 1H), 1.2 (s, 1H). ^{13}C NMR (125 MHz, CDCl_3): δ 202.2, 156.3, 143.9, 141.4, 127.9, 127.2, 125.0, 120.1, 84.1, 67.2, 48.2, 47.3. HRMS (ESI) [$\text{C}_{23}\text{H}_{26}\text{FNO}_3 + \text{Na}$] calculated 399.1846, 422.1744 (Na adduct) found 422.1751.

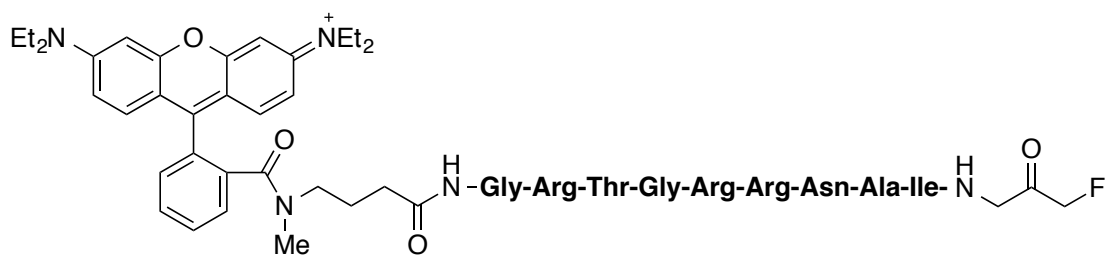
4.10.7



(2-(fluoromethyl)-5,5-dimethyl-1,3-dioxan-2-yl)methanamine (**47**). **46** (52 mg) was taken up in 3 mL ACN. To the solution was added 0.23 mL diethyl amine and reaction monitored by TLC. Solvent removed under vacuum. Crude reaction mixture used as is in the following steps.

4.11 Synthesis of Remaining Peptide Probes.

4.11.1

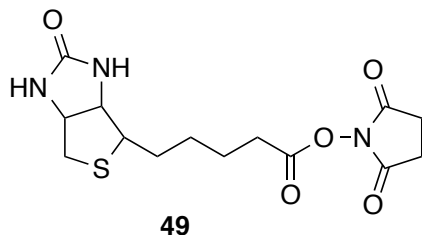


48

Rhodamine-PKI(14-22)-OH (0.05 mmol, **40**) was taken up in DCM (5 mL). PyBOP (0.065 mmol), DIEA (0.2 mmol), and fluoromethyl ketone **47** (0.065 mmol) were added to the solution. The reaction was stirred for 16 h. Solvent was removed and the purified on a silica gel gravity column, washed with DCM, and eluted with 20% MeOH/DCM. The solid was then globally deprotected with 95:2.5:2.5 TFA:TIS:H₂O (5 mL) for 1 hr. Then triturated with ether to afford

the crude product. Product purified on HPLC (95:5 to 75:25 H₂O:ACN over 20 minutes). MS (MALDI) C₁₄₂H₁₉₅FN₂₃O₂₅S₃ calculated 2737.3841, found 2737.3524.

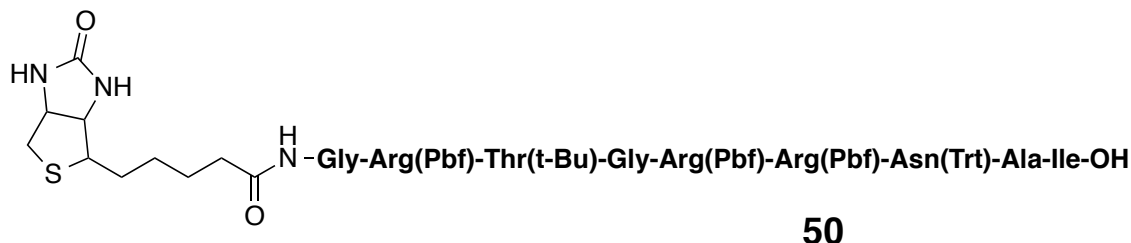
4.11.2



2,5-dioxopyrrolidin-1-yl 5-(2-oxohexahydro-1*H*-thieno[3,4-*d*]imidazol-4-yl)pentanoate (**49**).

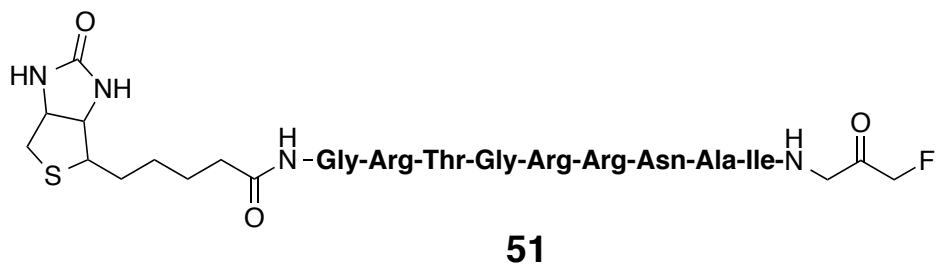
Procedure adapted from JACS 2007, 129, 13987.¹³⁸ To a round bottom flask add 17.2 mL DMF, 590 mg D-biotin (2.41 mmol), and 277 mg N-hydroxysuccinimide (2.41 mmol). To the mixture add *N,N'*-Dicyclohexylcarbodiimide (DCC, 645 mg, 3.13 mmol). Heat until dissolved, stir then allow to reach ambient T. Allow to react for 16 hr. Triturate with ether and collect precipitate. Spectral data matched previously reported.¹³⁸

4.11.3



50. To the peptide on resin was added **49** (6 eq) and TEA (10 eq) in DMF (0.05 M of **35**). The reaction was stirred for 3 h, washed with DMF 5x, then DCM 5x. The resin-bound product was taken directly to the next step. The Biotin-peptide bound to resin was cleaved under soft conditions with 2% TFA in DCM. Solvent removed in vacuo. MS (MALDI) $C_{111}H_{157}N_{21}O_{23}S_4$ calculated 2280.0644 [$C_{111}H_{157}N_{21}O_{23}S_4 + Na$] calculated 2303.0542 found 2301.0534.

4.11.4



Biotin-PKI(14-22)-OH (0.05 mmol, **50**) was taken up in DCM (5 mL). PyBOP (0.065 mmol), DIEA (0.2 mmol), and fluoromethyl ketone **47** (0.065 mmol) were added to the solution. The reaction was stirred for 16 h. Solvent was removed and the purified on a silica gel gravity column, washed with DCM, and eluted with 20% MeOH/DCM. The solid was then globally

deprotected with 95:2.5:2.5 TFA:TIS:H₂O (5 mL) for 1 hr. Then triturated with ether to afford the crude product. Product purified on HPLC (95:5 to 75:25 H₂O:ACN over 20 minutes). MS (MALDI) C₅₂H₉₄FN₂₂O₁₄S calculated 1301.7008, found 1302.1126.

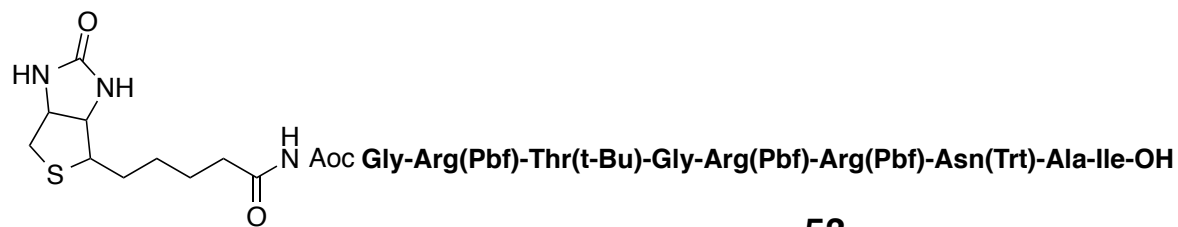
4.11.5



52

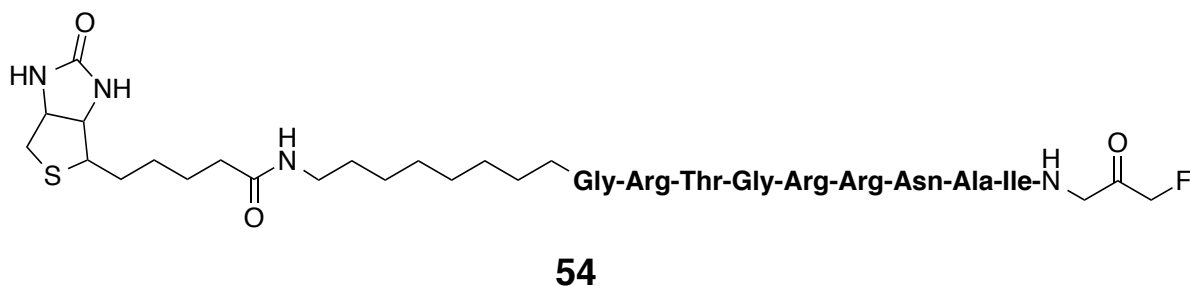
Aoc-PKI(14-22)-2-Cl-trityl Resin Synthesis (52). 2-Chlorotrityl Chloride (2-CTC) resin preloaded with Ile was purchased from ChemImpex (200-400 mesh, Catalog #03472). Peptide couplings were carried out automatically via standard Fmoc amino acid protection chemistry. After the final deprotection (Aoc) with 20% piperidine in DMF, the resin-bound product was taken directly to the next step.

4.11.6



53. To the peptide on resin was added **49** (6 eq) and TEA (10 eq) in DMF (0.05 M of **35**). The reaction was stirred for 3 h, washed with DMF 5x, then DCM 5x. The resin-bound product was taken directly to the next step. The Biotin-peptide bound to resin was cleaved under soft conditions with 2% TFA in DCM. Solvent removed in vacuo. MS (MALDI) $C_{119}H_{172}N_{22}O_{24}S_4$ calculated 2421.1798 found 2422.4553.

4.11.7



54. Biotin-Aoc-PKI(14-22)-OH (0.05 mmol, **53**) was taken up in DCM (5 mL). PyBOP (0.065 mmol), DIEA (0.2 mmol), and fluoromethyl ketone **47** (0.065 mmol) were added to the solution. The reaction was stirred for 16 h. Solvent was removed and the purified on a silica gel gravity column, washed with DCM, and eluted with 20% MeOH/DCM. The solid was then globally

deprotected with 95:2.5:2.5 TFA:TIS:H₂O (5 mL) for 1 hr. Then triturated with ether to afford the crude product. Product purified on HPLC (95:5 to 75:25 H₂O:ACN over 20 minutes). MS (MALDI) C₆₀H₁₀₉FN₂₃O₁₅S³⁺ calculated 1442.8162, found 1442.8860.

4.12 Biology Experimentals:

Overlap of Figure 43.

To overlap the gels, they were saved as .tiff files and inserted into a Microsoft Word document. Once in the word document the transparency of the images were adjusted so that both could be observed when overlapped. By positioning the images such that the reference points in the C199A mutant lanes were in line (lanes 7 and 8) immediately the predominant species was identified as the bottom band. This is a curious find in that the upper band always had a more robust signal intensity, but it is actually present in significantly less quantities than the lower band. This leads into the hypothesis of the probe having significant isoform selectivity; however, the differences between the two band at this point were unknown and further characterization was required.

Overlap of Figure 46.

To overlap the gels, the fluorescence and Coomassie images were saved as .tiff files and inserted into a Microsoft Word document. Then the transparency of the overlapping images was adjusted such that both could be observed simultaneously. By positioning the images such that the reference points in the BSA and PKA α were aligned the predominant species was again identified as the bottom band. This spurred a return to the literature were this issue had previously been reported. The two bands differ by phosphorylation at Thr197, the top band is the phosphorylated form (pThr197) and the bottom is the non phosphorylated species.^{87,130,131} To

confirm the new hypothesis that the double banding issue is the same reported in the literature, recombinant PKAC α was exposed to physiologically relevant phosphorylating conditions detailed below.

Figure 47:

To examine the effect of phosphorylation of Thr197 on labeling with Rh-PKI(14-22)-G-(CMK) recombinant PKAC α was phosphorylated *in vitro*. To promote phosphorylation at Thr197, the enzyme that performs this catalytic action *in vivo* (3-phosphoinositide-dependent protein kinase 1, PDK1) was purchased from Invitrogen. Recombinant PKAC α was diluted to 0.1mg/mL in MOPS buffer (50 mM MOPS, pH 7.4, 100 mM NaCl, 10 mM BME, 10 mM MgCl₂, and 1 mM ATP). To the solution of PKAC α was added 6 μ L of a 0.33 mg/mL solution of PDK1. The resulting solution was allowed to react for 90 minutes at ambient temperature. After the reaction was complete the solution was buffer exchanged back in to phosphate buffer solution (25 mM PO₄ pH 7.2, for labeling reactions). In Figure 47, the labeling characteristics of the probe were examined against the wild-type recombinant PKAC α and with recombinant PKAC α that was treated with PDK1. Both protein solution concentrations were determined by absorbance at 280 nM and diluted to 1 mg/mL in phosphate buffer (25 mM PO₄ pH 7.2). Appropriate amounts of protein were added to reaction vessels (epindorf tubes). The probe was made as a 10 mM stock solution in DMSO and diluted accordingly for appropriate final concentrations in the gel experiments. The gel was cast as 1.5 mm thick and the wells were a total volume of 20 μ L. The the samples were incubated with probe for 1 hr. The samples were quenched with a denaturing sample buffer (made in house and detailed in the biological experimental section) and incubated at 100°C for 5 minutes. The denaturing sample buffer contained a disulfide reducing agent

(betamercaptoethanol, BME). Coomassie staining was performed with blue G250 in a H₂O/MeOH/AcOH solution, and destained with a H₂O/MeOH/AcOH solution. Images of the Coomassie stained gel were taken with a galaxy S4 smart phone camera (13 megapixels, autofocus and default settings).

Bradford assay

Standard solutions of bovine serum albumin (BSA, provided in kit) were prepared at 0.5, 0.25, 0.125, 0.1, 0.05 mg/mL in 25 mM NaPO₄ buffer pH 7.2. The BioRad Bradford assay reagent is 5X and must be diluted to 1X in H₂O. A 96 well clear bottom plate from Greiner was used. To a well was added 10 µL of analyte solution and 200 µL Bradford detection solution. The resulting solution was allowed to incubate for 5 minutes. The absorbance was read on a FlexStation 3 at 595 nM. Absorbance values were graphed in excel and used to determine the concentration of unknown (linear range of assay is from 0.05 to 0.5 mg/mL).

Preparation of Lysates

MCF7 Lysates. The MCF7 cell line was grown up in T75 flasks in RPMI buffer with 10% FBS (no antibiotic present). Every second or third day (whichever time the cell line was 75% confluent) they were passaged at 1:10. Once three consecutive T75 flasks were growing the MCF7 cell line, they were grown to complete confluence and harvested and gently centrifuged (1000 rpm for 4 minutes) into a pellet. The pellet was resuspended in 5 mL phosphate buffer (25 mM NaPO₄, pH 7.2). The suspension was homogenized with a Dounce homogenizer and the

debris removed by centrifugation (31,200 rpm for 45 minutes). Supernatant was decanted and aliquoted. Protein concentration determined by Bradford assay.

Bradford Assay for MCF7 Cell Lysates:

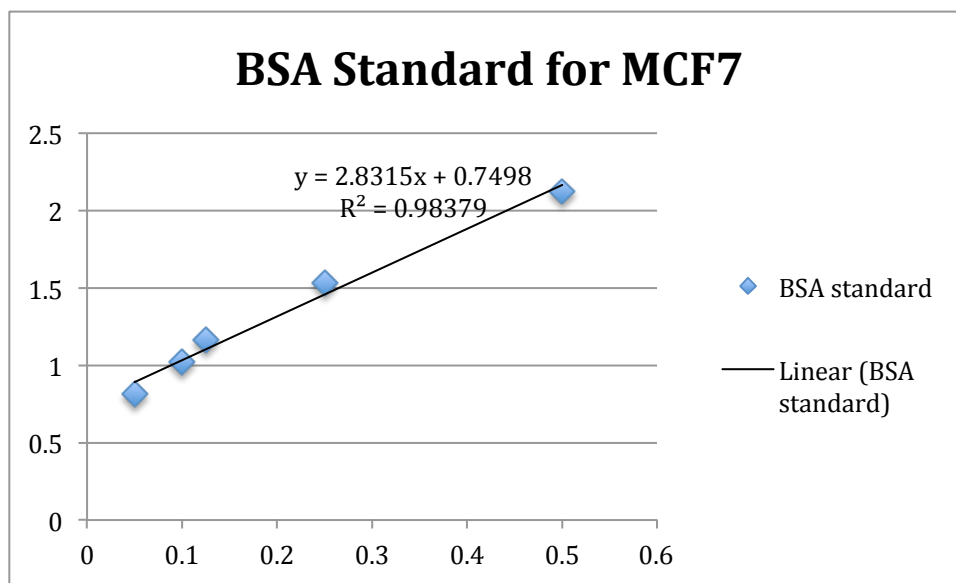


Figure 70. Bradford assay graph for MCF7 lysates.

Table 13. Results of Bradford assay for MCF7 cell lysates.

	Absorbance	Concentration (mg/mL)
MCF7	0.9692	0.077

Preparation of MDA-MB-231 Cell Lysates

MDA-MB-231 Lysates. The MDA-MB-231 cell line was grown up in T75 flasks in RPMI buffer with 10% FBS, and 1% ampicillin. Every second or third day (whichever time the cell line was

75% confluent) they were passaged at 1:5. Once four consecutive T75 flasks were growing the MDA-MB-231 cell line, they were grown to complete confluence and harvested and gently centrifuged (1000 rpm for 4 minutes) into a pellet, cell count was 2,820,000 (89.36% viable). The pellet was resuspended in 3 mL phosphate buffer (25 mM NaPO₄, pH 7.2) with 1X Rouche Protease Inhibitor Cocktail and 1 mM EDTA. The suspension was homogenized with a Dounce homogenizer and the debris removed by centrifugation (31,200 rpm for 45 minutes). Supernatant was decanted and aliquoted. Protein concentration determined by Bradford assay.

Bradford Assay for MDA-MB-231 Cell Lysates:

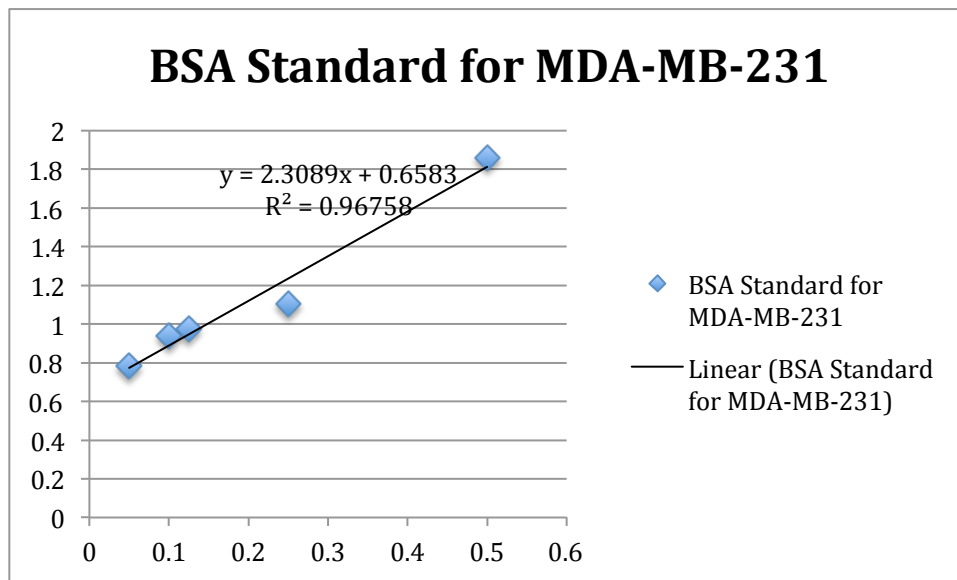


Figure 71. Bradford assay graph for MDA-MB-231 cell lysates.

Table 14. Results of Bradford assay for MDA-MB-231 cell lysates.

	Absorbance	Concentration (mg/mL)
MDA-MB-231	1.2321	0.25

Preparation of bovine heart lysates.

Bovine heart was obtained from a local butcher shop and immediately cut into equal 10 g portions and the portions not being used were frozen. One 10g portion was submerged in phosphate buffer (25 mM NaPO₄, pH 7.2) with 1X Rouche Protease inhibitor cocktail with 1 mM EDTA. The tissue was homogenized with a tissue homogenizer and the debris removed by sequential centrifugation (8,000 rpm for 30 minutes then 31,200 rpm for 45 minutes). The soluble fraction was collected and aliquoted out. The concentration was determined by Bradford Assay.

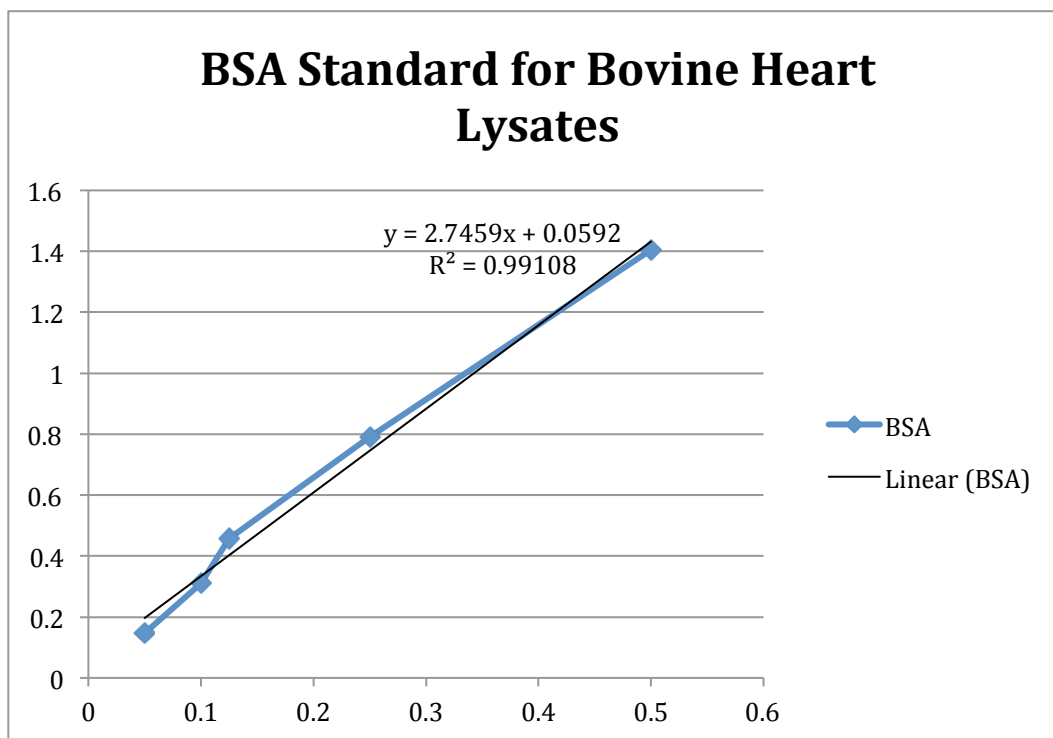


Figure 72. Bradford assay graph for bovine heart lysates.

Table 15. Results from Bradford assay of bovine heart lysates.

	Absorbance (0.1x)	Concentration (mg/mL)	Actual (mg/mL)
Bovine heart lysates	0.7516	0.25	2.5

Preparation of mouse heart lysates.

Mouse hearts harvested from HEB6 mice were a generous gift from Dr. Jolene Windle. Intact hearts were submerged in PBS buffer with Roche Protease Inhibitor at 1X concentration (at 0 °C) immediately after harvesting. The tissue was homogenized with a tissue homogenizer on ice and cellular debris removed by sequential centrifugation (8,000 rpm for 30 min, then 31,200 rpm for 45 min). The soluble fraction was collected and concentration determined by Bradford assay.

Figure 73. Bradford assay graph for mouse heart lysates.

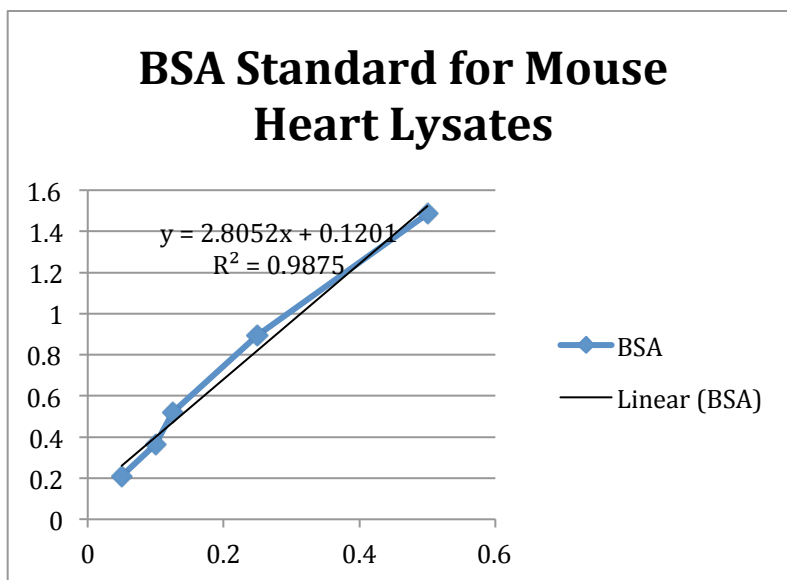


Table 16. Results from Bradford assay for mouse heart lysates.

	Absorbance (.01x)	Concentration (mg/mL)	Actual (mg/mL)
Mouse Heart Lysates	0.83945	0.26	26

4.1 Gel Electrophoresis

Gel recipes:

Resolving gel (10%)	1 gel	2 gels
Water	3.20 ml	6.40 ml
Lower buffer	2.00 ml	4.00 ml
Glycerol	0.80 ml (1.01 g)	1.60 ml (2.02 g)
40% acrylamide	2.00 ml	4.00 ml
10% APS (freshly prep.)	40 µl	80 µl

TEMED	10 μ l	20 μ l
-------	------------	------------

Stacking gel	1 gel	2 gels
Water	1.95 ml	3.90 ml
Upper buffer	750 μ l	1.5 ml
40% acrylamide	300 μ l	600 μ l
10% APS (freshly prep.)	30 μ l	60 μ l
TEMED	7.5 μ l	15 μ l

Lower buffer - 100 ml (pH 8.8)

Final conc.	Component	M.W.	Amount (g)	Volume (ml)
1.5 M	Tris	121.14	18.171	–
0.40%	SDS	–	0.4	–
	Water	–	–	q.s.

Adjust to pH 8.8 with HCl

Upper buffer - 100 ml (pH 6.8)

Final conc.	Component	M.W.	Amount (g)	Volume (ml)
0.5 M	Tris	121.14	6.057	–
0.40%	SDS	–	0.4	–
	Water	–	–	q.s.

Adjust to pH 6.8 with HCl

General Sample preparation procedure for gel electrophoresis

In vitro labeling of wild type and C199A PKA α . 2.0 mg of protein was diluted into 40 mL PBS (25 mM NaPO₄ pH 7.2), final concentration ~1.2 mM. The proteins were incubated with the relevant concentration of probe for 1 hr. 10 mL of a 5x SDS-Page Sample buffer was added and

separated on a 10% SDS-PAGE gel. Fluorescent imaging was performed on an Amersham Imager 600 (AI600) instrument. The gel was then stained with Coomassie and imaged on the AI600.

In vitro oxidation and labeling of wild type PKA α . 2.0 mg of protein was diluted into 40 mL PBS (25 mM NaPO₄ pH 7.2), final concentration ~1.2 mM. Wild type PKA α was incubated with 2 mM Ellman's reagent for 1 and 4 hours. The oxidized and non-treated proteins were then incubated with 300 nM probe for 1 hr. 10 mL of a 5x SDS-Page Sample buffer was added and separated on a 10% SDS-PAGE gel. Fluorescent and Coomassie imaging was performed on an AI600 instrument.

In vitro saturation of labeling of wild type PKA α . 2.0 mg of protein was diluted into 40 mL PBS (25 mM NaPO₄ pH 7.2), final concentration ~1.2 mM. Wild type PKA α was incubated with increasing concentrations of PKI(14-22)Amide for 1 hr. The treated and non-treated proteins were then incubated with relevant concentrations of probe for 1 hr. 10 mL of a 5x SDS-Page Sample buffer was added and separated on a 10% SDS-PAGE gel. Fluorescent and Coomassie imaging was performed on an AI600 instrument.

In vitro labeling of mouse heart lysates. Lysates were diluted in 1X protease inhibitor cocktail to a concentration of 2.5 mg/mL, with or without cAMP at 100 mM and with or without Probe at 300 nM for 1hr. The resulting proteome solution was concentrated to 25 mg/mL with a 10 kDa molecular weight cut off spin filter. 10 mL of a 5x SDS-Page Sample buffer was added and separated on a 10% SDS-PAGE gel. Fluorescent imaging was performed on an Amersham

Imager 600 instrument. The gel was then transferred to a PVDF membrane and bands detected by colorimetric HRP reaction with a T197 specific rabbit antibody, image taken on AI600 instrument.

In vitro labeling of bovine heart lysates. Lysates were diluted in 1X protease inhibitor cocktail to a concentration of 2.5 mg/mL, with or without cAMP at 100 mM and with or without Probe at 300 nM for 1hr. The resulting proteome solution was concentrated to 25 mg/mL with a 10 kDa molecular weight cut off spin filter. 10 μ L of a 5x SDS-Page Sample buffer was added and separated on a 10% SDS-PAGE gel. Fluorescent imaging was performed on an Amersham Imager 600 instrument. The gel was then transferred to a PVDF membrane and bands detected by colorimetric HRP reaction with a T197 specific rabbit antibody, image taken on AI600 instrument.

In vitro labeling of MCF7 lysates. Lysates were used at the concentration harvested, with or without cAMP at 100 mM and with or without Probe at 300 nM for 1hr. The resulting proteome solution denatured with 10 μ L of a 5x SDS-Page Sample buffer and separated on a 10% SDS-PAGE gel. Fluorescent imaging was performed on an Amersham Imager 600 instrument. The gel was then transferred to a PVDF membrane and bands detected by colorimetric HRP reaction with a T197 specific rabbit antibody, image taken on AI600 instrument.

In vitro labeling of MDA-MB-231 lysates. Lysates were used at the concentration harvested, with or without cAMP at 100 mM and with or without Probe at 300 nM for 1hr. The resulting proteome solution denatured with 10 μ L of a 5x SDS-Page Sample buffer and separated on a

10% SDS-PAGE gel. Fluorescent imaging was performed on an Amersham Imager 600 instrument. The gel was then transferred to a PVDF membrane and bands detected by colorimetric HRP reaction with a T197 specific rabbit antibody, image taken on AI600 instrument.

Gel Electrophoresis

- 1) Cast the gel (add reagents in order listed in recipe, TEMED starts the solidifying reaction)
- 2) Prepare the electrophoresis setup
- 3) Prepare the samples
- 4) Prepare the sample buffer, add 0.1x volume of BME to the amount of sample buffer required (10uL per well, calculate for a few extra ie. 7 wells you should make 100uL of buffer)
- 5) Denature the Samples with 5x Sample Buffer (10uL to 40uL for a total of 50uL)
 - a. 5minutes at 100°C
- 6) Spin the samples in microcentrifuge for 30 seconds to collect all volume at bottom
- 7) Load 40uL of the denatured sample into respective lanes on the gel (50 is max but it does not all fit properly)
- 8) Load 2uL undiluted Ladder to lane(s)
- 9) Place top of gel electrophoresis chamber on
- 10) Turn on the instrument

11) Set to constant voltage of 170, for 60 minutes

Western Blot:

Transfer to membrane

- 1) Collect the gel and wash with tap water 5x, leave in Petri dish submerged in water until needed
- 2) Submerge membrane in MeOH for 3 minutes
- 3) Prepare 1L of transfer buffer (see buffer bottle for dilution instructions)
- 4) Submerge filter paper and fiber pads in transfer buffer
- 5) Decant MeOH off the membrane and then immediately submerge in transfer buffer (do not let dry, if it does and you see white spots, repeat step 2)
- 6) Follow the setup depicted for the Western blot (ie black side of cartridge down, then in this order: Fiber pad, filter paper, gel, membrane, filter paper, fiberpad)
- 7) Place second cartridge into the electrophoresis chamber and fill chamber up with remaining buffer
- 8) Place cold pack into electrophoresis chamber
- 9) Top off chamber to Western blot line with buffer (or water if only a small amount is required)
- 10) Set to constant 100 mAmps and run for 60 minutes

Protein Detection (for colorimetric only, for ECL see manufacturer instructions)

- 1) Collect the membrane and submerge in blocking buffer (5% BSA) for 1hr.
- 2) Decant blocking buffer off

- 3) Incubate with primary antibody for 2hrs (dilute antibody 1:1000 in blocking buffer, 10mL total)
- 4) Wash with TBS 5x
- 5) Incubate with secondary antibody for 1hr (dilute antibody 1:1000 in blocking buffer, 10mL total)
- 6) Wash 5x with TBS
- 7) Leave submerged in TBS until ready for staining
- 8) Prepare colorimetric staining solution according to BioRad specifications (ie 9 mL of H₂O, 1 mL of 10x buffer, 60 uL of reagent B; then right before adding to membrane 2 mL reagent A)
- 9) Allow to develop until color change stops
- 10) Quench with tap water and let dry
- 11) Image on gel imager

General Procedure for the trypsin digest mass spectrometry

Unmodified PKAC α or PKAC α incubated with probe was buffer exchanged into a lysis buffer (25 mM Tris pH 7.6, 1 mM EDTA, 150 mM NaCl, 1% Triton X-100, 0.1% SDS, and 10 mM DTT). The protein solution was mixed with trypsin at a ratio of 20:1 protein to protease. The resulting solution was incubated at 37°C for 24 hr. The sample was analyzed by MALDI mass spectrometry with CHCA matrix (Sigma) on a Voyager DE-ProTM MALDI TOF Mass Spectrometer.

Procedure for Biotin Pull-Down Experiment.

Streptavidin column and buffers were purchased from BioRad as a complete kit. The column was washed with biotin solution to block all irreversible binding sites prior to usage. Subsequent

reactivation of the streptavidin column (stripping of reversible binding sites) with acidic buffer was then performed according to manufacturers instructions, followed by neutralization with supplied PBS. Then, 1 mL of mouse heart lysates was incubated with the streptavidin resin for 45 minutes. The lysate solution was eluted with PBS and the appropriate fractions were collected (determined by absorbance at 280 nm on spectrophotometer). The collected fractions were pooled and diluted to a final volume of 10 mL with 25 mM PO₄ buffer with 1X Rouché Protease inhibitor cocktail and 1 mM EDTA. To the resulting solution was added biotinylated probe and allowed to react for 1 hr. The solution was then incubated with the streptavidin column for an additional 45 minutes. The column was washed with PBS until no absorbance was detected on the spectrophotometer. Then biotinylated compounds were eluted with a 2 mM biotin solution provided in the kit. The appropriate fractions were collected (as determined by absorbance at 280 nM) and pooled. Gel electrophoresis experiments and Western blots were conducted to confirm.

Procedure for generation of plasmids

Initial cultures for plasmid isolation were grown up in 10 mL LB buffer at 37 °C for 16 hr with gentle shaking. The plasmids were collected with a QIA prep Spin miniprep kit w/ centrifuge according to manufacturers instructions as follows:

- 1) cell centrifuged to a pellet and solution decanted (1600xG 5 min)
- 2) cells taken up in 250µL Buffer P1 and transferred to an epindorf tube
- 3) to the solution was added 250 µL buffer P2 and inverted 5 times (solution turns blue)
- 4) to the solution was added 350 µL of Buffer N3, inverted 5 times (precipitate forms)
- 5) centrifuge for 10 minutes at 17,900xG for 3 minutes
- 6) decant solution into QIA prep spin column
- 7) centrifuge for 1 minute and discard flowthrough

- 8) Add 500 μL of Buffer PB and centrifuge for 1 minute, discard flowthrough
- 9) Add 750 μL of Buffer PE centrifuge for 1 minute, discard flowthrough
- 10) Centrifuge an additional time for 1 minute and discard flowthrough
- 11) Place QIAprep column in new (clean) epindorf tube
- 12) Add 50 μL Buffer EB and let equilibrate for 1 minute
- 13) Centrifuge for 1 minute
- 14) Collect flowthrough and freeze

Procedure for prep scale production of proteins (by day)

Day 1: Initial culture.

To a sterile test tube add 5 mL of LB media (solution of tryptone, yeast extract, and NaCl) with amp or kan (for dual expression use both antibiotics) selection. Cells directly from the $-80\text{ }^{\circ}\text{C}$ were added, without freezing and as small amount as could be reliably harvested (a pipette tip was used to scratch the surface of the frozen cells and the end submerged in the test tube media). Incubated at $37\text{ }^{\circ}\text{C}$ with gentle shaking for 16 hrs.

Day 2: Scale up from initial culture.

Prepared 1 L vessels for growing by adding auto induction media to each (1 L amount) and autoclaving. To the auto induction media add 20 mL of 50x glycerol, glucose, lactose solution, 1 mL of 1 M MgCl_2 salt, and 1 mL of amp solution (50 mg/mL) (and kan solution for dual expression). From the initial culture on the previous day, extract 1 mL and add to the auto induction media that has been treated to promote growth. Incubate at $37\text{ }^{\circ}\text{C}$ for 16 hr with gentle shaking.

Day 3: Isolation and Purification.

Collect media and spin down at 6000 rpm for 10 minutes. Collect cells in minimal amount of solvent you wish to lyse into (PBS is fine, but solvent for the Ni column is preferred). Lyse cells. Spin lysates for 30 minutes at 20,000 RPM to remove debris. Decant onto activated nickel column. Wash with 1 mM imidazole solution until no absorbance detected. Elute with 100 mM imidazole. Collect appropriate fractions.

Procedure for moving PDK1 into pRSF Duet vector.

PDK1 initially in pMCSG10 vector and the plasmid was isolated as described above. The pRSF duet vector (kan resistance) plasmid was simultaneously isolated in the same manner. To a micro centrifuge tube was added: 10 μ L of PDK1 Plasmid, 2 μ L Green buffer, 1 μ L BglII, 1 μ L NdeI, and 6 μ L H₂O. To a separate micro centrifuge tube was added: 10 μ L of pRSF Plasmid, 2 μ L Green buffer, 1 μ L BamHI, 1 μ L NdeI, and 6 μ L H₂O. Digested at 37 °C for 30 minutes. The resulting solutions were run on agarose gel that was made in house (50 mL stock Tris Acetate EDTA (TAE) in H₂O, 0.5 g agarose, bring to boil then add 5 μ L ethidium bromide and pour onto plate after solution has slightly cooled). Gel was run at 100 V for ~45 minutes with observation until adequate separation for isolation had occurred. Bands excised with scalpel. The appropriate excised gel fragments were placed in an epindorf tube with a solution of 1:3 isopropanol:buffer QG (100 mg gel = 100 μ L volume). Incubate at 50 °C for 10 minutes (or until dissolved). Transfer to QIAquick spin column and spin for 1 minute, discard flowthrough. Add 0.5 mL buffer QG, spin 1 minute, discard flowthrough. Add 0.75 mL buffer PE incubate for 5 minutes, spin 1 min, discard flowthrough. Spin down an additional 1 minute and discard flowthrough. Move QIAquick column to a 1.5 mL centrifuge tube and add 30 μ L of elution buffer allow to equilibrate for 1 minute. Spin for 1 minute and collect flowthrough. To a fresh microcentrifuge

tube add 17 μL DNA mixture, 2 μL of ligation buffer, 1 μL ligase and incubate at room temp for 30 minutes. Competent scarab cells were transformed with the resultant mixture as follows:

200 μL of competent scarab cells were thawed from the $-80\text{ }^{\circ}\text{C}$ freezer. To the cells was added 10 μL ligation mixture. Cells made to sit in ice for 30 minutes. Heat shock at $42\text{ }^{\circ}\text{C}$ in water bath for 1 minute. Plate onto antibiotic plate. Incubate at $37\text{ }^{\circ}\text{C}$ overnight.

Literature Cited

1. Kristensen, V. N.; Lingjaerde, O. C.; Russnes, H. G.; Vollan, H. K.; Frigessi, A.; Borresen-Dale, A. L. Principles and methods of integrative genomic analyses in cancer. *Nat Rev Cancer* **2014**, *14*, 299-313.
2. Phillips, C. I.; Bogyo, M. Proteomics meets microbiology: technical advances in the global mapping of protein expression and function. *Cell Microbiol* **2005**, *7*, 1061-1076.
3. Anderson, L.; Seilhamer, J. A comparison of selected mRNA and protein abundances in human liver. *Electrophoresis* **1997**, *18*, 533-537.
4. Hanahan, D.; Weinberg, R. A. Hallmarks of cancer: the next generation. *Cell* **2011**, *144*, 646-674.
5. Rix, U.; Superti-Furga, G. Target profiling of small molecules by chemical proteomics. *Nat Chem Biol* **2009**, *5*, 616-624.
6. Guo, Y.; Wilderman, A.; Zhang, L.; Taylor, S. S.; Insel, P. A. Quantitative proteomics analysis of the cAMP/protein kinase A signaling pathway. *Biochemistry* **2012**, *51*, 9323-9332.
7. Weerapana, E.; Wang, C.; Simon, G. M.; Richter, F.; Khare, S.; Dillon, M. B.; Bachovchin, D. A.; Mowen, K.; Baker, D.; Cravatt, B. F. Quantitative reactivity profiling predicts functional cysteines in proteomes. *Nature* **2010**, *468*, 790-795.
8. Longsworth, L. G.; Shedlovsky, T.; MacInnes, D. A. Electrophoretic patterns of normal and pathological human blood serum and plasma. *The Journal of Experimental Medicine* **1939**, *70*, 399-413.

9. Hanash, S.; Taguchi, A. The grand challenge to decipher the cancer proteome. *Nat Rev Cancer* **2010**, *10*, 652-660.
10. Verhelst, S.; Bogyo, M. Chemical proteomics applied to target identification and drug discovery. *Biotechniques* **2005**, *38*, 175-177.
11. Jessani, N.; Cravatt, B. F. The development and application of methods for activity-based protein profiling. *Curr Opin Chem Biol* **2004**, *8*, 54-59.
12. Speers, A. E.; Cravatt, B. F. Chemical strategies for activity-based proteomics. *Chembiochem* **2004**, *5*, 41-47.
13. Jeffery, D. A.; Bogyo, M. Chemical proteomics and its application to drug discovery. *Current opinion in biotechnology* **2003**, *14*, 87-95.
14. Uttamchandani, M.; Li, J.; Sun, H.; Yao, S. Q. Activity-based protein profiling: new developments and directions in functional proteomics. *Chembiochem* **2008**, *9*, 667-675.
15. Cravatt, B. F.; Wright, A. T.; Kozarich, J. W. Activity-based protein profiling: from enzyme chemistry to proteomic chemistry. *Annu Rev Biochem* **2008**, *77*, 383-414.
16. Barglow, K. T.; Cravatt, B. F. Activity-based protein profiling for the functional annotation of enzymes. *Nat Methods* **2007**, *4*, 822-827.
17. Lanning, B. R.; Whitby, L. R.; Dix, M. M.; Douhan, J.; Gilbert, A. M.; Hett, E. C.; Johnson, T. O.; Joslyn, C.; Kath, J. C.; Niessen, S.; Roberts, L. R.; Schnute, M. E.; Wang, C.; Hulce, J. J.; Wei, B.; Whiteley, L. O.; Hayward, M. M.; Cravatt, B. F. A road map to evaluate the proteome-wide selectivity of covalent kinase inhibitors. *Nat Chem Biol* **2014**, *10*, 760-767.
18. Liu, Y.; Patricelli, M. P.; Cravatt, B. F. Activity-based protein profiling: the serine hydrolases. *Proc Natl Acad Sci U S A* **1999**, *96*, 14694-14699.

19. Sanman, L. E.; Bogyo, M. Activity-based profiling of proteases. *Annu Rev Biochem* **2014**, *83*, 249-273.
20. Kato, D.; Boatright, K. M.; Berger, A. B.; Nazif, T.; Blum, G.; Ryan, C.; Chehade, K. A.; Salvesen, G. S.; Bogyo, M. Activity-based probes that target diverse cysteine protease families. *Nat Chem Biol* **2005**, *1*, 33-38.
21. Saghatelian, A.; Jessani, N.; Joseph, A.; Humphrey, M.; Cravatt, B. F. Activity-based probes for the proteomic profiling of metalloproteases. *Proc Natl Acad Sci U S A* **2004**, *101*, 10000-10005.
22. Jost, C.; Nitsche, C.; Scholz, T.; Roux, L.; Klein, C. D. Promiscuity and selectivity in covalent enzyme inhibition: a systematic study of electrophilic fragments. *J Med Chem* **2014**, *57*, 7590-7599.
23. Knight, Z. A.; Shokat, K. M. Features of selective kinase inhibitors. *Chem Biol* **2005**, *12*, 621-637.
24. Sogabe, Y.; Matsumoto, T.; Hashimoto, T.; Kirii, Y.; Sawa, M.; Kinoshita, T. 5Z-7-Oxozeaenol covalently binds to MAP2K7 at Cys218 in an unprecedented manner. *Bioorg Med Chem Lett* **2015**, *25*, 593-596.
25. Barf, T.; Kaptein, A. Irreversible protein kinase inhibitors: balancing the benefits and risks. *J Med Chem* **2012**, *55*, 6243-6262.
26. Cohen, M. S.; Zhang, C.; Shokat, K. M.; Taunton, J. Structural bioinformatics-based design of selective, irreversible kinase inhibitors. *Science* **2005**, *308*, 1318-1321.
27. Perez, D. I.; Palomo, V.; Perez, C.; Gil, C.; Dans, P. D.; Luque, F. J.; Conde, S.; Martinez, A. Switching reversibility to irreversibility in glycogen synthase kinase 3

- inhibitors: clues for specific design of new compounds. *J Med Chem* **2011**, *54*, 4042-4056.
28. Leproult, E.; Barluenga, S.; Moras, D.; Wurtz, J. M.; Winssinger, N. Cysteine mapping in conformationally distinct kinase nucleotide binding sites: application to the design of selective covalent inhibitors. *J Med Chem* **2011**, *54*, 1347-1355.
29. Schirmer, A.; Kennedy, J.; Murli, S.; Reid, R.; Santi, D. V. Targeted covalent inactivation of protein kinases by resorcylic acid lactone polyketides. *Proc Natl Acad Sci U S A* **2006**, *103*, 4234-4239.
30. Krysiak, J.; Breinbauer, R. Activity-based protein profiling for natural product target discovery. *Top Curr Chem* **2012**, *324*, 43-84.
31. Zhou, W.; Hur, W.; McDermott, U.; Dutt, A.; Xian, W.; Ficarro, S. B.; Zhang, J.; Sharma, S. V.; Brugge, J.; Meyerson, M.; Settleman, J.; Gray, N. S. A structure-guided approach to creating covalent FGFR inhibitors. *Chem Biol* **2010**, *17*, 285-295.
32. Lewis, J. A.; Lebois, E. P.; Lindsley, C. W. Allosteric modulation of kinases and GPCRs: design principles and structural diversity. *Curr Opin Chem Biol* **2008**, *12*, 269-280.
33. Saldanha, S. A.; Kaler, G.; Cottam, H. B.; Abagyan, R.; Taylor, S. S. Assay principle for modulators of protein-protein interactions and its application to non-ATP-competitive ligands targeting protein kinase A. *Anal Chem* **2006**, *78*, 8265-8272.
34. Nguyen, T.; Coover, R. A.; Verghese, J.; Moran, R. G.; Ellis, K. C. Phenylalanine-Based Inactivator of AKT Kinase: Design, Synthesis, and Biological Evaluation. *ACS Med Chem Lett* **2014**, *5*, 462-467.

35. Anjum, R.; Pae, E.; Blenis, J.; Ballif, B. A. TPCK inhibits AGC kinases by direct activation loop adduction at phenylalanine-directed cysteine residues. *FEBS Lett* **2012**, *586*, 3471-3476.
36. Toral-Barza, L.; Zhang, W. G.; Huang, X.; McDonald, L. A.; Salaski, E. J.; Barbieri, L. R.; Ding, W. D.; Krishnamurthy, G.; Hu, Y. B.; Lucas, J.; Bernan, V. S.; Cai, P.; Levin, J. I.; Mansour, T. S.; Gibbons, J. J.; Abraham, R. T.; Yu, K. Discovery of lactoquinomycin and related pyranonaphthoquinones as potent and allosteric inhibitors of AKT/PKB: mechanistic involvement of AKT catalytic activation loop cysteines. *Mol Cancer Ther* **2007**, *6*, 3028-3038.
37. Humphries, K. M.; Juliano, C.; Taylor, S. S. Regulation of cAMP-dependent protein kinase activity by glutathionylation. *J Biol Chem* **2002**, *277*, 43505-43511.
38. Humphries, K. M.; Deal, M. S.; Taylor, S. S. Enhanced dephosphorylation of cAMP-dependent protein kinase by oxidation and thiol modification. *J Biol Chem* **2005**, *280*, 2750-2758.
39. Kornev, A. P.; Haste, N. M.; Taylor, S. S.; Eyck, L. F. Surface comparison of active and inactive protein kinases identifies a conserved activation mechanism. *Proc Natl Acad Sci U S A* **2006**, *103*, 17783-17788.
40. Steichen, J. M.; Kuchinskas, M.; Keshwani, M. M.; Yang, J.; Adams, J. A.; Taylor, S. S. Structural basis for the regulation of protein kinase A by activation loop phosphorylation. *J Biol Chem* **2012**, *287*, 14672-14680.
41. Taylor, S. S.; Yang, J.; Wu, J.; Haste, N. M.; Radzio-Andzelm, E.; Anand, G. PKA: a portrait of protein kinase dynamics. *Biochim Biophys Acta* **2004**, *1697*, 259-269.

42. Taylor, S. S.; Zhang, P.; Steichen, J. M.; Keshwani, M. M.; Kornev, A. P. PKA: lessons learned after twenty years. *Biochim Biophys Acta* **2013**, *1834*, 1271-1278.
43. Nolen, B.; Taylor, S.; Ghosh, G. Regulation of protein kinases; controlling activity through activation segment conformation. *Mol Cell* **2004**, *15*, 661-675.
44. Bramson, H. N.; Thomas, N.; Matsueda, R.; Nelson, N. C.; Taylor, S. S.; Kaiser, E. T. Modification of the catalytic subunit of bovine heart cAMP-dependent protein kinase with affinity labels related to peptide substrates. *J Biol Chem* **1982**, *257*, 10575-10581.
45. First, E. A.; Taylor, S. S. Induced interchain disulfide bonding in cAMP-dependent protein kinase II. *J Biol Chem* **1984**, *259*, 4011-4014.
46. First, E. A.; Taylor, S. S. Selective modification of the catalytic subunit of cAMP-dependent protein kinase with sulfhydryl-specific fluorescent probes. *Biochemistry* **1989**, *28*, 3598-3605.
47. Kupfer, A.; Gani, V.; Jimenez, J. S.; Shaltiel, S. Affinity labeling of the catalytic subunit of cyclic AMP-dependent protein kinase by N alpha-tosyl-L-lysine chloromethyl ketone. *Proc Natl Acad Sci U S A* **1979**, *76*, 3073-3077.
48. Kupfer, A.; Jiménez, J. S.; Shaltiel, S. Distinct conformational changes in the catalytic subunit of cAMP-dependent protein kinase around physiological conditions. Do these changes reflect an ability to assume different specificities? *Biochemical and Biophysical Research Communications* **1980**, *96*, 77-84.
49. Mobashery, S.; Kaiser, E. T. Identification of amino acid residues involved in substrate recognition by the catalytic subunit of bovine cyclic AMP dependent protein kinase: peptide-based affinity labels. *Biochemistry* **1988**, *27*, 3691-3696.

50. Miller, W. T.; Kaiser, E. T. Probing the peptide binding site of the cAMP-dependent protein kinase by using a peptide-based photoaffinity label. *Proc Natl Acad Sci U S A* **1988**, *85*, 5429-5433.
51. Mobashery, S.; Doughty, M.; Kaiser, E. T. Inactivation of the catalytic subunit of bovine cAMP-dependent protein kinase by a peptide-based affinity inactivator. *Biopolymers* **1990**, *29*, 131-138.
52. Katz, B. M.; Lundquist, L. J.; Walsh, D. A.; Glass, D. B. Synthesis, characterization and inhibitory activities of (4-N³[3,5-³H]Phe¹⁰)PKI(6-22)amide and its precursors: photoaffinity labeling peptides for the active site of cyclic AMP-dependent protein kinase. *International Journal of Peptide and Protein Research* **2009**, *33*, 439-445.
53. Puri, R. N.; Bhatnagar, D.; Roskoski, R. Adenosine cyclic 3',5'-monophosphate dependent protein kinase: fluorescent affinity labeling of the catalytic subunit from bovine skeletal muscle with o-phthalaldehyde. *Biochemistry* **1985**, *24*, 6499-6508.
54. Puri, R. N.; Bhatnagar, D.; Glass, D. B.; Roskoski, R. Inactivation of guanosine cyclic 3',5'-monophosphate dependent protein kinase from bovine lung by o-phthalaldehyde. *Biochemistry* **1985**, *24*, 6508-6514.
55. Salerno, A.; Lawrence, D. S. Covalent modification with concomitant inactivation of the cAMP-dependent protein kinase by affinity labels containing only L-amino acids. *J Biol Chem* **1993**, *268*, 13043-13049.
56. Prorok, M.; Lawrence, D. S. An affinity label of absolute peptidic origin. *Journal of the American Chemical Society* **1990**, *112*, 8626-8627.
57. Yan, X. Precision Substrate Targeting of Protein Kinases. *Journal of Biological Chemistry* **1996**, *271*, 174-179.

58. Law, B.; Weissleder, R.; Tung, C. H. Mechanism-based fluorescent reporter for protein kinase A detection. *Chembiochem* **2005**, *6*, 1361-1367.
59. Willems, L. I.; Overkleeft, H. S.; van Kasteren, S. I. Current developments in activity-based protein profiling. *Bioconjug Chem* **2014**, *25*, 1181-1191.
60. Nodwell, M. B.; Sieber, S. A. ABPP methodology: introduction and overview. *Top Curr Chem* **2012**, *324*, 1-41.
61. Findeisen, P.; Neumaier, M. Functional protease profiling for diagnosis of malignant disease. *Proteomics Clin Appl* **2012**, *6*, 60-78.
62. Serwa, R.; Tate, E. W. Activity-based profiling for drug discovery. *Chem Biol* **2011**, *18*, 407-409.
63. Dijkstra, H. P.; Sprong, H.; Aerts, B. N.; Kruithof, C. A.; Egmond, M. R.; Klein Gebbink, R. J. Selective and diagnostic labelling of serine hydrolases with reactive phosphonate inhibitors. *Org Biomol Chem* **2008**, *6*, 523-531.
64. Kaschani, F.; Nickel, S.; Pandey, B.; Cravatt, B. F.; Kaiser, M.; van der Hoorn, R. A. Selective inhibition of plant serine hydrolases by agrochemicals revealed by competitive ABPP. *Bioorg Med Chem* **2012**, *20*, 597-600.
65. Nickel, S.; Kaschani, F.; Colby, T.; van der Hoorn, R. A.; Kaiser, M. A para-nitrophenol phosphonate probe labels distinct serine hydrolases of Arabidopsis. *Bioorg Med Chem* **2012**, *20*, 601-606.
66. Bachovchin, D. A.; Ji, T.; Li, W.; Simon, G. M.; Blankman, J. L.; Adibekian, A.; Hoover, H.; Niessen, S.; Cravatt, B. F. Superfamily-wide portrait of serine hydrolase inhibition achieved by library-versus-library screening. *Proc Natl Acad Sci U S A* **2010**, *107*, 20941-20946.

67. Zuhl, A. M.; Mohr, J. T.; Bachovchin, D. A.; Niessen, S.; Hsu, K. L.; Berlin, J. M.; Dochnahl, M.; Lopez-Alberca, M. P.; Fu, G. C.; Cravatt, B. F. Competitive activity-based protein profiling identifies aza-beta-lactams as a versatile chemotype for serine hydrolase inhibition. *J Am Chem Soc* **2012**, *134*, 5068-5071.
68. Jessani, N.; Niessen, S.; Wei, B. Q.; Nicolau, M.; Humphrey, M.; Ji, Y.; Han, W.; Noh, D. Y.; Yates, J. R., 3rd; Jeffrey, S. S.; Cravatt, B. F. A streamlined platform for high-content functional proteomics of primary human specimens. *Nat Methods* **2005**, *2*, 691-697.
69. Li, N.; Overkleeft, H. S.; Florea, B. I. Activity-based protein profiling: an enabling technology in chemical biology research. *Curr Opin Chem Biol* **2012**, *16*, 227-233.
70. Powers, J. C.; Asgian, J. L.; Ekici, O. D.; James, K. E. Irreversible inhibitors of serine, cysteine, and threonine proteases. *Chem Rev* **2002**, *102*, 4639-4750.
71. Heal, W. P.; Dang, T. H.; Tate, E. W. Activity-based probes: discovering new biology and new drug targets. *Chem Soc Rev* **2011**, *40*, 246-257.
72. Botta, M. New frontiers in kinases: special issue. *ACS Med Chem Lett* **2014**, *5*, 270.
73. Liu, Q.; Sabnis, Y.; Zhao, Z.; Zhang, T.; Buhrlage, S. J.; Jones, L. H.; Gray, N. S. Developing irreversible inhibitors of the protein kinase cysteinome. *Chem Biol* **2013**, *20*, 146-159.
74. Bogoyevitch, M. A.; Fairlie, D. P. A new paradigm for protein kinase inhibition: blocking phosphorylation without directly targeting ATP binding. *Drug Discov Today* **2007**, *12*, 622-633.
75. Cohen, P.; Alessi, D. R. Kinase drug discovery--what's next in the field? *ACS Chem Biol* **2013**, *8*, 96-104.

76. Cohen, M. S.; Hadjivassiliou, H.; Taunton, J. A clickable inhibitor reveals context-dependent autoactivation of p90 RSK. *Nat Chem Biol* **2007**, *3*, 156-160.
77. Honigberg, L. A.; Smith, A. M.; Sirisawad, M.; Verner, E.; Loury, D.; Chang, B.; Li, S.; Pan, Z. Y.; Thamm, D. H.; Miller, R. A.; Buggy, J. J. The Bruton tyrosine kinase inhibitor PCI-32765 blocks B-cell activation and is efficacious in models of autoimmune disease and B-cell malignancy. *Proceedings of the National Academy of Sciences of the United States of America* **2010**, *107*, 13075-13080.
78. Yee, M. C.; Fas, S. C.; Stohlmeyer, M. M.; Wandless, T. J.; Cimprich, K. A. A cell-permeable, activity-based probe for protein and lipid kinases. *J Biol Chem* **2005**, *280*, 29053-29059.
79. Hanks, S. K.; Hunter, T. Protein kinases 6. The eukaryotic protein kinase superfamily: kinase (catalytic) domain structure and classification. *FASEB J* **1995**, *9*, 576-596.
80. Gerlits, O.; Das, A.; Keshwani, M. M.; Taylor, S.; Waltman, M. J.; Langan, P.; Heller, W. T.; Kovalevsky, A. Metal-free cAMP-dependent protein kinase can catalyze phosphoryl transfer. *Biochemistry* **2014**, *53*, 3179-3186.
81. Masterson, L. R.; Cheng, C.; Yu, T.; Tonelli, M.; Kornev, A.; Taylor, S. S.; Veglia, G. Dynamics connect substrate recognition to catalysis in protein kinase A. *Nat Chem Biol* **2010**, *6*, 821-828.
82. Bastidas, A. C.; Deal, M. S.; Steichen, J. M.; Guo, Y.; Wu, J.; Taylor, S. S. Phosphoryl transfer by protein kinase A is captured in a crystal lattice. *J Am Chem Soc* **2013**, *135*, 4788-4798.

83. Knighton, D. R.; Zheng, J.; Ten Eyck, L. F.; Ashford, V. A.; Xuong, N.-H.; Taylor, S. S.; Sowadski, J. M. Crystal structure of the catalytic subunit of cyclic adenosine monophosphate-dependent protein kinase. *Science* **1991**, *253*, 407-414.
84. Aberg, E.; Lund, B.; Pflug, A.; Gani, O. A.; Rothweiler, U.; de Oliveira, T. M.; Engh, R. A. Structural origins of AGC protein kinase inhibitor selectivities: PKA as a drug discovery tool. *Biol Chem* **2012**, *393*, 1121-1129.
85. Vandamme, J.; Castermans, D.; Thevelein, J. M. Molecular mechanisms of feedback inhibition of protein kinase A on intracellular cAMP accumulation. *Cell Signal* **2012**, *24*, 1610-1618.
86. Burns-Hamuro, L. L.; Ma, Y.; Kammerer, S.; Reineke, U.; Self, C.; Cook, C.; Olson, G. L.; Cantor, C. R.; Braun, A.; Taylor, S. S. Designing isoform-specific peptide disruptors of protein kinase A localization. *Proc Natl Acad Sci U S A* **2003**, *100*, 4072-4077.
87. Steichen, J. M.; Iyer, G. H.; Li, S.; Saldanha, S. A.; Deal, M. S.; Woods, V. L., Jr.; Taylor, S. S. Global consequences of activation loop phosphorylation on protein kinase A. *J Biol Chem* **2010**, *285*, 3825-3832.
88. Guo, L.; Lee, A. A.; Rizvi, T. A.; Ratner, N.; Kirschner, L. S. The protein kinase A regulatory subunit R1A (Prkar1a) plays critical roles in peripheral nerve development. *J Neurosci* **2013**, *33*, 17967-17975.
89. Day, M. E.; Gaietta, G. M.; Sastri, M.; Koller, A.; Mackey, M. R.; Scott, J. D.; Perkins, G. A.; Ellisman, M. H.; Taylor, S. S. Isoform-specific targeting of PKA to multivesicular bodies. *J Cell Biol* **2011**, *193*, 347-363.
90. Kennedy, E. J.; Yang, J.; Pillus, L.; Taylor, S. S.; Ghosh, G. Identifying critical non-catalytic residues that modulate protein kinase A activity. *PLoS One* **2009**, *4*, e4746.

91. Taylor, S. S.; Kim, C.; Vigil, D.; Haste, N. M.; Yang, J.; Wu, J.; Anand, G. S. Dynamics of signaling by PKA. *Biochim Biophys Acta* **2005**, *1754*, 25-37.
92. Kim, C.; Xuong, N. H.; Taylor, S. S. Crystal structure of a complex between the catalytic and regulatory (RIalpha) subunits of PKA. *Science* **2005**, *307*, 690-696.
93. Paulucci-Holthauzen, A. A.; O'Connor, K. L. Use of pseudosubstrate affinity to measure active protein kinase A. *Anal Biochem* **2006**, *355*, 175-182.
94. Glass, D. B.; Cheng, H. C.; Mende-Mueller, L.; Reed, J.; Walsh, D. A. Primary structural determinants essential for potent inhibition of cAMP-dependent protein kinase by inhibitory peptides corresponding to the active portion of the heat-stable inhibitor protein. *J Biol Chem* **1989**, *264*, 8802-8810.
95. Skroblin, P.; Grossmann, S.; Schäfer, G.; Rosenthal, W.; Klussmann, E. Mechanisms of Protein Kinase A Anchoring. **2010**, *283*, 235-330.
96. Sastri, M.; Haushalter, K. J.; Panneerselvam, M.; Chang, P.; Fridolfsson, H.; Finley, J. C.; Ng, D.; Schilling, J. M.; Miyanochara, A.; Day, M. E.; Hakozaiki, H.; Petrosyan, S.; Koller, A.; King, C. C.; Darshi, M.; Blumenthal, D. K.; Ali, S. S.; Roth, D. M.; Patel, H. H.; Taylor, S. S. A kinase interacting protein (AKIP1) is a key regulator of cardiac stress. *Proc Natl Acad Sci U S A* **2013**, *110*, E387-396.
97. Naviglio, S.; Caraglia, M.; Abbruzzese, A.; Chiosi, E.; Di Gesto, D.; Marra, M.; Romano, M.; Sorrentino, A.; Sorvillo, L.; Spina, A.; Illiano, G. Protein kinase A as a biological target in cancer therapy. *Expert Opinion on Therapeutic Targets* **2009**, *13*, 83-92.
98. Walsh, D. A.; Van Patten, S. M. Multiple pathway signal transduction by the cAMP-dependent protein kinase. *The FASEB Journal* **1994**, *8*, 1227-1236.

99. Beristain, A. G.; Molyneux, S. D.; Joshi, P. A.; Pomroy, N. C.; Di Grappa, M. A.; Chang, M. C.; Kirschner, L. S.; Prive, G. G.; Pujana, M. A.; Khokha, R. PKA signaling drives mammary tumorigenesis through Src. *Oncogene* **2015**, *34*, 1160-1173.
100. Iglesias-Bartolome, R.; Torres, D.; Marone, R.; Feng, X.; Martin, D.; Simaan, M.; Chen, M.; Weinstein, L. S.; Taylor, S. S.; Molinolo, A. A.; Gutkind, J. S. Inactivation of a Galpha-PKA tumour suppressor pathway in skin stem cells initiates basal-cell carcinogenesis. *Nat Cell Biol* **2015**.
101. Mantovani, G.; Bondioni, S.; Lania, A. G.; Rodolfo, M.; Peverelli, E.; Polentarutti, N.; Veliz Rodriguez, T.; Ferrero, S.; Bosari, S.; Beck-Peccoz, P.; Spada, A. High expression of PKA regulatory subunit 1A protein is related to proliferation of human melanoma cells. *Oncogene* **2008**, *27*, 1834-1843.
102. Naviglio, S.; Spina, A.; Marra, M.; Sorrentino, A.; Chiosi, E.; Romano, M.; Improta, S.; Budillon, A.; Illiano, G.; Abbruzzese, A.; Caraglia, M. Adenylate cyclase/cAMP pathway downmodulation counteracts apoptosis induced by IFN-alpha in human epidermoid cancer cells. *J Interferon Cytokine Res* **2007**, *27*, 129-136.
103. Sands, W. A.; Palmer, T. M. Regulating gene transcription in response to cyclic AMP elevation. *Cell Signal* **2008**, *20*, 460-466.
104. Kita, T.; Goydos, J.; Reitman, E.; Ravatn, R.; Lin, Y.; Shih, W. C.; Kikuchi, Y.; Chin, K. V. Extracellular cAMP-dependent protein kinase (ECPKA) in melanoma. *Cancer Lett* **2004**, *208*, 187-191.
105. Calebiro, D.; Hannawacker, A.; Lyga, S.; Bathon, K.; Zabel, U.; Ronchi, C.; Beuschlein, F.; Reincke, M.; Lorenz, K.; Allolio, B.; Kisker, C.; Fassnacht, M.; Lohse, M. J. PKA

- catalytic subunit mutations in adrenocortical Cushing's adenoma impair association with the regulatory subunit. *Nat Commun* **2014**, *5*, 5680.
106. Lyons, J.; Landis, C. A.; Harsh, G.; Vallar, L.; Grunewald, K.; Feichtinger, H.; Duh, Q.-Y.; Clark, O. H.; Kawasaki, E.; Bourne, H. R. Two G protein oncogenes in human endocrine tumors. *Science* **1990**, *249*, 655-659.
107. Parma, J.; Duprez, L.; Van Sande, J.; Cochaux, P.; Gervy, C.; Mockel, J.; Dumont, J.; Vassart, G. Somatic mutations in the thyrotropin receptor gene cause hyperfunctioning thyroid adenomas. *Nature* **1993**, *365*, 649-651.
108. Vallar, L.; Spada, A.; Giannattasio, G. Altered Gs and adenylate cyclase activity in human GH-secreting pituitary adenomas. **1987**.
109. Landis, C. A.; Masters, S. B.; Spada, A.; Pace, A. M.; Bourne, H. R.; Vallar, L. GTPase inhibiting mutations activate the α chain of Gs and stimulate adenylyl cyclase in human pituitary tumours. **1989**.
110. Agnes, R. S.; Jernigan, F.; Shell, J. R.; Sharma, V.; Lawrence, D. S. Suborganelle sensing of mitochondrial cAMP-dependent protein kinase activity. *J Am Chem Soc* **2010**, *132*, 6075-6080.
111. Lee, H. M.; Xu, W.; Lawrence, D. S. Construction of a photoactivatable profluorescent enzyme via propinquity labeling. *J Am Chem Soc* **2011**, *133*, 2331-2333.
112. Shults, M. D.; Imperiali, B. Versatile fluorescence probes of protein kinase activity. *J Am Chem Soc* **2003**, *125*, 14248-14249.
113. Viht, K.; Vaasa, A.; Raidaru, G.; Enkvist, E.; Uri, A. Fluorometric TLC assay for evaluation of protein kinase inhibitors. *Anal Biochem* **2005**, *340*, 165-170.

114. Donal A. Walsh, C. D. A., Carmen Gonzalez, Dianne Calkins, Edmond H. Fischer, and Edwin G. Krebs Purification and Characterization of a Protein Inhibitor of Adenosine 3',5'-Monophosphate-dependent Protein Kinases. *J. Biol. Chem.* **1971**, *246*, 1977-1985.
115. Donal A. Walsh, C. D. A. Protein Kinases. Aspects of their regulation and diversity. *Recent progress in hormone research* **1973**, *29*, 329-359.
116. Scott, J. D.; Fischer, E. H.; Demaille, J. G.; Krebs, E. G. Identification of an inhibitory region of the heat-stable protein inhibitor of the cAMP-dependent protein kinase. *Proceedings of the National Academy of Sciences* **1985**, *82*, 4379-4383.
117. H C Cheng, B. E. K., R B Pearson, A J Smith, L Misconi, S M Van Patten, and D A Walsh A potent synthetic peptide inhibitor of the cAMP-dependent protein kinase. *J. Biol. Chem.* **1986**, *261*, 989-992.
118. David B Glass, M. R. E.-M., Simon J. Pilgis Synthetic peptides corresponding to the site phosphorylated in 6-phosphofructo-2-kinase/fructose-2,6-bisphosphatase as substrates of cyclic nucleotide-dependent protein kinases. *J. Biol. Chem.* **1986**, *261*, 2987-2993.
119. Glass, D. B.; Cheng, H. C.; Kemp, B. E.; Walsh, D. A. Differential and common recognition of the catalytic sites of the cGMP-dependent and cAMP-dependent protein kinases by inhibitory peptides derived from the heat-stable inhibitor protein. *J Biol Chem* **1986**, *261*, 12166-12171.
120. Dalton, G. D.; Dewey, W. L. Protein kinase inhibitor peptide (PKI): a family of endogenous neuropeptides that modulate neuronal cAMP-dependent protein kinase function. *Neuropeptides* **2006**, *40*, 23-34.

121. Glass, D. B.; Feller, M. J.; Levin, L. R.; Walsh, D. A. Structural basis for the low affinities of yeast cAMP-dependent and mammalian cGMP-dependent protein kinases for protein kinase inhibitor peptides. *Biochemistry* **1992**, *31*, 1728-1734.
122. Guergnon, J.; Dessauge, F.; Traincard, F.; Cayla, X.; Rebollo, A.; Bost, P. E.; Langsley, G.; Garcia, A. A PKA survival pathway inhibited by DPT-PKI, a new specific cell permeable PKA inhibitor, is induced by *T. annulata* in parasitized B-lymphocytes. *Apoptosis* **2006**, *11*, 1263-1273.
123. Bray, B. L. Large-scale manufacture of peptide therapeutics by chemical synthesis. *Nat Rev Drug Discov* **2003**, *2*, 587-593.
124. Harre, M.; Nickisch, K.; Tilstam, U. An efficient method for activation and recycling of trityl resins. *Reactive & Functional Polymers* **1999**, *41*.
125. Zhang, Y.; Ren, L.; Tu, Q.; Wang, X.; Liu, R.; Li, L.; Wang, J.-C.; Liu, W.; Xu, J.; Wang, J. Fabrication of reversible poly (dimethylsiloxane) surfaces via host-guest chemistry and their repeated utilization in cardiac biomarker analysis. *Analytical chemistry* **2011**, *83*, 9651-9659.
126. Arden-Jacob, J.; Drexhage, K.-H.; Hamers-Schneider, M.; Kemnitzer, N.; Zilles, A., Carboxamide-substituted dyes for analytical applications. Google Patents: 2011.
127. Gonzalez-Muniz, R.; Garcia-Lopez, M. T.; Gomez-Monterrey, I.; Herranz, R.; Jimeno, M. L.; Suarez-Gea, M. L.; Johansen, N. L.; Madsen, K.; Thogersen, H.; Suzdak, P. Ketomethylene and (Cyanomethylene)amino Pseudopeptide Analogs of the C-Terminal Hexapeptide of Neurotensin. *Journal of Medicinal Chemistry* **1995**, *38*, 1015-1021.

128. Moore, M. J.; Adams, J. A.; Taylor, S. S. Structural basis for peptide binding in protein kinase A. Role of glutamic acid 203 and tyrosine 204 in the peptide-positioning loop. *J Biol Chem* **2003**, *278*, 10613-10618.
129. Narayana, N.; Cox, S.; Shaltiel, S.; Taylor, S. S.; Xuong, N. Crystal structure of a polyhistidine-tagged recombinant catalytic subunit of cAMP-dependent protein kinase complexed with the peptide inhibitor PKI(5-24) and adenosine. *Biochemistry* **1997**, *36*, 4438-4448.
130. Moore, M. J.; Kanter, J. R.; Jones, K. C.; Taylor, S. S. Phosphorylation of the catalytic subunit of protein kinase A. Autophosphorylation versus phosphorylation by phosphoinositide-dependent kinase-1. *J Biol Chem* **2002**, *277*, 47878-47884.
131. Steinberg, R. A.; Cauthron, R. D.; Symcox, M. M.; Shuntoh, H. Autoactivation of catalytic (C alpha) subunit of cyclic AMP-dependent protein kinase by phosphorylation of threonine 197. *Mol Cell Biol* **1993**, *13*, 2332-2341.
132. Zoller, M.; Taylor, S. Affinity labeling of the nucleotide binding site of the catalytic subunit of cAMP-dependent protein kinase using p-fluorosulfonyl-[14C] benzoyl 5'-adenosine. Identification of a modified lysine residue. *Journal of Biological Chemistry* **1979**, *254*, 8363-8368.
133. Schwiebert, E. M.; Zsembery, A. Extracellular ATP as a signaling molecule for epithelial cells. *Biochimica et Biophysica Acta (BBA) - Biomembranes* **2003**, *1615*, 7-32.
134. Myers, A. G.; Barbay, J. K. On the Inherent Instability of α -Amino α' -Fluoro Ketones. Evidence for Their Transformation to Reactive Oxyvinyliminium Ion Intermediates. *Organic Letters* **2001**, *3*, 425-428.

135. Dobrota, C.; Fasci, D.; Hadade, N. D.; Roiban, G. D.; Pop, C.; Meier, V. M.; Dumitru, I.; Matache, M.; Salvesen, G. S.; Funeriu, D. P. Glycine fluoromethylketones as SENP-specific activity based probes. *ChemBiochem* **2012**, *13*, 80-84.
136. Cho, Y. S.; Park, Y. G.; Lee, Y. N.; Kim, M. K.; Bates, S.; Tan, L.; Cho-Chung, Y. S. Extracellular protein kinase A as a cancer biomarker: Its expression by tumor cells and reversal by a myristate-lacking Calpha and RIIbeta subunit overexpression. *Proceedings of the National Academy of Sciences* **2000**, *97*, 835-840.
137. Jimenez, J. S.; Kupfer, A.; Gani, V.; Shaltiel, S. Salt-induced conformational changes in the catalytic subunit of adenosine 3',5'-phosphate dependent protein kinase. Use for establishing a connection between one sulfhydryl group and the .gamma.-P subsite in the ATP site of this subunit. *Biochemistry* **1982**, *21*, 1623-1630.
138. Susumu, K.; Uyeda, H. T.; Medintz, I. L.; Pons, T.; Delehanty, J. B.; Mattoussi, H. Enhancing the Stability and Biological Functionalities of Quantum Dots via Compact Multifunctional Ligands. *Journal of the American Chemical Society* **2007**, *129*, 13987-13996.
139. Madhusudan; Akamine, P.; Xuong, N. H.; Taylor, S. S. Crystal structure of a transition state mimic of the catalytic subunit of cAMP-dependent protein kinase. *Nat Struct Biol* **2002**, *9*, 273-277.
140. Yang, J.; Kennedy, E. J.; Wu, J.; Deal, M. S.; Pennypacker, J.; Ghosh, G.; Taylor, S. S. Contribution of non-catalytic core residues to activity and regulation in protein kinase A. *J Biol Chem* **2009**, *284*, 6241-6248.

141. Bastidas, A. C.; Deal, M. S.; Steichen, J. M.; Keshwani, M. M.; Guo, Y.; Taylor, S. S. Role of N-terminal myristylation in the structure and regulation of cAMP-dependent protein kinase. *J Mol Biol* **2012**, *422*, 215-229.
142. Helmboldt, H.; Köhler, D.; Hiersemann, M. Synthesis of the Norjatrophone Diterpene (-)-15-Acetyl-3-propionyl- 17-norcharaciol. *Organic Letters* **2006**, *8*, 1573-1576.
143. Inci, B.; Wagener, K. B. Decreasing the Alkyl Branch Frequency in Precision Polyethylene: Pushing the Limits toward Longer Run Lengths. *Journal of the American Chemical Society* **2011**, *133*, 11872-11875.
144. Guzi, T.; Rane, D. F.; Mallams, A. K.; Cooper, A. B.; Doll, R. J.; Girijavallabhan, V. M.; Taveras, A. G.; Strickland, C.; Kelly, J. M.; Chao, J., Farnesyl protein transferase inhibitors. Google Patents: 2002.
145. Chandler, B. D.; Roland, J. T.; Li, Y.; Sorensen, E. J. Seebach's Conjunctive Reagent Enables Double Cyclizations. *Organic Letters* **2010**, *12*, 2746-2749.
146. Concellón, J. M.; Riego, E.; Rodríguez-Solla, H.; Plutín, A. M. Enantiopure Preparation of the Two Enantiomers of the Pseudo-C₂-Symmetric N,N-Dibenzyl-1,2:4,5-diepoxy-pentan-3-amine. *The Journal of Organic Chemistry* **2001**, *66*, 8661-8665.

Vita

Robert Anthony Coover was born on February 11, 1988 in Durham, North Carolina and is a citizen of the United States of America. He graduated from the University of North Carolina at Greensboro in 2011 with a Bachelor of Science in chemistry. During which time he interned at Targacept Inc. for the summer of 2009 (Winston-Salem, NC) and at Research Triangle Institute International (RTP, NC) for the summer of 2010.